TECHNISCHE
UNIVERSITÄT
WIEN
Vienna University of Technology

Diese Dissertation haben begutachtet:

....

DISSERTATION

Holographic Predictions for Strongly Coupled Quarks

ausgeführt zum Zwecke der Erlangung des akademischen Grades eines Doktors der technischen Wissenschaften unter der Leitung von

Univ.-Prof. DI Dr. Anton Rebhan
Institutsnummer: E 136
Institut für Theoretische Physik

eingereicht an der Technischen Universität Wien
Fakultät für Physik

von

Stefan A. Stricker
Matrikelnummer: e9925903
Erne Sedergasse 8/3/3.504
A-1030 Wien

Wien, am 22. März 2011 .....

Dedicated to my two girls, Viara and Sophia, who truly understand me.

Abstract

In this work we use the AdS/CFT correspondence to study properties of strongly coupled matter in the presence of fundamental matter fields. The AdS/CFT correspondence relates string theories living in a geometry that is asymptotically $AdS_5 \times S^5$ with gauge theories living on the boundary of AdS_5 which is four-dimensional Minkowski space. When one side is weakly coupled the other side is strongly coupled and vice versa, and therefore we can study properties of strongly coupled field theories by studying classical supergravity. We use two models, the Karch-Katz model based on a D3-D7-brane system and the Sakai-Sugimoto model based on a D4-D8-brane system.

Within the model by Karch and Katz we compute the energy spectrum of heavy-light mesons in an $\mathcal{N} = 2$ super Yang-Mills theory which on the gravity side corresponds to the fluctuation modes of a string stretching between two flavor branes. In the heavy quark limit, similar to QCD, we find that the excitation energies are independent of the heavy quark mass. We also find degeneracies in the spectrum which can be removed upon breaking supersymmetry. We consider two supersymmetry breaking scenarios. In one we tilt one of the fundamental branes leading to the emergence of hyperfine splitting, in the other we apply an external magnetic field leading to the Zeeman effect.

In the Sakai-Sugimoto model, which, in a certain limit, is dual to large N_c QCD, we study the effect of large magnetic fields on chiral matter. First, we discuss the proper implementation of the covariant anomaly and calculate chiral currents in the confined and deconfined phase. We introduce axial/vector chemical potentials in the system, where in the presence of a magnetic field a vector/axial current is induced. This is of relevance in the interior of compact stars and in non-central heavy-ion collisions where in both systems large magnetic fields are present. In heavy-ion collisions an imbalance in left and right-handed fermions may lead to a vector current parallel to the magnetic field, termed the chiral magnetic effect. After implementing the correct covariant anomaly we find an axial current in accordance with previous studies and a vanishing vector current, in apparent contrast to previous weak-coupling calculations. Second, we construct a charged and a neutral pion condensate and investigate their properties in an external magnetic field. In the case of a neutral pion condensate, a magnetic field is found to induce nonzero gradients of the Goldstone boson fields corresponding to meson supercurrents. A charged pion condensate, on the other hand, acts as a superconducter and expels the magnetic field due to the Meissner effect. Upon comparing the free energies of the two phases we find a critical magnetic field where a first order phase transition between the charged pion phase and the neutral pion phase occurs.

Zusammenfassung

In dieser Arbeit verwenden wir die AdS/CFT Korrespondenz um Eigenschaften von stark gekoppelter Materie in der Gegenwart von fundamentalen Materiefeldern zu untersuchen. Die AdS/CFT Korrespondenz verbindet Stringtheorien, welche in einem Raum leben, der asymptotisch die Geometrie von $AdS_5 \times S^5$ hat, mit Eichtheorien am Rand des AdS_5 Raumes, welcher ein vier-dimensionaler Minkowski Raum ist. Wenn die Stringtheorie stark gekoppelt ist, ist die Feldtheorie schwach gekoppelt und umgekehrt. Deshalb können wir mittels klassischer Supergravitation stark gekoppelte Feldtheorien untersuchen. Wir verwenden zwei Modelle, das Karch-Katz Modell, welches auf einem D3-D7-Branen-System basiert, und das Sakai-Sugimoto Modell, welches aus einem D4-D8-Branen-System besteht.

Unter Verwendung des Karch-Katz Modells berechnen wir das Energiespektrum von Mesonen, die aus einem schweren und einem leichten Quark bestehen, in einer $\mathcal{N} = 2$ Super-Yang-Mills Theorie. Auf der Gravitationsseite entspricht das Energiespektrum der Mesonen den Fluktuationsmoden von Strings, die zwischen zwei Flavor-Branen hängen. Im Limes für schwere Quarks finden wir Anregungsenergien, ähnlich wie in QCD, die unabhängig von der Masse des schweren Quarks sind. Wir finden auch Entartungen im Energiespektrum, die durch Brechen der Supersymmetrie aufgelöst werden. Wir brechen Supersymmetrie mit zwei verschiedenen Mechanismen. Einerseits verdrehen wir eine der fundamentalen Branen, woraus eine hyperfeine Struktur im Spektrum resultiert. Andererseits setzen wir ein externes Magnetfeld ein, das den Zeeman-Effekt zur Folge hat.

Im Sakai-Sugimoto Modell, das in einem bestimmten Limes dual zu QCD mit vielen Farbladungen ist, untersuchen wir den Effekt großer Magnetfelder auf chirale Materie. Zuerst diskutieren wir, wie die korrekte kovariante Anomalie im Modell implementiert wird und berechnen chirale Ströme in der gebundenen und ungebundenen Phase. Wir führen axiale/vektorielle chemische Potentiale ein, wobei in der Gegenwart eines Magnetfeldes vektorielle/axiale Ströme induziert werden. Dies ist im Inneren von kompakten Sternen und in nicht zentralen Schwerionen Kollisionen von Bedeutung, wo in beiden Systemen große Magnetfelder auftreten. In Schwerionen-Kollisionen kann ein Ungleichgewicht von links-und rechts-händigen Fermionen zu einem Vektorstrom führen, der sogenannte Chirale Magnetische Effekt. Nach der Berücksichtigung der korrekten kovarianten Anomalie finden wir einen axialen Strom, der mit vorhergehenden Studien übereinstimmt und einen verschwindenden Vektorstrom, im Widerspruch zu vorhergehenden Studien mittels schwacher Kopplung.

Danach konstruieren wir geladene und neutrale Pion-Kondensate und untersuchen deren Eigenschaften in der Gegenwart eines externen magnetischen Feldes. Einerseits finden wir im Fall des neutralen Pion-Kondensates, dass das Magnetfeld einen nicht verschwindenden Gradienten der Goldstone Bosonen induziert, welcher einem Superstrom von Mesonen entspricht. Andererseits verhält sich das geladene Pion-Kondensat wie ein Supraleiter und verdrängt das Magnetfeld aufgrund des Meissner-Effekts. Durch Vergleich der freien Energien der beiden Phasen finden wir ein kritisches Magnetfeld, bei dem ein Phasenübergang erster Ordnung zwischen geladener und neutraler Pion Phase auftritt.

Contents

Chapter 1

Introduction

1.1 Motivation

The ultimate goal in theoretical high energy physics is a theory that unifies the four known fundamental forces into a single theory on the quantum level.

Electromagnetism, the weak nuclear force, and the strong nuclear force have been combined into a single quantum field theory, called the standard model [1, 2, 3]. How to quantize gravity is still a big mystery, and one promising candidate for a quantum theory of gravity is string theory.

Quantum electrodynamics is very well understood and as of yet the most accurate theory that has ever been constructed. The weak force, responsible for the β-decay, is fairly well understood but still a few puzzles remain, like the existence of the Higgs particle. Quantum chromodynamics (QCD), the theory that describes the strong nuclear force, is not fully explored. QCD describes the interactions between quarks and gluons which form hadrons (baryons and mesons). It is a non-Abelian gauge theory with gauge group SU(3). The quarks transform in the fundamental representation and the gluons in the adjoint representation of the gauge group.

QCD is asymptotically free [4, 5]. This means that the effective coupling between the quarks and gluons decreases as the energy increases. The coupling constant is not a parameter of the theory but a function of energy scale. At sufficiently large momentum transfer QCD becomes a system of weakly interacting quarks and gluons and one can use perturbation theory. Perturbation theory relies on a valid expansion parameter. One assumes that the theory is almost free and observables are computed in a term by term expansion in the coupling constant. At low energies QCD becomes strongly coupled and it is not easy to perform calculations. The energy scale that separates the strongly coupled regime from the weakly coupled regime is $\Lambda_{QCD} \approx 200$ MeV, where the coupling constant is of order one. Let us have a look at the QCD phase diagram shown in Figure 1.1 in the plane of quark chemical potential μ and temperature T.

Above the deconfinment phase transition the ground state is the so called quark gluon plasma (QGP), where the fundamental degrees of freedom are the quarks and gluons. It is believed that the QGP existed until 10^{-5} seconds after the big bang. At very high temperatures, several times above the deconfinement temperature, the QCD coupling constant is perturbatively small and (hard thermal loop) perturbation theory can be applied to study QCD thermodynamics. For example the pressure of the QGP has been calculated to high order in the coupling constant [6, 7]. Before the experiments at the Relativistic Heavy Ion Collider (RHIC) in Brookhaven National Laboratory, where QGP was created, it was widely believed that the QGP is weakly coupled, even at moderately small temperatures, about twice the deconfinement temperature. However, it turned out the QGP rather behaves as a strongly

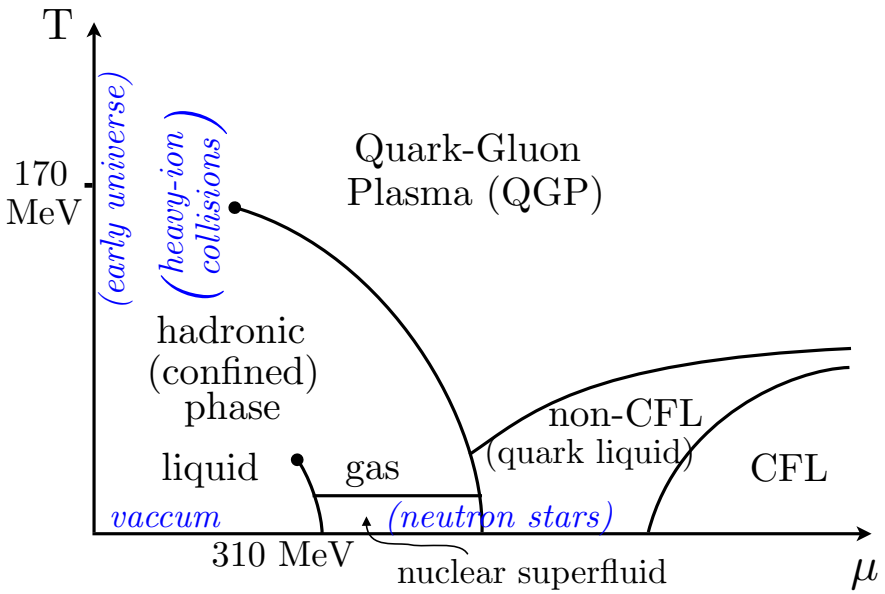

Figure 1.1: Conjectured phase diagram of QCD in the plane for quark chemical potential μ and temperature T. For asymptotically high chemical potentials and low temperature the ground state is the color-flavor-locked (CFL) phase. Going to lower chemical potentials one enters an unknown region, such as in neutron stars, which might consist of superfluid nuclear matter or deconfined quark matter or mixture of both. At high temperatures and low density the ground state is the quark-gluon-plasma (QGP) phase, probed in heavy-ion collisions.

coupled liquid than a weakly interacting gas of quarks and gluons.

Another region of interest where QCD becomes weakly coupled is for comparably cold and dense matter ($T \ll \mu \gg \Lambda_{QCD}$), which is called quark matter. For asymptotically high densities the ground state of QCD is the highly symmetric color-flavor locked (CFL) phase [8, 9]. The CFL phase is a superfluid and an electromagnetic insulator and chiral symmetry is broken. To go to more realistic densities, such as in neutron stars, first principle calculations are no longer possible, and extrapolation methods must be used and it is not clear how trustworthy they are.

Inside the hadronic phase, where quarks and gluons are confined, it is possible to use effective theories such as heavy quark effective theory or chiral perturbation theory. Effective field theories use the fact that physics at different energy scales are separated. Effective theories are approximate theories below some characteristic energy scale, *e.g.*, Λ_{QCD}, while ignoring the degrees of freedom at higher energies. They only take into account the relevant degrees of freedom while the others are integrated out from the action. See Refs. [10, 11] for reviews on effective field theories.

One example of such an effective theory is chiral perturbation theory (ChPT), which is the low energy realization of QCD in the light quark sector. Due to confinement in QCD the relevant degrees of freedom at low energies are not quarks and gluons but hadrons, and a description in terms of hadrons seems more adequate. At very low energies the hadronic spectrum only contains an octet of very light pseudo-Goldstone bosons (π, η, K) whose interactions can be understood with global symmetry considerations. ChPT has been very successful in calculating meson decay constants, quark mass ratios, etc., but also has its limitations and is not a theory built from the fundamental degrees of freedom, namely the quarks and gluons.

Another prominent effective theory is the heavy quark effective theory (HQET). Instead of the chiral symmetry for massless quarks one uses the heavy quark symmetry for infinitely

heavy quarks. In HQET one exploits the fact that in a system with one infinitely heavy quark, the light degrees of freedom cannot resolve the spin and flavor of the heavy quark. This heavy quark symmetry leads to simplifications and an effective action can be constructed. We will say more about HQET in Section 3.1.

Clearly some nonperturbative methods are needed to explore QCD at strong coupling from the fundamental degrees of freedom, with the most prominent one being lattice gauge theory (see *e.g.* the textbooks [12, 13]). In lattice gauge theory spacetime is discretized on a lattice and Wick-rotated to Euclidean space. It has been very successful in calculating hadron spectra and properties of states in thermal equilibrium such as the pressure of the QGP. However, lattice gauge theory faces conceptual problems for calculating out of equilibrium states, that is time dependent quantities such as transport coefficients, and for physics including chemical potentials. The reason for the conceptual problems originates from the use of the Euclidean space. By including a chemical potential the action is no longer real, making standard Monte Carlo methods unreliable. The same problem appears by studying time dependent dynamics, where analytic continuation to Minkowski space is necessary and the action becomes imaginary again. This is the famous sign problem of lattice QCD.

So there is still a big area of the QCD phase diagram where the above methods can not be applied and new tools are needed to gain a better understanding of the properties of QCD.

In 1997, with the discovery of the anti-de Sitter/conformal field theory (AdS/CFT) correspondence from string theory a new way for studying strongly coupled gauge theory became available. The original AdS/CFT correspondence states that type IIB string theory living on a background that is asymptotically $AdS_5 \times S_5$ is dual to $\mathcal{N} = 4$ supersymmetric Yang-Mills (SYM) theory living on the conformal boundary of AdS_5 which is four dimensional Minkowski space [14]. AdS spaces are negatively curved spacetimes, or in other words, solutions to the Einstein equation with negative cosmological constant. We will review AdS spaces and $\mathcal{N} = 4$ SYM theory in Sections 2.1 and 2.2. By duality we mean that the two theories describe exactly the same physics, but when one side is weakly coupled the other side is strongly coupled and vice versa.

In the discovery of the AdS/CFT correspondence D-branes were the crucial ingredient. Dp-branes are nonperturbative p+1 dimensional massive objects in string theory where open strings can end. One can think of them as hyperplanes embedded in spacetime. The discovery of the correspondence is based on the low energy limit of D-branes in two different regimes. Roughly speaking the argument goes as follows. Let us consider a stack of N_c D3-branes. Since Dp-branes are massive objects they can curve spacetime and the parameter measuring the effect of Dp-branes on the geometry is given by $g_s N_c$, where g_s is the string coupling constant. For $g_s N_c \ll 1$ spacetime is nearly flat and for $g_s N_c \gg 1$ we have a highly curved spacetime. In the low energy limit for $g_s N_c \ll 1$ the physics of the bulk and the stack of D3-branes decouples and one is left with $\mathcal{N} = 4$ SYM theory living on the brane and a theory of closed strings on flat space. Taking the low energy limit in the highly curved regime, again one ends up with two decoupled theories. This time with a theory of closed strings on flat space and type IIB string theory on $AdS_5 \times S_5$. This led to the conjecture that, since in both regimes one has closed strings on flat space, $\mathcal{N} = 4$ super Yang-Mills theory is equivalent to type IIB string theory on $AdS_5 \times S_5$.

In order to connect the two theories one needs a dictionary that relates the field theory with the string theory. A key relation is

$$\frac{L^4}{l_s^4} = 4\pi g_s N_c \,, \qquad 2\pi g_s = g_{YM}^2$$

where l_s is the string length, N_c the number of colors, L the curvature radius of AdS_5 space and the S_5 and g_{YM} the Yang-Mills coupling constant. The above entry from the dictionary tells

us the following. If the curvature radius is larger then the string length $L/l_s \gg 1$, where string theory is approximated by classical supergravity, then the field theory is strongly coupled because $g^2_{YM}N_c \gg 1$, showing us the nature of the duality between weakly and strongly coupled theories. Therefore we can calculate properties of strongly coupled gauge theories by considering classical supergravity. We will repeat in detail Maldacena's argument of the correspondence in Section 2.7.

However, the correspondence has not been proven and remains a conjecture, but it has passed many nontrivial tests, *e.g.*, the sets of fields living on the gravitational side has been matched with the set of field operators.

One might ask what this has to do with QCD. After all, $\mathcal{N} = 4$ SYM theory is a supersymmetric conformal theory with no running of the coupling constant. Firstly, it is helpful to have a new tool to calculate properties of a strongly coupled gauge theory, which might also result in a better understanding of other theories, like statements about universalities [15]. Secondly, it turns out that some theories have a conformal window. For example, at high enough temperatures lattice calculations suggest that the QGP becomes conformal [16], and the AdS/CFT correspondence turned out to be amazingly useful to study its properties such as the ratio of shear viscosity over entropy density [17], where the AdS/CFT calculation is surprisingly close to the measured result. (See Ref. [18] for a nice review on QGP and AdS/CFT.) Or the duality can be used to study certain condensed matter systems which are strongly coupled and conformal at the critical point [19].

After the original correspondence was discovered the more general conjecture was made that every non-Abelian gauge theory has a dual string theory which now goes under the name gauge/gravity duality [20]. And indeed, more dualities have been found [21, 22]. The gauge/gravity duality is an example of the holographic principle [23, 24, 25], which states that a theory of quantum gravity in some region of spacetime can be represented by a theory that lives on the boundary of this region. The holographic principle is motivated by black hole physics where the entropy of a black hole is proportional to the area of the horizon and not to its volume and is similar to optics, where a three dimensional image can be recorded onto a two dimensional plate. The AdS/CFT correspondence is a concrete example of the holographic principle in the sense that the SYM theory, which captures all the physics of the interior of the ten-dimensional spacetime, provides a holographic description of the gravitational world.

Of course, the ultimate goal is to find the gravitational dual to QCD. There are two approaches to reach this goal. The so called "*bottom up* " approach, where one starts with the gauge theory and constructs the holographic dual, like in [26, 27, 28]. Or the "*top down*" approach, where the starting point is a consistent theory of quantum gravity, like string theory, and one aims to derive a geometry which is dual to QCD in some limit [29].

One step towards more realistic holographic models was the inclusions of so called *probe branes* [30]. By adding a new type of branes one introduces new degrees of freedom to the system, namely fields transforming in the fundamental representation of the gauge group which are interpreted as quarks. With this setup it is possible to study the dynamics of quarks and to construct chiral condensates, mesons, and to investigate their properties like their energy spectrum. This will be the main theme of this thesis. We study properties of strongly coupled matter from holography in the presence of fundamental fields from different perspectives. We will use two models in the spirit of the *top down* approach: the Karch-Katz setup [30] and the Sakai-Sugimoto model [29].

Clearly, the discovery of the AdS/CFT correspondence is one of the milestones in theoretical physics and changed our view on fundamental theories and raises many deep questions about quantum gravity and gauge theories. In this thesis we will not try to tackle this fundamental question but rather use the gauge/gravity duality as a tool to learn something about

QCD by asking the right questions in theories where the gravitational dual is known.

1.2 Outline

This thesis is organized as follows. We will give a detailed introduction into the AdS/CFT correspondence in Chapter 2. We start by reviewing the necessary ingredients in order to understand the correspondence. We begin with the properties of AdS spaces and $\mathcal{N} = 4$ SYM theory. After introducing the physics of D-branes we will give Maldacena's derivation of the AdS/CFT correspondence [14] and then explain how to compute correlation functions of the gauge theory using the correspondence. We end this chapter by explaining how fundamental degrees of freedom can be introduced in the gravity picture.

In Chapter 3 we use a setup by Karch and Katz [30] and construct heavy-light mesons by placing probe D7 branes in a D3 brane background. The heavy-light mesons are strings stretching between the probe branes. We then study the energy spectrum of our heavy-light mesons in different scenarios. First we study the spectrum of supersymmetric mesons and then we investigate the effect of supersymmetry breaking on the spectrum by tilting one of the branes and by applying an external magnetic field. These results were first presented in [31, 32].

In Chapter 4 we give an introduction to the second holographic model we will use in the last two chapters: The Sakai-Sugimoto model [29], which is based on probe D8 branes embedded in a D4 background geometry.

In Chapter 5 we study holographic chiral currents in the confined and deconfined phase. We start with a discussion of the proper implementation of the "*consistent*" and "*covariant*" anomaly into the model and derive the general form of the currents. We then discuss the ambiguity of the currents, defined on the one hand via the general definition from the AdS/CFT correpondence, and on the other hand from the thermodynamic potentials. We calculate the axial and vector current in both phases which might be of relevance in compact stars and heavy-ion collisions (like the chiral magnetic effect). This chapter is based on [33].

Finally, in Chapter 6 we use the Sakai-Sugimoto model to investigate chirally broken phases in an external magnetic field at finite isospin and baryon chemical potentials. We construct two phases, a neutral pion condensate and a charged pion condensate. We find that a magnetic field induces nonzero gradients of the Goldstone boson fields corresponding to meson supercurrents. The charged pion condensate, on the other hand, expels the magnetic field due to the Meissner effect. Finally we compare the Gibbs free energies of the two phases and give the resulting phase diagram. This chapter is based on [34].

Chapter 2

The AdS/CFT correspondence

In this chapter we will review the necessary ingredients for understanding the duality between string theories and gauge theories. We will start with the properties of anti-de Sitter (AdS) spaces, followed by a summary of $SU(N_c)$ $\mathcal{N}=4$ Super Yang Mills theory. In Section 2.6 we will introduce the physics of D-branes and then, in Section 2.7, we will repeat Maldacena's beautiful argument [14] that relates string theory on $AdS_5 \times S_5$ to $\mathcal{N}=4$ SYM theory living on the boundary of AdS_5. Section 2.8 explains how one can calculate correlation functions from supergravity using the correspondence. Finally, in Section 4.1.2 we show how fundamental degrees of freedom can be added to the system via probe branes.
For more information on the subjects presented in this introduction, see the AdS/CFT reviews [35, 36, 37] and the string theory textbooks [38, 39, 40] and references therein.

2.1 Anti-de Sitter space

The properties of Anti-de Sitter spacetimes are essential for the AdS/CFT correspondence. Therefore we will take our time to review this geometry in detail. Before studying the structure of AdS space let us study the conformal structure[1] of flat spacetime [41] because the identification of the isometry of group of AdS_{p+2} with the conformal symmetry of flat Minkowski space $\mathbb{R}^{1,p}$ will be important for the AdS/CFT correspondence.

2.1.1 Conformal structure of flat space

We start with two-dimensional Minkowski space $\mathbb{R}^{1,1}$ because it is easier to visualize, but all arguments hold for higher dimensions as well. The metric is given by

$$ds^2 = -dt^2 + dx^2\,, \qquad (-\infty < t,\, x < \infty). \tag{2.1}$$

Performing a coordinate transformation

$$\tan u_\pm = t \pm x\,, \qquad u_\pm = \frac{\tau \pm \theta}{2}, \tag{2.2}$$

we can write the metric as

$$ds^2 = \frac{1}{4\cos^2 u_+ \cos^2 u_-}(-d\tau^2 + d\theta^2). \tag{2.3}$$

In this way we can map Minkowski space into a compact region, $|u_\pm| < \pi/2$. Since the causal structure does not change by a conformal transformation

$$g_{\mu\nu} \to g'_{\mu\nu}(x') = \Omega(x) g_{\mu\nu}(x)\,, \tag{2.4}$$

[1] After reading the following it should be clear what we mean by conformal structure.

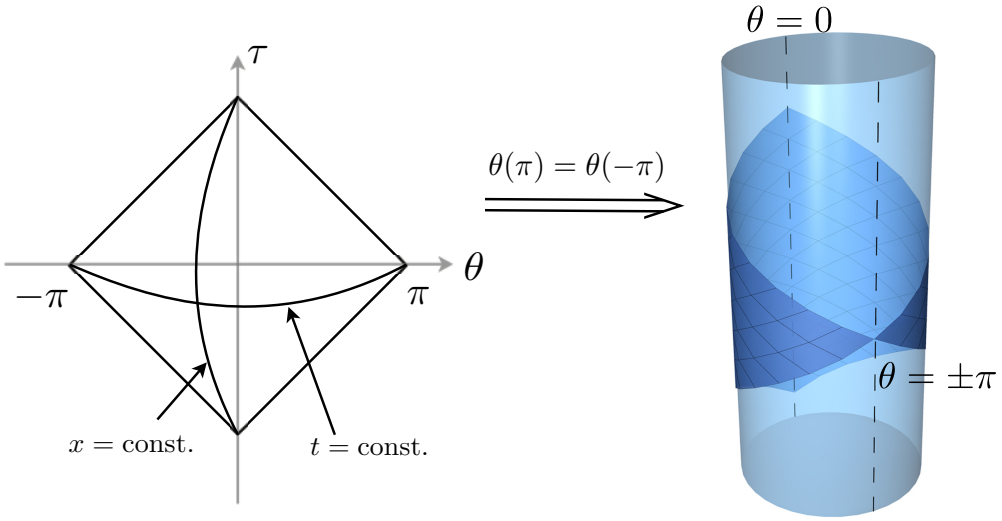

Figure 2.1: Left: Penrose diagram for $\mathbb{R}^{1,1}$. Right: By identifying $\theta = -\pi$ with $\theta = \pi$ $\mathbb{R}^{1,1}$ can be embedded in a cylinder.

we can multiply the above metric by $4\cos^2 u_+ \cos^2 u_-$ to obtain

$$ds'^2 = -d\tau^2 + d\theta^2. \tag{2.5}$$

The new coordinates are well defined at the asymptotic region of flat space and a spacetime is called *asymptotically flat* if it has the same boundary structure as flat space after conformal compactification. Conformal compactifications are very useful for studying the causal structure of spacetimes. Since the causal structure does not change under conformal transformations we speak of the conformal structure of a spacetime at infinity. The Penrose diagram of two dimensional Minkowski space is given in Figure 2.1. It is a square, where the two corners at $(\tau, \theta) = (0, \pm\pi)$ correspond to the spatial infinities at $x = \pm\infty$. We can embed the rectangular image of $\mathbb{R}^{1,1}$ in a cylinder $\mathbb{R} \times S^1$ by identifying the two corners as shown in Figure 2.1. The dark blue region is conformal to the whole of Minkowski spacetime.
The Einstein static universe in two dimensions with topology $\mathbb{R}^1 \times S^1$ can be represented as a cylinder embedded in three-dimensional Minkowski space.
It is possible to analytically continue (2.5) to the entire cylinder. This means that Minkowski space can be conformally mapped into the Einstein static universe. The generalization to (p+1)-dimensional Minkowski space is straightforward. After a series of coordinate changes and conformal rescaling, the metric for $\mathbb{R}^{1,p}$ can be written as

$$ds^2 = -d\tau^2 + d\theta^2 + \sin^2\theta d\Omega^2_{p-1}. \tag{2.6}$$

with $0 \leqslant \theta \leqslant \pi$. This time the Penrose diagram is a triangle because of the different interval for the θ coordinate but can be analytically continued outside the triangle and the maximally extended space has again the topology of the Einstein static universe $\mathbb{R} \times S^p$.

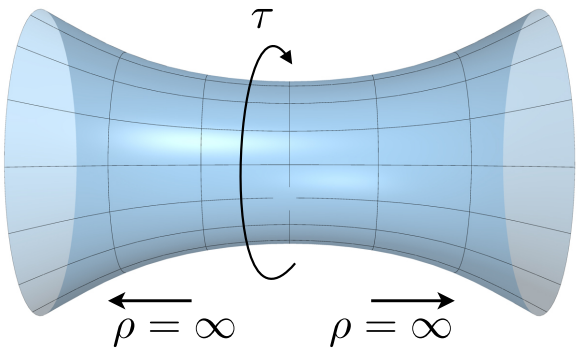

Figure 2.2: AdS_{p+1} realized as a hyperbolic space embedded in $\mathbb{R}^{2,p+1}$

2.1.2 Geometry of anti-de Sitter space

Anti-the Sitter space is an extension of hyperbolic space with a time direction. It is a solution to the Einstein equations

$$R_{\mu\nu} - \frac{1}{2} R g_{\mu\nu} = 8\pi G \Lambda g_{\mu\nu} \,, \tag{2.7}$$

with a negative cosmological constant Λ, or in other words it is a maximally symmetric negatively curved spacetime with constant curvature. A sphere on the contrary is a maximally symmetric positively curved spacetime. AdS_{p+2} space can be represented as the hyperboloid

$$\left(X^0\right)^2 + \left(X^{p+2}\right)^2 - \sum_{i=1}^{p+1} \left(X^i\right)^2 = L^2, \tag{2.8}$$

embedded in a flat $p+3$ dimensional space with the metric

$$ds^2 = -dX_0^2 - dX_{p+2}^2 + \sum_{i=1}^{p+1} \left(dX^i\right)^2 \,, \tag{2.9}$$

where L is the curvature radius of AdS_{p+2}. Its symmetry group is $SO(2, p+1)$.
The algebraic constraint equation (2.8) can be solved by setting

$$X_0 = L \cosh\rho \cos\tau \,, \qquad X_{p+2} = L \cosh\rho \sin\tau \,, \tag{2.10}$$

$$X_i = L \sinh\rho \, \Omega_i \qquad \left(i = 1, ..., p+1, \, \sum_{i=1}^{p+1} \Omega_i^2 = 1 \right) , \tag{2.11}$$

where the Ω_i are the standard coordinates of a p-dimensional sphere. Substituting this parametrization into (2.9) we obtain the AdS_{p+2} metric as

$$ds^2 = L^2 \left(-\cosh^2\rho \, d\tau^2 + d\rho^2 + \sinh^2\rho \, d\Omega_p^2 \right) . \tag{2.12}$$

By taking $\rho \in (0, \infty)$ and $\tau \in [0, 2\pi]$ we can cover the whole hyperboloid (Fig. 2.2) once and therefore the coordinates ρ, τ, Ω_i are called global coordinates. Near $\rho = 0$ the metric behaves as $ds^2 \simeq L^2(-d\tau^2 + d\rho^2 + \rho^2 d\Omega^2)$, showing that the hyperboloid has the topology of $S^1 \times \mathbb{R}^{p+1}$, with S^1 representing closed timelike curves in the τ direction. This is not what we want because in a universe with closed timelike curves one could travel for a while and get back before one's departure. To obtain a causal space-time we have to take the universal cover

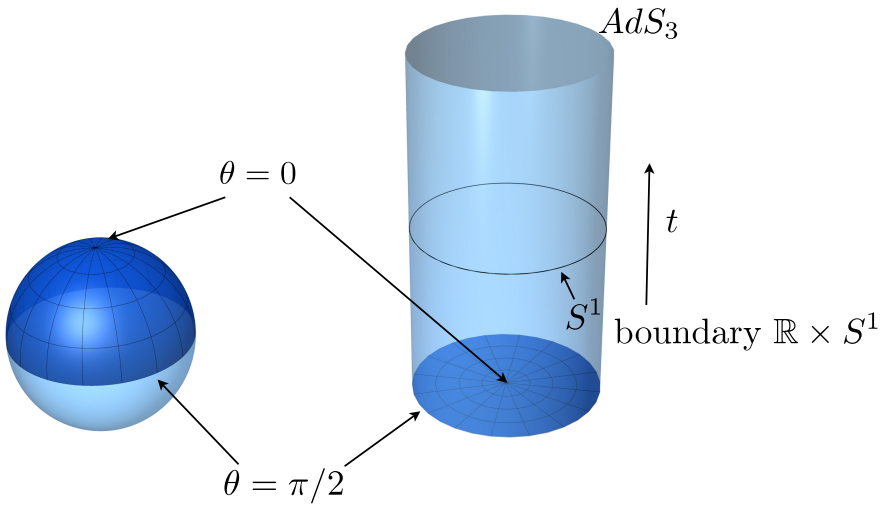

Figure 2.3: AdS_3 can be conformally mapped into one half of the Einstein static universe $\mathbb{R} \times S^2$. The conformal boundary is the surface $\mathbb{R} \times S^1$.

of the S^1. Practically this means we can simply unwrap the circle by taking $-\infty < \tau < \infty$ and there are no closed timelike curves anymore.

Let us now study the conformal structure of AdS_{p+2}. The most convenient way to do so is by introducing a new coordinate θ, related to ρ by $\tan\theta = \sinh\rho$, $(0 \leq \theta < \pi/2)$, which brings the endpoints of the ρ coordinate to finite values. Then, the metric (2.12) takes the form

$$ds^2 = \frac{L^2}{\cos^2\theta}\left(-d\tau^2 + d\theta^2 + \sin^2\theta d\Omega_p^2\right), \tag{2.13}$$

where $0 \leq \theta \leq \pi/2$ for all dimensions except for 2 (where $-\pi/2 \leq \theta \leq \pi/2$). Note that there is a second order pole at $\theta = \pi/2$. This is where the boundary of AdS is located. Because of this second order pole the bulk metric does not yield a metric at the boundary, it yields a conformal structure instead [42]. In order to analyze this conformal structure we make a conformal transformation by multiplying the metric with $L^{-2}\cos^2\theta$ to obtain

$$d\tilde{s}^2 = -d\tau^2 + d\theta^2 + \sin^2\theta d\Omega_p^2\,. \tag{2.14}$$

This allows us to understand the Penrose diagram of AdS. The equator at $\theta = \pi/2$ is a boundary of the space with the topology of S^p. The Penrose diagram of AdS_{p+2} is a solid cylinder whose boundary has the topology of $S^p \times \mathbb{R}$ where $\mathbb{R}$ corresponds to the time direction. We show this for AdS_3 in Figure 2.3.
Now comes the crucial point. We observe that the boundary of the conformally compactified AdS_{p+2} is identical to the conformal compactifaction of the (p+1)-dimensional Minkowski space. This will be important later because the field theory will be defined on that boundary. Also note that the metric (2.14) is the same as for the Einstein static universe (2.6) with dimension lower by one, with the only difference that the coordinate θ takes values in $0 \leq \theta < \pi/2$, rather than $0 \leq \theta < \pi$. Namely, AdS can be conformally mapped into one half of the Einstein static universe. In general, if a spacetime can be conformally compactified into a region which has the same boundary structure as one half of the Einstein static universe, the spacetime is called *asymptotically AdS*.

In addition to the global parametrization there is another set of coordinates, called the Poincaré

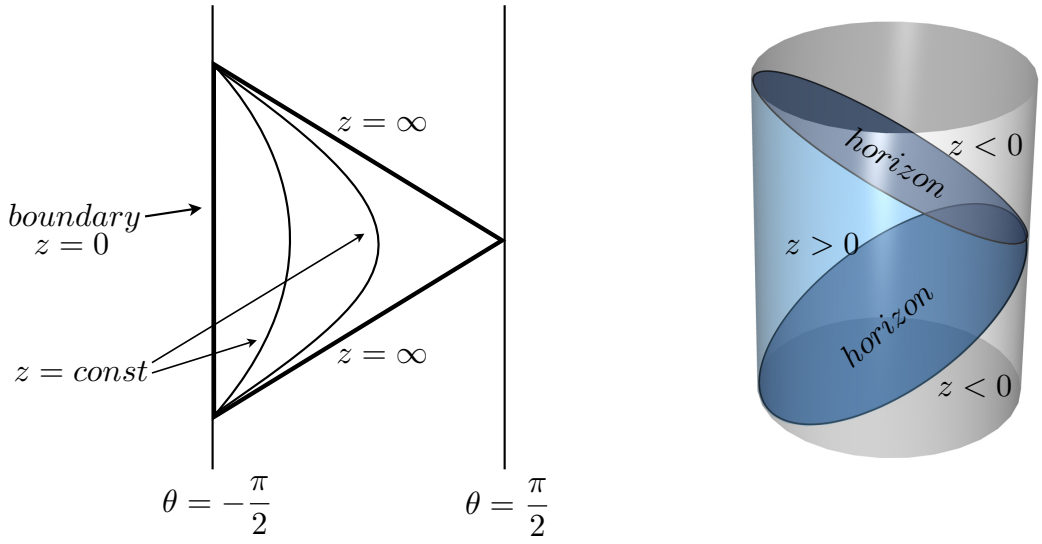

Figure 2.4: Left: Penrose diagram for AdS_2. Global AdS can be conformally mapped into the strip between $\theta = -\pi/2$ and $\theta = \pi/2$. The triangular region is the Penrose diagram for the Poincaré coordinates. Right: Boundary regions of AdS_3 in the Poincaré patch. The blue shaded area in the interior of the cylinder corresponds to the region covered by the Poincaré coordinates and is bounded by two lightlike hyperplanes. By crossing these hyperplanes one reaches the other Poincaré patch. The boundary of the cylinder is the conformal region of AdS_3 covered by Minkowski space.

coordinates $(z, t, \vec{x})$, where $0 < z, \vec{x} \in \mathbb{R}^{p+1}$, which we will use later. It is defined as

$$X_0 = \frac{1}{2z}\left(L^2 + z^2 - t^2 + \vec{x}^2\right), \qquad X_{p+2} = \frac{Lt}{z} \tag{2.15}$$

$$X^{p+1} = \frac{1}{2z}\left(L^2 - z^2 + t^2 - \vec{x}^2\right), \qquad X^i = \frac{Lx^i}{z} \quad (i = 1, ..., p). \tag{2.16}$$

In these coordinates the the AdS_{p+2} metric takes the form

$$ds^2 = \frac{L^2}{z^2}\left(-dt^2 + dz^2 + d\vec{x}^2\right). \tag{2.17}$$

In these coordinates the space is essentially (p+1) dimensional flat space with an extra warped dimension, z, which is the radial coordinate of AdS. The boundary of the AdS space is located at $z = 0$ and there is a horizon at $z = \infty$ since $g_{tt} \to 0$, called the Poincaré horizon. The horizon has zero area because $g_{x_i x_i} \to 0$ as $z \to \infty$, but has finite area in global coordinates. For a complete list of mappings between global and Poincaré coordinates see Ref. [43]. These coordinates only cover one half of the hyperboloid (2.8) for $z > 0$. By crossing the horizon one reaches the other Poincaré patch, covering the other half of the hyperboloid $z < 0$. The coordinate singularity at $z = 0$ does not belong to the AdS space but is part of its boundary. In Figure 2.4 we show the Penrose diagram in Poincaré coordinates for AdS_2, which is the triangular region and its embedding into the Einstein static universe for AdS_3. The conformal compactification of global AdS_2 is the infinite strip between $\theta = -\pi/2$ and $\theta = \pi/2$. The Poincaré patch is often very useful for calculations and we will use it in Chapter 3.
Performing the coordinate transformation $u = L^2/z$ the metric (2.17) can be written as

$$ds^2 = L^2\left[\frac{du^2}{u^2} + u^2(-dt^2 + d\vec{x}^2)\right], \tag{2.18}$$

where now the boundary is located at $u = \infty$. We will encounter this form of the metric in Section 2.7 when we look at the near horizon geometry of extremal D3-branes.
Sometimes we will also use the Euclidean version of AdS_{p+2} space, given by

$$ds^2 = \frac{L^2}{z^2}\left(dz^2 + \sum_{i=1}^{p+1} dx_i^2\right), \tag{2.19}$$

which has the topology of a (p+2)-dimensional disk. To close this section we want to point out a peculiar property of AdS space. A light ray can reach the boundary located at infinity in a finite amount of time. This is possible because AdS space acts as a gravitational potential well.

2.2 Supersymmetry

In flat four dimensional space-time $\mathbb{R}^{1,3}$ the Poincaré algebra is the Lie algebra of the symmetry group of Minkowski space and is generated by translations and Lorentz transformations $SO(1,3)$, with generators P_μ and $L_{\mu\nu}$ respectively. In the 60's people were asking if it is possible to combine the Poincaré symmetry and the internal symmetries of particle physics, such as the $U(1)$ of electromagnetism or the $SU(3)$ of QCD into a larger group? At first the answer turned out to be no, due to the famous Coleman-Mandula theorem [44], which says that if the Poincaré and internal symmetries were to combine, the S matrices for all processes would be zero and hence only trivial theories could be constructed. However, this theorem only holds if the final algebra is a Lie algebra but one can evade the theorem by generalizing the notion of a Lie algebra to a *graded Lie algebra*. A graded Lie algebra is an algebra that has some generators Q_α^i that satisfy an anticommuting law instead of a commuting law, namely

$$\{Q_\alpha^i, Q_\beta^j\} = \text{other generator.} \tag{2.20}$$

Then it is possible to combine Poincaré with internal symmetries. The anticommuting symmetry generators Q_α^i, called supercharges, are spinors

$$i = 1, ..., \mathcal{N} \qquad \begin{cases} Q_\alpha^i \quad \alpha = 1,2 & \text{left Weyl spinor} \\ \bar{Q}_{\dot{\alpha} i} = (Q_\alpha^i)^\dagger & \text{right Weyl spinor.} \end{cases} \tag{2.21}$$

Here, $\mathcal{N}$ is the number of independent supersymmetries of the algebra. Weyl spinors have two components, thus the total number of real supercharges is $2 \times 2 \times \mathcal{N}$. When acting with Q_α^i on a boson field we will get a spinor field. Therefore Q_α^i gives a symmetry between bosons and fermions called **supersymmetry** (susy). (A standard textbook on supersymmetry is [45].)

The supercharges transform as Weyl spinors of $SO(1,3)$ and commute with translations. The remaining susy structure relations are

$$\{Q_\alpha^i, \bar{Q}_{\dot{\beta} j}\} = 2\sigma^\mu_{\alpha\dot{\beta}} P_\mu \delta_i^j, \qquad \{Q_\alpha^i, Q_\beta^j\} = 2\epsilon_{\alpha\beta} Z^{ij}, \tag{2.22}$$

where Z^{ij} are bosonic symmetry generators, called central charges and σ^μ are the 2×2 Pauli matrices together with $\sigma^0 = \mathbf{1}_{2\times 2}$. The supersymmetry algebra possesses a group of automorphisms, rotations of supercharges into one another, forming a group $U(\mathcal{N})_R$, called the R-symmetry group. The supercharges act as raising and lowering operators for helicity. Theories with one supercharge are called simple susy theories and with $\mathcal{N} > 1$ are called extended supersymmetric theories.
If the central charge of a theory is nonzero then there are massive particle representations. There are many different supersymmetric theories. In the next section we will review the properties of a very special supersymmetric theory, namely supersymmetric Yang-Mills theory with four supercharges.

2.3 Supersymmetric Yang-Mills theory

It is possible to extend four dimensional Yang-Mills (YM) theory and make it supersymmetric. Actually there are different supersymmetric Yang-Mills (SYM) theories, depending on the number of supercharges. The maximally supersymmetric gauge theory is $\mathcal{N} = 4$ supersymmetric Yang-Mills theory ($\mathcal{N} = 4$ SYM) with 16 real supercharges. The Lagrangian for $\mathcal{N} = 4$ SYM is unique and is determined completely by demanding gauge invariance and supersymmetry. The field content of $\mathcal{N} = 4$ SYM is a vector A_μ, six scalars ϕ^I $(I = 1, ..., 6)$ and four Majorana fermions $\lambda_{\alpha,i}$, $\lambda_{\dot{\alpha},\bar{i}}$, where the α, $\dot{\alpha}$ are four-dimensional chiral and anti-chiral spinor indices respectively and $i = 1, ..., 4$ is an index in the **4** representation of the $SU(4)$ and $\bar{i}$ in the $\bar{\mathbf{4}}$. The scalars transform in the **6** representation. Due to supersymmetry all fields transform in the same representation, the adjoint representation, and must have the same mass. To ensure gauge invariance the gauge field has to be massless, hence the scalars and fermions are also massless. Schematically the Lagrangian can be written as [46, 36]

$$\mathcal{L}_{\mathcal{N}=4} = \mathrm{Tr}\left[\frac{1}{g^2}F^2 + \theta F\tilde{F} + (D\phi)^2 + \bar{\lambda}\not{D}\lambda + g\,\lambda[\phi,\lambda] + g\,\bar{\lambda}[\Phi,\bar{\lambda}] + g^2[\phi^I,\phi^J]^2\right], \qquad (2.23)$$

with two parameters, the coupling constant g and the θ angle.

Classically the $\mathcal{N} = 4$ SYM is scale invariant. In a relativistic field theory, scale invariance and Poincaré invariance combine into a larger *conformal symmetry*, forming the group $SO(2, 4)$. Combining supersymmetry and conformal invariance produces an even larger symmetry, the superconformal symmetry given by the supergroup $SU(2, 2|4)$. Remarkably, $\mathcal{N} = 4$ SYM theory remains scale invariant even quantum mechanically. Moreover the theory is renormalizable and the β-function vanishes identically.

By definition, the conformal group is the subgroup of coordinate transformation that leaves the metric invariant up to a scale change

$$g_{\mu\nu} \to g'_{\mu\nu}(x') = \Omega(x)g_{\mu\nu}(x). \qquad (2.24)$$

These are the coordinate transformations that preserve the angles between two vectors. The conformal group consists of the following transformations:

- Translations: $x^\mu \to x^\mu + a^\mu$
- Lorentz transformations: $x^\mu \to \Lambda^\mu_\nu x^\nu$
- Scale transformations: $x^\mu \to \lambda x^\mu$
- Special conformal transformations: $x^\mu \to \frac{x^\mu + b^\mu x^2}{1+2b_\mu x^\mu + b^2 x^2}$

The first two are the transformations of the Poincaré group. The third is a scale transformation, and the fourth is a combination of an inversion and a translation.

Together with the R-symmetry of the supercharges, which locally is the $SU(4)_R$ subgroup of the $U(4)_R$ and isomorphic to $SO(6)$, the bosonic symmetry group of $\mathcal{N} = 4$ SYM is $SO(4, 2) \times SO(6)$.

2.4 Large N field theories

One of the first hints that gauge theories have some stringy features appeared in the investigation of SU(N) gauge theories in the large N limit. In theories like QCD the coupling constant at low energy is not a good expansion parameter because the coupling constant becomes energy dependent (dimensional transmutation) and the theory is strongly coupled below some

characteristic energy scale. In 1974 't Hooft [47] suggested one should generalize QCD from three colors and an SU(3) gauge theory to N colors and an SU(N) gauge theory. The hope was that the theory can be solved in the large N limit and has some similarities with real QCD. So far QCD hasn't been solved in the large N limit but it proved very useful to gain insight into renormalizable theories with spontaneous symmetry breaking and asymptotic freedom. Some toy models with these properties, like the Gross-Neveu model [48], can be solved exactly in the large N limit.

Let us have a look at SU(N) Yang Mills theory and estimate the behavior of correlation functions in the large N limit. The β-function equation for this theory is given by

$$\mu \frac{\partial g_{YM}}{\partial \mu} = -\frac{11}{3} N \frac{g_{YM}^3}{16\pi^2} + \mathcal{O}(g_{YM}^5), \tag{2.25}$$

where g_{YM} is the Yang-Mills coupling constant and μ is some energy scale. Clearly, this equation has no sensible large N limit. To get a sensible large N limit we define a new coupling constant $\lambda = g_{YM}^2 N$ and keep λ fixed as N $\to \infty$. This is known as the 't Hooft limit. The Lagrangian is given by

$$S = \frac{1}{4g_{YM}^2} \int d^4x \mathrm{Tr}\left(F_{\mu\nu}^2\right), \quad F_{\mu\nu} = \partial_\mu A_\nu - \partial_\nu A_\mu + [A_\mu, A_\nu], \quad (A_\mu)_j^i = A_\mu^a (T^a)_j^i, \tag{2.26}$$

where $(T^a)_j^i$ are the generators of the SU(N) gauge group. We may now estimate the behavior of the correlation function in the 't Hooft limit. To keep track of the color indices in the Feynman diagrams one can think of the gluon as a quark- antiquark combination, $(A_\mu)_j^i \sim q^i \bar{q}_j$. In this so called "double-line notation" each of the two indices i, j is given their own line with an arrow, the direction of the arrow distinguishing quark from antiquark. For simplicity let us consider vacuum to vacuum graphs, graphs with no external lines (every index line must close) and count the powers of λ and N. Each interaction vertex has a factor of N/λ and each propagator has a factor of λ/N, since a vertex is a term in the Lagrangian and the propagator is the inverse of the quadratic parts in the Lagrangian. Every closed loop gives a factor of N, because we have to sum over all possible configurations.

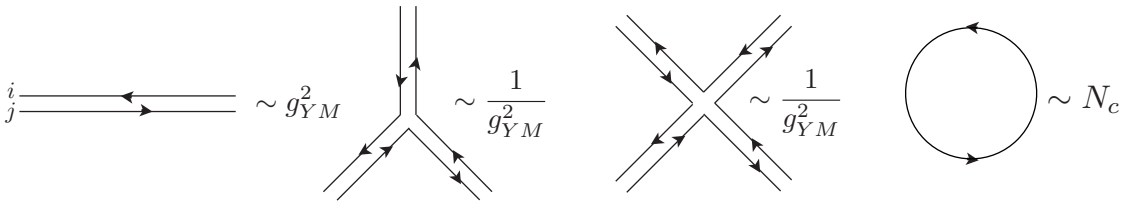

Figure 2.5: Feynman rules for SU(N) gauge theory in the double line notation

There are planar and non-planar diagrams. Non-planar diagrams can not be drawn on a plane without lines crossing like the last diagram in Figure 2.6.

We can also compactify space by adding a point at infinity. Then each diagram corresponds to a compact, closed oriented surface. In such a diagram we can view the propagators (double lines) as forming the edges (E) and the loops as faces (F) in a simplicial decomposition (*e.g.* a triangulation) of a surface. A diagram with V vertices, E propagators and F loops is proportional to

$$\left(\frac{\lambda}{N}\right)^{prop-vert} N^F = N^{V-E+F} \lambda^{E-V} = N^\chi \lambda^{E-V} = N^{2-2g} \lambda^{E-V}, \tag{2.27}$$

where $\chi = 2 - 2g$ is a topological invariant known as the Euler number and g is the number of handles. We see that planar diagrams are proportional to N^2 and non-planar ones are suppressed by additional factors of $1/N^2$. The important point now is that non planar diagrams can be made planar by drawing them on a surface of higher genus, like a torus, as shown in Figure 2.6. Therefore Feynman diagrams are organized by their topology and the sum over

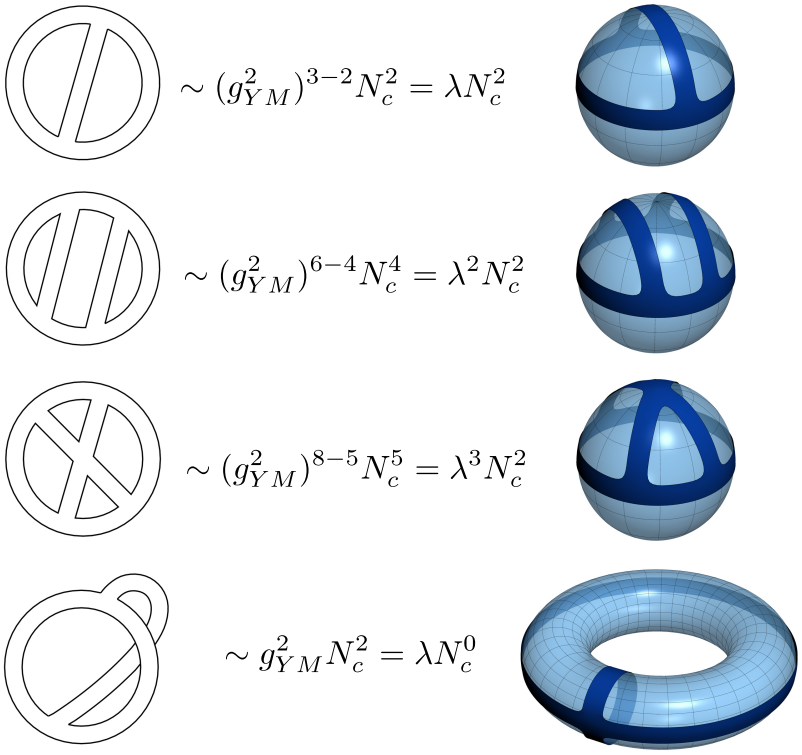

Figure 2.6: Counting factors of g_{YM} and N_c for planar and non planar diagrams. Planar diagrams are proportional to N_c^2 and can be drawn on a sphere. Non planar diagrams can not be drawn on a plane without lines crossing but can be drawn as planar ones on surfaces of higher genus, like the torus. Non planar diagrams are suppressed by a factor of N_c^{-2}.

connected vacuum-to-vacuum amplitudes can be written at large N as

$$\ln Z = \sum_{g=0}^{\infty} N^{2-2g} \sum_{i=0}^{\infty} c_{g,i} \lambda^i = \sum_{g=0}^{\infty} N^{2-2g} f_g(\lambda), \tag{2.28}$$

where $c_{g,i}$ are numerical coefficients depending on the detailed evaluation of each Feynman graph and f_g is some polynomial in λ. This indicates that there is some dual relationship between Feynman diagrams of an SU(N) gauge theory and two dimensional surfaces.

One can also include quarks, ore more generally matter in the fundamental representation. Quarks have N_c degrees of freedom. In a theory with N_f flavors the contribution of a single quark loop to the vacuum amplitude is proportional to $\ln Z \sim N_f N_c$ in contrast to N_c^2 as in (2.28). Thus, in the large N_c limit quark loops are suppressed by powers of N_f/N_c. Classifying quark loops by their topologies of two-dimensional surfaces as for gluons one has to include surfaces with boundaries, each boundary corresponding to a quark loop.

In the next section we will show an intriguing relation between the organization of Feynman diagrams by their topology and perturbative string theory.

2.5 String theory

String theory is one attempt to unify QFT with a quantum theory of gravity. In string theory the fundamental objects are not pointlike particles but rather one-dimensional extended objects called strings. Strings are very small objects with one dimensionful fundamental parameter, the string length l_s, which is taken to be the order of the Planck length. Every string comes with an energy per unit length, the string tension

$$T = \frac{1}{2\pi\alpha'} \equiv \frac{1}{2\pi l_s^2}, \tag{2.29}$$

which sets the characteristic length scale l_s of the theory. α' is the so called Regge slope[2]. There are two kinds of strings, open and closed strings. Strings live in a higher dimensional space-time given by the metric $G_{\mu\nu}$. As time passes by a string will sweep out a two-dimensional surface, called the string world-sheet. The action for such a string, the Nambu-Goto action, is just the area of the string world-sheet which we extremize to get the string equations of motion.

Suppose $\xi^\alpha = (\tau, \sigma)$ are the coordinates on the world-sheet and $X^\mu(\xi^\alpha)$ are the coordinates of the string describing its embedding in space-time. Then $G_{\mu\nu}$ induces a metric on the world-sheet:

$$ds^2 = G_{\mu\nu} dX^\mu dX^\nu = G_{\mu\nu} \frac{\partial X^\mu}{\partial \xi^\alpha} \frac{\partial X^\nu}{\partial \xi^\beta} d\xi^\alpha d\xi^\beta = h_{\alpha\beta} d\xi^\alpha d\xi^\beta, \tag{2.30}$$

where the induced metric is

$$h_{\alpha\beta} = G_{\mu\nu} \frac{\partial X^\mu}{\partial \xi^\alpha} \frac{\partial X^\nu}{\partial \xi^\beta}. \tag{2.31}$$

This metric can be used to calculate the surface area swept out by the string. The action, invariant under general world-sheet and target-space coordinate transformations and proposed by Nambu and Goto is given by

$$S_{NG} = -T \int d^2\xi \sqrt{-\det h_{\alpha\beta}} = -T \int d^2\xi \sqrt{(\dot{X} \cdot X')^2 - (\dot{X}^2)(X'^2)}, \tag{2.32}$$

where $X \cdot Y = G_{\mu\nu} X^\mu Y^\nu$ and $\partial_\sigma X = X'$ and $\partial_\tau X = \dot{X}$.

In order to solve the equation of motion we have to implement boundary conditions depending on the type of string we are studying. For a closed string the world-sheet is a tube and we impose the periodicity condition

$$X^\mu(\sigma + 2\pi) = X^\mu(\sigma). \tag{2.33}$$

For open strings the world-sheet is a strip and we can use two kinds of boundary conditions:

$$\text{Neumann}: \quad \frac{\delta \mathcal{L}}{\delta X'^\mu}\Big|_{\sigma=0,\pi} = 0, \qquad \text{Dirichlet}: \quad \frac{\delta \mathcal{L}}{\delta \dot{X}^\mu}\Big|_{\sigma=0,\pi} = 0. \tag{2.34}$$

Neumann conditions imply that no momentum flows off the endpoints of the string, whereas Dirichlet boundary conditions fix the endpoints of the string. It is also possible to impose linear combinations of the two boundary conditions. We will encounter this situation in Section 3.7.1.

Quantizing the string imposes restrictions on the dimensionality in which the string can propagate. It turns out that for the bosonic string a consistent string theory only exists in 26 dimensions. Otherwise one would have negative norm states. Physically, the vibrational

[2]The name comes from the early stages of string theory, where string theory was an attempt to describe hadron resonances with a spin mass relation described by Regge trajectories $J = m^2\alpha' + \beta_0$

modes of the string correspond to different states in the spectrum. On distances larger than the string length these modes appear as particles of different mass and spin. In analyzing the string spectrum one finds massive and massless modes. Among the massless states there is a spin-1 particle in the open string sector, the photon, and a spin-2 particle in the closed string sector, the graviton. The graviton describes fluctuations of spacetime and although we started with a fixed metric, we have a graviton in the spectrum indicating that the background geometry is dynamical. This is why string theory is a theory of quantum gravity.

The problem with bosonic string theory is that it is inconsistent. The spectrum contains a tachyon, that is a state whose mass squared is negative and it only contains bosons. Realistic string theories must also contain fermions. To get fermions one introduces new anticommuting dynamical world-sheet variables $\Psi^{\mu}_{\alpha}(\tau, \sigma)$ with $\alpha = 1, 2$, which behave as spacetime fermions. Then it is possible to construct a consistent string theory action that is invariant under supersymmetry transformations. This theory is called *superstring* theory and the absence of negative norm states requires the spacetime to be 10-dimensional. By including fermions the tachyon disappears from the spectrum. In addition to the graviton the massless spectrum now contains fermions, antisymmetric tensor fields generalizing the photon and two scalars. One of these scalars is the dilaton ϕ which plays an important role. It determines the string self-interaction $g_s \sim e^{\phi}$.

There are five known superstring theories. In this work we will use two of them, type IIA and type IIB superstring theories, which include spacetime fermions of opposite and even chirality respectively.

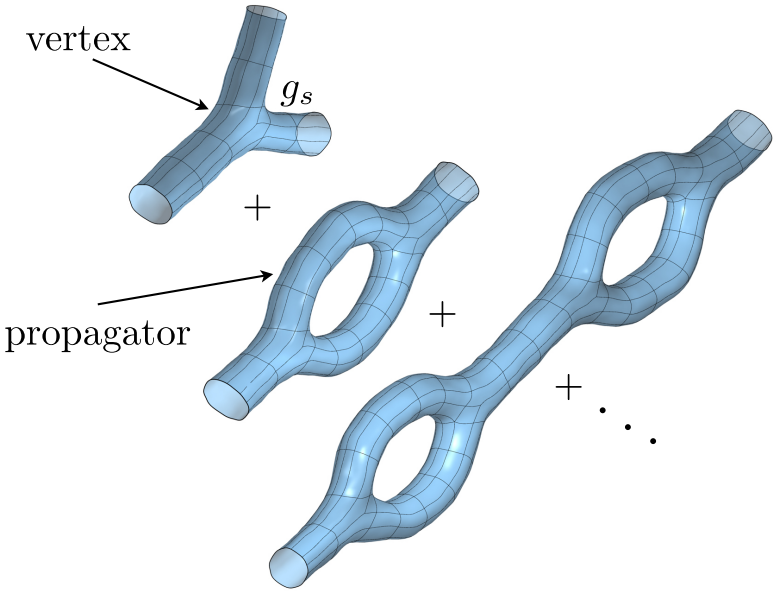

Figure 2.7: Perturbative string theory diagram for the interaction of three closed strings and its sum over topologies.

We also want to comment on perturbative string theory and point out a very important connection between the perturbative expansion of string theory and gauge theory in the 't Hooft limit. Strings interact with a coupling strength g_s which is the probability for a string to split into two strings or for two strings to join, see Figure 2.7. Remarkably string theory dynamically determines its own coupling strength. In perturbative string theory interactions are represented by diagrams similar to Feynman diagrams in field theory. The difference is that

instead of point particles interacting at vertices, strings sweep out two dimensional Riemann surfaces which are arranged according to their topology. Such surfaces are characterized by a topological invariant, called Euler number $\chi = 2 - 2g - b$, where g is the genus of a Riemann surface (=number of handles) and b is the number of boundaries. *E.g.* the Euler number of a sphere is $\chi = 2$ ($g = 0, b = 0$), of a disk is $\chi = 1$ ($g = 0, b = 1$) and of a torus is $\chi = 0$ ($g = 1, b = 0$). It turns out that string diagrams are weighted by a factor of $g_s^{-\chi}$. For $g_s \ll 1$ a sphere with $\chi = 2$ will dominate the expansion, followed by the torus. If we include open strings the sub-leading term will be from the disk. The vacuum to vacuum amplitude in closed string theory can be written as

$$\mathcal{A} = \sum_{g=0}^{\infty} g_s^{2g-2} F_g(\alpha'), \tag{2.35}$$

where $F_g(\alpha')$ is the contribution of two-dimensional surfaces with g holes. Identifying g_s with $1/N$ we see that string diagrams and Feynman diagrams (2.28) have the same form of the expansion, if the string tension is given as some function of the 't Hooft coupling λ. If we also want to make the connection to quark loops we have to include open strings, where boundaries of the worldsheet correspond to worldlines of the open strings. The first contribution to the vacuum amplitude (2.35) from open strings will be from the disk, scaling like $\mathcal{A} \sim g_s$. This is the same scaling behavior as we found for a single quark loop in the large N_c expansion.

This connection, due to 't Hooft, is one of the strongest motivations for believing that string theories and gauge theories are related and that this relation is more visible in the large N limit.

2.6 D-branes

D-branes were the essential ingredient in the discovery of the AdS/CFT correspondence and we will review their most important properties here. D-branes can be viewed from two perspectives:

- As a semiclassical solution of supergravity, which is the low energy limit of string theory.
- As hyperplanes in the full string theory where open strings can end.

We start with the supergravity description. In the low energy limit string theory admits classical solutions corresponding to extended black holes. Such solutions are called p-branes, where p stands for the number of spatial dimensions. The supergravity action is given by

$$S_p = \frac{1}{2\kappa_{10}} \int d^{10}x \sqrt{-g} \left[e^{-2\Phi} \left(R + 4(\nabla\Phi)^2 \right) - \frac{2}{2(p+2)!} F_{p+2}^2 \right], \tag{2.36}$$

where R is the Ricci scalar, Φ is the dilaton and $F_{p+2} = dC_{p+1}$ is the field strength of the (p+1)-form potential. For type IIB p is odd and for type IIA p is even. The C_{p+1} form potential is called Ramond-Ramond (R-R) form and is a fully antisymmetric (p+1)-index tensor. In superstring theory p-branes exhibit an important feature. They carry conserved charges, the RR-charges, which ensure the stability of the D-branes and act as a source for the R-R form fields. In Appendix B we write down the equations of motion and discuss their solutions in detail. In a nutshell, we start from the supergravity action and look for a black hole solution carrying electric charge with respect to the R-R form C_{p+1}. In order to find a solution to the equations of motion we assume that the metric is spherically symmetric in the transverse (10-p) directions with the R-R source at the origin. In addition we also impose the Dirac quantization condition on the R-R charge. There is a special solution, where the mass of the p-brane equals its charge, called extremal p-brane with the line-element given in (B.14). An

extremal p-brane is a BPS object (see B.13) and is the ground state of a p-brane. It turns out that extremal p-branes are D-branes.

From the full string theory perspective, Dirichlet branes, in short D-branes, are dynamical fundamental objects in superstring theory. By definition a Dp-brane is a p+1 dimensional hyperplane on which open strings must end. By the worldsheet duality [3] , this means that a D-brane is also a source for closed strings. Closed strings propagate in the bulk of spacetime, but sense the hyperplane through the usual open-closed interaction. This is a consistent string theory, provided p is even in the IIA theory or odd in the IIB theory. D-branes carry conserved charges, called Ramond-Ramond (R-R) charges [49], which ensure their stability. In particular they act as the fundamental source for a R-R (p+1)-form field. To specify a D-brane one needs as many conditions as there are spatial coordinates normal to the brane. A string that ends on a D-brane has Dirichlet boundary conditions in the directions normal to the brane and Neumann boundary conditions in the tangential directions. This means that the endpoints of a string can move freely along the world-volume of a D-brane. Since D-branes are dynamical objects we need to construct a world-volume action to describe their dynamics. The basic idea is that that the modes of the open string with its endpoints attached to the D-brane can be described by fields that are restricted to the world-volume of the brane. At low energies, low compared to the string scale, only the massless open string modes need to be considered and we can construct an effective action.

D-branes support scalar and gauge fields. To see this one has to quantize the open string in the presence of a D-brane, determine the open string states and investigate how they transform under Lorentz transformations. It turns out that a Dp-brane has a gauge field living on its world-volume and a massless scalar for each normal direction.

To see how the scalars arise, let us consider a drumhead, positioned in the x-y plane, that can fluctuate in the z direction. We would write down a "scalar field" $z(t, y, x)$ to describe these fluctuations. A D-brane is just like a drumhead.

Like a string, a D-brane is embedded in some background geometry with coordinates X^μ and metric $G_{\mu\nu}$. The map $X^\mu(\xi^\alpha)$, where $\xi^\alpha,\ \alpha = 0, 1, ..., p$ are the coordinates on the brane, specifies the embedding of the brane. p of these functions describe the fluctuations along the brane, while $9 - p$ describe fluctuations orthogonal to the brane which are fluctuations of scalar fields. The scalars parametrize the transverse position of the D-brane in the target space. In other words, D-branes have a tension and part of its action is the (p+1)-dimensional worldvolume, which it wants to minimize. This is the generalization of the Nambu-Goto action (2.32) to p+1 dimensions.

The gauge field arises in the following way. A string with both endpoints on a brane can minimize its length and shrink to a point giving massless degrees of freedom which is a U(1) gauge field living on the D-brane. For a U(1) field strength $F_{\mu\nu}$ the dynamics of the brane is given by the Dirac- Born-Infeld (DBI) action

$$S_{DBI} = -T_p \int d^{p+1}\xi e^{-\Phi} \sqrt{-\det(h_{\alpha\beta}) + 2\pi\alpha' F_{\alpha\beta}}, \tag{2.37}$$

where T_p is the D-brane tension, Φ is the dilaton and $h_{\alpha\beta}$ is the induced metric like in (2.31). The dilaton dependence arises because the DBI action is an open string tree level action. In terms of fundamental parameters the D-brane tension is given by [49]

$$T_p = \frac{\sqrt{\pi}}{\kappa_{10}(2\pi l_s)^{p-3}} = \frac{1}{(2\pi)^p g_s l_s^{p+1}}. \tag{2.38}$$

[3] An example of the worldsheet-duality is the equivalence of a closed string exchange between two D-branes and the vacuum loop of an open string with one end on each D-brane.

However, this is not the whole story. We still have to include the background fields, namely the antisymmetric NS-NS tensor $B_{\mu\nu}$ and the R-R (p+1) form C_{p+1}. The NS-NS tensor ensures gauge invariance of the DBI part. The R-R form couples to the brane through a Chern-Simons (CS) term. The whole action is known to leading order in g_s and is given by [39]

$$S_{D_p} = S_{DBI} + S_{CS} = T_p \int d^{p+1}\xi e^{-\Phi} \sqrt{-\det(h_{\alpha\beta}) + \mathcal{F}_{\alpha\beta}} + iT_p \int \left(C\, \mathrm{e}^{\mathcal{F}_{\alpha\beta}}\right)_{p+1}. \tag{2.39}$$

Here $\mathcal{F}_{\alpha\beta} = 2\pi\alpha' F_{\alpha\beta} + B_{\alpha\beta}$.

So far we have only considered a single brane. If we consider N parallel coincident D-branes the gauge symmetry is enhanced to a non-Abelian $U(N)$ gauge theory. Note that a $U(N)$ gauge theory can always be decomposed into a $U(1) \times SU(N)$, where the $U(1)$ part describes the center of mass motion of the stack of D-branes. When we are interested only in the motion relative to the stack we will ignore the overall $U(1)$ and refer to the gauge group of the worldvolume theory as $SU(N)$. The worldvolume theory for N coincident D-branes is the $SU(N)$ SYM theory with 16 supercharges. In order to find a precise relation between the string coupling g_s and the Yang-Mills coupling g_{YM} we expand the action (2.37) for small field strengths and its derivatives (small compared to the string coupling), and add a trace over the gauge indices. The action becomes

$$S_{DBI} = -T_p \int d^{p+1}\xi \sqrt{\det h_{\alpha\beta}}\, tr\left[1 + (2\pi\alpha')^2 F_{\alpha\beta}F^{\alpha\beta} + \mathcal{O}\left(\alpha'^4 F^4\right)\right]. \tag{2.40}$$

The first term is the worldvolume and the second term is the Lagrangian for $SU(N)$ Yang Mills theory $1/(4g_{YM}^2) trF^2$ if we identify

$$g_{YM}^2 = \frac{2}{(2\pi l_s^2)^2 T_p} = 2(2\pi l_s)^{p-4} l_s g_s, \tag{2.41}$$

where we used $\alpha' = l_s^2$ and (2.38). The additional factor of two comes from the normalization of the nonabelian generators,

$$F_{\alpha\beta} = F^a_{\alpha\beta} T^a\,, \qquad [T^a, T^b] = \frac{\delta^{ab}}{2}\,, \tag{2.42}$$

which we use throughout this work.

Now consider the case where we have two stacks of D-branes separated by some distance, with the number of branes for each stack given by N_1 and N_2. Then we will have strings with both endpoints attached to the same stack, giving each stack a gauge theory with gauge groups $U(N_1)$ and $U(N_2)$. In addition there are open strings stretching between the two stacks. The endpoints of the string will act as point charges, *i.e.*, as sources in the fundamental representation of $U(N_1)$ and $U(N_2)$. In this case the string cannot shrink to zero length and the point charges acquire a mass given by the length of the string times its tension. So in addition to the massless fields transforming in the adjoint representation we also have massive excitations transforming in the fundamental representation. These massive excitations are vector fields. This is the D-brane description of the Higgs mechanism.

2.7 The correspondence

Now we have all the necessary tools at hand to follow Maldacena's beautiful argument on how gauge theories are related to string theories. In Section 2.6 we have seen that D branes can be described in terms of open strings or closed strings. Now we will investigate both descriptions

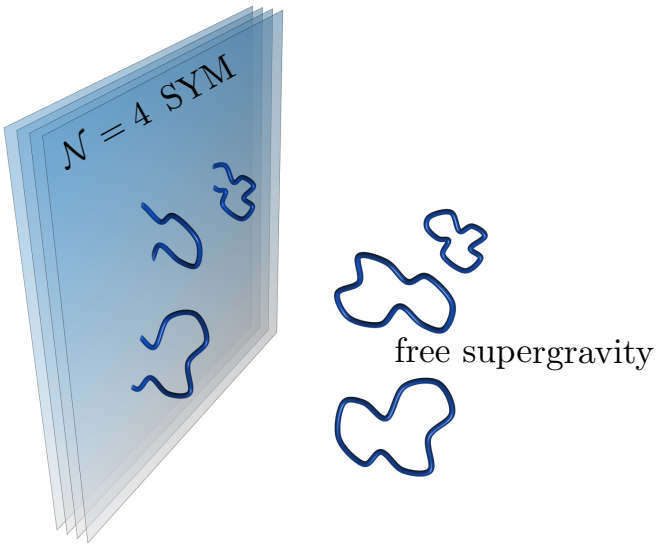

Figure 2.8: Open string description of D3-branes. In the low energy limit $\mathcal{N} = \triangle$ SYM living on the stack of D3-branes and closed strings living in ten-dimensional Minkowski space decouple.

for D3-branes in the low energy limit.

Let us start with type IIB string theory in flat, ten-dimensional Minkowski space and consider a stack of N parallel D3 branes. They are (3+1)-dimensional hyperplanes, embedded in the higher dimensional space, and are located at some point of the transverse six-dimensional space. The theory contains two kinds of excitations: open strings and closed strings. In the low energy description, at energies below the string scale $1/l_s$, the open degrees of freedom are described by $\mathcal{N} = 4$, U(N) super Yang Mills theory, whereas the low energy description of the closed string excitations is given by type IIB supergravity. Note that in the low energy regime only massless string states can be excited and we can write an effective Lagrangian describing their interaction schematically as

$$S = S_{bulk} + S_{brane} + S_{int}. \tag{2.43}$$

S_{bulk} is the ten dimensional supergravity action, S_{brane} is the action that describes open string states on the (3+1) dimensional brane worldvolume, and contains $\mathcal{N} = 4$ super-Yang-Mills theory. S_{int} describes the interaction between the open and closed strings.

We can expand the bulk part in powers of the gravitational constant κ by making an ansatz of the form $g_{\mu\nu} = \eta_{\mu\nu} + \kappa h_{\mu\nu}$. Schematically we have

$$S_{bulk} \sim \frac{1}{2\kappa^2} \int d^{10}x \sqrt{g} R + ... \sim \int d^{10}x \left[(\partial h)^2 + \kappa h (\partial h)^2 + ... \right], \tag{2.44}$$

where the dots indicate other bulk fields. Since all the interaction terms of the closed string modes come with positive powers of the gravitational constant κ, these interactions become weaker at low energies. Similarly, expanding the interaction term gives

$$S_{int} \sim \int d^4x \sqrt{g} \mathrm{Tr}[F^2] + ... \sim \kappa \int d^4x h_{\mu\nu} \mathrm{Tr} \left[F_{\mu\nu} - \delta_{\mu\nu} F^2 \right] + ... \tag{2.45}$$

To obtain the low energy limit we may take all energies to be small or equivalently keep the energy fixed and send the characteristic scale of the theory $l_s \to 0$, keeping all the dimensionless parameters fixed. In this limit the coupling $\kappa \sim g_s \alpha' \to 0$, and all interaction terms vanish

as well as the higher derivative terms in S_{brane} and S_{bulk}. So we are left with two decoupled theories: $\mathcal{N} = 4$ super-Yang-Mills theory living on the brane and free supergravity in the bulk as indicated in Figure 2.8.

Now let us consider the same system from a different point of view. D-branes are massive charged objects and act as a source for the supergravity fields. The extremal D3-brane solution of type IIB supergravity is given by (B.14)

$$\begin{aligned} ds^2 &= H^{-1/2}(u)\left(\eta_{\mu\nu}dx^\mu dx^\nu\right) + H^{1/2}(u)\left(du^2 + u^2 d\Omega_5^2\right), \\ H(u) &= 1 + \frac{L^4}{u^4}, \qquad L^4 = 4\pi g_s l_s^4 N\,. \end{aligned} \tag{2.46}$$

To understand this geometry better we will take two limits. Suppose we are far away from the stack of branes, $u^2 \gg L^2$. Then the harmonic function $H(u) \to 1$ and we are left with 10-dimensional Minkowski space. On the other hand, if we are close to the D3-branes, $u \ll L$, we can approximate $H(u) \sim L^4/u^4$ and the geometry becomes

$$ds^2 = \frac{u^2}{L^2}\left(\eta_{\mu\nu}dx^\mu dx^\nu\right) + \frac{L^2}{u^2}\left(du^2 + u^2 d\Omega_5^2\right), \tag{2.47}$$

which is the geometry of $AdS_5 \times S_5$ in Poincaré coordinates (2.18).

Roughly speaking the geometry is divided into three parts as shown in Figure 2.9. The asymptotic region, which is flat Minkowski space, the near horizon region which is $AdS_5 \times S_5$, and the interpolating region called the throat. The throat acts as a gravitational potential well. Since the metric component g_{tt} is not constant the energy measured at infinity will be

$$E_\infty = H^{-1/4} E_u, \tag{2.48}$$

due to the red shift. This means that the same object brought closer and closer to $u = 0$ would appear to have lower and lower energy for an observer at infinity.

Now we want to ask the following question: What low energy physics will we observe in the asymptotic flat region? From the point of view of an observer at infinity there are two types of low energy excitations. In the asymptotic region we can have massless large wavelength excitations, which is just free supergravity in flat space. Or we can have any kind of excitations that approach the near horizon region around $u = 0$, which will be highly redshifted and appear as low energy excitations for an observer at infinity. Therefore we have to take the full string theory in the near horizon region into account. In the low energy limit these two excitations decouple from each other. As we bring the excitations closer and closer to the horizon they find it harder and harder to escape to the asymptotic region due the gravitational potential well they have to climb. We end up with two sets of noninteracting modes. On the one hand we have free type IIB supergravity in the asymptotic region and on the other hand we have type IIB string theory on $AdS_5 \times S_5$ in the near horizon region.

We investigated the low energy description of D-branes from two perspectives. From the field theory point of view (open strings) and from the supergravity point of view (closed strings). In both descriptions we end up with two decoupled theories in the low energy limit. In both cases one of the decoupled system is free supergravity in flat space. Maldacena then conjectured that the two other theories have to be equivalent, namely $\mathcal{N} = 4$ *super Yang-Mills theory in 3+1 dimensions is the same as type IIB superstring theory on* $AdS_5 \times S_5$.

An important question is how to relate field theory parameters to string theory parameters and when do we have a reliable description of these theories? From the section about D-branes we

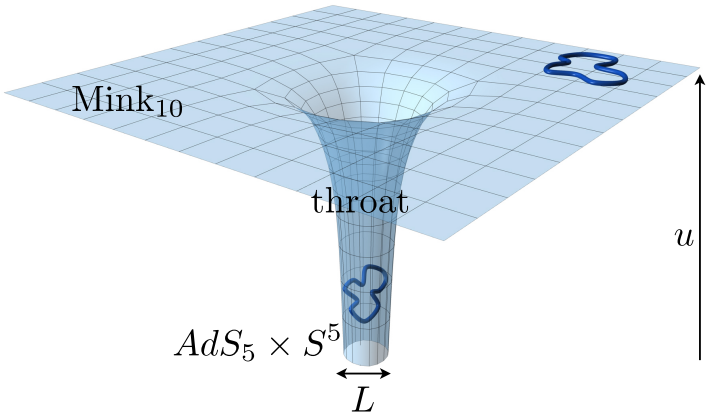

Figure 2.9: Closed string description of D-branes. In the low energy we have again two decoupled theories. On the one hand we have type II B string theory living on $AdS_5 \times S_5$ far down the throat. And on the other hand we have low energy closed strings on 10-dimensional Minkowski space in the asymptotic region.

know that the YM coupling is related to the string coupling via $g^2_{YM} = 4\pi g_s$ and the number of colors N of the gauge theory appears as as the four form flux in the string theory as

$$\frac{1}{2\kappa_{10}} \int F_5 = T_3 N. \tag{2.49}$$

The characteristic parameters, g_{YM} and N_c, of the gauge theory are all dimensionless. On the string theory side we have an additional dimensionful parameter, the string length l_s, which sets all the scales. Actually only the ratio of the radius of curvature L and the string length l_s is a parameter, since only relative scales are meaningful and thus l_s will disappear from any physical quantity we will compute. So let us check when we trust our solution (2.46) which was derived from classical supergravity, the low energy limit of string theory. On the one hand we have classical supergravity if the radius of curvature is bigger than the string length, $L^4/l_s^4 \gg 1$. On the other hand we understand string theory best in the perturbative regime, when $g_s \ll 1$. The relation between these parameters is (2.46)

$$\frac{L^4}{l_s^4} = 4\pi g_s N = g^2_{YM} N = \lambda, \tag{2.50}$$

telling us that in the perturbative regime, if N is finite, we would have $L^4/l_s^4 \ll 1$, exactly the opposite what we want to have. To satisfy both criteria at once we have to take $N \to \infty$ as we take $g_s \to 0$ in such a way that $4\pi g_s N$ remains finite and then take $L^4/l_s^4 \gg 1$.

On the field theory side this "double" limit corresponds to the 't Hooft limit: first let $g_{YM} \to 0$ and $N_c \to \infty$ with λ fixed and then take $\lambda \to \infty$. This shows us that when one side is weakly coupled the other side is strongly coupled and vice versa. We can now state the correspondence: *type IIB supergravity on $AdS_5 \times S_5$ is dual to $\mathcal{N} = 4$ SYM theory at large 't Hooft coupling.* This is the "weak" form of the correspondence. In its strongest form the statement of the conjecture is that the duality between type IIB string theory and $\mathcal{N} = 4$ SYM is valid in general for all values of N and λ. The strongest form can not be tested because we don't know how to quantize string theory on a curved background with R-R fields. The AdS/CFT correspondence has not been proven and remains a conjecture but has passed many nontrivial tests. Especially in its weakest form the correspondence is almost guaranteed to hold due to the large amount of symmetries. The simplest test is to check if the symmetries on both sides are the same. As we have seen in Section 2.3 the symmetry group of $\mathcal{N} = 4$

SYM is $SO(4,2) \times SO(6)$. On the gravity side we have an $SO(6)$ symmetry which rotates the S^5 and a $SO(2,4)$ symmetry which is the isometry group AdS_5. We see that the symmetries on both sides match. A more complicated test involves the matching of special correlation functions, which are related to anomalies and do not depend on the 't Hooft coupling λ [50, 51].

With the correspondence we now have a tool at hand where we can compute properties of a strongly coupled gauge theory by solving classical supergravity. However, so far we have not specified how the two theories can be matched to each other.

2.8 The heart of the correspondence

In the previous section we set up the AdS/CFT correspondence but so far we do not have a precise description how the two theories can be matched to each other. Now let us discuss how computations on the string theory side can be related to those one would like to do on the gauge theory side. This was first worked out in Refs. [52, 53] where it was shown that the two sides of the correspondence can be related via

$$Z_{string} = \exp\left[S_{Sugra}\left(\phi(\vec{x},z)|_{z=0} = z^{4-\Delta}\phi_0(\vec{x})\right)\right] + ... = \left\langle \exp^{\int d^4x \phi_0(\vec{x})\, \mathcal{O}(\vec{x})} \right\rangle_{CFT}, \quad (2.51)$$

where the dots indicate string corrections to the supergravity action. This formula says that the supergravity field $\phi(\vec{x})$ with a certain boundary behavior evaluated at the boundary acts as a source for a field theory operator $\mathcal{O}$ or in other words, for each field in the 5 dimensional bulk, we have a corresponding operator in the dual field theory.

Correlation functions on the gauge theory side now follow simply by computing repeated derivatives with respect to the sources

$$\frac{\delta^n Z_{string}}{\delta\phi_0(\vec{x}_1)...\delta\phi_0(\vec{x}_n)} = \langle T\mathcal{O}(\vec{x}_1)...\mathcal{O}(\vec{x}_n)\rangle\,. \quad (2.52)$$

Here we just want to state the most important points. In general the recipe for calculating correlation functions goes as follows. First, determine which field ϕ is dual to the operator $\mathcal{O}$. This can be very hard but usually the dimension and symmetries of the operator are enough to identify the dual field. For example, the graviton is associated with the stress tensor operator. Then solve the supergravity equations for the field ϕ and use this solution to calculate the on-shell action. Plugging this action into (2.51) and taking the variational derivatives with respect to the leading asymptotic value ϕ_0 leads to the correlation function. In Appendix A we show in detail how this is done for a massive scalar field in (d+1)-dimensional AdS space. Here we want to investigate the physics behind the asymptotic solution more closely.

The general classical solution for a massive scalar in AdS_{d+1} near the boundary, $z = 0$, behaves as

$$\phi(z,\vec{x}) = z^{4-\Delta}\left(\phi_0(\vec{x}) + O(z^2)\right) + z^{\Delta}\left(A(\vec{x}) + O(z^2)\right), \quad (2.53)$$

where Δ is one of the roots of

$$\Delta(\Delta - d) = m, \qquad \Delta_{\pm} = \frac{d}{2} \pm \sqrt{\frac{d^2}{4} + m^2}. \quad (2.54)$$

Here ϕ_0 is a prescribed source function and is called the non-normalizable mode and $A(\vec{x})$ describes a physical fluctuation as we will now show and is called the normalizable mode.

As in Appendix A.2 we begin with the usual case $\Delta = \Delta_+$. The form of $A(\vec{x})$ can be read off from the subleading term in (A.25) and is given by

$$A(\vec{x}) = \pi^{-\frac{d}{2}} \frac{\Gamma(\Delta)}{\Gamma\left(\Delta - \frac{d}{2}\right)} \int d^d\vec{x}' \frac{\phi_0(\vec{x}')}{|\vec{x} - \vec{x}'|^{2\Delta}}, \quad (2.55)$$

where Δ is the conformal dimension of the operator $\mathcal{O}$. Comparing (2.55) with the one point function in (A.28) it turns out that $A(\vec{x})$ is related to the expectation value of the operator $\mathcal{O}(\vec{x})$ [54]. The precise relation is

$$A(\vec{x}) = \frac{1}{2\Delta - d}\langle \mathcal{O}(\vec{x})\rangle. \tag{2.56}$$

From the point of view of the d-dimensional CFT, $(2\Delta - d)A(\vec{x})$ is the variable conjugate to $\phi_0(\vec{x})$. In other words, the prescribed boundary field $\phi_0(\vec{x})$ acts as a source for the expectation value of the operator $\mathcal{O}$ given by the subleading term in the expansion (2.53).

We considered the bigger of the two roots in (2.54) which certainly seems like the right choice for positive m^2 because then the ϕ_0 term in (2.53) dominates over the A term. However, Breitenlohner and Freedman showed [55] that in the mass range

$$-\frac{d^2}{4} < m^2 < -\frac{d^2}{4} + 1 \tag{2.57}$$

both roots of (2.54) can be chosen. This means that a single classical AdS supergravity action (A.18) can give rise to two different quantum field theories on AdS space, depending on the choice of boundary conditions. According to the AdS/CFT correspondence, the two theories correspond to two different conformal field theories on the boundary, one with an operator of conformal dimension Δ_- and one with an operator of conformal dimension Δ_+. In order to go to the Δ_- theory, it is clear from (2.53) that we have to interchange $\phi_0(\vec{x})$ and $(2\Delta - d)A(\vec{x})$. Therefore the two theories are not independent of each other, in fact they are related to each other by a canonical transformation that interchanges the roles of $\phi_0(\vec{x})$ and $A(\vec{x})$. We conclude that the generator of connected correlators of the Δ_- theory is obtained by Legendre transforming the generator of the of connected correlators of the Δ_+ theory.

2.9 Adding flavor

So far we only have a dual gravity theory for $\mathcal{N} = 4$ SYM theory with all the fields being massless and transforming in the adjoint representation. In QCD however only the gluons transform in the adjoint representation, but the quarks transform in the fundamental representation and are massive. To come closer to QCD we want to introduce additional fields that transform in the fundamental representation, *i.e.*, flavor fields. On the field theory side this can be achieved by adding, *e.g.*, a $\mathcal{N} = 2$ hypermultiplet. On the gravity side one needs to add more degrees of freedom by adding additional D-branes to the system [30]. In this section we will explain the holographic setup in order to introduce fundamental degrees of freedom.

Let us start with a stack of N_c D3-branes. We know that the open string description leads to a $SU(N_c)$ gauge theory with all fields transforming in the adjoint representation and being massless. In order to introduce fields in the fundamental representation, *e.g.*, flavor fields, we need to add the open string sector. This can be done by placing a new type of N_f coincident D-branes (where N_f is the number of the new D-branes) to the D3 system . These new branes are called flavor branes. Strings between the D3's and the new branes have only one end on the stack of D3-branes and hence generate matter in the fundamental representation.

If the new D-branes can be separated from the D3-branes in some direction transverse to both branes then the fundamental fields acquire a mass. Strings with both endpoints on the flavor branes are in the adjoint of the $U(N_f)$ flavor symmetry of the quarks and hence describe mesonic degrees of freedom. In string theory this states describe fluctuations of the brane in the background geometry.

So what kind of branes should we add? The system has to be stable and therefore some supersymmetry should be preserved. The amount of supersymmetries preserved by a D-brane in some background are those generated by Killing spinors that satisfy the κ-symmetry condition [56],

$$\Gamma\epsilon = \epsilon \tag{2.58}$$

where ϵ is a Killing spinor of the background and Γ's are curved space Γ matrices. First one has to write down the Killing spinors for a given background and then find out how many of them satisfy (2.58). A D-brane preserves as many supersymmetries as there are solutions to (2.58). We will comment more on supersymmetry in Section 3.3.

The analysis of intersecting D-branes shows that half of the supersymmetries will be preserved if we have four or eight directions in which one stack is extending and the other is not [39]. In addition we require that the new branes share all the coordinates of the D3-branes so that the endpoint of the string can propagate in all directions of the worldvolume of the D3-brane. The only possible choice left is to add N_f D7-branes to the system in the following way

	X_0	X_1	X_2	X_3	X_4	X_5	X_6	X_7	X_8	X_9
D3	x	x	x	x						
D7	x	x	x	x	x	x	x	x		

(2.59)

Here an x denotes the directions in which the branes are extending. We see that the D7-branes share all of the D3-brane's directions and also extend in four more directions orthogonal to the D3-branes. The X_8, X_9 directions are orthogonal to both stacks of D-branes. If we separate the D7-branes from the D3-branes in the X_8, X_9 directions by some distance d the field in the fundamental representation will acquire a mass $m_q = d/(2\pi\alpha')$.

To summarize, we have constructed a system where the 3-3 strings correspond to fields transforming in the adjoint representation of $SU(N_c)$. The endpoints of the 3-7 strings on the D3-branes behave as point charges in the fundamental representation of $SU(N_c)$ and the 7-7 strings describe mesonic degrees of freedom transforming in the adjoint representation of $SU(N_f)$.

Adding D7-branes breaks the $SO(6)$ to $SO(4) \times SO(2)$, where the SO(4) rotates in the X_4, X_5, X_5, X_7, while the $SO(2)$ group acts on X_8, X_9. When the D7-branes are separated from the D3-branes in the X_8, X_9 directions the $SO(2)$ will be broken. These symmetries are also realized in the dual field theory.

The field theory dual corresponding to this brane set-up is the usual $\mathcal{N} = 4$ Super Yang-Mills theory coupled to N_f $\mathcal{N} = 2$ hypermultiplets transforming in the fundamental representation of the gauge group. The hypermultiplet consists of two complex scalars Φ_i and two Weyl fermions Ψ_i of opposite chirality. In analogy with QCD we refer to the hypermultiplet fermions as quarks. The Lagrangian is that of $\mathcal{N} = 4$ SYM (2.23) plus terms that account for the hypermultiplet fields. Very schematically the Lagrangian looks as follows

$$\begin{aligned} \mathcal{L}_{\mathcal{N}=2} &= \mathcal{L}_{\mathcal{N}=4} + \Psi^\dagger(D^2 + M^2)\Psi + \bar{\Psi}(\not{D} + M)\Psi + g\left(\bar{\Psi}\lambda\Phi + \bar{\Psi}\phi\Psi + M\Phi^\dagger\phi\Phi\right) \\ &+ g^2\Phi^\dagger\phi\phi\Phi \ . \end{aligned} \tag{2.60}$$

The breaking of the $SO(6)$ on the gravity side is realized as a breaking of the R-symmetry on the field theory side to $SO(4)_R \times SO(2)_R$. The global $SO(4)_R \sim SU(2)_\Phi \times SU(2)_R$ consists of the $\mathcal{N} = 2$ R-symmetry and the $SU(2)_\Phi$ that rotates the scalars in the adjoint hypermultiplet as a doublet.

The $SO(2)_R \sim U(1)_R$ symmetry acts as a chiral symmetry and is similar to the axial symmetry in QCD. The $U(1)_R$ is explicitly broken by a quark mass, like in QCD where a finite quark mass breaks the axial symmetry. However, in the D3-D7 system one cannot introduce chiral quarks. In Section (4) we will introduce the Sakai-Sugimoto model which is also capable of describing definite chirality of fields in the fundamental representation.

We know that D-branes are massive charged objects and therefore curve space-time. If we add new branes to the system they will have an effect on the structure of space-time. However, if we take $N_f \ll N_c$ we can neglect the backreaction of the flavor branes on the geometry. This is know as the probe brane approximation. This means that we can place a D7-brane into the geometry produced by the D3-branes without deforming it. The dynamics of the probe D7-branes is governed by the DBI action (2.37). For N_f D7-branes the action is just N_f copies of the action of a single D7-brane. In field theory quantities the action scales like $N_f N_c \lambda$. This is a factor of N_c smaller compared to the supergravity action, justifying our neglect of the backreaction on the geometry.

Now we want to show how to find the embedding of a single static D7-brane (vanishing $F_{\mu\nu}$) in a sample calculation. Let us write the $AdS_5 \times S_5$ metric in the following form

$$ds^2 = \frac{u^2}{L^2}\eta_{ij}dx^i dx^j + \frac{L^2}{u^2}(d\rho^2 + \rho^2 d\Omega_3^2 + dy_5^2 + dy_6^2), \tag{2.61}$$

with $\rho^2 = y_1^2 + ... + y_4^2$, $u^2 = \rho^2 + y_5^2 + y_6^2$. The D7-brane can fluctuate in the directions orthogonal to its worldvolume, y_5, y_6. For simplicity we set $y_6 = 0$. We work in a gauge where y_5 depends on the worldsheet coordinate ρ. Then the action for a static D7-brane is given by

$$S_{D_7} = T_7 \int d^8\xi \sqrt{1 + y_5'^2}, \tag{2.62}$$

where $y_5' = \partial_\rho y_5$. The ground state configuration of the D7-brane corresponds to a solution to the equation of motion

$$\partial_\rho \left(\frac{\rho^3\ y_5'}{\sqrt{1 + y_5'}} \right) = 0. \tag{2.63}$$

Clearly, $y_5'(\rho) = 0$ is a solution, so a constant $y_5(\rho)$ is a solution. The embedding of the D7-brane is given by $y(\rho) = d$, for any constant d. This means that we can choose the position of the brane by hand, and therefore we can also choose the mass of the hypermultiplet, since $m = \frac{d}{2\pi\alpha'}$. In general, the asymptotic solution ($\rho \to \infty$) to the equation of motion has the form

$$y_5(\rho) = d + \frac{c}{\rho^2} + ..., \tag{2.64}$$

where d is related to the quark mass as discussed above and c describes the degree of bending of the D7-brane. From the holographic dictionary we know that the leading term in the above expansion acts as a source for an operator in the subleading term. The parameter c must correspond to an operator with mass dimension three since ρ carries energy dimension. We conclude that c corresponds to the quark condensate $\langle \bar{\psi}\psi \rangle \propto c$. In the case of a static D7-brane with no gauge field turned on, solutions with non-zero values of c are not regular in AdS space and these solutions are excluded. However, when a magnetic field is included a condensate can form, even for zero quark masses [57]. This effect is known as *magnetic catalysis*.

A few comments about conformal symmetry are in order. The induced metric on the D7-brane is

$$ds^2 = \frac{\rho^2 + d^2}{L^2}\eta_{ij}dx^i dx^j + \frac{L^2}{\rho^2 + d^2} + \frac{L^2\rho^2}{\rho^2 + d^2}d\Omega_3^2\,. \tag{2.65}$$

If we set $d = 0$ we see that the induced metric is exactly $AdS_5 \times S_3$. The AdS_5 factor suggests that theory should still be conformally invariant. Indeed, in the probe limit with vanishing quark masses the theory is classically conformal. This is also true quantum mechanically. The β-function for the 't Hooft coupling is is proportional to the ratio N_f/N_c between the number of D7-and D3-branes, which goes to zero in the probe limit [30]. Now, if we separate the D7-branes from the D3-branes the above metric becomes $AdS_5 \times S_3$ only asymptotically ($\rho \gg d$). This reflects the fact that conformal symmetry is explicitly broken by the mass of the hypermultiplet, but is restored at energies $E \gg m_q$.

With the possibility of including fields in the fundamental representation, quarks, it is possible to study systems that are closer to QCD. This is what we will do in the rest of this work. We will study the properties of strongly coupled systems in the presence of fundamental fields in two different models.

Chapter 3

Heavy-light mesons

In the last section we have shown how fundamental fields can be included in the framework of the AdS/CFT correspondence. In the following we will investigate various strongly coupled systems with fundamental matter and explore their properties. In this chapter we use the correspondence to compute the energy spectrum of heavy-light mesons. We start with $\mathcal{N} = 2$ super Yang-Mills theory with two massive hypermultiplets. In the heavy quark limit, similar to QCD, we find that the excitation energies are independent of the heavy quark mass. We also find some degeneracies in the spectrum which can be attributed to the presence of supersymmetry, protecting the masses of mesons inside supermultiplets. Then we inspect the mass spectrum of heavy-light mesons in deformed $\mathcal{N} = 2$ super Yang-Mills theory and demonstrate how some of the degeneracies of the supersymmetric mesons can be removed upon breaking supersymmetry.

This chapter is organized as follows. We begin with an introduction and motivate our work. In Section 3.3 we review the dual supergravity construction of $\mathcal{N} = 2$ SYM theory with two massive fundamental hypermultiplets, and in addition we make some remarks about related constructions with less supersymmetry. Section 3.4 fixes our notation and sets up the supergravity calculation of the heavy-light meson spectrum. In Section 3.5, we analyze small fluctuations of the string dual to the heavy-light meson. Section 3.6 follows with a discussion of spinning strings dual to heavy-light mesons with large charge and angular momentum. In Section 3.7 we break supersymmetry by two different mechanisms, one leading to the emergence of hyperfine splitting and the other to the Zeemann effect. This chapter is based on [31, 32].

3.1 Heavy quark effective theory

The heavy quark limit of QCD has been an important tool in understanding the spectrum and decays of mesons and baryons with a heavy quark constituent; see Ref. [58] for a review. When the mass of the heavy quark is large compared to the QCD scale, $m_h \gg \Lambda_{\rm QCD}$, the interaction between the heavy quark and the light quarks and gluons becomes independent of the spin and flavor of the heavy quark. This independence yields predictions for the m_h dependence of the meson spectrum and weak decay amplitudes.

One reason why heavy quarks are easier to understand in QCD than light quarks is asymptotic freedom; at short distance scales and high energies, the strong force becomes weak. Roughly speaking, for energies sufficiently above $\Lambda_{\rm QCD}$, the coupling constant α_s becomes small, and thus the interactions of the heavy quarks, charm, bottom and top, are governed by a weak effective coupling $\alpha_s(m_h)$. The light quarks, up, down, and strange, on the other hand experience a much stronger coupling $\alpha_s(\Lambda)$, with Λ only slightly above $\Lambda_{\rm QCD}$, where the coupling diverges. Indeed, the strong force between two heavy quarks is weak enough to be treated perturbatively, and is similar to the force between an electron and a positron.

Heavy-heavy mesons, which are bound states of two heavy quarks, therefore have measured properties very similar to positronium.[1]

Heavy-light mesons, in contrast, are more complicated objects, as their light quark constituent experiences strong interactions. Qualitatively, the heavy quark is a small object of size $1/m_h$ surrounded by the"brown muck", of size $1/\Lambda_{\rm QCD}$, of virtual strongly interacting light quarks, antiquarks, and gluons. However, the small size of the heavy quark leads to simplifications. The "brown muck" cannot resolve the spin or flavor of the heavy quark to leading order in $1/m_h$, which means the interaction is spin and flavor blind. The light degrees of freedom only experience its color field, which extends over large distances due to confinement. Suppose we have a hadron with one single heavy quark $Q(v,s)$ with spin s and velocity v surrounded by the light degrees of freedom. If we replace the quark by another heavy quark $Q'(v,s')$ with different flavor or spin but with the same velocity the configuration of the light degrees of freedom does not change. Both heavy quarks lead to the same static color field. This is the heavy quark symmetry. The heavy quark symmetry is an approximate symmetry and corrections arise since the quark masses are not infinite. This symmetry is similar to the isotopic symmetry in atomic physics, where different isotopes (same number of protons but different number if neutrons) of an atom have the same chemical properties to a very good approximation.
Heavy Quark Effective theory predicts a heavy-light spectrum of the parametric form

$$M_{hl} = m_h + \Lambda_{\rm QCD} + \frac{\Lambda_{\rm QCD}^2}{m_h} + \mathcal{O}\left(\frac{\Lambda_{\rm QCD}^3}{m_h^2}\right). \tag{3.1}$$

The second term in the above equation originates from the light quark quantum numbers and is called *fine structure*. The third term, called *hyperfine structure*, is due to the coupling of the heavy quark spin to the light degrees of freedom. In the heavy quark limit $m_h \to \infty$ there are degenerate states of mesons. For example, there is a degenerate doublet of S-wave mesons. At large but finite quark mass this doublet is not exactly degenerate. *Hyperfine splitting* proportional to Λ^2/m_h appears.

Equation (3.1) and the effect of hyperfine splitting are our main motivations to study heavy-light mesons from holography. Concretely we are interested if holography can reproduce predictions from HQET and/or give new predictions.

3.2 Holographic heavy-light mesons

We investigate the heavy quark limit not in QCD but in a cousin of $\mathcal{N} = 4$ SU(N) super Yang-Mills (SYM) theory. We add two fundamental hypermultiplets, with masses m_l and m_h, to $\mathcal{N} = 4$ SYM, breaking the supersymmetry to $\mathcal{N} = 2$. Using the AdS/CFT correspondence [59, 52, 53], we study the spectrum of heavy-light mesons in this theory at large N and large 't Hooft coupling $\lambda = g_{\rm YM}^2 N$.

We want to know, what parallels exist between heavy-light mesons in real world QCD and in strongly coupled $\mathcal{N} = 2$ SU(N) SYM theory with two massive hypermultiplets. The parent theory $\mathcal{N} = 4$ SU(N) SYM is clearly very different from QCD. Most importantly for our comparison, $\mathcal{N} = 4$ SYM is conformal, and we thus have no equivalent notion of the coupling constant being m_h dependent. We also have no notion of a confinement or QCD scale $\Lambda_{\rm QCD}$; for us the IR scale will be m_l. It is true that adding $N_f = 2$ hypermultiplets to $\mathcal{N} = 4$ SYM breaks the conformal symmetry (see Section 4.1.2), but the nonzero beta function in fact runs

[1] Note however that highly excited charmonium and bottomonium states are expected to be sensitive to the details of confinement. For these excited states, the quarks are separated by relatively large distances and experience a linear confining potential rather than a Coulombic potential. To reproduce the full spectrum, the Cornell potential, which interpolates between these two limiting forms, is often used.

in the wrong direction, toward strong coupling in the UV. We will, however, work in the limit $N_f \ll N$, and therefore ignore N_f/N suppressed effects.

Despite these differences, there is persistent hope that we may gain insights into QCD by asking the right questions about $\mathcal{N} = 4$ SYM and its relatives at strong coupling. For example, at zero temperature, the Klebanov-Strassler model [60] provides a geometric understanding of abelian chiral symmetry breaking and confinement for a $\mathcal{N} = 1$ supersymmetric gauge theory in this AdS/CFT context. Regarding nonzero temperature physics, where the arguments are perhaps more compelling, Refs. [61, 62] made the following two observations. First, consider the ratio of the pressure at strong and weak coupling. The ratio for $\mathcal{N} = 4$ SYM was computed by Ref. [63] to be 3/4. QCD is not conformal, but lattice simulations can be used to compute the pressure at a few times the deconfinement temperature where the theory is relatively strongly interacting and the pressure slowly varying. The ratio of this pressure to the free result is about 0.8. The second observation is that at strong coupling, both $\mathcal{N} = 4$ SYM and QCD are believed to have very small viscosities (see *e.g.* Refs. [64, 65])

The AdS/CFT correspondence maps $\mathcal{N} = 4$ SU(N) SYM theory to type IIB string theory in the curved background $AdS_5 \times S^5$. We will work in the large N and λ limit, where the string theory becomes classical and can be well approximated by supergravity. As described by Ref. [30], a hypermultiplet can be added to the gauge theory by placing a D7-brane in the dual geometry. The heavy-light mesons we consider then, according to the duality, correspond to strings stretching between two parallel D7-branes, and the energy spectrum consists of the vibrational and rotational modes of the strings. Consistent with our large N limit, we will neglect the back reaction of the D-branes on the geometry, as well as the back reaction of the strings on the D-branes and the geometry.

Despite the conformal nature of the theory we consider, we find that the meson spectrum is, in an appropriate sense, spin and flavor blind in the heavy quark and strong coupling limit. The mass M_{hl} of the heavy-light mesons we find has the form

$$M_{hl} = m_h + m_l \, f_1\left(\frac{J}{\sqrt{\lambda}}, \frac{Q}{\sqrt{\lambda}}, \frac{n}{\sqrt{\lambda}}\right) + \mathcal{O}\left(\frac{m_l^2}{m_h}\right) \ , \tag{3.2}$$

where J is the angular momentum of the meson, Q an R-charge, and n a quantum number specifying a radial excitation.[2] We have not introduced a confinement scale and thus m_l takes the place of $\Lambda_{\rm QCD}$.

One important aspect of this heavy-light meson spectrum is its m_h independence, which can be understood in the following way. The excitations (at least in n and J) we find are closely analogous to the modes of a guitar string, the length of which is proportional to $1/m_l - 1/m_h$. In the heavy quark limit, the length of the string becomes independent of $1/m_h$, and hence it is expected that also the frequencies of the modes become $1/m_h$ independent.

The fluctuation analysis also shows a degeneracy in the spectrum. For example, we find that a scalar meson and a vector meson have the same energy. By breaking supersymmetry this degeneracy gets lifted and hyperfine structure appears.

Let us also comment on the existing literature. After the appearance of Ref. [30], there have been many detailed studies of the meson spectrum of the $\mathcal{N} = 2$ SU(N) SYM theory beginning with Refs. [66, 67]. In fact, a nice review [68] has appeared to which we point the interested reader for a more complete list of references. To understand what is new about our work, it is useful to outline the differences of our work from Ref. [67], where the authors considered the meson spectrum for $\mathcal{N} = 2$ SYM theory with a single massive hypermultiplet of

[2]Recall that $\mathcal{N} = 2$ supersymmetric gauge theories have a global R-symmetry. Geometrically, Q is an angular momentum in the internal S^5.

mass m. They considered two different types of mesons. The first type have a very small mass $M \sim m/\sqrt{\lambda}$ and spin 0, 1/2, or 1, and are dual to fluctuations of the D7-brane embedding. The second type are dual to U-shaped semiclassical strings with much larger angular momentum J and mass. For $J \ll \sqrt{\lambda}$, the mass obeys Regge scaling $M \sim m\sqrt{J}/\lambda^{1/4}$ while for $J \gg \sqrt{\lambda}$, the potential is Coulombic $M = 2m - \text{const}/J^2$. While the behavior of these types of mesons are qualitatively diffferent, there is expected to be a way in which as we consider mesons with larger and larger angular momentum, the D7-brane fluctuations in fact morph into semiclassical string configurations.

The ground state of our heavy-light meson is a string, which stretches between two D7-branes separated by a finite distance proportional to the mass difference between the hypermultiplets. Having taken the heavy-quark limit, there is no sense in which our meson spectrum is well approximated by D7-brane fluctuations. To find the spectrum, we therefore instead consider fluctuations of the string itself, which will correspond to radial excitations of the meson. We also consider the dependence of the string energy on its angular momentum J and charge Q, and this part of the analysis is similar to the second half of Ref. [67] and Section 2 of [69].

The types of heavy-light mesons we consider have been studied before, in Refs. [70, 71, 69]. Ref. [69], is very similar in spirit to ours. Indeed, Section 2 of Ref. [69] overlaps to some extent with our discussion of the spinning strings in Section 3.6.1. In Refs. [70, 71], it was pointed out that the ground state heavy-light mesons have a mass which scales as the difference of the heavy quark masses, $M = m_h - m_l$. This scaling is very different from the D7-brane fluctuations considered in Ref. [67], which yielded masses $M \sim m/\sqrt{\lambda}$ for the heavy-heavy and light-light mesons. Ref. [70] also demonstrated that the excitation energies above the ground state are suppressed by a power of λ. This work should in principle be very similar to what we do here, as the authors of Ref. [70] also study the fluctuation spectrum of a semiclassical string stretching between two D7-branes in the $AdS_5 \times S^5$ geometry. However, they work in an approximation where the strings do not bend and find that the excitation energies for heavy-light mesons scale with m_h instead of m_l. Ref. [71] in contrast is a calculation in a different limit: They consider the case where the masses of the two hypermultiplets become degenerate and thus non-abelian effects on the D7-branes are important.

3.3 Holographic setup and supersymmetry considerations

We know that type IIB strings in an $AdS_5 \times S^5$ space-time are dual to $\mathcal{N} = 4$ SU(N) super Yang-Mills theory through the AdS/CFT correspondence. The space $AdS_5 \times S^5$ has the line element

$$ds^2 = L^2 \left[u^2 \eta_{\mu\nu} dx^\mu dx^\nu + \frac{\delta_{ij} dy^i dy^j}{u^2} \right] , \tag{3.3}$$

where the indices i and j run from one to six, μ and ν run from zero to three, and L is the radius of curvature. The coordinate $u^2 \equiv \sum_i (y^i)^2$ is a radial coordinate, and as $u \to \infty$, we reach the boundary of AdS_5. In this notation, the metric is clearly a warped product of Minkowski space $\mathbb{R}^{1,3}$ with $\mathbb{R}^6$. The line element can also be written to make the AdS_5 more explicit:

$$ds^2 = \frac{L^2}{z^2}(\eta_{\mu\nu} dx^\mu dx^\nu + dz^2) + L^2 d\Omega^2 , \tag{3.4}$$

where $d\Omega^2$ is a line element on the S^5 and $u = 1/z$. The SO(6) isometry group of the S^5 geometrically realizes the SO(6) R-symmetry of the dual field theory.

As described by Karch and Katz [30], adding an $\mathcal{N} = 2$ hypermultiplet to the gauge theory is dual to placing a D7-brane in the dual geometry. The D7-brane spans the Minkowski directions x^μ and four of the remaining directions in $\mathbb{R}^6$. With this ansatz, the D7-brane is

insensitive to the RR-five form flux in the curved geometry, and its behavior is determined solely through the DBI action

$$S_{DBI} = -T_7 \int d^8\xi \sqrt{-\det(G_{ab} + 2\pi\alpha' \mathcal{F}_{ab})} \ , \tag{3.5}$$

where $T_7 = 1/(2\pi)^7 \alpha'^4 g_s$ is the D7-brane tension, $1/2\pi\alpha'$ is the string tension, g_s is the string coupling constant, G_{ab} is the induced metric on the D7-brane, and $\mathcal{F}_{ab}$ is the gauge field on the D7-brane. We will consider only the case $\mathcal{F}_{ab} = 0$ in these remarks. Recall that the AdS/CFT dictionary relates

$$\frac{L^2}{\alpha'} = \sqrt{\lambda} \quad \text{and} \quad 4\pi g_s = g_{\rm YM}^2 \ , \tag{3.6}$$

where $\lambda = g_{\rm YM}^2 N$ is the 't Hooft coupling.

To correspond to a hypermultiplet, the D7-brane must span $\mathbb{R}^{1,3}$, and thus the four remaining dimensions of the D7-brane lie in $\mathbb{R}^6$. It seems natural to choose a gauge in which four of the coordinates on the D7-brane are the x^μ. Moreover we pick an embedding in $\mathbb{R}^6$ that does not depend on the x^μ. Given this independence, the determinant of the induced metric on the D7-brane will not depend on the warp factor u^2 in the ten dimensional metric (3.3). Dividing out by the volume of Minkowski space, the DBI action can be written in the form

$$S_{DBI} = -T_7 L^8 \int d^4\xi \sqrt{\det\left(\frac{\partial \vec{y}}{\partial \xi^a} \cdot \frac{\partial \vec{y}}{\partial \xi^b}\right)} \ . \tag{3.7}$$

The D7-brane will satisfy the same equations of motion that it does in flat space; the D7-brane describes a minimal four dimensional hypersurface in $\mathbb{R}^6$. Note that the normalization of the DBI action can be written in gauge theory language as

$$T_7 L^8 = \frac{2\lambda N}{(2\pi)^6} \ .$$

The DBI action is smaller by a factor of N compared to the supergravity action, justifying our neglect of the back reaction of the D7-brane on the geometry.

A particularly simple class of hypersurfaces which satisfy the equations of motion are surfaces described by a holomorphic embedding equation. If we think of $\mathbb{R}^6 = \mathbb{C}^3$ as a complex manifold and define coordinates $w^j = y^{2j-1} + iy^{2j}$, a D7-brane which satisfies an equation of the form $f(w^1, w^2, w^3) = 0$ for an arbitrary function f will locally satisfy the equations of motion away from singularities.

The Karch-Katz D7-brane is a hyperplane described by two linear equations $\vec{a}_1 \cdot \vec{y} = c_1$ and $\vec{a}_2 \cdot \vec{y} = c_2$. Given the SO(6) rotational symmetry of the sphere, such a hyperplane can be rotated so that the two equations become $y^5 = c$ and $y^6 = 0$.[3] In complex coordinates, the hyperplane is the complex submanifold described by $f = w^3 - c$. The parameter c is dual to the mass of the hypermultiplet.

The Karch-Katz D7-brane preserves $\mathcal{N} = 2$ supersymmetry, while the more general case $f(w^1, w^2, w^3) = 0$ preserves only $\mathcal{N} = 1$ supersymmetry (see *e.g.* Ref. [72]). In brief, there are 32 real spinors generating supersymmetry transformations that leave invariant the $AdS_5 \times S^5$ type IIB supergravity background, 16 of which correspond to ordinary supercharges and the remainder of which are superconformal. This number of supercharges is sufficient to generate the $\mathcal{N} = 4$ superconformal algebra of the dual Yang-Mills field theory. Of these 32 spinors, only four of the ordinary and none of the superconformal generate supersymmetry transformations

[3] Use the SO(6) symmetry to rotate $\vec{a}_1$ into the y^5 direction and $\vec{a}_2$ into the y^5–y^6 plane. The problem reduces to considering the intersection of two lines in a plane. There is a residual $SO(2)$ symmetry in the y^5–y^6 plane which always allows us to rotate the intersection point onto the y^5 axis.

which leave a general D7-brane satisfying $f(w^1, w^2, w^3) = 0$ invariant. The four invariant spinors are independent of the choice of $f(w^1, w^2, w^3)$. The Karch-Katz D7-brane, on the other hand, is left invariant by 8 of the ordinary spinors.

Given that a single Karch-Katz D7-brane corresponds to adding a single $\mathcal{N} = 2$ hypermultiplet, adding two such D7-branes should correspond to adding two hypermultiplets. In the literature [70, 71, 73], we find that the second D7-brane is usually added in a way such that the embedding equation for the second D7-brane is parallel to the first, $w^3 = c'$ where $c' \in \mathbb{R}$. Adding the second D7-brane in such a way has a number of desirable features. The theory remains $\mathcal{N} = 2$ supersymmetric. Moreover, an unbroken $\mathrm{SO}(4) \subset \mathrm{SO}(6)$ of the global R-symmetry is preserved. Note that $c' \in \mathbb{C}$ still preserves $\mathcal{N} = 2$ supersymmetry and the $\mathrm{SO}(4)$ R-symmetry. The relative phase of c and c' affects the relative phase of the hypermultiplet masses and also the mass of the heavy-light meson, a fact we will return to in the discussion.

However, a generic second D7-brane would not be parallel to the first. Assuming the second D7-brane is also described by a four dimensional hyperplane inside $\mathbb{R}^6$, the two D7-branes will generically intersect along a plane $\mathbb{R}^2$. Such an intersection generically breaks all the supersymmetry. If supersymmetry is broken, then there will probably be a tachyon, *i.e.* an instability, and the D7-branes will recombine; it's not clear what the final state will be, and we have little to say about this nonsupersymmetric situation.

While the remaining $\mathrm{SO}(4)$ symmetry is not enough to guarantee the second Karch-Katz D7-brane can be described by a complex equation as well, there will be a special case where both D7-brane embeddings are described by complex equations in $\mathbb{C}^3$. This special case preserves $\mathcal{N} = 1$ supersymmetry. Indeed, if we add any number of Karch-Katz D7-branes such that they are all described by complex equations in $\mathbb{C}^3$, $\mathcal{N} = 1$ supersymmetry is preserved. The reason is that the four spinors preserved by both the supergravity background and the D7-brane are independent of the choice of $f(w^1, w^2, w^3)$. These intersecting brane configurations should lead to a heavy-light meson spectrum similar to the heavy-heavy and light-light meson spectra found in Ref. [67]. There will be short strings localized at the intersection of the two D-branes whose masses should scale as the distance of the intersection from the origin of the geometry divided by $\sqrt{\lambda}$. These intersecting configurations also provide a novel way of thinking about meson decay, which is different from what has been considered in the literature before [74, 75]. The case of three intersecting Karch-Katz D7-branes would be especially interesting to consider because the intersection of three four dimensional hyperplanes in $\mathbb{R}^6$ is in general a point. We, however, leave a study of such spectra and decays for the future.

Finally, we make a short remark on the field theory aspects of the system we are studying. We know that $\mathcal{N} = 4$ $\mathrm{SU}(N)$ SYM has the superpotential

$$W = \mathrm{Tr}\, X[Y, Z] \tag{3.8}$$

where X, Y, and Z are chiral superfields transforming in the adjoint of $\mathrm{SU}(N)$. The Karch-Katz D7-brane leads to the modified superpotential

$$W = \mathrm{Tr}\, X[Y, Z] + \tilde{Q}(m - X)Q \ , \tag{3.9}$$

where Q and $\tilde{Q}$ are chiral superfields that transform in the fundamental of $\mathrm{SU}(N)$ and combine to form a hypermultiplet.[4] The $\mathcal{N} = 2$ supersymmetry preserving case of two parallel D7-branes has the superpotential

$$W = \mathrm{Tr}\, X[Y, Z] + \tilde{Q}_h(m_h - X)Q_h + \tilde{Q}_l(m_l - X)Q_l \ . \tag{3.10}$$

When m_h and m_l are both real, we chose above both c and $c' \in \mathbb{R}$. However, we may introduce a relative phase between m_h and m_l as well corresponding to $c' \in \mathbb{C}$. Adding the D7-branes

[4] We have been careless of the relative normalizations of the different terms in W, but they will be fixed by supersymmetry. See *e.g.* Ref. [76] for details.

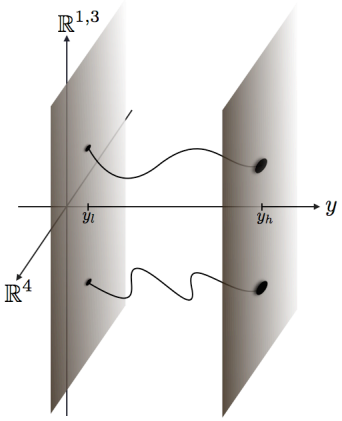

Figure 3.1: A cartoon of our heavy-light mesons as strings stretched between two D7-branes.

in a way that preserves only $\mathcal{N} = 1$ superysmmetry corresponds to more general types of superpotentials, for example

$$W = \mathrm{Tr}\, X[Y, Z] + \tilde{Q}_h(m_h - X)Q_h + \tilde{Q}_l(m_l - Y)Q_l \ . \tag{3.11}$$

In most of the rest of what follows, we will restrict to the case where m_h and m_l are real and the two D7-branes preserve $\mathcal{N} = 2$ supersymmetry.

3.4 Mass spectra of heavy-light mesons: Preliminaries

We consider the special configuration of two parallel D7-branes in the $\mathcal{N} = 2$ supersymmetric scenario described above where the ground state string will have a nonzero length. The string hangs from one brane to the other and the string endpoints correspond to one heavy and one light quark. Our aim is to derive the mass spectrum of heavy-light mesons by investigating the spectrum of fluctuations of strings hanging between the branes.

The $AdS_5 \times S_5$ metric (3.3) can be thought of as a warped product metric on $\mathbb{R}^{1,3} \times \mathbb{R}^6$. We will write the line element on $\mathbb{R}^6$ as

$$\delta_{ij} dy^i dy^j = d\rho^2 + \rho^2 d\theta^2 + \rho^2 \sin^2\theta \, d\Omega_2^2 + dy^2 + (dy^6)^2 \ , \tag{3.12}$$

where $d\Omega_2^2$ is a metric on a unit S^2 and we have defined $\rho^2 \equiv u^2 - (y^5)^2 - (y^6)^2$ and $y \equiv y^5$. The metric on Minkowski space $\mathbb{R}^{1,3}$ we will write as

$$\eta_{\mu\nu} dx^\mu dx^\nu = -dt^2 + dr^2 + r^2 d\phi^2 + dx^2 \ . \tag{3.13}$$

In this geometry, strings that stretch from one D7-brane to another are dual to mesons, as illustrated in Figure 3.1 which displays our geometric picture of heavy-light mesons. Classical strings are described by the Nambu-Goto action

$$S_{NG} = \int d\tau d\sigma \mathcal{L} = -\frac{1}{2\pi\alpha'} \int d\tau d\sigma \sqrt{(\dot{X} \cdot X')^2 - (\dot{X})^2 (X')^2} \ , \tag{3.14}$$

where $X^A(\tau, \sigma)$ describes the embedding of the string in $AdS_5 \times S^5$. In our notation, $X \cdot Y = g_{AB} X^A Y^B$ is contracted with the ten dimensional metric, and we have defined $\partial_\sigma X \equiv X'$ and

$\partial_\tau X \equiv \dot{X}$. We choose a gauge in which the worldsheet coordinates are $\tau = t$, $\sigma = y$. The locations of the light and heavy D7-branes will be denoted by $y = y_l$ and $y = y_h$, and the light and heavy quark masses [30] read

$$m_l = \frac{L^2}{2\pi\alpha'}\, y_l \; ; \quad m_h = \frac{L^2}{2\pi\alpha'}\, y_h \; , \tag{3.15}$$

where $L^2/\alpha' = \sqrt{\lambda}$. The Nambu-Goto action is suppressed by a relative power of N with respect to the DBI action, and thus we are justified in neglecting the back reaction of the string on the D7-brane and the geometry in the large N limit.

We wish to study the profile that a string stretching between the D7-branes takes, assuming that the string sits at a constant position in the internal unit S^2. The Nambu-Goto action (3.14) produces the equation of motion

$$\begin{aligned} 0 \;\; &= \;\; \frac{\partial}{\partial\tau}\left(g_{AB}\frac{(\dot{X}\cdot X')(X')^B - (X')^2\dot{X}^B}{\sqrt{(\dot{X}\cdot X')^2 - (\dot{X})^2(X')^2}}\right) + \frac{\partial}{\partial\sigma}\left(g_{AB}\frac{(\dot{X}\cdot X')\dot{X}^B - (\dot{X})^2(X')^B}{\sqrt{(\dot{X}\cdot X')^2 - (\dot{X})^2(X')^2}}\right) \\ &- \;\; \frac{1}{\sqrt{(\dot{X}\cdot X')^2 - (\dot{X})^2(X')^2}}\frac{\partial g_{AB}}{\partial X^C}\left(\dot{X}^A X'^B (X')^2 - \frac{1}{2}\dot{X}^A\dot{X}^B(X')^2 - \frac{1}{2}X'^A X'^B(\dot{X})^2\right). \end{aligned} \tag{3.16}$$

The second line will only give a contribution to the equation of motion when we consider spinning strings in Section 3.6. The various scalar products have the forms

$$\dot{X}\cdot X' \;\; = \;\; L^2\Big\{ u^2\left(\dot{x}x' + \dot{r}r' + r^2\dot{\phi}\phi'\right) + \frac{1}{u^2}\left(\dot{\rho}\rho' + \rho^2\dot{\theta}\theta' + \dot{y}_6 y_6'\right)\Big\}, \tag{3.17}$$

$$(\dot{X})^2 \;\; = \;\; L^2\Big\{ u^2(-1 + \dot{x}^2 + \dot{r}^2 + r^2\dot{\phi}^2) + \frac{1}{u^2}\left(\dot{\rho}^2 + \rho^2\dot{\theta}^2 + \dot{y}_6^2\right)\Big\}, \tag{3.18}$$

$$(X')^2 \;\; = \;\; L^2\Big\{ u^2\left((x')^2 + (r')^2 + r^2(\phi')^2\right) + \frac{1}{u^2}\left(1 + (\rho')^2 + \rho^2(\theta')^2 + (y_6')^2\right)\Big\}, \tag{3.19}$$

where we have rewritten y^6 as y_6 to avoid confusing superscripts. The energy and momentum densities of the string are

$$\pi^0_A = \frac{\partial\mathcal{L}}{\partial\dot{X}^A} = -\frac{1}{2\pi\alpha'}g_{AB}\frac{(\dot{X}\cdot X')(X')^B - (X')^2(\dot{X})^B}{\sqrt{(\dot{X}\cdot X')^2 - (X')^2(\dot{X})^2}} \; , \tag{3.20}$$

while the energy and momentum currents read

$$\pi^1_A = \frac{\partial\mathcal{L}}{\partial(X')^A} = -\frac{1}{2\pi\alpha'}g_{AB}\frac{(\dot{X}\cdot X')(\dot{X})^B - (\dot{X})^2(X')^B}{\sqrt{(\dot{X}\cdot X')^2 - (X')^2(\dot{X})^2}} \; . \tag{3.21}$$

We will apply Neumann boundary conditions in the D7-brane directions at $y = y_l$ and $y = y_h$

$$\pi^1_A\big|_{y=y_h,y_l} = 0 \; , \tag{3.22}$$

for $A = x$, r, ϕ, ρ, and θ, implying that no momentum is assumed to flow into the string from the D7-brane in these directions. The coordinate y_6 is in contrast subject to Dirichlet boundary conditions.

3.5 Fluctuations in x, ρ and y_6

In this section, we study radial excitations of the heavy-light mesons. Specializing to the background of $\dot{\theta} = 0$, $r = 0$ and a constant $\rho = \rho_0$, we consider infinitesimal fluctuations of the string action in the form of $x = x(t, y)$, $\rho(t, y) = \rho_0 + \delta\rho(t, y)$ and $y_6 = y_6(t, y)$. Applying Eqs. (3.17)–(3.19) where now $u^2 = y^2 + (\rho_0 + \delta\rho)^2$, we expand the action to second order in the fluctuations, and obtain

$$S_{NG} = \frac{L^2}{2\pi\alpha'} \int d\tau d\sigma \left\{ 1 - \frac{1}{2}\,\dot{x}^2 + \frac{1}{2}\,u_0^4 (x')^2 + \frac{1}{2}\,((\delta\rho')^2 + (y_6')^2) - \frac{1}{2u_0^4}\,\left(\delta\dot{\rho}^2 + \dot{y}_6^2\right) \right\} , \quad (3.23)$$

with $u_0^2 \equiv y^2 + \rho_0^2$.

Translational symmetry in the Minkowski directions guarantees that a constant value of x is a solution to the equation of motion and thus that there is a zero mode in the spectrum corresponding to motion of the string at constant velocity in the x direction. Perhaps surprisingly, a constant value of ρ is also a solution and thus there is another zero mode in the spectrum corresponding to translations of the ρ coordinate, even though we do not have translational symmetry in these directions. However, we will see below that this zero mode is only present for the ground state string. The fluctuating string can minimize its energy by moving to $\rho = 0$.

There exists an interesting relationship between the equation of motion for the fluctuations in the y_6 and $\delta\rho$ directions and the equation of motion for the fluctuations in x which we believe may be a consequence of supersymmetry. We will assume that the fluctuations have the time dependence $X^A \sim e^{-i\omega t}$ so that $\ddot{X}^A = -\omega^2 X^A$. The equations of motion thus become

$$\frac{\partial}{\partial y}\Big(f(y)\,x'\Big) = -\omega^2 x \ , \quad (3.24)$$

$$f(y)\delta\rho'' = -\omega^2\delta\rho \ , \qquad \text{and} \qquad f(y)y_6'' = -\omega^2 y_6 \ , \quad (3.25)$$

where $f(y) = (y^2 + \rho_0^2)^2$. From these expressions, it is clear that if we have a solution x to Eq. (3.24), then $\delta\rho = f(y)x'$ (or $y_6 = f(y)x'$) satisfies Eq. (3.25). Moreover, given a solution $\delta\rho$ (or y_6) to Eq. (3.25), then $x = \delta\rho'$ (or $x = y_6'$) satisfies Eq. (3.24).

A consideration of boundary conditions now reveals that the fluctuations in x and y_6 have the same spectrum up to a zero mode. While x and $\delta\rho$ satisfy Neumann boundary conditions, y_6 satisfies Dirichlet boundary conditions. If we solve Eq. (3.24) for the allowed fluctuation modes x satisfying Neumann boundary conditions, then the relations between the two equations of motion give us all the fluctuation modes y_6 satisfying Dirichlet boundary conditions. We have to perform a separate calculation for the $\delta\rho$ fluctuations, but had the x fluctuations satisfied Dirichlet boundary conditions instead of Neumann, they would, too, be trivially related to the $\delta\rho$ fluctuations. We begin with the x fluctuations.

3.5.1 The x fluctuations

The equation (3.24) for the x fluctuations can be solved to yield

$$\begin{aligned} x(t,y) &= \frac{C\rho_0}{\sqrt{y^2+\rho_0^2}} \left\{ \sqrt{1+\frac{\omega^2}{\rho_0^2}}\,\cos\left[\sqrt{1+\frac{\omega^2}{\rho_0^2}}\,\arctan\left[\frac{y}{\rho_0}\right]+\alpha\right] \right. \\ &+ \left. \frac{y}{\rho_0}\,\sin\left[\sqrt{1+\frac{\omega^2}{\rho_0^2}}\,\arctan\left[\frac{y}{\rho_0}\right]+\alpha\right] \right\} e^{-i\omega t} \ , \end{aligned} \quad (3.26)$$

where C and α are the two integration constants. We now apply Neumann boundary conditions $x'(y_l) = x'(y_h) = 0$ to determine the allowed spectrum ω. Doing this at the light D7-brane,

we find

$$\alpha \;=\; -\sqrt{1+\frac{\omega^2}{\rho_0^2}}\,\arctan\left[\frac{y_l}{\rho_0}\right], \tag{3.27}$$

while applying the boundary conditions at the heavy brane then yields the discrete spectrum:

$$\omega_n^x = \rho_0\sqrt{\frac{n^2\pi^2}{\left(\arctan[\rho_0/y_l]-\arctan[\rho_0/y_h]\right)^2}-1}\,, \tag{3.28}$$

where $n \in \mathbb{Z}^+$. In addition to these values of n however, the spectrum also contains a zero mode, the trivial solution of $\omega = 0$.

Before moving onto the y_6 fluctuations, we note that in the $\rho_0 = 0$ limit, the mode functions and spectrum become simpler:

$$x \;=\; C(\omega z\cos(\omega(z-z_l))-\sin(\omega(z-z_l)))e^{-i\omega t}\,, \tag{3.29}$$

$$\omega_n^x \;=\; \frac{\pi n}{z_l-z_h}\,, \qquad \text{where} \qquad z=1/y\,. \tag{3.30}$$

The frequencies are the same as those of a guitar string of length $z_l - z_h$, and we thus see that in the heavy quark limit, $z_h \to 0$, the frequencies become m_h independent.

3.5.2 The y_6 fluctuations

The solution to the equation of motion (3.25) is now related in a trivial way to the x fluctuations studied above:

$$y_6 = (y^2+\rho_0^2)^2x' = -C\omega^2\sqrt{\rho_0^2+y^2}\sin\left[\sqrt{1+\frac{\omega^2}{\rho_0^2}}\,\arctan\left[\frac{y}{\rho_0}\right]+\alpha\right]e^{-i\omega t}\,. \tag{3.31}$$

In the $\rho_0 = 0$ limit, the mode function again takes a simpler form

$$y_6 = \frac{C\omega^2}{z}\sin(\omega(z-z_l))e^{-i\omega t} \qquad \text{where} \qquad z=1/y\,. \tag{3.32}$$

The Dirichlet boundary conditions $y_6(y_l) = 0 = y_6(y_h)$ are equivalent to the Neumann boundary conditions applied to the x fluctuations above, leading to the same value of α given in Eq. (3.27) and the same spectrum

$$\omega_n^y \;=\; \rho_0\sqrt{\frac{n^2\pi^2}{\left(\arctan[\rho_0/y_l]-\arctan[\rho_0/y_h]\right)^2}-1}\,, \tag{3.33}$$

where $n \in \mathbb{Z}^+$. This time, however, there is no zero mode.

3.5.3 The $\delta\rho$ fluctuations

For the $\delta\rho$ fluctuations, we will not be able to find an analytic spectrum, but will eventually attempt to understand the spectrum's features both qualitatively and numerically. We begin with the general solution to Eq. (3.25),

$$\delta\rho(t,y) = C\sqrt{\rho_0^2+y^2}\sin\left[\sqrt{1+\frac{\omega^2}{\rho_0^2}}\,\arctan\left[\frac{y}{\rho_0}\right]+\alpha\right]e^{-i\omega t}\,. \tag{3.34}$$

Applying Neumann boundary conditions at the light brane $\delta\rho'(y_l) = 0$, we find

$$\alpha \;=\; -\sqrt{1+\frac{\omega^2}{\rho_0^2}}\,\arctan\left[\frac{y_l}{\rho_0}\right] - \arctan\left[\sqrt{1+\frac{\omega^2}{\rho_0^2}}\,\frac{\rho_0}{y_l}\right], \tag{3.35}$$

while demanding that the boundary conditions are satisfied at the heavy brane leads to

$$\begin{aligned}&\tan\left[\sqrt{1+\frac{\omega^2}{\rho_0^2}}\left(\arctan\left[\frac{y_l}{\rho_0}\right]-\arctan\left[\frac{y_h}{\rho_0}\right]\right)+\arctan\left[\sqrt{1+\frac{\omega^2}{\rho_0^2}}\,\frac{\rho_0}{y_l}\right]\right]\\ =\;&\sqrt{1+\frac{\omega^2}{\rho_0^2}}\,\frac{\rho_0}{y_h}\;.\end{aligned} \tag{3.36}$$

The solutions of this equation give us the spectrum of the fluctuations ω_n^ρ.

Unfortunately, the transcendental nature of the above equation prevents us from solving it analytically. There are, however, various limits, where we can simplify the numerical solution. The first simplification occurs in the limit of large y_h, in which one may attempt a power expansion in y_l/y_h. To this end, we write

$$\omega_n^\rho \;\equiv\; \omega_n \,=\, y_l \times \sum_{i=0}^{\infty} \omega_{n,i} \left(\frac{y_l}{y_h}\right)^i, \tag{3.37}$$

substitute this into Eq. (3.36), and proceed to solve the equation order by order in the small parameter y_l/y_h. At leading order, we easily obtain for $\omega_{n,0}$

$$\sqrt{1+\frac{\omega_{n,0}^2\,y_l^2}{\rho_0^2}}\left(\frac{\pi}{2}-\operatorname{arccot}\left[\frac{\rho_0}{y_l}\right]\right)-\arctan\left[\sqrt{1+\frac{\omega_{n,0}^2\,y_l^2}{\rho_0^2}}\,\frac{\rho_0}{y_l}\right] \;=\; n\pi, \tag{3.38}$$

with $n \in \mathbb{Z}^+$. The numerical solution to this equation quickly leads to the forms of the functions $\omega_{n,0}\,(\rho_0/y_l)$. The next two terms in the power series expansion of Eq. (3.36) are solved trivially by setting $\omega_{n,1}$ and $\omega_{n,2}$ equal to zero, and it is only at order $i = 3$ that we find the next nonzero term in the expansion of Eq. (3.37). The forms of the resulting functions $\omega_{n,0}\,(\rho_0/y_l)$ and $\omega_{n,3}\,(\rho_0/y_l)$ will be displayed for $n = 1, 2, ..., 5$ in the next section in a slightly different notation.

One limit, where the functions $\omega_{n,i}$ are in fact analytically solvable is that of large ρ_0/y_l. There, it is straightforward to see that Eq. (3.38) reduces to the solution

$$\omega_{n,0} \;=\; \sqrt{(2n+1)^2-1}\,\frac{\rho_0}{y_l}\,, \tag{3.39}$$

while the three next orders produce

$$\omega_{n,1} = \omega_{n,2} \,=\, 0 \qquad \text{and} \qquad \omega_{n,3} = \frac{4}{3\pi}\,\sqrt{n(n+1)}(2n+1)^2\left(\frac{\rho_0}{y_l}\right)^4. \tag{3.40}$$

It is interesting to contrast Eq. (3.39) with the spectra of the x and y_6 fluctuations, which in the same limit ($y_h \to \infty$ and ρ_0/y_l large) produce from Eq. (3.28)

$$\omega_n^x \;=\; \sqrt{(2n)^2-1}\,\rho_0. \tag{3.41}$$

We thus see that at least in this limit, the fluctuation energies in the x and y_6 direction lie exactly in between the energies of the ρ fluctuations.

Finally, we note that in the limit $\rho_0 = 0$, Eq. (3.34) reduces to

$$\delta\rho = \frac{-C}{z\sqrt{1+\omega^2 z_l^2}} \left(\omega z_l \cos(\omega(z-z_l)) + \sin(\omega(z-z_l))\right) e^{-i\omega t} \ , \tag{3.42}$$

while condition (3.36) on the frequencies reduces to the simple expression

$$\omega(z_h - z_l) = \arctan(\omega z_h) - \arctan(\omega z_l) - \pi n \ , \tag{3.43}$$

where n is an integer. This equation, however, is not of an analytically solvable type either, so it must be dealt with numerically. In the limit $y_h \to \infty$, the first few solutions are $\omega z_l = 4.493$, 7.725, and 10.904.

3.5.4 The meson mass spectrum

Let us finally look at the energy spectrum of the string fluctuations in more detail. Using the result

$$E = -\int \mathrm{d}\sigma \, \pi_t^0 \ , \tag{3.44}$$

we see that to quadratic order in the fluctuations the energy of the string can be obtained by integrating the canonical momentum density

$$\pi_t^0 \ = \ -\frac{L^2}{2\pi\alpha'} \left(1 + \frac{1}{2}\, u^4 (x')^2 + \frac{1}{2}\, \dot{x}^2 + \frac{1}{2}\, (\delta\rho')^2 + \frac{1}{2u^4}\, (\delta\dot{\rho})^2 + \frac{1}{2}\, (y_6')^2 + \frac{1}{2u^4}\, (\dot{y}_6)^2\right).$$

From a classical perspective, the energies will depend on the amplitudes of the fluctuations, while from a quantum perspective, these amplitudes can only take on discrete values corresponding to the occupation number of a given mode. At quadratic order, we essentially have a version of the quantum harmonic oscillator. The equal time commutation relation $[X^A(y), \pi_A^0(y')] = i\delta(y-y')$ implies, in units where $\hbar = 1$, that the smallest quanta of excitation are the frequencies we determined before, the ω_n^w where $w = x$, ρ, or y. We find the simple result

$$E \ = \ m_h - m_l + \sum_{w,n} N_w^n \omega_n^w, \tag{3.45}$$

where N_w^n is the occupation number of the mode (w, n).[5] We therefore note that in order to inspect the mass spectrum of the heavy-light mesons below, we merely need to consider the frequencies ω_n^w obtained above. We anticipate Eq. (3.45) remains valid provided $N_w^n \ll \sqrt{\lambda}$ and we can neglect the nonlinearities in the string equation of motion.

The x and y_6 fluctuations

Denoting $q \equiv \rho_0 L^2/2\pi\alpha'$ and using the relation $L^2/\alpha' = \sqrt{\lambda}$, we can write the energy spectrum of the x or y_6 fluctuations in the form

$$E_n^x = E_n^y \ = \ m_h - m_l + \frac{2\pi q}{\sqrt{\lambda}} \sqrt{\frac{n^2\pi^2}{\left(\arctan[q/m_l] - \arctan[q/m_h]\right)^2} - 1} \ . \tag{3.46}$$

This formula gives the energy for a string with a single quantum of excitation in the nth mode of the y_6 or x fluctuations. In the Introduction, we claimed that in the heavy quark limit,

[5] Calculating the zero point energy contribution to these oscillators requires also investigating the fermionic fluctuations of the superstring. We suspect supersymmetry implies that the zero point energy vanishes.

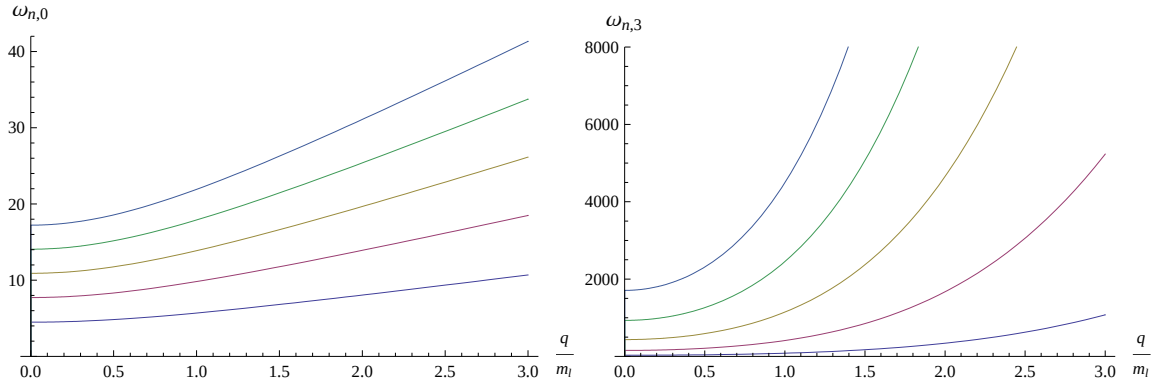

Figure 3.2: Plots of the functions $\omega_{n,0}(q/m_l)$ and $\omega_{n,3}(q/m_l)$, respectively. The index n grows from 1 to 5 from the bottom to the top curve in both figures.

$m_h \gg m_l$, the energy of the excitations scaled with m_l. Here, seemingly in contradiction with the earlier claim, we find that in the limit $m_h \gg q$, we may expand the ω_n^x in inverse powers of m_h, producing

$$E_n^x = m_h - m_l + \frac{2\pi q}{\sqrt{\lambda}} f_n\left(\frac{q}{m_l}\right) + \frac{2\pi^3 n^2 q^2}{\sqrt{\lambda}\, m_h} \frac{1}{\arctan^3[q/m_l] f_n(q/m_l)} + \mathcal{O}\left(\frac{1}{m_h^2}\right), \quad (3.47)$$

where we have denoted

$$f_n(x) \equiv \sqrt{\frac{n^2\pi^2}{\arctan^2[x]} - 1}\ . \quad (3.48)$$

Thus, the excitation spectrum depends on both light scales m_l and q.

We now give two reasons why the scale q should disappear. First, the derivative of the excitation energies with respect to q is non-negative

$$\frac{\partial E_n^x}{\partial q} = \frac{\partial E_n^y}{\partial q} \geq 0\ , \quad (3.49)$$

and is equal to zero at $q = 0$, implying that fluctuations about $q \neq 0$ have more energy than the equivalent fluctuations about $q = 0$. This inequality suggests that a string fluctuating about a nonzero value ρ_0 will in addition begin to oscillate about $\rho = 0$. In the case of $q = 0$, the energy spectra reduce to

$$E_n^x = E_n^y = m_h - m_l + \frac{m_h m_l}{m_h - m_l} \frac{2\pi^2 n}{\sqrt{\lambda}}\ , \quad (3.50)$$

where $n \in \mathbb{Z}^+$. In the heavy quark limit $m_h \gg m_l$, the excitation spectrum does indeed depend only on m_l to leading order in m_l/m_h.

The second reason for the disappearance of the scale q will be developed more in Section 3.6, where we will see that for slowly spinning strings in the ρ–θ plane, a nonzero value of ρ_0 is stabilized. Thus what would seem to be a zero mode in the ρ direction is lifted and a continuous change of q will not be possible for these spinning strings. However, the stable value of ρ_0 is of order m_l or zero, regardless of the angular momentum, and thus the extra scale q again disappears from the excitation spectrum.

The $\delta\rho$ fluctuations

For the $\delta\rho$ fluctuation spectrum given by Eq. (3.36), we have to resort to numerics. In the limit of large $y_h \gg y_l$, we may use our earlier numerical solution utilizing a power series expansion in y_l/y_h, in terms of which the spectrum can be written in the form

$$E_n^\rho = m_h - m_l + m_l\,\omega_{n,0}(q/m_l)\frac{2\pi}{\sqrt{\lambda}} + \frac{m_l^4}{m_h^3}\,\omega_{n,3}(q/m_l)\frac{2\pi}{\sqrt{\lambda}} + \mathcal{O}(m_l^5/m_h^4)\ . \qquad (3.51)$$

This formula corresponds to the energy of a string with a single quantum of energy in the nth mode of the ρ fluctuations. We plot the functions $\omega_{n,0}$ and $\omega_{n,3}$ in Figure 3.2. From there, we see that the energies of the fluctuations are always minimized at $\rho_0 = 0$ or $q = 0$, just as it was for the x and y_6 fluctuations. Another interesting aspect of these excitation energies is the absence of the two first leading corrections in m_l/m_h in the heavy quark limit.

3.6 Spinning strings

To supplement our discussion of the small fluctuations of strings around static quark-antiquark solutions, we now turn to consider the case where the string joining the heavy and the light brane is spinning. First, we consider strings spinning in the real space where they have a conserved angular momentum, and then look into strings spinning in the internal θ direction where the corresponding angular momentum can be reinterpreted as a charge. Our analysis is purely classical, but we expect valid, provided the angular momentum and charge of the strings are large.

As we have discussed briefly already, there is an interesting wrinkle in the discussion of the ρ–θ spinning strings. A straight, motionless string stretching between the D7-branes at a nonzero value of ρ_0 is a solution for all ρ_0. That such a string is a solution is surprising given the lack of translation invariance in ρ. As we saw before in the analysis of the fluctuations, if we excite one of these straight strings with $\rho_0 \neq 0$, it will experience a force pulling it toward $\rho = 0$. In this section on spinning strings, we will find that a string spinning in the ρ–θ plane is not free to sit at an arbitrary average value of ρ_0 either.

3.6.1 Strings spinning in real space

We start by looking into the profile and energy spectrum of a string spinning in real space, more specifically in the x^1–x^2 plane, assuming that $x^3 = \rho = y_6 = 0$. To begin with, we transform from Cartesian (x^1, x^2) to polar coordinates (r, ϕ), and make the uniformly rotating ansatz of Ref. [67], where $\phi = \Omega t$ is independent of the worldsheet coordinate σ. At the same time, we assume that $z(\sigma)$ and $r(\sigma)$ are t independent, which leads to an action of the form

$$S = -\frac{L^2}{2\pi\alpha'}\int dt\,d\sigma\,\frac{1}{z^2}\sqrt{(1-\Omega^2 r^2)((z')^2+(r')^2)}\ , \qquad (3.52)$$

invariant under reparametrizations of the worldsheet coordinate $\sigma = f(\sigma')$. For the most part, we will choose $\sigma = z$, though for the numerical studies we will shortly present, we found it sometimes convenient to make other choices, such as $\sigma = r$. This action leads to the following formulae for the energy and angular momentum of the string:

$$E = \frac{L^2}{2\pi\alpha'}\int d\sigma\,\frac{1}{z^2}\sqrt{\frac{(z')^2+(r')^2}{1-\Omega^2 r^2}}\ , \qquad (3.53)$$

$$J = \frac{L^2\Omega}{2\pi\alpha'}\int d\sigma\,\frac{r^2}{z^2}\sqrt{\frac{(z')^2+(r')^2}{1-\Omega^2 r^2}}\ . \qquad (3.54)$$

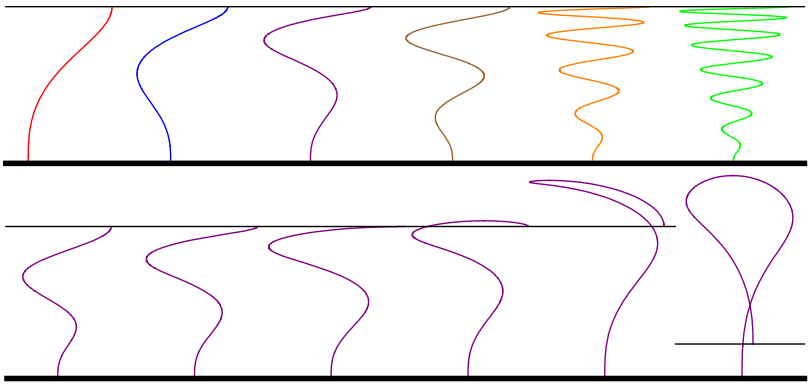

Figure 3.3: Top: A schematic plot showing the forms of the spinning string solutions $r(z)$ for various n. The lower (thick) horizontal line corresponds to the heavy brane sitting at $z_h = 1/100$ and the upper (thin) line to the light brane at $z_l = 1$, with the coordinate z growing vertically. The six curves, from left to right, correspond to the cases of $n = 1, 2, 3, 4, 9$ and 13, respectively. Bottom: Another schematic plot showing the evolution of the $n = 3$ branch as Ω is decreased from 9.52 (left) to 0.5 (right). The critical solution $\Omega_{3c} = 5.84$ is the third from the left. For the smallest value of Ω, corresponding to large J and E, we have rescaled the solution in the z direction by a factor of 4.4 in order to make it fit in the figure. In the $\Omega \to 0$ limit, the solution becomes symmetric in the r direction about the center of mass.

Choosing now $\sigma = z$, the equation of motion for $r(z)$ has the form

$$\frac{r''}{1+(r')^2} - \frac{2}{z}r' + \frac{\Omega^2 r}{1-\Omega^2 r^2} = 0 \ , \tag{3.55}$$

which we now proceed to solve, demanding that Neumann boundary conditions be satisfied on the heavy and light branes at $z = z_h$ and $z = z_l$. Neumann boundary conditions for ϕ are satisfied trivially because $\phi' = 0$, while for r the boundary conditions read

$$r' \sqrt{\frac{1-\Omega^2 r^2}{1+(r')^2}}\Bigg|_{z=z_h,z_l} = 0 \ . \tag{3.56}$$

Thus, we must either require that $r' = 0$ at the boundary or that $\Omega^2 r^2 = 1$, which physically is the condition that the endpoint of the string is moving at the local speed of light. We will in general choose $r' = 0$, but will nevertheless find certain "critical" solutions that satisfy the light-like boundary conditions.

The linearized form of Eq. (3.55) provides a good place to begin our study, as this form

$$z^2 \left(\frac{r'}{z^2}\right)' + \Omega^2 r = 0 \ , \tag{3.57}$$

of Eq. (3.55), valid when r' and $\Omega r \ll 1$, is easy to solve. Indeed, we already solved it; Eq. (3.57) is identical to Eq. (3.24) in the case $\rho_0 = 0$. Assuming then that the string takes the form

$$r = A\left(\omega_n z \cos(\omega_n(z - z_l)) - \sin(\omega_n(z - z_l))\right) , \tag{3.58}$$

$$\phi = \omega_n t = \frac{\pi n}{z_l - z_h} t \tag{3.59}$$

for small A, where we have adapted Eq. (3.29), the energy and angular momentum are given

by the approximate expressions

$$E = \frac{L^2}{2\pi\alpha'}\left(\frac{1}{z_h}-\frac{1}{z_l}-\frac{(\pi n)^4 A^2}{2(z_h-z_l)^3}+\mathcal{O}(A^4)\right), \tag{3.60}$$

$$J = \frac{L^2}{2\pi\alpha}\left(\frac{(\pi n)^3 A^2}{2(z_h-z_l)^2}+\mathcal{O}(A^4)\right). \tag{3.61}$$

Eliminating A from here, we find that[6]

$$E \approx m_h - m_l + n\pi\frac{m_l m_h}{m_h-m_l}\frac{2\pi J}{\sqrt{\lambda}}, \tag{3.62}$$

which corresponds to the dashed straight lines in Figure 3.4 (left), where we display the E vs. J dependence of our spinning strings. This linear scaling of E with J is characteristic of a particle in a Hooke's law potential, where the constant of proportionality is given by the frequency of the oscillator.

As the E and J of the string get larger, r will get larger as well, and eventually our linearized approximation breaks down. To make further progress, we resort to numerics to calculate the profile (r,z) of the spinning strings. For simplicity, we rescale our variables so that $z_l = 1$, and have z_h take the values $1/10$ and $1/100$, corresponding roughly to the heavy-to-light quark mass ratios one finds in QCD for charm and bottom quarks. We find that for each n, there is a continuous family of rotating string solutions for all Ω such that $0 < \Omega < \omega_n$. The index n parametrizes the number of turning points in the solutions: For the branch n, the string profile (r,z) has always $n-1$ (local) extremal values in r. Examples of the profile (r,z) for various n are exhibited in Figure 3.3 (top).

Once the results for (r,z) are obtained in a numerical form, we insert them into the integrals of Eqs. (3.53) and (3.54), thus obtaining the energies of the spinning strings in terms of their angular momenta. The resulting curves $f(x)$, parametrizing the energies through

$$E = m_h - m_l + m_l\, f(2\pi J/\sqrt{\lambda}), \tag{3.63}$$

are shown for $n = 1,2,3,4$ and $z_h = 1/100$ in Figure 3.4 (left) and in more detail for the $n=1$ branch in Figure 3.5. Intriguingly, reducing Ω increases both E and J. A similar behavior was observed for the heavy-heavy mesons in Ref. [67], and is explained by the fact that the decrease in Ω is made up for by the growing size of the string. The evolution of the profile of the $n=3$ branch string as a function of Ω is shown in Figure 3.3 (bottom).

The dependence of the $E(J)$ curves on m_h is relatively mild and easily modeled. The Eq. (3.62) suggests a rescaling of the variable J by $1/(1-m_l/m_h)$, defining

$$\tilde{J} = \frac{m_h}{m_h-m_l}\frac{2\pi J}{\sqrt{\lambda}}. \tag{3.64}$$

With this small correction, we see from Figure 3.4 (right) that the curves corresponding to $z_h = 1/10$ and $1/100$ practically overlap.

As Ω is decreased, there is a critical Ω_{nc} for each family of solutions where the light quark endpoint of the string is moving at the local speed of light, $\Omega_{nc}\, r(z_l) = 1$. For the *short strings* with $\Omega > \Omega_{nc}$, the string is contained entirely between the two D7-branes, while for the *long strings* with $\Omega < \Omega_{nc}$, there is a loop of string in the region $z > z_l$. Like the ω_n, the critical Ω_{nc} depend to some extent on the choice of the heavy and light quark masses. For the first few n, we find that

$$z_h = 1/10:\ \Omega_{1c} = 1.54,\ \Omega_{2c} = 3.98,\ \Omega_{3c} = 6.22,\ \Omega_{4c} = 8.41,$$
$$z_h = 1/100:\ \Omega_{1c} = 1.38,\ \Omega_{2c} = 3.72,\ \Omega_{3c} = 5.84,\ \Omega_{4c} = 7.91.$$

[6]The $n=1$ version of this formula (3.62) was first presented in Ref. [69].

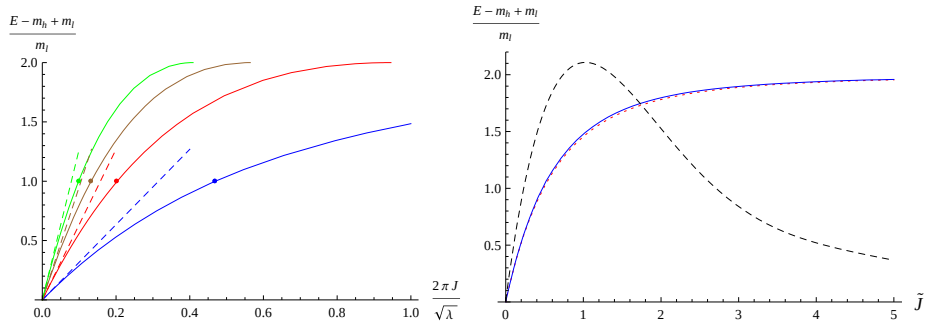

Figure 3.4: Left: The dependence of E versus J for the spinning heavy-light mesons. We display the curves for $m_h = 100m_l$ and $n = 1, 2, 3, 4$ from right to left, with the adjacent dashed straight lines corresponding to the respective analytic small-J approximations of Eq. (3.62) and the dots on the curves denoting the critical solutions at $\Omega = \Omega_{nc}$. Right: The $E(\tilde{J})$ curves for both the $m_h = 100m_l$ (solid blue curve) and $m_h = 10m_l$ (dotted red) cases for the $n = 1$ branch, together with their difference multiplied by a factor of 100 (dashed black).

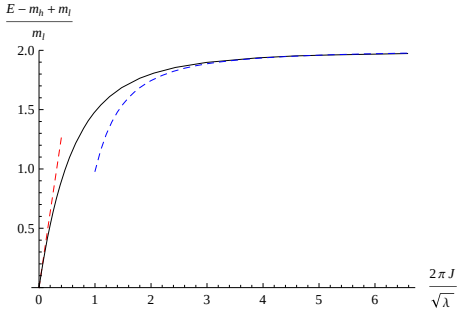

Figure 3.5: We plot E versus J for the $n = 1$ branch of the spinning heavy-light mesons. The solid curve is the numerical result for the case $m_h = 100m_l$, while the red and blue dashed curves are the analytic small and large-J approximations of Eqs. (3.62) and (3.67), respectively.

We furthermore observe that for $n = 1$, the critical energies and angular momenta obey the results

$$E_c = m_h - \frac{m_l^2}{2m_h} + \mathcal{O}\left(\frac{m_l^3}{m_h^2}\right), \tag{3.65}$$

$$\tilde{J}_c = 0.473 - 0.262\,\frac{m_l}{m_h} + \mathcal{O}\left(\frac{m_l^2}{m_h^2}\right), \tag{3.66}$$

and that for $n > 1$, the forms of the equations stay intact, while the numbers in the latter relation somewhat change. Especially the former of these results deserves some attention; we have verified this relation to more than 1 part in 10000, but have so far no explanation for why the limiting energy should obtain such a simple form.

As Ω is decreased below Ω_{nc}, the strings quickly begin to get very large compared to the separation between the D7-branes, and in the $\Omega \to 0$ limit, their size in fact diverges both in the r and z directions. Indeed, in this limit the spinning string solutions can be seen to approach those of the heavy-heavy mesons considered in Ref. [67], where both ends of the string end on the same D7-brane. The limit $\Omega \to 0$ of the $n = 1$ branch is special because the velocity of any point on the $n = 1$ string approaches zero as Ω decreases, while for the $n > 1$ branches, there always exists a finite set of points σ_i along the string where, due to the large

size of the string, $r(\sigma_i)\Omega \to 1$ as $\Omega \to 0$. As noticed originally by Refs. [67, 69], the small size of Ωr allows for an analytic treatment of the E and J of the $n = 1$ branch in the $\Omega \to 0$ limit.

In the $\Omega \to 0$ limit, the strings correspond to marginally bound heavy-light mesons with an energy $E \approx m_h + m_l$. By marginally bound, we mean that the binding energy becomes very small. For the $\Omega \to 0$ limit of the $n = 1$ branch, the string profile must be well approximated by the static configuration that determines the potential between two infinitely massive quarks. As shown in Ref. [69], in this limit the energy of the string obeys the relation

$$E = m_h + m_l - \kappa \frac{m_l m_h}{m_h + m_l} \frac{\lambda}{J^2} , \tag{3.67}$$

where

$$\kappa = 2 \left(\frac{\Gamma(3/4)}{\Gamma(1/4)} \right)^4 \approx 0.0261 ,$$

consistent with a Coulombic attraction between the quarks. We see from Figure 3.5 that Eq. (3.67) is quite a good approximation to the $E(J)$ curve already at moderately large J. In contrast, the $\Omega \to 0$ limit of the $n > 1$ branches all terminate at finite values of J. Numerically, for the case of $m_h = 100 m_l$, these terminal values of $2\pi J/\sqrt{\lambda}$ are 0.946, 0.546, and 0.409 for the $n = 2$, 3 and 4 branches, respectively.

We believe that the long strings are much less stable than the short strings. For one, they intersect the D7-brane and thus can break in two. For another, they are much bigger in size than the short strings, and thus it is likely that they are subject to instabilities, which do not respect the uniformly rotating $\phi = \Omega t$ ansatz.

3.6.2 String profile in ρ and θ

Next, we look at the profile of a string spinning inside the $\mathbb{R}^6$, in the ρ–θ directions. Let Q be the corresponding angular momentum. Although Q is an angular momentum from the ten dimensional point of view, in the four dimensional field theory it is a charge, namely the R-charge of the R-symmetry of our supersymmetric field theory. From the point of view of QCD, Q could be viewed as a model of the electromagnetic charge of the meson.

To begin with, we assume that $x = r = y_6 = 0$, and in analogy with our discussion of strings spinning in real space, make an ansatz where $\rho(y)$ is time independent and $\theta = \Omega t$ is y independent. The Neumann boundary conditions for θ are then again trivially satisfied because $\theta' = 0$. With these simplifications, the action for the string reduces to

$$S_{NG} = -\frac{L^2}{2\pi\alpha'} \int dt\, dy \sqrt{(1 - \rho^2\Omega^2/u^4)\,(1 + (\rho')^2)} , \tag{3.68}$$

leading to the equation of motion for $\rho(y)$,

$$\frac{u^2\rho''}{1 + (\rho')^2} + \Omega^2\rho \frac{u^2 - 2\rho^2 + 2y\rho\rho'}{u^4 - \Omega^2\rho^2} = 0 . \tag{3.69}$$

The energy E and internal angular momentum Q of the spinning strings are given by

$$E = \frac{L^2}{2\pi\alpha'} \int dy \sqrt{\frac{1 + (\rho')^2}{1 - \rho^2\Omega^2/u^4}} , \tag{3.70}$$

$$Q = \frac{L^2}{2\pi\alpha'} \int dy \frac{\rho^2\Omega}{u^4} \sqrt{\frac{1 + (\rho')^2}{1 - \rho^2\Omega^2/u^4}} . \tag{3.71}$$

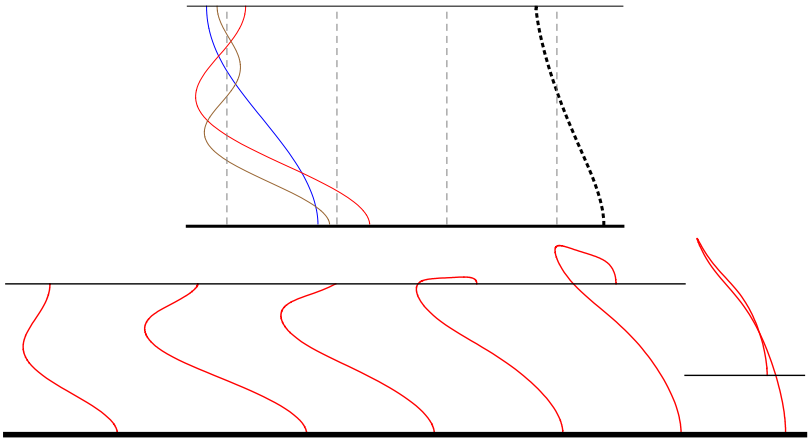

Figure 3.6: Top: Profiles of the spinning strings $\rho(z)$ stretching between the two branes at $z_l = 1$ and $z_h = 1/100$, with $z \equiv 1/y$ and the notation as in Figure 3.3. The black dotted line corresponds to the $n = 0$ branch, while the blue, red and brown solid curves correspond to the $n = 1, 2, 3$ cases, respectively. The gray dashed lines, from left to right, mark the points $\rho = 0, 1/2, 1, 3/2$. Bottom: The evolution of the $n = 2$ branch of solutions as Ω is decreased from 7.725 to 1. The critical solution is again the third from the left, while the smallest Ω solution has been rescaled in the z direction by a factor 2.55. In the $\Omega \to 0$ limit, the part of the solution extending beyond the light brane doubles back on itself.

The Neumann boundary conditions for ρ on the other hand reduce to the requirement

$$\rho' \sqrt{\frac{1 - \rho^2\Omega^2/u^4}{1 + (\rho')^2}}\Bigg|_{y=y_h,y_l} = 0 \ , \tag{3.72}$$

from where we see that we must again either require that $\rho' = 0$ at the boundary or that the ends of the string move at the local speed of light. Similar to the strings spinning in real space, we generically enforce $\rho' = 0$, but in addition find certain special solutions that satisfy the light-like boundary conditions. Note that a motionless string with $\rho = \rho_0$ and $\Omega = 0$ is a solution to the equations of motion for all ρ_0. Once $\Omega \neq 0$, however, the story becomes much more interesting.

For non-zero Ω, the equation of motion for ρ, Eq. (3.69), seems difficult to solve analytically at least in full generality, and we will therefore resort to numerics, setting again $y_l = 1$ and varying the location of the heavy brane y_h. The story we encounter is strongly reminiscent of the strings spinning in real space. We again find multiple branches of solutions indexed by an integer n, $n \geq 1$, with the corresponding string profiles $\rho_n(y)$ containing exactly $n-1$ extrema in ρ.

The low energy behavior of our strings can again be understood analytically through the fluctuation analysis of the previous Section. In this $E \to 0$ limit, we may take the string profiles to be complex combinations of ρ fluctuations with infinitesimal amplitude. The complex combination produces a string spinning in the ρ–θ plane with angular velocity $\Omega = \omega_n$, corresponding to the solutions to Eq. (3.43). Consistent with the results from Section 4.3, we see that for $y_h = 100$, the values of the first few ω_n's are 4.493, 7.725, 10.904.

For a given $n > 0$, we find a continuous family of solutions in the range $0 < \Omega < \omega_n$. Decreasing Ω corresponds to increasing E and J, the increase in the size of the string more than making up for the loss of angular velocity. There are again critical angular frequencies Ω_{nc} which separate the *long strings* with $\Omega < \Omega_{nc}$ from the *short strings* with $\Omega > \Omega_{nc}$, the former extending to the region $y < y_l$. For the critical solution, the endpoint of the string

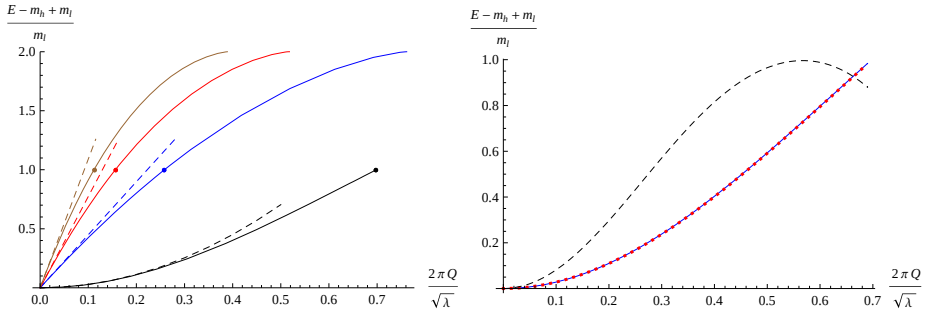

Figure 3.7: Left: E versus Q for the spinning heavy-light mesons. From right to left, the solid curves correspond to the $n = 0, 1, 2, 3$ branches, and the corresponding dashed curves to the analytic small Q approximations of Eqs. (3.75) and (3.88). The value of y_h is set to 100, and the dots on the curves again denote the critical solutions. Right: The effect of changing the heavy brane location from $y_h = 100$ (solid blue curve) to $y_h = 10$ (dotted red) in the $n = 0$ case. The difference of the two curves is also shown as the dashed black line, magnified by a factor of 500.

sitting on the light brane is moving at the local speed of light. For $y_h = 100$, the critical angular velocities for the first three branches are found to equal $\Omega_{1c} = 3.260$, $\Omega_{2c} = 5.152$ and $\Omega_{3c} = 7.108$.

In addition to the branches with $n \geq 1$, we find an additional branch of solutions, $n = 0$, which has no analog for the strings spinning in real space. This branch of the spinning strings emerges from the lifting of the zero fluctuation mode corresponding to translations in the ρ direction, and as we will show shortly, it is possible to understand its low-energy properties in a semi-analytic fashion. Earlier in our fluctuation analysis, we saw that while the ground state string sitting at $\rho \neq 0$ with $\Omega = 0$ did not experience a potential, excited strings felt a force pulling them toward $\rho = 0$. Here, we instead find that strings with even an arbitrarily small Ω are not free to move in the ρ direction, but must sit at a constant $\rho = \rho_0$ in the limit where Ω tends to zero.

Inspecting the $n = 0$ branch numerically for $y_h = 100$, we observe that Ω can be arbitrarily close to zero, with the $\Omega \to 0$ limit corresponding to small angular momenta and energies, in contrast to the branches with $n \geq 1$. In this limit, the string profile becomes a constant, equaling $\rho(y) \equiv \rho_0 \approx 1.825$. This time there is no maximal angular velocity at which the solution breaks down, but we rather find that the curve that this branch of solutions draws on the $(\Omega, \rho(y_l))$ plane is not a single valued function of Ω. For the $y_h = 100$ case we are considering, it starts from the point $(0, 1.825)$, follows monotonically to the point $(2.082, 1.361)$ and finally turns back to end at $(2.069, 1.300)$, where the light end of the string is spinning at the local speed of light. We exhibit the forms of the string profiles for $n = 0, 1, 2, 3$ in Figure 3.6.

In Figure 3.7, we plot the E vs. Q dependence of the different branches of spinning string solutions we have encountered. Let us first focus on the $n \geq 1$ branches, and specifically on their small Q limits. Similar to the analysis of the strings spinning in real space, we can consider the approximate solution, valid for small A,

$$\delta\rho = A\frac{1}{z}\left(\omega_n z_l \cos(\omega_n(z - z_l)) + \sin(\omega_n(z - z_l))\right) , \tag{3.73}$$

$$\theta = \omega_n t , \tag{3.74}$$

with $z \equiv 1/y$ and the ω_n's given by our ρ fluctuation spectrum. This solution leads to the

approximate small Q relation

$$E \approx m_h - m_l + m_l\,\omega_n z_l\,\frac{2\pi Q}{\sqrt{\lambda}}\ , \tag{3.75}$$

which is shown as the dashed straight lines in Figure 3.7 (left).

Decreasing Ω towards the critical angular velocities Ω_{nc}, $n \geq 1$, we observe that the charge Q approaches a critical value Q_{nc}, varying according to n, while the energy E approaches a universal constant $E_c \approx m_h$, independent of the branch in question. Both values, as well as the forms of the $E(Q)$ curves, are highly independent of the location of the heavy brane at sufficiently large values of y_h, and for $y_h \geq 10$, the first few values of Q_{nc} are $Q_{1c} = 0.258\sqrt{\lambda}/2\pi$, $Q_{2c} = 0.156\sqrt{\lambda}/2\pi$, and $Q_{3c} = 0.112\sqrt{\lambda}/2\pi$. This m_h independence can be understood by inspecting the form of the canonical momentum densities appearing in Eqs. (3.70)–(3.71). The charge density π^0_θ behaves at large y as $1/y^4$. The energy density scales at leading order as $\sqrt{\lambda}$, giving rise to the ground state mass $m_h - m_l$ of the heavy-light meson, but the first correction also behaves as $1/y^4$. These $1/y^4$ terms mean that the excitation energy as a function of the charge of the spinning string is highly insensitive to the form of the string profile at $y \gtrsim 10 y_l$.

If we proceed to even smaller frequencies, $0 < \Omega < \Omega_{nc}$, we notice that these $n > 0$ branches persist all the way down to zero. In the limit $\Omega \to 0$, the strings become marginally bound, like their real-space spinning counterparts, with an energy $E \approx m_h + m_l$. In contrast, the charges Q for the terminal solutions are not universal. For the case $m_h = 100 m_l$, we find that the terminal values of $2\pi Q/\sqrt{\lambda}$ are 0.762, 0.518, and 0.390 for the $n = 1$, 2, and 3 branches respectively. Like their real-space spinning counterparts, we suspect that these long strings are not stable for the exact same reasons.

Switching then to following the $n = 0$ branch on the (Q, E) plane, we observe that for a given value of the charge, these strings are always energetically favored in comparison with their $n \geq 1$ counterparts. In the limit $y_h \to \infty$, we find that the energy and charge of the critical solution on the $n = 0$ branch very quickly approach

$$E_{0c} \;=\; m_h - 6(1)\,\frac{m_l^4}{m_h^3} + \mathcal{O}\left(\frac{m_l^5}{m_h^4}\right), \tag{3.76}$$

$$\frac{2\pi Q_{0c}}{\sqrt{\lambda}} \;=\; 0.69868(1) - 4.0(5)\,\frac{m_l^3}{m_h^3} + \mathcal{O}\left(\frac{m_l^4}{m_h^4}\right), \tag{3.77}$$

where the coefficients of the first terms have been found by fitting a variety of trial functions to our numerical data and the errors have been estimated in a very conservative manner. The vanishing of the first few corrections in $1/m_h$ is similar to the suppression of $1/m_h$ corrections in the ρ fluctuation analysis of Section 3.5.3. The $n = 0$ branch does not appear to admit long string solutions.

Small Ω limit of the $n = 0$ branch

To conclude our inspection of the string spinning in the θ direction, we will now take a closer look at the limit of infinitesimally small Ω in order to gain more understanding of the behavior of the $n = 0$ solutions there. We note that this limit corresponds to approximating $y_l \gg \Omega$, and therefore implies that we may use the relation $u^4 - \Omega^2\rho^2 \approx u^4$ in the equation of motion for ρ. On the other hand, the observed fact that ρ is nearly a constant in this case implies that

$$\left(u^2 - 2\rho^2 + 2y_5\rho\rho'\right)\left(1 + (\rho')^2\right)\rho \;\approx\; \left(u^2 - 2\rho^2\right)\rho, \tag{3.78}$$

finally giving as the equation to solve

$$u^6\rho'' + \Omega^2\left(u^2 - 2\rho^2\right)\rho \;=\; 0. \tag{3.79}$$

In the last form, we note that we may write

$$\rho(y) \;=\; \rho_0 + \delta\rho(y), \tag{3.80}$$

where ρ_0 is a constant and $\delta\rho(y)$ satisfies the Neumann boundary conditions at $y = y_l$ and $y = y_h$. We define ρ_0 by the constraint that $\delta\rho \to 0$, as $y \to y_h$. Using this parametrization and the fact that $y_l \gg \Omega$, we see that $\delta\rho$ satisfies the equation of motion

$$\delta\rho'' \;=\; -\Omega^2 \frac{(y^2-\rho_0^2)}{(y^2+\rho_0^2)^3}\,\rho_0\ . \tag{3.81}$$

If we enforce the boundary condition at $y = y_h$, this differential equation can then be integrated to yield

$$\begin{aligned}\delta\rho(y)/\Omega^2 \;&=\; \frac{(y-y_h)\left(\rho_0^4(y-2y_h)-\rho_0^2 y y_h(3y-y_h)-y^2y_h^3\right)}{4\rho_0(y^2+\rho_0^2)(y_h^2+\rho_0^2)^2}\\ &+\; \frac{y}{4\rho_0^2}\left(\arctan\left[\frac{y}{\rho_0}\right]-\arctan\left[\frac{y_h}{\rho_0}\right]\right),\end{aligned} \tag{3.82}$$

from where — demanding that the derivative of this expression vanish also at $y = y_l$ — we finally obtain as the equation for ρ_0

$$\frac{(y_l^2+3\rho_0^2)y_l\rho_0}{(y_l^2+\rho_0^2)^2}-\frac{(y_h^2+3\rho_0^2)y_h\rho_0}{(y_h^2+\rho_0^2)^2} \;=\; \arctan\left[\frac{y_h}{\rho_0}\right]-\arctan\left[\frac{y_l}{\rho_0}\right]. \tag{3.83}$$

Solving this equation numerically produces two solutions, $\rho_0 = 0$ and $\rho_0 = F(y_h/y_l) \times y_l$, of which we can throw out the former, as it is not consistent with our assumption of a small $\delta\rho$ and furthermore leads to a vanishing angular momentum. The latter result, on the other hand, is a slowly varying function of y_h/y_l for large values of this ratio, approaching in the $y_h/y_l \to \infty$ limit the result $\rho_0 \approx 1.82526\, y_l$. In contrast, for $y_h \approx y_l$, $F(y_h/y_l) \approx 1$.

Properties of the small-Ω solution

To get some feeling for the physical properties of the above solutions obtained for small $\Omega \ll y_l$, we will next compute their energy E and internal angular momentum Q using Eq. (3.70), where the canonical momentum and internal angular momentum densities read approximately

$$\pi_t^0 \approx -\frac{L^2}{2\pi\alpha'}\left(1+\frac{\rho_0^2\Omega^2}{2u_0^4}\right) \qquad \text{and} \qquad \pi_\theta^0 \approx \frac{L^2}{2\pi\alpha'}\,\frac{\rho_0^2\Omega}{u_0^4}\,, \tag{3.84}$$

with $u_0^2 \equiv y^2 + \rho_0^2$. Here, we have neglected higher order corrections in Ω and used the approximate solution (3.82). Performing the integrals, we obtain

$$E \approx \frac{L^2}{2\pi\alpha'}\left(y_h - y_l + \frac{\Omega^2}{2y_l}\,\Upsilon\right) \qquad \text{and} \qquad Q \approx \frac{L^2}{2\pi\alpha'}\,\frac{\Omega}{y_l}\,\Upsilon, \tag{3.85}$$

in which we have defined the dimensionless constant

$$\Upsilon \;\equiv\; \rho_0^2 y_l \int_{y_l}^{y_h} dy\,\frac{1}{(y^2+\rho_0^2)^2} \;=\rho_0^2 y_l\left(\frac{y_l}{(\rho_0^2+y_l^2)^2}-\frac{y_h}{(\rho_0^2+y_h^2)^2}\right)\ . \tag{3.86}$$

In deriving Eq. (3.86), we have made use of Eq. (3.83). Note that we have

$$\lim_{y_h\to\infty}\Upsilon \approx 0.17757 \qquad \text{while} \qquad \lim_{y_h\to y_l}\Upsilon = \frac{y_h-y_l}{4y_l}\ . \tag{3.87}$$

We may now easily solve Ω in terms of Q from Eq. (3.85) above, which allows us to write E in terms of Q

$$E \approx m_h - m_l + \frac{m_l}{2\Upsilon}\left(\frac{2\pi Q}{\sqrt{\lambda}}\right)^2. \tag{3.88}$$

Thus we find again that the excitation spectrum does not depend on m_h at leading order in the heavy quark mass limit. As we can see from Figure 3.7, this analytic approximation is quite good even for moderately large values of Q.

3.7 Hyperfine splitting and the Zeeman effect

In the previous sections we have calculated the spectrum of heavy-light mesons and found that the spectrum is m_h independent in the heavy quark limit but we could not see hyperfine splitting (3.50). But in our fluctuation analysis, there are degeneracies in the spectrum, which provide us with a starting point to look for hyperfine splitting. For example, the lowest lying mode in the x direction is a vector meson with the same energy as the scalar meson corresponding to the lowest lying excitation in the y_6 direction. This the degeneracy is a consequence of supersymmetry, protecting the masses of mesons inside supermultiplets.

We will now demonstrate how some of the degeneracies of the supersymmetric meson spectrum can be removed upon breaking supersymmetry, thus leading to the emergence of hyperfine structure. The explicit SUSY breaking scenarios we consider involve on one hand tilting one of the two fundamental D7-branes inside the internal $\mathbb{R}^6$ space, and on the other hand applying an external magnetic field on the (untilted) branes. The latter scenario leads to the well-known Zeeman effect, which we inspect for both weak and strong magnetic fields.

3.7.1 Hyperfine splitting

Now we are breaking SUSY by tilting the heavy brane. Consider a slight deformation of the setup introduced in the previous Section 3.4, in which the embedding equations of the heavy brane are shifted to $y = y_h$ and

$$\cos\theta\, y_6 - \sin\theta\, y_4 = 0, \tag{3.89}$$

corresponding to tilting the brane in the y_4, y_6 plane by an angle θ. (From now on, we will write the 4 and 6 as lower indices.) On the field theory side, the redefinition of the $AdS_5 \times S^5$ coordinates that would keep the tilted D7-brane at $y_6 = 0$ corresponds to an SU(4) R symmetry transformation acting on the $\mathcal{N} = 4$ scalars and fermions in the **6** and **4** representations, respectively. Hence, the Lagrangian of the deformed, non-SUSY theory can be obtained from that of pure $\mathcal{N} = 2$ SYM theory by applying suitable transformations on its fields, which has indeed been performed in Ref. [77].

In Ref. [77], it was pointed out that for massless and thus overlapping D7-branes, the tilting produces tachyonic modes which translate into a Coleman-Weinberg instability in the effective potential for the fundamental scalars. In our theory, we assume that the D7-branes are separated by a large enough distance that the tachyon is absent. In field theory terms, this assumption implies that the difference in mass between the hypermultiplets is large compared to the string scale. However, because SUSY is broken, the force between the D7-branes will not vanish and the form of the potential can be found in Ref. [78]. We ignore this force in this Section and assume some unspecified physical effect has stabilized the D7-branes at their rotated positions [7].

[7] While we can specify the asymptotic behavior of the D7-branes through boundary conditions, a stabilization mechanism is needed to keep the branes from deforming in the interior of the geometry.

On the gravity side, the tilting of the heavy brane affects the spectra of string fluctuations by modifying the boundary conditions that the y_6 and y_4 fluctuations have to satisfy. The respective Dirichlet and Neumann boundary conditions of these two modes at $y = y_h$ now become

$$\cos\theta\, y_6(y_h) - \sin\theta\, y_4(y_h) = 0, \tag{3.90}$$
$$\sin\theta\, y_6'(y_h) + \cos\theta\, y_4'(y_h) = 0, \tag{3.91}$$

which leads to a shift in the frequencies ω that in the $\theta \to 0$ limit can be read off from (3.33). To see this shift quantitatively, we now choose the worldsheet coordinate as $\sigma = 1/y$ and assume a time dependence $y_i \sim e^{-i\omega t}$ for the fluctuations. In this case, both fluctuations satisfy the same linearized differential equation

$$y_i'' + \frac{2}{\sigma} y_i' = -\omega^2 y_i, \tag{3.92}$$

where $y_i' \equiv \partial_\sigma y_i$ [31].

It is easily verified that the solutions to Eq. (3.92) that satisfy the correct boundary conditions at the untilted light brane can be written in the forms $y_6 = C_6 D(\sigma)$ and $y_4 = C_4 N(\sigma)$, where

$$D(\sigma) = \frac{1}{\sigma}\sin(\omega(\sigma - \sigma_l)), \tag{3.93}$$
$$N(\sigma) = \frac{1}{\sigma}\left[\omega\sigma_l \cos(\omega(\sigma - \sigma_l)) + \sin(\omega(\sigma - \sigma_l))\right]. \tag{3.94}$$

We may now write the boundary conditions at the heavy brane as a two-by-two matrix equation for the vector $v \equiv (C_6, C_4)$, $Mv = 0$, from which we immediately see that the condition for having non-zero solutions is that the determinant of the matrix M vanish,

$$\cos^2\theta\, D(\sigma_h)N'(\sigma_h) + \sin^2\theta\, D'(\sigma_h)N(\sigma_h) = 0. \tag{3.95}$$

The solutions to this equation and the corresponding eigenvectors of M correspond to linear combinations of the y_6 and y_4 fluctuations that are the physical fluctuation modes of the new system.

An observation important for understanding the solutions to Eq. (3.95) in the heavy quark limit $\sigma_h \sim 1/m_h \approx 0$ is that because of the prefactor $1/\sigma$ in Eqs. (3.93) and (3.94),

$$N'(\sigma_h) = -\frac{1}{\sigma_h}N(\sigma_h) + \mathcal{O}(1), \tag{3.96}$$
$$D'(\sigma_h) = -\frac{1}{\sigma_h}D(\sigma_h) + \mathcal{O}(1). \tag{3.97}$$

This implies that to leading order in σ_h, the θ dependence vanishes from Eq. (3.95) and the allowed frequencies are given by the solutions to $N'(\sigma_h) = 0$ and $D(\sigma_h) = 0$ that can be read off from (3.50). For the y^6 case, the unperturbed solutions read

$$\omega_n = \frac{\pi n}{\sigma_l - \sigma_h}, \quad n \in \mathbb{Z}^+, \tag{3.98}$$

while for the y_4 fluctuations, we have to solve the transcendental equation

$$\frac{\omega\,(\sigma_l - \sigma_h)}{1 + \sigma_l\sigma_h\omega^2} = \tan(\omega(\sigma_l - \sigma_h)) \tag{3.99}$$

that also leads to a discrete spectrum.

To determine the leading order corrections to the frequency spectra due to the tilting of the heavy brane, we proceed as follows. Anticipating that the eigenvectors of M can at least to leading order still be identified with the y_6 and y_4 fluctuations, we make a frequency ansatz of the form

$$\omega = \omega_0 + \omega_1 \frac{\sigma_h}{\sigma_l} + \mathcal{O}\left(\frac{\sigma_h^2}{\sigma_l^2}\right), \tag{3.100}$$

where ω_0 corresponds to the $\theta = 0$ frequencies of Eqs. (3.98) and (3.99). Looking first at fluctuations in the (mostly) y_6 direction, we expand Eq. (3.95) around $\omega_{0n} \equiv \pi n/(\sigma_l - \sigma_h)$, obtaining

$$\omega_n = \frac{\pi n}{\sigma_l - \sigma_h} - \frac{n\pi\sigma_h}{\sigma_l^2}\sin^2\theta + \mathcal{O}\left(\frac{\sigma_h^2}{\sigma_l^3}\right). \tag{3.101}$$

For the y_4 direction, we similarly get

$$\omega_n = \omega_{0n} + \frac{2\sigma_h}{\sigma_l^2}\csc[2\omega_{0n}\sigma_l]\,\sin^2\theta + \mathcal{O}\left(\frac{\sigma_h^2}{\sigma_l^3}\right), \tag{3.102}$$

where the ω_{0n}'s are now obtained from Eq. (3.99).

Eqs. (3.101) and (3.102) describe the energy spectra of our heavy-light mesons. To make the existence of hyperfine structure clear, recall that $\sigma_h \sim 1/m_h$ and $\sigma_l \sim 1/m_l$. Recall also that the energy spectra of the heavy-light excitations that correspond to fluctuations in the x^i and y^i, $i = 1, 2, 3$, directions were unchanged in the tilting, and are thus given by the $\theta \to 0$ limit of Eqs. (3.101) and (3.102), respectively. Thus, there exist energy splittings between the y_4, y_6 fluctuations and the the x^i and y^i fluctuations of order m_l^2/m_h. It would be a very interesting exercise in perturbation theory to try to produce a similar structure in the energies of the weakly coupled bound states of the deformed theory, proceeding along the lines of Ref. [79]. We, however, leave this investigation for future work.

3.7.2 The Zeeman effect

Another possibility for breaking SUSY in the setup of Section 3.3 is to apply an external magnetic field on one or both of the D7-branes in the system. In general this will lead to a force between the branes, but there are certain configurations, *e.g.* if the same magnetic field is applied to both branes, where the system will be a stable BPS configuration [80] . However, in what follows we will use arbitrary magnetic fields and again assume a stabilizing mechanism.

Here, we will for simplicity study a setting in which the U(1) gauge fields living on the branes correspond to a constant magnetic field pointing in the x^3 direction, *i.e.*

$$2\pi F_{(2)} = 2\pi H\, dx^1 \wedge dx^2 = \sqrt{\lambda} b\, dx^1 \wedge dx^2, \tag{3.103}$$

where we have introduced a rescaled field $b \equiv 2\pi H/\sqrt{\lambda}$. In general, the magnetic field will change the embedding profiles of the branes, which become functions of the radial coordinate of the AdS space [57].

In order to study the change in embedding, we need to consider the DBI action (3.5), which governs the dynamics of the D7-branes at leading order in α'. We will set $B_{(2)} = 0$. For the following analysis it will be convenient to break $\mathbb{R}^6 = \mathbb{R}^4 \times \mathbb{R}^2$ and write the transverse part of the metric (3.3) as

$$\frac{L^2}{\chi^2 + \xi^2}\left[d\chi^2 + \chi^2 d\theta^2 + d\xi^2 + \xi^2 d\Omega_3^2\right] . \tag{3.104}$$

We will assume that the D7-brane sits at constant θ and is described by two functions $\chi(\sigma)$ and $\xi(\sigma)$, leading to an effective Lagrangian

$$\mathcal{L} = -\frac{\lambda N}{(2\pi)^4}\,\xi^3\sqrt{\chi'^2+\xi'^2}\sqrt{1+\frac{b^2}{(\xi^2+\chi^2)^2}}\ , \tag{3.105}$$

where we have made use of the normalization

$$\tau_7 L^8 \mathrm{Vol}(S^3) = \frac{\lambda N}{(2\pi)^4}\ . \tag{3.106}$$

We will analyze this Lagrangian in a gauge where $\sigma = \xi$.

A consequence of introducing a magnetic field on the brane is that the profile is not a constant but a more complicated function of the radial coordinate. The AdS/CFT dictionary relates asymptotics of χ to the bare mass of the quark m_0 and the chiral condensate $\langle\bar\psi\psi\rangle$:[8]

$$m_0 = \frac{\sqrt{\lambda}}{2\pi}\lim_{\xi\to\infty}\chi(\xi)\ ;\quad \langle\bar\psi\psi\rangle = \frac{\sqrt{\lambda}N}{(2\pi)^3}\lim_{\xi\to\infty}\xi^3\chi'(\xi)\ . \tag{3.107}$$

The kinetic mass of the quark [73] on the other hand can be computed from the length of the lightest straight string that stretches from the D7-brane to the origin

$$m_{\rm kin} = \frac{\sqrt{\lambda}}{2\pi}\chi(\xi_{min})\ . \tag{3.108}$$

Following Ref. [57] we can solve the equation of motion that comes from (3.105) in the limit $m_0^2 \gg H$. We find that

$$\chi(\xi) = \chi_0 + \frac{b^2}{4\chi_0(\xi^2+\chi_0^2)} + \mathcal{O}(H^4) \quad \text{where} \quad m_0 = \frac{\sqrt{\lambda}}{2\pi}\chi_0\ . \tag{3.109}$$

From this perturbative solution, we can determine the relation between the bare and kinetic mass and also the value of the chiral condensate:

$$m_{\rm kin} = m_0 + \frac{\lambda H^2}{16\pi^2 m_0^3} + \mathcal{O}(H^4)\ , \tag{3.110}$$

and

$$\langle\bar\psi\psi\rangle = -\frac{N}{(2\pi)^2}\left[\frac{H^2}{m_0} + \mathcal{O}(H^4)\right]\ . \tag{3.111}$$

The most important conclusion for what follows is that the difference between m_0 and $m_{\rm kin}$ in the limit $m_0^2 \gg H$ is suppressed by a power of $H^2/m_{\rm kin}^4$. The suppression implies that unless we consider very large magnetic fields, we may ignore these bending effects at least for the heavy brane.

We may also consider the embedding of a general D7-brane with a magnetic field of an arbitrary size by numerically solving the equation of motion derived from Eq. (3.105). Normalizing the various quantities in the natural way, we obtain the chiral condensate $\sqrt{\lambda}\langle\bar\psi\psi\rangle/(Nm_{\rm kin}^2)$ as functions of the magnetic field $\sqrt{\lambda}H/(2\pi m_{\rm kin}^2)$ in the form shown in Figure 3.8.

Now we will study the effect of an external magnetic field on the heavy-light mesons. Starting from the most general case possible, we introduce independent magnetic fields, H_h and H_l (or b_h and b_l) for the heavy and light branes, respectively, and study small fluctuations of the

[8] Note that defining $S = \int \mathcal{L} d\xi$, the action evaluated on-shell for our static configuration is minus the free energy $S = -F$. Then we have $\langle\bar\psi\psi\rangle = \frac{\partial F}{\partial m_0}$.

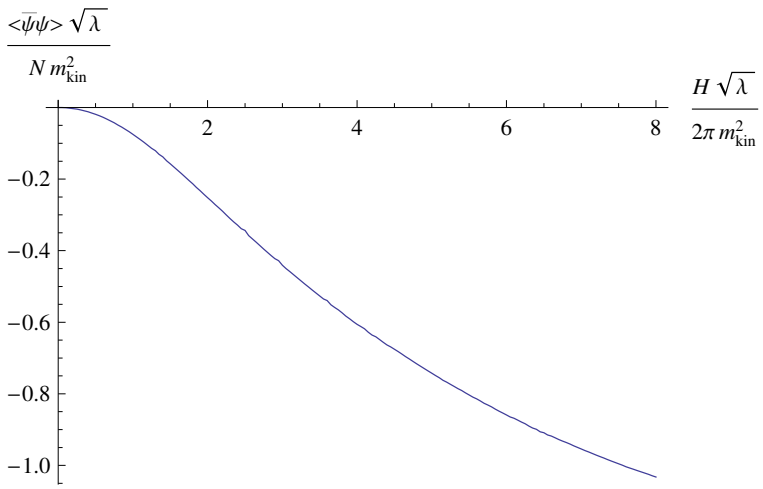

Figure 3.8: Plot of the chiral condensate, $\sqrt{\lambda}\langle\bar{\psi}\psi\rangle/(Nm_{\rm kin}^2)$, as function of the magnetic field H.

string around the unperturbed solution. The unperturbed straight string is orthogonal to the D7-brane at the point where they meet, and thus the fluctuations don't experience the bending of the brane to linear order. Neglecting bending effects, we may simply repeat the analysis of the previous section. The only difference is that it is now the coupling of the magnetic field to the endpoints of the string (which behave just like charged particles) that changes the boundary conditions and thus the fluctuation spectra.

The new boundary conditions of the string can be read off from the equation

$$\partial_\sigma X^\mu + 2\pi\alpha' F^\mu{}_\nu \partial_\tau X^\nu = 0, \tag{3.112}$$

where X^μ are the coordinates of the string on the world volume of the brane and $F_{\mu\nu}$ is our field strength tensor. Working in the gauge $\sigma = 1/y$, we again assume a time dependence of the form $x_i \sim e^{-i\omega t}$, in which case the fluctuations in the x_1 and x_2 directions satisfy the linearized differential equation

$$x_i'' - \frac{2}{\sigma} x_i' = -\omega^2 x_i. \tag{3.113}$$

This equation has the general solution $x_i = \sum_{j=1}^2 C_{ij} f_j(\sigma)$, where

$$f_1 = \sin\omega\sigma - \omega\sigma\cos\omega\sigma\ , \quad f_2 = \cos\omega\sigma + \omega\sigma\sin\omega\sigma, \tag{3.114}$$

using which the boundary conditions of Eq. (3.112) can be expressed in the form of a four-by-four matrix equation $Mv = 0$, with $v = (C_{11}, C_{12}, C_{21}, C_{22})$.

The condition for the allowed frequencies becomes again that the determinant of the matrix M vanish. While the full expression for the determinant is too messy to reproduce here, we can study various limits thereof. One particularly simple one is that of small $b_l\sigma_l^2$ and $b_h\sigma_h^2$, in which case we easily obtain

$$\omega_{n\pm} = \frac{\pi n \pm (b_l\sigma_l^2 - b_h\sigma_h^2)}{\sigma_l - \sigma_h}, \tag{3.115}$$

the $b_l = b_h = 0$ limit of which naturally agrees with Eq. (3.98). Moreover, if we set $b_l = 0$, then the magnetic field on the heavy brane leads to meson mass splittings proportional to $1/m_h^2$.

Finally, we study in some more detail the case where a magnetic field of an arbitrary magnitude is applied on the heavy brane but $b_l = 0$. Here, the vanishing of the determinant leads to the condition

$$b_h = \pm\,\frac{\omega/\sigma_h}{|1 + \omega\sigma_h\cot((\sigma_l - \sigma_h)\omega)|}\,, \tag{3.116}$$

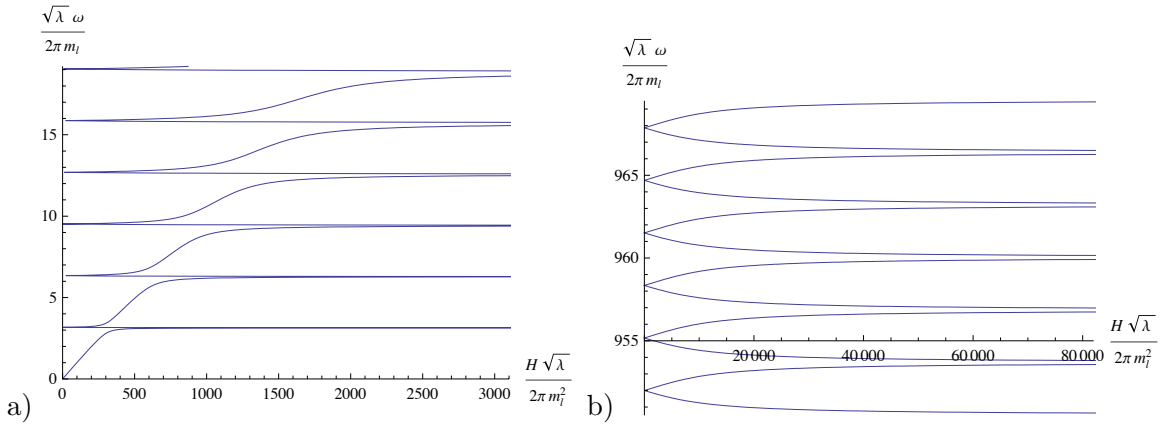

Figure 3.9: The dependence of the x_1 and x_2 fluctuation frequencies ω on the magnitude of the magnetic field H in the case where $m_h/m_l = 100$: a) the branches $n = 1, 2, ..., 6$ (and half of the zero branch) are displayed; b) the branches $n = 301, 302, ..., 306$. In the limit of small H, the frequencies can be read off from Eq. (3.115), while for large values of the magnetic field, the behavior of the curves is given by Eq. (3.118).

which we may attempt to invert to find the allowed frequency spectrum. While the small-b_h limit is given by Eq. (3.115), for very large values of the magnetic field we clearly obtain the b_h independent equation

$$\tan((\sigma_l - \sigma_h)\omega) = -\omega\sigma_h, \tag{3.117}$$

which comes with the approximate solutions

$$\begin{aligned} \omega_n &\approx \frac{\pi n}{\sigma_l}, \quad n \approx 1, \\ \omega_n &\approx \frac{\pi n}{\sigma_l - \sigma_h} - \frac{1}{\sigma_l - \sigma_h} \arctan\left[\frac{\pi n}{\sigma_l/\sigma_h - 1}\right], \quad n \gg 1. \end{aligned} \tag{3.118}$$

In Figure 3.9, we display the behavior of the frequencies as functions of b_h, obtained after numerically inverting Eq. (3.116). From here, we can identify both the usual Zeeman splitting, described by Eq. (3.115), as well as the subsequent rejoining of the frequencies according to Eq. (3.118).

3.8 Discussion

Although different in many respects, the heavy-light mesons we have studied have a spectrum which shares certain properties of real-world heavy-light mesons. For example, consider the case where there are two heavy quarks h and h' and two light quarks l and l'. We find for the ground state heavy-light mesons that

$$M_{hl} - M_{hl'} = m_{l'} - m_l = M_{h'l} - M_{h'l'} \ . \tag{3.119}$$

This kind of relation is similar to the real world relation (see for example Ref. [58]) for mesons containing a charm or bottom quark,

$$m_{B_s} - m_B \approx m_{D_s} - m_D \approx 100 \text{ MeV} \ . \tag{3.120}$$

Of course, the sign of the above difference is wrong: While for us, given that $m_l > m_{l'}$, we would find a negative difference, in the real world the difference is positive. This sign

difference is, however, of little significance in this $\mathcal{N} = 2$ SYM theory. In Section 3.3, we noted that we could let the lighter D7-brane end along $w^3 = c'$ where $c' \in \mathbb{C}$ and $|c'| = 1/z_l$. This case still preserves $\mathcal{N} = 2$ supersymmetry and allows us to tune the mass of the ground state heavy-light meson to be anything between $m_h - m_l$ and $m_h + m_l$.

Continuing the comparison with QCD, we can consider the mass difference between an excited and a ground state heavy-light meson in QCD. From the review [58], we learn that a typical QCD prediction of this heavy quark limit is that the difference in energy between excited and ground state heavy-light mesons should obey the relations

$$m_{B_2^*} - m_B \approx m_{D_2^*} - m_D \approx 593 \text{ MeV} , \quad m_{B_1} - m_B \approx m_{D_1} - m_D \approx 557 \text{ MeV} . \tag{3.121}$$

Unfortunately, there is no good data yet for $m_{B_2^*}$ and m_{B_1}. These differences are consistent with our result that the energy excitations scale with m_l, although in real world QCD, we expect to have m_l replaced with Λ_{QCD}.

The electromagnetic mass splittings of heavy-light mesons in QCD are typically tiny [81]. For example, $m_{D^\pm} - m_{D^0} \approx 5$ MeV while $m_{B^0} - m_{B^\pm} \approx 0.4$ MeV. It is suggestive that in the large λ limit, our approximate formula (3.88) for the Q dependence of the masses is suppressed by an additional power of $Q/\sqrt{\lambda}$ compared with the linear scaling of Eq. (3.62) on $J/\sqrt{\lambda}$. However, we have no good understanding of the relative sizes of the splittings for these D and B mesons.

Finally, we make some comments regarding two specific open questions related to our work.

Hybrid mesons

In phenomenological QCD literature, one finds discussion of hybrid mesons. In perturbative language, such an object would be a bound state of a quark, antiquark, and gluon [82], while at strong coupling, there exist models of a heavy quark and antiquark joined by a vibrating flux tube [83]. This second picture is similar to but also rather different from our model. Like us, the authors of Ref. [83] begin by finding the modes of the vibrating flux tube joining the quarks. However, in their model, both quarks are heavy. Also, and perhaps more importantly, the quarks themselves have a mass large compared to the energy of the flux tube, whereas in ours, the mass of the meson is the mass of the flux tube. As a next step, the authors of Ref. [83] use the vibrating flux tube to construct a phenomenological Cornell like potential through which the massive quarks interact. Despite these differences, one wonders if there exists a closer connection between our heavy-light mesons in $\mathcal{N} = 2$ SYM and hybrid heavy-light mesons in QCD — if such things exist — rather than the "ordinary" heavy-light mesons of QCD.

W bosons

One may also consider Higgsing the $\mathcal{N} = 4$ SU(N) SYM theory down to SU($N-2$) $\times U(1)^2$. In the dual gravitational picture, this Higgsing corresponds to pulling two D3 branes off of the stack of N D3 branes, whose low energy description this SYM theory is. As long as we keep the D3 branes parallel in this $AdS_5 \times S^5$ geometry, they do not experience a potential and we can imagine placing them at nonzero values of y, just as we did for the D7-branes. There is then a semi-classical string that stretches between the two D3 branes, whose fluctuations we may study and which has a dual field theory interpretation as a W boson.[9]

We mention this D3 brane and string construction because we can at this point in our analysis treat it very easily. The treatment of the string spinning in real space and corresponding to a heavy-light meson is identical for the W bosons. Also, the x fluctuations of such a string

[9] We would like to thank I. Klebanov for suggesting we think about this extension of our results.

are identical to the x fluctuations for the heavy-light meson. Finally, the y_6 fluctuations are identical, except that there are now four additional y_6-like directions perpendicular to the D3 brane string configuration. Whereas for the heavy-light meson, the x and y_6 fluctuations gave us four towers of identical modes, and the ρ fluctuations gave us another four towers, for the W boson, the x and y_6 fluctuations give us eight towers of identical modes. We believe this regrouping of one pair of four identical towers into eight identical towers is related to the doubling in the amount of supersymmetry. The $\mathcal{N} = 2$ SYM relevant for the heavy-light mesons has eight supercharges, whereas the $\mathcal{N} = 4$ SYM, after the Higgsing which breaks conformal invariance, should have 16.

Chapter 4

The Sakai-Sugimoto model

The model by Karch and Katz is the simplest model at hand where fundamental fields are introduced. But in order to come closer to QCD one wants models that exhibit dynamical chiral symmetry breaking, have less or no supersymmetry and also incorporate the chirality of fermions. A popular supergravity solution dual to a confining gauge theory is the Klebanov-Strassler background [60]. The dual field theory has $\mathcal{N} = 1$ supersymmetry and exhibits chiral symmetry breaking.

An example where supersymmetry is completely broken and confinement is present is the Constable-Mayers background [84]. This background has a non-constant dilaton and is convenient for embedding probe D7-branes because it preserves $SO(6)$ symmetry.

A model that can also account for chiral fermions is a setup where D6 and $\overline{\text{D6}}$-brane probes are embedded in a D4 background geometry [85]. On the gauge theory side one has a $\mathcal{N} = 2$ supersymmetric five dimensional gauge theory that exhibits chiral symmetry breaking and confinement. But this model is still supersymmetric and can not account for the massless Goldstone bosons associated with the spontaneous breaking of chiral symmetry in QCD.

In another model, which comes even closer to QCD, D8 and $\overline{\text{D8}}$-branes are embedded in a D4 background geometry. This model has very nice features. It provides a holographic description for chiral symmetry breaking in a very intuitive geometrical form and can account for chiral fermions. It exhibits confinement and supersymmetry is completely broken, and it also contains the massless Goldstone bosons associated with chiral symmetry breaking. This model is based on an idea by Witten [21] and was improved by Sakai and Sugimoto [29]. In this chapter we give an introduction into this model and we will use it in Chapter 5 and 6.

4.1 The model

The idea is the following. One starts with N_c D4-branes in type IIA superstring theory. The D4-brane theory is a five dimensional supersymmetric $SU(N_c)$ gauge theory whose field content includes fermions, scalars and gauge fields in the adjoint representation of $SU(N_c)$. Then one compactifies one direction of the D4-branes on a circle with radius M_{KK}^{-1}, where M_{KK} is the Kaluza-Klein mass and imposes anti-periodic boundary conditions for the worldvolume fermions on this circle. This breaks supersymmetry completely by giving Kaluza-Klein masses to the fermions and scalars. The fermions acquire a mass at tree level and the scalars acquire a mass through one loop-effects. At energies sufficiently below the compactification scale the theory is effectively a four dimensional $SU(N_c)$ gauge theory without supersymmetry.

In the dual string theory the D4-branes are replaced by their near horizon supergravity background with one compact dimension. There are two different solutions for the metric, realized in two different temperature regimes. The transition from one to the other is interpreted as the deconfinement phase transition. Similar to the original AdS/CFT setting at

finite temperature [21], the deconfined phase has a black hole which is absent in the confined phase.

4.1.1 D4 background

We start with the confined phase. The type IIA supergravity (euclidean) metric of the confined phase is given by [85]

$$ds^2_{\rm conf} = \left(\frac{u}{R}\right)^{3/2}[d\tau^2+\delta_{ij}dx^i dx^j+f(u)dx_4^2]+\left(\frac{R}{u}\right)^{3/2}\left[\frac{du^2}{f(u)}+u^2 d\Omega_4^2\right] \quad (4.1)$$

$$e^{\phi} = g_s\left(\frac{u}{R}\right)^{3/4}, \qquad F_4 = dC_3 = \frac{2\pi N_c}{V_4}\epsilon_4, \qquad f(u)=1-\frac{u_{\rm KK}^3}{u^3} \quad (4.2)$$

Here, ϕ is the dilaton, $d\Omega_4^2$ is the metric of a four-sphere, F_4 is the field strength, ϵ_4 is the volume form on the unit four-sphere and $V_4 = 8\pi^2/3$ is its volume. u has dimension of length and can be interpreted as a radial coordinate in the directions transverse to the D4-branes. R is the curvature radius of the background which is related to the string coupling g_s and the string length ℓ_s via (B.15)

$$R^3 = \pi g_s N_c \ell_s^3 \,. \quad (4.3)$$

A crucial feature of the model is the compactified dimension x_4. In order to avoid a conical singularity at $u = u_{\rm KK}$, x_4 must be identified with period

$$x_4 \sim x_4 + \delta x_4, \qquad \delta x_4 = \frac{4\pi}{3}\frac{R^{1/2}}{u_{\rm KK}^{3/2}}. \quad (4.4)$$

We can relate the radius of the compact dimension to the Kaluza-Klein mass by identifying x_4 with the compact direction in the gauge theory

$$M_{\rm KK} \equiv \frac{2\pi}{\delta x_4} = \frac{3}{2}\frac{u_{\rm KK}^{1/2}}{R^{3/2}}. \quad (4.5)$$

This breaks supersymmetry completely by giving Kaluza-Klein masses to the adjoint fermions of the dual gauge theory and the analogue of thermal masses to the adjoint scalars, leaving only gauge bosons in the spectrum of the low-energy limit as the latter are protected by gauge symmetry [21]. The point $u = u_{\rm KK}$ is the tip of the cigar-shaped subspace spanned by x_4 and the holographic coordinate u. The subspace spanned by the euclidean time τ and the coordinate u is cylinder-shaped, with the circumference given by the inverse temperature, $\tau \equiv \tau + 1/T$.

In the deconfined phase the coordinates τ and x_4 interchange their roles, i.e., now the subspace spanned by x_4 and u is cylinder-shaped while the subspace spanned by τ and u is cigar-shaped. In this case, the metric is

$$ds^2_{\rm deconf} = \left(\frac{u}{R}\right)^{3/2}[\tilde{f}(u)d\tau^2+\delta_{ij}dx^i dx^j+dx_4^2]+\left(\frac{R}{u}\right)^{3/2}\left[\frac{du^2}{\tilde{f}(u)}+u^2 d\Omega_4^2\right], \quad (4.6)$$

where

$$\tilde{f}(u) \equiv 1-\frac{u_T^3}{u^3}\,. \quad (4.7)$$

Again, by avoiding a conical singularity at $u = u_T$ and identifying $\tau \equiv \tau + 1/T$ we can relate the temperature to the tip of the cigar-shaped τ-u space u_T via

$$T = \frac{3}{4\pi}\frac{u_T^{1/2}}{R^{3/2}}\,. \quad (4.8)$$

The deconfinement phase transition is located at a critical temperature $T = T_c$ where the free energies corresponding to the two phases are identical. This occurs at $u_{\rm KK} = u_{T_c}$ and thus $T_c = M_{\rm KK}/(2\pi)$. This critical temperature is independent of the chemical potential. Consequently, the model predicts a horizontal phase transition line in the T-μ_B plane, in accordance with expectations from QCD at infinite number of colors N_c [86].

The supergravity prescription depends on having the background weakly curved compared to the string scale. This is the case for large four-dimensional 't Hooft coupling [85] (see also Section 2.7)

$$\lambda = g_{\rm YM}^2 N_c = \frac{g_5^2 N_c}{2\pi M_{\rm KK}^{-1}} \gg 1\,, \tag{4.9}$$

where the five-dimensional gauge coupling g_5 is given by $g_5^2 = (2\pi)^2 g_s \ell_s$.

The Kaluza-Klein mass sets the energy scale below which the dual field theory is effectively four-dimensional. For large 't Hooft coupling, this scale is of the same order as the mass gap of the field theory; only for small λ, where string corrections become important, does one have duality with non-supersymmetric large-N_c QCD in four dimensions. However, there is already ample evidence that the limit of large 't Hooft coupling, where supergravity calculations are meaningful, does provide a useful tool for unravelling certain nonperturbative features of QCD.

4.1.2 Adding flavor branes

As explained in Section 2.9 one can introduce fields in the fundamental representation by adding flavor branes to the system to obtain a more realistic holographic model. Sakai and Sugimoto [29] extended Wittens model by adding N_f pairs of D8 and $\overline{\rm D8}$-branes which are transverse to the circle along x_4. The D8 and $\overline{\rm D8}$-branes extend in all dimensions except for the coordinate x_4 (whereas the D4-branes extend in the t, x_i, $i = 1, \ldots, 4$ directions)

	X_0	X_1	X_2	X_3	X_4	X_5	X_6	X_7	X_8	X_9
D4	x	x	x	x	x					
D8	x	x	x	x		x	x	x	x	x

(4.10)

This leaves only one function to specify the embedding of the probe branes in the background. As long as $N_f \ll N_c$, the D8/$\overline{\rm D8}$-branes can be treated as probe branes, i.e., the backreaction on the background geometry is neglected. The induced metrics on the probe branes in the confined and deconfined backgrounds are

$$ds^2_{\rm D8,conf} = \left(\frac{u}{R}\right)^{3/2}\left(d\tau^2 + \delta_{ij}dx^i dx^j\right) + \left(\frac{R}{u}\right)^{3/2}\left[\frac{v^2(u)}{f(u)}du^2 + u^2 d\Omega_4\right], \tag{4.11a}$$

$$ds^2_{\rm D8,deconf} = \left(\frac{u}{R}\right)^{3/2}\left[\tilde{f}(u)d\tau^2 + \delta_{ij}dx^i dx^j\right] + \left(\frac{R}{u}\right)^{3/2}\left[\frac{\tilde{v}^2(u)}{\tilde{f}(u)}du^2 + u^2 d\Omega_4\right], \tag{4.11b}$$

where we abbreviated

$$v(u) \equiv \sqrt{1 + f^2(u)\left(\frac{u}{R}\right)^3 (\partial_u x_4)^2}\,, \qquad \tilde{v}(u) \equiv \sqrt{1 + \tilde{f}^2(u)\left(\frac{u}{R}\right)^3 (\partial_u x_4)^2}\,. \tag{4.12}$$

Here the function $x_4(u)$ gives the embedding of the D8-branes in the x_4-u subspace.

By adding the flavor branes we introduced new degrees of freedom, namely strings with one endpoint attached to the D4-brane and the other attached to the D8 or the $\overline{\rm D8}$-branes. From these new strings we obtain N_f flavors of massless fermions in the fundamental representation

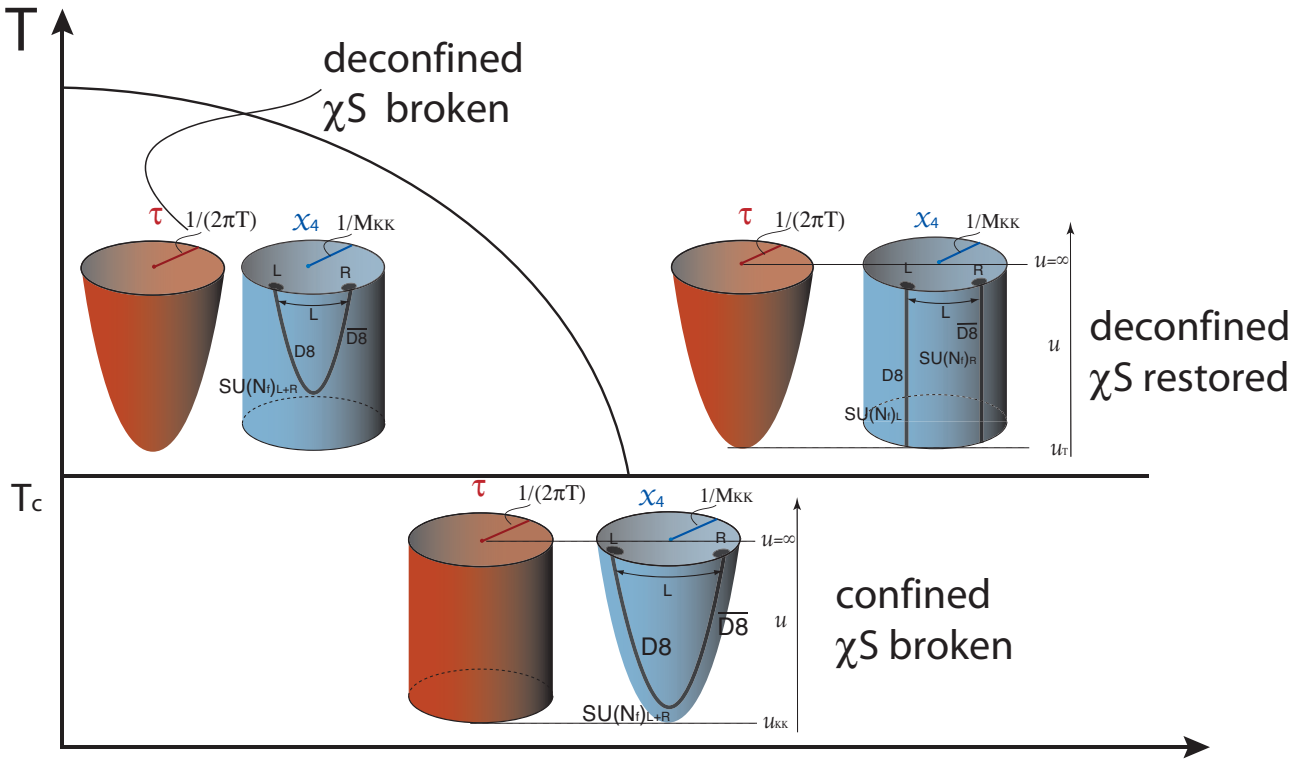

Figure 4.1: T-μ phase diagram as predicted by the Sakai-Sugimoto model. The horizontal line separates the confined phase from the deconfined phase. In the confined phase the $\tau - u$ subspace is cylinder-shaped and the $x_4 - u$ subspace is cigar-shaped. In the deconfined phase their roles are exchanged. We also show the embedding of the D8 and $\overline{\text{D8}}$-branes. In the confined phase the probe branes must connect, and the gauge fields living on them can not be rotated separately, giving a symmetry group $U(N_f)_{L+R}$. In the deconfined phase there are two possible embeddings for the D8-branes. If they are connected one is in the deconfined chiraly broken phase and if they are separated one is in deconfined phase with chiral symmetry $U(N_f)_L \times U(N_f)_R$.

of the color group of opposite chirality, which are located on the intersection of the D8 and and $\overline{\text{D8}}$-branes with the N_c D4-branes. We interpret these fermions as massless quarks of QCD.

The D4/D8-$\overline{\text{D8}}$ setup provides the tools to study not only the deconfinement phase transition but also the chiral phase transition. In the x_4 direction, the D8-branes are separated from the $\overline{\text{D8}}$-branes by a distance L. The maximal separation of the branes is $L = \pi/M_{\text{KK}}$ in which case the branes are attached at opposite sides of the circle spanned by x_4. Gauge fields on the D8 and $\overline{\text{D8}}$-branes transforming under a local symmetry group $U(N_f)$ induce a global symmetry group $U(N_f)$ on the five-dimensional boundary at $u = \infty$. More precisely, a gauge symmetry on the D8-branes induces a global symmetry at the four-dimensional subspace of the holographic boundary at $x_4 = 0$, while the gauge symmetry on the $\overline{\text{D8}}$-branes induces a separate global symmetry on the four-dimensional subspace at $x_4 = L$. Therefore the total global symmetry can be interpreted as the chiral group $U(N_f)_L \times U(N_f)_R$.

So far we have viewed the gauge symmetry on the D8-branes as independent from that on the $\overline{\text{D8}}$-branes. This is correct if the branes are geometrically separate. For example in the deconfined background, where the x_4-u subspace is cylinder-shaped, the branes follow straight lines from $u = u_T$ up to $u = \infty$, and thus are disconnected. However, it may also be

energetically favored for the branes to be connected. In this case, the gauge symmetry reduces to joint rotations, given by the vectorial subgroup $U(N_f)_{L+R}$. This is exactly the symmetry breaking pattern induced by a chiral condensate. In fact, in the confined phase, where the x_4-u subspace is cigar-shaped, the branes *must* connect. In other words, chiral symmetry is always broken in the confined phase. Whether the branes are disconnected in the deconfined phase depends on the separation scale L. For sufficiently large L they are always disconnected, while for smaller L the connected phase may be favored for certain temperatures [87]. In other words, in the former case, deconfinement and the chiral phase transition are identical while in the latter case they differ and there exists a deconfined but chirally broken phase in the T-μ_B plane [88]. We show the phase diagram in Figure 4.1. In this work, we shall use maximally separated branes, i.e., $L = \pi/M_{\rm KK}$. This simplifies the treatment since in this case we always have $\partial_u x_4 = 0$ because the D8-branes follow geodesics. The case of not maximally separated planes, more precisely the limit where the radius of the compactified dimension is much larger than the separation distance, $1/M_{\rm KK} \gg L$, corresponds to an NJL model on the field theory side [89].

Temperature and chemical potentials enter the model in very different ways. As explained above, temperature has a geometric effect on the background metric, in particular a black hole forms for sufficiently large T. Chemical potentials, however, enter as boundary conditions for the gauge fields on the D8 and $\overline{\rm D8}$-branes, i.e., in the subsequent Sections we will fix the baryon and isospin components of the temporal components of the "right-handed" and "left-handed" gauge fields at the boundary $u = \infty$ by the isospin and baryon chemical potentials. Analogously, nontrivial boundary values of the spatial components of the gauge fields have the interpretation of spatial gradients in chiral condensates, corresponding to supercurrents. We shall discuss the gauge field action associated with the flavor branes in more detail now.

4.2 Yang-Mills and Chern-Simons action

Now we write down the action that describes the dynamics of the flavor branes. We will at most work with two flavors and therefore we derive everything for a two flavor system and take the one flavor limit when we need to. The total action for the D8 and $\overline{\rm D8}$-branes is given by the sum of the Dirac-Born-Infeld (DBI) and the Chern-Simons (CS) actions. As indicated in the introduction and as will become clear below, the Chern-Simons term is necessary to account for nonzero baryon and isospin numbers. For simplicity, we shall expand the DBI action for small gauge fields such that we obtain a Yang-Mills contribution instead. This was also done for instance in Ref. [90], while other works used the full DBI action in a similar context, however for the simpler cases of a one-flavor system without isospin chemical potential [91] and without currents and magnetic field [92]. Our action takes the form

$$S_{\rm D8} = S_{\rm YM} + S_{\rm CS}\,. \tag{4.13}$$

Here, the Yang-Mills contribution is

$$S_{\rm YM} = 2N_f T_8 V_4 \int d^4x\, du\, e^{-\Phi}\sqrt{g}\left(1 - \frac{(2\pi\alpha')^2}{4N_f} g^{\mu\nu} g^{\rho\sigma} {\rm Tr}[\mathcal{F}_{\nu\rho}\mathcal{F}_{\sigma\mu}]\right), \tag{4.14}$$

where $T_8 = 1/[(2\pi)^8 \ell_s^9]$ is the D8-brane tension, where $\alpha' = \ell_s^2$, and where $V_4 = 8\pi^2/3$ is the volume of the unit 4-sphere. The remaining integrations are done over four-dimensional space-time t, x_1, x_2, x_3, and over the holographic coordinate u. In the confined (deconfined) phase the limits for this integration are $u_{\rm KK}(u_T) < u < \infty$, and the factor 2 on the right-hand side of Eq. (4.14) accounts for integration over D8 and $\overline{\rm D8}$-branes. In this section, all expressions are thus valid for both confined and deconfined phase, which differ, besides the integration

limits for u, by the metric g. The dilaton is $e^{\Phi} = g_s(u/R)^{3/4}$, and the trace is taken over the internal $U(2)$ space (from now on $N_f = 2$). Our convention for the field strength tensor is

$$\mathcal{F}_{\mu\nu} = \partial_\mu \mathcal{A}_\nu - \partial_\nu \mathcal{A}_\mu - i[\mathcal{A}_\mu, \mathcal{A}_\nu]\,, \tag{4.15}$$

where $\mu, \nu = 0, 1, 2, 3, u$, and where $\mathcal{A}_\mu$ is the $U(2)$ gauge field. It is convenient to separate the $U(1)$ part from the gauge fields and field strengths,

$$\mathcal{A}_\mu = \frac{\hat{A}_\mu}{2}\mathbf{1} + \frac{A^a_\mu}{2}\tau_a\,, \qquad \mathcal{F}_{\mu\nu} = \frac{\hat{F}_{\mu\nu}}{2}\mathbf{1} + \frac{F^a_{\mu\nu}}{2}\tau_a\,, \tag{4.16}$$

where $a = 1, 2, 3$ and τ_a are the Pauli matrices. With these conventions we have

$$\hat{F}_{\mu\nu} = \partial_\mu \hat{A}_\nu - \partial_\nu \hat{A}_\mu\,, \qquad F^a_{\mu\nu} = \partial_\mu A^a_\nu - \partial_\nu A^a_\mu + A^b_\mu A^c_\nu \epsilon_{abc}\,. \tag{4.17}$$

The Chern-Simons contribution in Eq. (4.13) is [93]

$$\begin{aligned} S_{\rm CS} &= -i\frac{N_c}{12\pi^2}\int \left\{\frac{3}{2}\hat{A}\mathrm{Tr}[F^2] + \frac{1}{4}\hat{A}\hat{F}^2 + \frac{1}{2}d\left[\hat{A}\mathrm{Tr}\left(2FA - \frac{i}{2}A^3\right)\right]\right\} \\ &= -i\frac{N_c}{96\pi^2}\int d^4x\, du \left\{\frac{3}{2}\hat{A}_\mu\left(F^a_{\nu\rho}F^a_{\sigma\lambda} + \frac{1}{3}\hat{F}_{\nu\rho}\hat{F}_{\sigma\lambda}\right)\right. \\ &\qquad \left. + 2\partial_\mu\left[\hat{A}_\nu\left(F^a_{\rho\sigma}A^a_\lambda + \frac{1}{4}\epsilon_{abc}A^a_\rho A^b_\sigma A^c_\lambda\right)\right]\right\}\epsilon^{\mu\nu\rho\sigma\lambda}\,, \end{aligned} \tag{4.18}$$

where, in the first line, we have used a notation in terms of differential forms in order to connect our expression to the one from Ref. [93] (our integration range is $u_{\rm KK} < u < \infty$; therefore, in order to integrate over D8 and $\overline{\rm D8}$-branes we need an additional factor 2 in the prefactor compared to Eq. (2.8) in Ref. [93]). The change of numerical prefactors in going from the first to the second line comes from performing the trace and from our convention of the field strength (4.15) (the factors for the latter are hidden in the wedge products in the first line). The boundary term does not enter the equations of motion but gives a contribution to the free energy.

4.3 Equations of motion

We can now derive the equations of motion for the gauge fields. We start by taking the variation with respect to the gauge fields of the Yang-Mills and Chern-Simons Lagrangians $\mathcal{L}_{\rm YM}$ and $\mathcal{L}_{\rm CS}$. They are given by the integrands (including the prefactors outside the integral) of the actions in (4.14) and (4.18). We present the general form of the variations for the confined phase in detail in Appendix C.1.

The equations of motion obtained from the variations (C.2), (C.3), (C.6), (C.7) are complicated coupled nonlinear differential equations for the gauge fields. We shall now simplify these equations by transforming the holographic coordinate u and by choosing a particular gauge. The new coordinate z we shall use from now on is defined through

$$u = (u_{\rm KK}^3 + u_{\rm KK} z^2)^{1/3}\,. \tag{4.19}$$

We have $z \in [-\infty, \infty]$ while $u \in [u_{\rm KK}, \infty]$. In the new coordinate, the boundaries of the connected D8 and $\overline{\rm D8}$-branes correspond to $z = -\infty$ for $x_4 = 0$ ("left-handed fermions") and $z = +\infty$ for $x_4 = L = \pi/M_{\rm KK}$ ("right-handed fermions"), while the point $z = 0$ corresponds to the tip of the cigar-shaped z-x_4 subspace in the bulk. We work in a gauge where $\mathcal{A}_z = 0$ [29, 94], see Section 6.2.1 for a discussion of this choice.

With the metric of the confined phase (4.1), the relations between the parameters of the model (4.3), (4.5), (4.9), and the new coordinate z (4.19), the Yang-Mills part of the action (5.2a) can be written as

$$S_{\rm YM} = \kappa \int d^4x \int_{-\infty}^{\infty} dz \left\{ \frac{16 M_{\rm KK}^2 k^{2/3}(z)}{9(2\pi\alpha')^2 u_{\rm KK}} + \frac{M_{\rm KK}^2}{u_{\rm KK}^2} k(z) {\rm Tr}[\mathcal{F}_{z\mu}^2] + \frac{1}{2} h(z) {\rm Tr}[\mathcal{F}_{\mu\nu}^2] \right\} , \qquad (4.20)$$

where $\mu, \nu = 0, 1, 2, 3$. Here,

$$h(z) \equiv (u_{\rm KK}^3 + u_{\rm KK} z^2)^{-1/3} , \qquad k(z) \equiv u_{\rm KK}^3 + u_{\rm KK} z^2 \qquad (4.21)$$

and

$$\kappa \equiv \frac{\lambda N_c}{216\pi^3} . \qquad (4.22)$$

In deriving Eq. (4.20) we have used that the field strengths are symmetric or antisymmetric functions of z.

Since we work at finite temperature, we need to work in Euclidean space. However, in what follows, it turns out to be more convenient to use Minkowski notation. More precisely, we start from the Euclidean action with imaginary time τ and replace $A_0 \to i A_0$, after which we may write the result using a Minkowski metric with signature $(-,+,+,+)$. The space-time integral is denoted by d^4x for simplicity but actually is an integral $d\tau\, d^3x$ over imaginary time τ and three-dimensional space. Our convention for the ϵ-tensor is $\epsilon_{0123} = 1$. In this notation the equations of motion for the confined phase in the new coordinate z are

$$\kappa M_{\rm KK}^2 \partial_z [k(z) \hat{F}^{z\mu}] + \kappa h(z) \partial_\nu \hat{F}^{\nu\mu} = \frac{N_c}{32\pi^2} (F_{z\nu}^{(a)} F_{\rho\sigma}^{(a)} + \hat{F}^{z\nu} \hat{F}^{\rho\sigma}) \epsilon^{\mu\nu\rho\sigma} , \quad (4.23a)$$

$$\kappa M_{\rm KK}^2 \partial_\mu [k(z) \hat{F}^{z\mu}] = \frac{N_c}{128\pi^2} (F_{\mu\nu}^{(a)} F_{\rho\sigma}^{(a)} + \hat{F}_{\mu\nu} \hat{F}_{\rho\sigma}) \epsilon^{\mu\nu\rho\sigma} , \quad (4.23b)$$

$$\kappa M_{\rm KK}^2 D_z [k(z) F^{(c)z\mu}] + \kappa h(z) D_z F^{(c)z\mu} = \frac{N_c}{16\pi^2} (\hat{F}_{z\nu} F_{\rho\sigma}^{(a)}) \epsilon^{\mu\nu\rho\sigma} \quad (4.23c)$$

$$\kappa M_{\rm KK}^2 D_\mu [k(z) F^{(c)z\mu}] = \frac{N_c}{64\pi^2} (\hat{F}_{\mu\nu} F_{\rho\sigma}^{a}) \epsilon^{\mu\nu\rho\sigma} , \quad (4.23d)$$

where the covariant derivative is given by

$$D_z F^{(a)z\mu} = (\delta_{ac} \partial_z + A_z^b \epsilon_{abc}) F^{(c)z\mu} \qquad D_\mu F^{(a)\mu\nu} = (\delta_{ac} \partial_\mu + A_z^b \epsilon_{abc}) F^{(c)\mu\nu} . \qquad (4.24)$$

The second and fourth equation of motion are obtained by varying $\hat{A}_z, A_z^{(a)}$ in the action prior to setting $A_z = 0$.
To obtain the equations of motion for the deconfined phase one has to replace $k(z) \to k_\mu(z)$ where

$$k_0(z) \equiv \frac{(u_T^3 + u_T z^2)^{3/2}}{z\, u_T^{1/2}} , \qquad k_3(z) \equiv z\, u_T^{1/2} (u_T^3 + u_T z^2)^{1/2} , \qquad (4.25)$$

due to different metric functions for the temporal and spatial coordinates in the metric (4.6).

Chapter 5

Anomalies and chiral currents in the Sakai-Sugimoto model

This chapter is based on [33]. Topologically charged gauge field configurations in QCD generate chirality due to the nonabelian axial anomaly. In the presence of a magnetic field, this chirality, *i.e.*, an imbalance in the number of right- and left-handed quarks, has been predicted to generate an electromagnetic current parallel to the applied magnetic field. This is a consequence of the QED axial anomaly and has been termed chiral magnetic effect [95, 96, 97]. As a result, electric charge separation may occur in noncentral heavy-ion collisions, where magnetic fields up to $10^{17}\,\mathrm{G}$ can be generated temporarily, and corresponding experimental evidence has in fact been reported in Refs. [98, 99] (see however Ref. [100]).

In a simplified picture, one may study the induced current for a static magnetic field. The generalization to time-dependent magnetic fields, as produced in heavy-ion collisions, in principle amounts to computing a frequency-dependent conductivity [97, 101]. However, the observed charge separation is proportional to the zero-frequency limit [97]. In this work, the currents we compute always correspond to the zero-frequency limits of the conductivities.

Another simplification of the highly nontrivial scenario of a heavy-ion collision is to mimic the (event-by-event) topologically induced chirality by a nonzero axial chemical potential μ_5, the difference of right- and left-handed chemical potentials. The resulting current is a vector current proportional to μ_5. In a more general setup, although negligible in the heavy-ion context, one may also include a quark chemical potential μ, which is the same for right- and left-handed fermions. Again via a nonzero magnetic field, an axial current is generated in this case [102, 103]. This effect may be of relevance for the physics of compact stars [104], where strongly interacting matter can reach densities of several times nuclear ground state density, and (surface) magnetic fields up to $10^{15}\,\mathrm{G}$ have been measured, indicating the possibility of even higher magnetic fields in the interior. Also the direct high-density analogue of the chiral magnetic effect has been studied in the context of neutron star physics [105].

We apply a strong-coupling approach, based on the AdS/CFT correspondence [14, 106, 107], to compute both kinds of currents. We use a general setup to account for nonzero temperatures, relevant in the context of heavy-ion collisions, as well as for nonzero quark chemical potentials, relevant in the astrophysical context. Besides the chirally symmetric phase we also consider the chirally broken phase which is important in both contexts: heavy-ion collisions are expected to probe the region of the QCD chiral phase transition; in quark matter at densities present in compact stars, chiral symmetry may also be spontaneously broken, for example in the color-flavor locked phase [8].

The Sakai-Sugimoto model [29] introduced in the previous Section is particularly suited for our purpose since it has a well-defined concept for chirality and the chiral phase transition. It is straightforward to introduce right- and left-handed chemical potentials independently. Several

previous works have considered currents in a magnetic field at nonzero chemical potentials in this model [91, 90, 34, 108]. The purpose of this chapter is two-fold. The physical motivation is to extend these calculations to the currents relevant for the chiral magnetic effect, and to compare our strong-coupling results to the weak-coupling results [96] as well as the lattice results [109] in the existing literature. There is also a more theoretical purpose of our work, addressing certain fundamental properties of the Sakai-Sugimoto model. We discuss in detail how to implement the covariant QED anomaly into the model in order to obtain physically acceptable predictions. Moreover, we elaborate on an ambiguity in the definition of the chiral currents in the presence of a Chern-Simons term that has been observed previously [91, 34, 108] (see also [110]).

This chapter is organized as follows. We start with a general discussion of the currents, in particular the appearance of consistent and covariant anomalies, in Section 5.1. In Section 5.2 we discuss the solution of the equations of motion in the presence of background magnetic and electric fields. We present analytical solutions for the chirally broken phase, Section 5.2.1, and the chirally symmetric phase, Section 5.2.2. We then discuss the ambiguity of the currents, defined on the one hand via the general definition from Section 5.1, and on the other hand from the thermodynamic potentials obtained in Section 5.2. In Section 5.3 we present our results for the axial and vector currents.

5.1 Anomalies in the Sakai-Sugimoto model

5.1.1 Action, equations of motion, and currents

In this section we give the one flavor version of the action and the equation of motion, discussed in Sections (4.2, 4.3), in the broken phase where the D8- and $\overline{\text{D8}}$-branes are connected. The equations for the symmetric phase are very similar and shall be given later where necessary. Throughout this chapter we shall work with one quark flavor, $N_f = 1$. The currents we compute are expected to be simple sums over quark flavors, each flavor contributing in the same way, distinguished only by its electric charge. This is rather obvious in the chirally symmetric phase. In the chirally broken phase, the flavor contributions may be more complicated in the case of charged pion condensation. However, since we work at vanishing isospin chemical potential, there is only neutral pion condensation and the different flavor contributions decouple.

To obtain the action for one quark flavor in the gauge $A_z = 0$ we simply have to set $\hat{A}_\mu = A_\mu$ in (4.20) and (4.18). Remember that we work in Minkowski signature and that $A_0 \to iA_0$. The (Euclidean) action for $N_f = 1$,

$$S = S_{\text{YM}} + S_{\text{CS}} \tag{5.1}$$

is given by

$$S_{\text{YM}} = \kappa M_{\text{KK}}^2 \int d^4x \int_{-\infty}^{\infty} dz \left[k(z) F_{z\mu} F^{z\mu} + \frac{h(z)}{2M_{\text{KK}}^2} F_{\mu\nu} F^{\mu\nu} \right] , \tag{5.2a}$$

$$S_{\text{CS}} = \frac{N_c}{24\pi^2} \int d^4x \int_{-\infty}^{\infty} dz\, A_\mu F_{z\nu} F_{\rho\sigma} \epsilon^{\mu\nu\rho\sigma} , \tag{5.2b}$$

with Greek indices running over $\mu, \nu, \ldots = 0, 1, 2, 3$. Our convention for the epsilon tensor is $\epsilon_{0123} = +1$. The metric functions $k(z)$ and $h(z)$ are given by (4.21) and the dimensionless constant κ is given by (4.22). The integration over the four-sphere has already been done, and we are left with the integral over space-time $(\tau, \mathbf{x})$ and the holographic coordinate z which extends from the left-handed boundary ($z = +\infty$) over the tip of the cigar-shaped (x^4, z) subspace ($z = 0$) to the right-handed boundary ($z = -\infty$). The coordinate z is dimensionless

and is obtained from the dimensionful coordinate z of (4.19) upon defining $z' = z/u_{\rm KK}$ ($T < T_c$) and then dropping the prime. Here, $u_{\rm KK} = 4R^3 M_{\rm KK}^2/9$, with R being the curvature radius of the background metric. The equations of motion (4.23) for $N_f = 1$ are

$$\kappa M_{\rm KK}^2\, \partial_z[k(z)F^{z\mu}] + \kappa h(z)\partial_\nu F^{\nu\mu} = \frac{N_c}{16\pi^2} F_{z\nu}F_{\rho\sigma}\epsilon^{\mu\nu\rho\sigma}\,, \tag{5.3a}$$

$$\kappa M_{\rm KK}^2\, \partial_\mu[k(z)F^{z\mu}] = \frac{N_c}{64\pi^2} F_{\mu\nu}F_{\rho\sigma}\epsilon^{\mu\nu\rho\sigma}\,, \tag{5.3b}$$

where the second equation is obtained from varying A_z in the action prior to setting $A_z = 0$.

Next we introduce the chiral currents. The usual way is to define them through the variation of the on-shell action with respect to the boundary values of the gauge fields (see however Ref. [110] for a discussion of possible alternatives). We thus replace $A_\mu(x,z) \to A_\mu(x,z) + \delta A_\mu(x,z)$ in the action and keep the terms linear in $\delta A_\mu(x,z)$ to obtain

$$\begin{aligned}\delta S_{\rm YM} &= 2\kappa M_{\rm KK}^2 \left\{ \int d^4x\, k(z) F^{z\mu}\delta A_\mu\Big|_{z=-\infty}^{z=\infty} + \int d^3x \int_{-\infty}^{\infty} dz\, \frac{h(z)}{M_{\rm KK}^2} F^{\nu\mu}\delta A_\mu\Big|_{x_\nu} \right. \\ &\quad \left. - \int d^4x \int_{-\infty}^{\infty} dz\, \left[\partial_z[k(z)F^{z\mu}] + \frac{h(z)}{M_{\rm KK}^2}\partial_\nu F^{\nu\mu}\right]\delta A_\mu \right\}\,, \end{aligned} \tag{5.4a}$$

$$\begin{aligned}\delta S_{\rm CS} &= \frac{N_c}{8\pi^2}\left\{ -\frac{1}{3}\int d^4x\, A_\nu F_{\rho\sigma}\delta A_\mu\Big|_{z=-\infty}^{z=\infty} - \frac{2}{3}\int d^3x \int_{-\infty}^{\infty} dz\, A_\sigma F_{z\nu}\delta A_\mu\Big|_{x_\rho} \right. \\ &\quad \left. + \int d^4x \int_{-\infty}^{\infty} dz\, F_{z\nu}F_{\rho\sigma}\delta A_\mu \right\}\epsilon^{\mu\nu\rho\sigma}\,. \end{aligned} \tag{5.4b}$$

In the total variation $\delta S = \delta S_{\rm YM} + \delta S_{\rm CS}$ the bulk terms vanish upon using the equation of motion for A_μ (5.3a) and we are left with boundary terms only. According to the holographic correspondence, we keep only the boundary terms at $|z| = \infty$ and drop any terms from space-time infinities. This may seem natural but possibly is problematic in our case as we shall discuss later after we have implemented our specific ansatz. The boundary terms at the holographic boundary $z = \pm\infty$ lead to the left- and right-handed currents

$$\mathcal{J}^\mu_{L/R} \equiv -\frac{\delta S}{\delta A_\mu(x, z = \pm\infty)} = \mp\left(2\kappa M_{\rm KK}^2 k(z) F^{z\mu} - \frac{N_c}{24\pi^2}\epsilon^{\mu\nu\rho\sigma}A_\nu F_{\rho\sigma}\right)_{z=\pm\infty}\,, \tag{5.5}$$

where the first (second) term is the YM (CS) contribution. This result of the currents is in agreement with Refs. [34, 110, 111], see also [112, 113]. The overall minus sign in the definition originates from our use of the Euclidean action which is minus the Minkowski action, and the functional derivative is taken with respect to the space-time coordinates x (and not also with respect to the holographic coordinate z plus a subsequent limit $z \to \pm\infty$). The currents (5.5) can also be obtained from

$$\mathcal{J}^\mu_{L/R} = \mp\, \frac{\partial\mathcal{L}}{\partial\,\partial_z A_\mu}\Big|_{z=\pm\infty}\,, \tag{5.6}$$

in accordance with the usual rules of the gauge/gravity correspondence.

As already pointed out in Ref. [34], it is only the YM part of the current, *i.e.*, the first term in eq. (5.5), which appears in the asymptotic expansion of the gauge fields. From the definition (5.5) and with $k(z) = 1 + z^2$ we find

$$A_\mu(x,z) = A_\mu(x, z = \pm\infty) \pm \frac{\mathcal{J}^{L/R}_{\mu,\rm YM}}{2\kappa M_{\rm KK}^2}\frac{1}{z} + \mathcal{O}\left(\frac{1}{z^2}\right)\,. \tag{5.7}$$

One can also confirm this relation from our explicit results in the subsequent sections.

5.1.2 Consistent and covariant anomalies

The divergence of the currents (5.5) can be easily computed with the help of the equation of motion for A_z (5.3b). One obtains

$$\partial_\mu \mathcal{J}^\mu_{L/R} = \partial_\mu (\mathcal{J}_{\rm YM} + \mathcal{J}_{\rm CS})^\mu_{L/R} = \mp \frac{N_c}{16\pi^2} \left(1 - \frac{2}{3}\right) F^{L/R}_{\mu\nu} \widetilde{F}^{\mu\nu}_{L/R} \,, \tag{5.8}$$

with the left- and right-handed field strengths $F^{L/R}_{\mu\nu}(x) \equiv F_{\mu\nu}(x, z = \pm\infty)$, and the left- and right-handed dual field strength tensors $\widetilde{F}^{\mu\nu}_{L/R} = \frac{1}{2} F^{L/R}_{\rho\sigma} \epsilon^{\mu\nu\rho\sigma}$. (For notational convenience we use the labels L, R and related labels such as V, A sometimes as superscript, sometimes as subscript.) With the vector and axial currents

$$\mathcal{J}^\mu \equiv \mathcal{J}^\mu_R + \mathcal{J}^\mu_L \,, \qquad \mathcal{J}^\mu_5 \equiv \mathcal{J}^\mu_R - \mathcal{J}^\mu_L \,, \tag{5.9}$$

and the vector and axial field strengths introduced as $F^R_{\mu\nu} = F^V_{\mu\nu} + F^A_{\mu\nu}$, $F^L_{\mu\nu} = F^V_{\mu\nu} - F^A_{\mu\nu}$, eq. (5.8) yields the vector and axial anomalies

$$\partial_\mu \mathcal{J}^\mu = \frac{N_c}{12\pi^2} F^V_{\mu\nu} \widetilde{F}^{\mu\nu}_A \,, \tag{5.10a}$$

$$\partial_\mu \mathcal{J}^\mu_5 = \frac{N_c}{24\pi^2} \left(F^V_{\mu\nu} \widetilde{F}^{\mu\nu}_V + F^A_{\mu\nu} \widetilde{F}^{\mu\nu}_A \right) . \tag{5.10b}$$

The coefficients on the right-hand side (which as we saw receive contributions from both the YM and CS parts of the currents) are in accordance with the standard field theoretic results for N_c chiral fermionic degrees of freedom coupled to left and right chiral gauge fields [114]. The above form of the anomaly, which is symmetric in vector and axial-vector gauge fields, is called *consistent* anomaly. If left- and right-handed Weyl spinors are treated separately, this form of the anomaly arises unambiguously. This is explained for instance in Ref. [115], where left- and right-handed fields are separated by an extra dimension. This is not unlike our present model and it is thus not surprising that the consistent anomaly arises naturally from the above definition of the currents. In QED, however, we must require that the vector current be strictly conserved, even in the presence of axial field strengths. As was first discussed by Bardeen [114], this can be achieved by the introduction of a counterterm that mixes left- and right-handed gauge fields. Having even parity, Bardeen's counterterm is uniquely given by [115]

$$\Delta S = c \int d^4x (A^L_\mu A^R_\nu F^L_{\rho\sigma} + A^L_\mu A^R_\nu F^R_{\rho\sigma}) \epsilon^{\mu\nu\rho\sigma} \,, \tag{5.11}$$

where c is a constant determined by requiring a strictly conserved vector current. Because this expression can be naturally written as a (metric-independent) integral over a hypersurface at $|z| = \Lambda \to \infty$ with left- and right-handed fields concentrated at the respective brane locations, ΔS can actually be interpreted as a (finite) counterterm in holographic renormalization. In particular, it does not change the equations of motion.

To obtain the contribution of Bardeen's counterterm to the chiral currents we replace $A^{L/R}_\mu \to A^{L/R}_\mu + \delta A^{L/R}_\mu$ to obtain

$$\begin{aligned} \delta\Delta S &= \pm c \int d^4x \left(A^{R/L}_\nu F^{R/L}_{\rho\sigma} - A^{L/R}_\nu F^{R/L}_{\rho\sigma} + 2 A^{R/L}_\nu F^{L/R}_{\rho\sigma} \right) \delta A^{L/R}_\mu \epsilon^{\mu\nu\rho\sigma} \\ &\quad \mp 2c \int d^3x \, A^{R/L}_\nu A^{L/R}_\sigma \delta A^{L/R}_\mu \Big|_{x_\rho} \epsilon^{\mu\nu\rho\sigma} \,. \end{aligned} \tag{5.12}$$

Again dropping the space-time surface terms, the contribution to the currents is therefore

$$\Delta \mathcal{J}^\mu_{L/R} = \mp c \left(A^{R/L}_\nu F^{R/L}_{\rho\sigma} - A^{L/R}_\nu F^{R/L}_{\rho\sigma} + 2 A^{R/L}_\nu F^{L/R}_{\rho\sigma} \right) \epsilon^{\mu\nu\rho\sigma} \,, \tag{5.13}$$

and the contribution to the divergence of the currents becomes

$$\partial_\mu \Delta \mathcal{J}^\mu_{L/R} = \mp c \left(F^{R/L}_{\mu\nu} \widetilde{F}^{\mu\nu}_{R/L} + F^{L/R}_{\mu\nu} \widetilde{F}^{\mu\nu}_{R/L} \right) . \tag{5.14}$$

Denoting renormalized left- and right-handed currents as

$$\bar{\mathcal{J}}^\mu_{L/R} \equiv \mathcal{J}^\mu_{L/R} + \Delta \mathcal{J}^\mu_{L/R} , \tag{5.15}$$

and similarly the renormalized axial and vector currents as $\bar{\mathcal{J}}_\mu$, $\bar{\mathcal{J}}^5_\mu$, we find that the choice

$$c = \frac{N_c}{48\pi^2} \tag{5.16}$$

leads to the *covariant* anomaly

$$\partial_\mu \bar{\mathcal{J}}^\mu = 0 , \tag{5.17a}$$

$$\partial_\mu \bar{\mathcal{J}}^\mu_5 = \frac{N_c}{8\pi^2} F^V_{\mu\nu} \widetilde{F}^{\mu\nu}_V + \frac{N_c}{24\pi^2} F^A_{\mu\nu} \widetilde{F}^{\mu\nu}_A . \tag{5.17b}$$

Note that the prefactor in front of the first term in the axial anomaly now has changed to $N_c/(8\pi^2)$, from $N_c/(24\pi^2)$ in eq. (5.10b), which is the well-known result for the Adler-Bell-Jackiw anomaly for QED [116, 117] and which is essential for getting the correct pion decay rate $\pi^0 \to 2\gamma$. The necessity of adding the counterterm (5.11) to the Sakai-Sugimoto model is in fact completely analogous to the very same and well-known procedure in chiral models where a Wess-Zumino-Witten term accounts for the anomaly [118].

In the literature sometimes the coefficient of the subleading term in the asymptotic behavior of $A_\mu(x, |z| \to \infty)$ and thus the YM part of the current (see eq. (5.7)) is identified with the full current [101], see also [119, 120, 121, 122]. Using this identification, it has also been assumed that the equation of motion for A_z (5.3b) represents the anomaly equation [108]. Indeed, from eq. (5.3b) one obtains the apparent anomaly

$$\partial_\mu \mathcal{J}^\mu_{\mathrm{YM},L/R} = \mp \frac{N_c}{16\pi^2} F^{L/R}_{\mu\nu} \widetilde{F}^{\mu\nu}_{L/R} , \tag{5.18}$$

which leads to

$$\partial_\mu \mathcal{J}^\mu_{\mathrm{YM}} = \frac{N_c}{4\pi^2} F^V_{\mu\nu} \widetilde{F}^{\mu\nu}_A , \tag{5.19a}$$

$$\partial_\mu \mathcal{J}^\mu_{\mathrm{YM},5} = \frac{N_c}{8\pi^2} \left(F^V_{\mu\nu} \widetilde{F}^{\mu\nu}_V + F^A_{\mu\nu} \widetilde{F}^{\mu\nu}_A \right) , \tag{5.19b}$$

and this does contain the same coefficient in front of $F^V_{\mu\nu} \widetilde{F}^{\mu\nu}_V$ as the full covariant anomaly (5.17). However, it differs from the latter in the presence of axial gauge fields. In particular, the vector current is then not strictly conserved. The renormalized current $\bar{\mathcal{J}}_{L/R}$ satisfies eq. (5.18) only for $F^L_{\mu\nu} = F^R_{\mu\nu}$.[1] Even when this issue may be ignored, because all axial vector field strengths are set to zero, it appears to be questionable to keep only part of the full current (5.5).

In the remainder of this chapter we shall consider the full currents for which Bardeen's counterterm is needed, and study the implications, which indeed differ from keeping only the YM part of the currents. (The effect of truncating to the YM part can be easily read off from the expressions that we shall give.)

[1] The more general validity of eq. (5.18) has been assumed incorrectly in eq. (2.1) of ref. [101] and eq. (36) of Ref. [96].

5.2 Background electromagnetic fields and chemical potentials

The discussion in the previous section was general in the sense that we have not specified any gauge fields except for the gauge choice $A_z = 0$. In this section we specify our ansatz according to the physical situation we are interested in. This includes a background magnetic field B as well as separate left- and right-handed chemical potentials. The left- and right-handed chemical potentials are defined as the boundary values of the temporal component of the gauge field

$$\mu_{L/R} = A_0(\pm\infty). \tag{5.20}$$

Equivalently, they can be written in terms of the ordinary quark chemical potential $\mu = (\mu_R + \mu_L)/2$ and an axial chemical potential $\mu_5 = (\mu_R - \mu_L)/2$. With these ingredients we can obtain results relevant for the heavy-ion context (nonzero μ_5, negligibly small μ) and for the astrophysical context (vanishing μ_5, large μ). In order to be able to check the axial anomaly explicitly, we also add an electric field E and an "axial electric field" ϵ parallel to the magnetic field. The electric field E is needed because the axial anomaly is proportional to $\mathbf{E}\cdot\mathbf{B}$. The (unphysical) field ϵ shall be used to check the absence of a vector anomaly, *i.e.*, the conservation of the vector current, which must be true even in the presence of ϵ, and would be trivial without ϵ. In our final results for the currents, the electric fields are however set to zero.

For previous discussions of background electric and magnetic fields in the Sakai-Sugimoto model see for instance Refs. [91, 90, 34, 123, 124]. We shall only consider spatially homogeneous systems. This is the simplest case, which might however require generalization when the true ground state is more complicated, for instance when Skyrme crystals are formed [125].

5.2.1 Chirally broken phase

In our ansatz the nonzero fields are $A_0(t,z)$, $A_1(x_2)$, $A_3(t,z)$, where the dependence on t will only be present for nonvanishing electric fields E and ϵ at the holographic boundary. The temporal component A_0 is needed to account for nonzero (left- and right-handed) chemical potentials which correspond to the values of A_0 at the boundary. The electromagnetic fields are encoded in the boundary values of the spatial components. Since the gauge symmetry in the bulk corresponds to a global symmetry for the dual field theory, the fields at the holographic boundary are not dynamical and merely serve as background fields. This is however sufficient for our purpose. The magnetic field $\mathbf{B}$ is assumed to point into the 3-direction, $\mathbf{B} = (0,0,B)$. Consequently, we can choose

$$A_1(x_2) = -x_2 B \tag{5.21}$$

at the holographic boundary. The equations of motion show that A_1 can be chosen to be constant in z throughout the bulk. (This is different in the presence of an isospin chemical potential [34].) Consequently, $F_{12}(x,z) = B$. For notational convenience we have absorbed the electric quark charge q_f into B, *i.e.*, actually $B \to q_f B$ with $q_f = 2/3\,e$ for $f = u$, and $q_f = -1/3\,e$ for $f = d$. With nonzero A_0 and A_1, accounting for the chemical potential and the magnetic field, a nonzero A_3 is induced, even without electric field. In the broken phase, A_3 develops a nonzero boundary value, corresponding to the gradient of the neutral pion [91, 90, 34] (see also Chapter 6). Just as for a usual superfluid, where the gradient of the phase of the order parameter is proportional to the superfluid velocity, this gradient of the pion field can be viewed as an axial supercurrent [34].

Next we introduce the electric field $\mathbf{E} = (0,0,E)$ parallel to $\mathbf{B}$ and, as explained above, an "axial electric field" $\boldsymbol{\epsilon} = (0,0,\epsilon)$. We thus have to add $-t(E \mp \epsilon)$ to the boundary value of A_3, such that, together with the axial supercurrent $\jmath_t$, we have

$$A_3(t, z = \pm\infty) = -t(E \mp \epsilon) \mp \jmath_t\,. \tag{5.22}$$

Due to the axial electric field we allow the supercurrent to become time-dependent. Strictly speaking the electric fields prevent us from using a thermodynamic description since it introduces a time-dependence and thus non-equilibrium physics. Therefore, our electric field should be considered infinitesimal. This is sufficient for our purpose since we can check the anomaly relations with an arbitrarily small electric field. Moreover, as mentioned above, the physical situations we are interested in do not require finite electric fields anyway.

With the above ansatz, the YM and CS contributions to the action (5.2) become

$$S_{\rm YM} = \kappa M_{\rm KK}^2 \int d^4x \int_{-\infty}^{\infty} dz\, k(z) \left[-(\partial_z A_0)^2 + (\partial_z A_3)^2\right] , \tag{5.23a}$$

$$S_{\rm CS} = \frac{N_c}{12\pi^2} \int d^4x \int_{-\infty}^{\infty} dz \Big\{ (\partial_2 A_1) \left[A_0(\partial_z A_3) - A_3(\partial_z A_0)\right] - A_1 \left[(\partial_2 A_0)(\partial_z A_3) - (\partial_2 A_3)(\partial_z A_0)\right] \Big\} . \tag{5.23b}$$

We have written all terms which are needed to derive the equations of motion, including the ones that vanish on-shell. More specifically, the second line in the CS action (5.23b) vanishes on-shell because neither A_0 nor A_3 depends on x_2, but yields a finite contribution to the equations of motion. The equations of motion are

$$\partial_z(k\partial_z A_0) = 2\beta\partial_z A_3 , \tag{5.24a}$$

$$\partial_z(k\partial_z A_3) = 2\beta\partial_z A_0 , \tag{5.24b}$$

$$\partial_t(k\partial_z A_0) = 2\beta\partial_t A_3 , \tag{5.24c}$$

with the dimensionless magnetic field

$$\beta \equiv \frac{\alpha B}{M_{\rm KK}^2} , \tag{5.25}$$

and $\alpha \equiv 27\pi/(2\lambda)$. We defer the details of solving the equations of motion to appendix C.6.1. The results for the gauge fields and field strengths are

$$A_0(t,z) = \mu_t - \mu_{5,t}\frac{\sinh(2\beta\arctan z)}{\sinh\beta\pi} - (\jmath_t - \epsilon t)\left[\frac{\cosh(2\beta\arctan z)}{\sinh\beta\pi} - \coth\beta\pi\right] , \tag{5.26a}$$

$$A_3(t,z) = -tE - \mu_{5,t}\left[\frac{\cosh(2\beta\arctan z)}{\sinh\beta\pi} - \coth\beta\pi\right] - (\jmath_t - \epsilon t)\frac{\sinh(2\beta\arctan z)}{\sinh\beta\pi} , \tag{5.26b}$$

and

$$k\partial_z A_0 = -2\beta\left[\mu_{5,t}\frac{\cosh(2\beta\arctan z)}{\sinh\beta\pi} + (\jmath_t - \epsilon t)\frac{\sinh(2\beta\arctan z)}{\sinh\beta\pi}\right] , \tag{5.27a}$$

$$k\partial_z A_3 = -2\beta\left[\mu_{5,t}\frac{\sinh(2\beta\arctan z)}{\sinh\beta\pi} + (\jmath_t - \epsilon t)\frac{\cosh(2\beta\arctan z)}{\sinh\beta\pi}\right] . \tag{5.27b}$$

Here we have denoted

$$\mu_t \equiv \mu + \epsilon t\coth\beta\pi , \qquad \mu_{5,t} \equiv \mu_5 + Et\tanh\beta\pi , \tag{5.28}$$

i.e., both boundary values of A_0 become time-dependent through the electric fields. As can be seen from the detailed derivation in appendix C.6.1, this time-dependence is unavoidable.

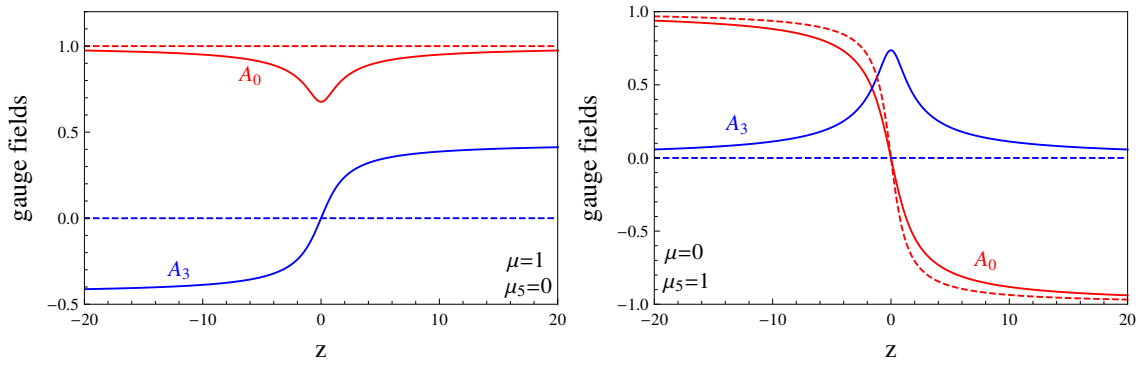

Figure 5.1: Gauge fields in the chirally broken phase as functions of the holographic coordinate $z \in [-\infty, \infty]$ for a finite quark chemical potential and vanishing axial chemical potential (left) and vice versa (right). Dashed lines: gauge fields with vanishing magnetic field; solid lines: gauge fields with a nonzero magnetic field $\beta = 0.6$. In both plots we have set the electric fields to zero, $E = \epsilon = 0$. The boundary values at $z = \pm\infty$ correspond to left- and right-handed quantities. The magnetic field induces an axial supercurrent (boundary value of A_3) in the case of a nonvanishing quark chemical potential. If both μ and μ_5 are nonvanishing, the gauge fields are neither symmetric nor antisymmetric in z. The analytic expressions for these curves are given in eqs. (6.27).

In Figure 5.1 we plot the gauge fields for $E = \epsilon = 0$ at the minimum, *i.e.*, after $\jmath_t$ has been determined to minimize the free energy, see below.

The thermodynamic potential $\Omega = \frac{T}{V} S_{\text{on-shell}}$ is obtained from eqs. (C.60), treating t as an external parameter,

$$\Omega = \frac{8\kappa M_{\text{KK}}^2}{3} \left\{ \left[(\jmath_t - \epsilon t)^2 - \mu_{5,t}^2 \right] \rho(\beta) + \beta \left[\mu_t (\jmath_t - \epsilon t) + t E \mu_{5,t} \right] \right\}, \tag{5.29}$$

where we have abbreviated

$$\rho(\beta) \equiv \beta \coth \beta\pi + \frac{\pi \beta^2}{2 \sinh^2 \beta\pi} \simeq \begin{cases} \dfrac{3}{2\pi} + \dfrac{\pi}{6}\beta^2 & \text{for } \beta \to 0 \\ |\beta| & \text{for } |\beta| \to \infty \end{cases} . \tag{5.30}$$

Minimization of Ω with respect to $\jmath_t$ yields the axial supercurrent

$$\jmath_t = -\frac{\beta\mu}{2\rho(\beta)} + \epsilon t \left[1 - \frac{\beta \coth \beta\pi}{2\rho(\beta)} \right] . \tag{5.31}$$

We see that the supercurrent depends neither on μ_5 nor on E. Therefore, at $t = 0$ it is simply the one-flavor limit of the result obtained in Ref. [34] (where the D8 and $\overline{\text{D8}}$ branes were identified with R and L, not with L and R, respectively, hence the different sign of the supercurrent).

5.2.2 Chirally symmetric phase

As explained in Section 4.1.2, in the chirally symmetric phase the D8 and $\overline{\text{D8}}$-branes are not connected. On both branes the holographic coordinate z now runs from $z = 0$, the black hole horizon, to the holographic boundary at $z = \infty$, and both branes yield separate contributions to the action,

$$S = (S_{\text{YM}}^L + S_{\text{YM}}^R) + (S_{\text{CS}}^L - S_{\text{CS}}^R) . \tag{5.32}$$

The CS action assumes different overall signs on the D8- and $\overline{\text{D8}}$-branes since its parity is odd. The YM and CS contributions are

$$S^h_{\rm YM} = \kappa M^2_{\rm KK}\theta^3 \int d^4x \int_0^\infty dz \left[-k_0(z)(\partial_z A^h_0)^2 + k_3(z)(\partial_z A^h_3)^2\right], \tag{5.33a}$$

$$S^h_{\rm CS} = \frac{N_c}{12\pi^2}\int d^4x \int_0^\infty dz \Big\{(\partial_2 A^h_1)[A^h_0(\partial_z A^h_3) - A^h_3(\partial_z A^h_0)] - A^h_1[(\partial_2 A^h_0)(\partial_z A^h_3) - (\partial_2 A^h_3)(\partial_z A^h_0)]\Big\}, \tag{5.33b}$$

with $h = L, R$. Here, we have defined the dimensionless temperature

$$\theta \equiv \frac{2\pi T}{M_{\rm KK}}. \tag{5.34}$$

In contrast to the broken phase there are different metric functions for temporal and spatial components of the gauge fields,

$$k_0(z) \equiv \frac{(1+z^2)^{3/2}}{z}, \qquad k_3(z) \equiv z(1+z^2)^{1/2}. \tag{5.35}$$

Note the slight difference in notation of the gauge fields: while in the broken phase $A^{L/R}_\mu(x) \equiv A_\mu(x, z = \pm\infty)$ always implies evaluation at the holographic boundary, here we label the bulk gauge fields $A^{L/R}_\mu(x, z)$ by L and R to indicate whether they live on the D8- or on the $\overline{\text{D8}}$-brane. Since we always discuss broken and symmetric phases separately, this should not cause any confusion.

The equations of motion on the separate branes become

$$\partial_z(k_0\partial_z A^{L/R}_0) = \pm\frac{2\beta}{\theta^3}\partial_z A^{L/R}_3, \tag{5.36a}$$

$$\partial_z(k_3\partial_z A^{L/R}_3) = \pm\frac{2\beta}{\theta^3}\partial_z A^{L/R}_0, \tag{5.36b}$$

$$\partial_t(k_0\partial_z A^{L/R}_0) = \pm\frac{2\beta}{\theta^3}\partial_t A^{L/R}_3. \tag{5.36c}$$

Details of solving the equations of motion are presented in appendix C.6.2. The final solution for the gauge fields is

$$A^{L/R}_0(t,z) = (\mu_t \mp \mu_{5,t})\left[p(z) - \frac{p_0}{q_0}\,q(z)\right], \tag{5.37a}$$

$$A^{L/R}_3(t,z) = -t(E \mp \epsilon) \pm \frac{\mu_t \mp \mu_{5,t}}{2\beta/\theta^3}\left[k_0\partial_z p - \frac{p_0}{q_0}(1 + k_0\partial_z q)\right], \tag{5.37b}$$

which is plotted in Figure 5.2 for $E = \epsilon = 0$. Below we shall also need the field strengths on the branes,

$$k_0\partial_z A^{L/R}_0 = (\mu_t \mp \mu_{5,t})\left(k_0\partial_z p - \frac{p_0}{q_0}k_0\partial_z q\right), \tag{5.38a}$$

$$k_3\partial_z A^{L/R}_3 = \pm\frac{2\beta}{\theta^3}(\mu_t \mp \mu_{5,t})\left[p(z) - \frac{p_0}{q_0}q(z)\right]. \tag{5.38b}$$

The functions $p(z)$, $q(z)$ are hypergeometric functions which we defined in eqs. (C.66) and which depend on the ratio β/θ^3. Their values at $z = 0$ are denoted by p_0, q_0, see eqs. (C.69), and the ratio p_0/q_0 behaves for small and large magnetic fields as

$$\frac{p_0}{q_0} \simeq \begin{cases} 1 + (2\beta/\theta^3)^2(\ln 4 - 1) & \text{for } \beta/\theta^3 \to 0 \\ 2|\beta|/\theta^3 & \text{for } |\beta|/\theta^3 \to \infty \end{cases}. \tag{5.39}$$

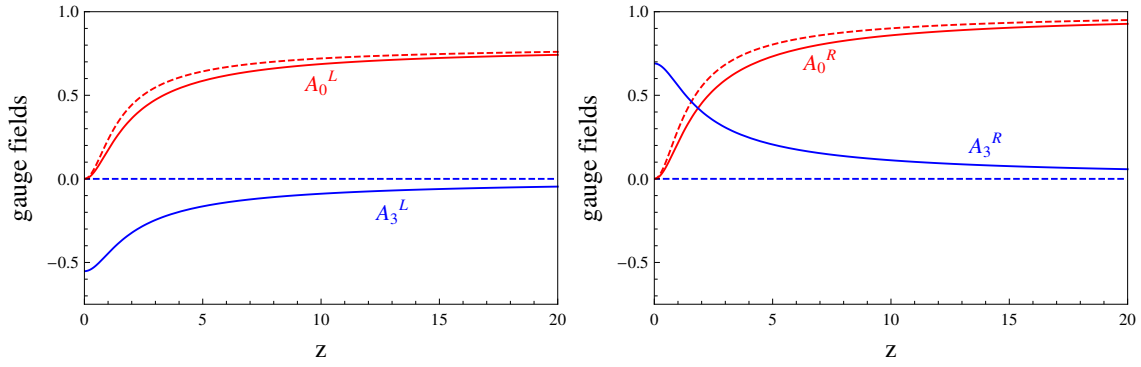

Figure 5.2: Left- and right-handed gauge fields (left and right panel, respectively) in the chirally symmetric phase as functions of the holographic coordinate $z \in [0, \infty]$ for $\mu = 0.9$, $\mu_5 = 0.1$. We have set the electric fields to zero, $E = \epsilon = 0$. The temporal components $A_0^{L/R}$ approach the chemical potentials $\mu \mp \mu_5$ at the boundary $z = \infty$, while the spatial components $A_3^{L/R}$ vanish at $z = \infty$. A finite magnetic field (solid lines, here $\beta/\theta^3 = 0.6$) distorts the gauge fields compared to the case of vanishing magnetic fields (dashed lines). In particular, the spatial component develops a nonzero value at $z = 0$. The different sign of this value for left- and right-handed fields, *i.e.*, on the D8- and $\overline{\text{D8}}$-branes, ensures the correct parity behavior of the fields. The analytical expressions for these curves are given in eqs. (5.37).

The boundary values of the temporal components are $A_0^{L/R}(t, z = \infty) = \mu_t \mp \mu_{5,t}$ with

$$\mu_t \equiv \mu + 2t\epsilon \frac{\beta}{\theta^3}\frac{q_0}{p_0}\,, \qquad \mu_{5,t} \equiv \mu_5 + 2tE\frac{\beta}{\theta^3}\frac{q_0}{p_0}\,. \tag{5.40}$$

It is instructive to compare this behavior of the axial chemical potential with the expected behavior for free fermions in a magnetic field. To this end, consider the lowest Landau level in which the spin of all (say, positively charged) fermions is aligned parallel to the magnetic field. As a consequence, all right- (left-) handed massless fermions move parallel (antiparallel) to the magnetic field. An electric field parallel to the magnetic field now shifts all momenta in the positive 3-direction by an amount Et. Consequently, some of the left- handed fermions are converted into right-handed fermions and a shift Et is induced in the difference of right- and left-handed Fermi momenta, $(p_F^R - p_F^L)/2 = Et$ [96, 126]. Interpreting $\mu_{5,t}$ as $(p_F^R - p_F^L)/2$ (strictly speaking there is no well-defined Fermi momentum in our model), eq. (5.40) reproduces this shift for asymptotically large magnetic fields because in this case $q_0/p_0 \to \theta^3/(2\beta)$. For small magnetic fields $q_0/p_0 \to 1$, and the shift becomes linear in the magnetic field. Since $\beta/\theta^3 \propto B/T^3$, we can in principle also obtain $\mu_{5,t} = \mu_5 + tE$ for sufficiently small temperatures and fixed magnetic field. However, we cannot reduce the temperature arbitrarily in the above expression since below the critical temperature T_c we are in the chirally broken phase. In this case the analogous, temperature-independent relation in eq. (5.28) holds.

The free energy, obtained from the YM and CS contributions (C.80), is

$$\Omega = -\frac{2\kappa M_{\text{KK}}^2}{3}\left[\theta^3(\mu_t^2 + \mu_{5,t}^2)\eta - 4\beta\, t\,(\mu_t\epsilon + \mu_{5,t}E)\right]\,, \tag{5.41}$$

where we introduced the function

$$\eta(\beta/\theta^3) \equiv I_0 - (2\beta/\theta^3)^2 I_3 + 2\frac{p_0}{q_0} \simeq \begin{cases} 3 + (2\beta/\theta^3)^2(\ln 4 - 1) & \text{for } \beta/\theta^3 \to 0 \\ 4|\beta|/\theta^3 & \text{for } |\beta|/\theta^3 \to \infty \end{cases}\,, \tag{5.42}$$

with integrals I_0 and I_3 defined in eqs. (C.81).

5.2.3 Ambiguity of currents

In the following discussion we restrict ourselves to the symmetric phase, but one can easily check that all arguments hold for the broken phase as well. Let us first give the analogue of the definition of the currents (5.5) for the symmetric phase,

$$\mathcal{J}^{\mu}_{L/R} = -\left(2\kappa M_{\rm KK}^2\theta^3 k_{(\mu)} F^{z\mu}_{L/R} \mp \frac{N_c}{24\pi^2}\epsilon^{\mu\nu\rho\sigma} A^{L/R}_{\nu} F^{L/R}_{\rho\sigma}\right)_{z=\infty}, \tag{5.43}$$

where the notation $k_{(\mu)}$ (no summation over μ) indicates the different metric functions for temporal and spatial components, see eq. (5.35). Equivalently, and in analogy to eq. (5.6), we can write the currents in the symmetric phase as

$$\mathcal{J}^{\mu}_{L/R} = -\frac{\partial\mathcal{L}}{\partial\,\partial_z A^{L/R}_{\mu}}\bigg|_{z=\infty}. \tag{5.44}$$

We shall now show that the currents defined via these equations are different from the ones obtained via taking the derivative of the free energy (5.41) with respect to the corresponding source. We do so for the vector density, *i.e.*, the sum of left- and right–handed 0-components of the currents. One can observe the same ambiguity for the other nonvanishing components. The following arguments do not depend on the electric fields, so we temporarily set $\epsilon = E = 0$ for simplicity (and for a truly equilibrated situation). From the definition (5.43) and the gauge fields (5.37) and field strengths (5.38) we obtain

$$\mathcal{J}^0 = \mathcal{J}^0_R + \mathcal{J}^0_L = 4\kappa M_{\rm KK}^2\theta^3\frac{p_0}{q_0}\mu\,. \tag{5.45}$$

On the other hand, the free energy Ω of the system should yield the number density via the thermodynamic relation

$$n = -\frac{\partial\Omega}{\partial\mu} = \frac{4\kappa M_{\rm KK}^2\theta^3}{3}\mu\,\eta\,. \tag{5.46}$$

This result shows that $n \neq \mathcal{J}^0$ which, given spatial homogeneity, is inconsistent. This inconsistency is absent for vanishing magnetic fields: using the behavior of the functions p_0/q_0 and η from eqs. (5.39) and (5.42) one sees that for $\beta = 0$ the expressions for $\mathcal{J}^0$ and n are identical. We can formulate this observation in a more general way. To this end we write the left- and right-handed on-shell Lagrangians, *i.e.*, the integrands of the on-shell action (5.32), as $\mathcal{L}_h(A^h_0, \partial_z A^h_0, A^h_3, \partial_z A^h_3)$, where all arguments of $\mathcal{L}_h$ depend on the chemical potentials μ_h with $h = L, R$ and $\mu_{L/R} = \mu \mp \mu_5$. Then, with $\Omega_h = T/V \int d^4x \int_0^\infty dz\,\mathcal{L}_h$ we have

$$\begin{aligned}
\frac{\partial\Omega_h}{\partial\mu_h} &= \frac{T}{V}\sum_{i=0,3}\int d^4x\int_0^\infty dz\left(\frac{\partial\mathcal{L}_h}{\partial A^h_i}\frac{\partial A^h_i}{\partial\mu_h} + \frac{\partial\mathcal{L}_h}{\partial\,\partial_z A^h_i}\frac{\partial\,\partial_z A^h_i}{\partial\mu_h}\right)\\
&= \frac{T}{V}\sum_{i=0,3}\left[\int d^4x\,\frac{\partial\mathcal{L}_h}{\partial\,\partial_z A^h_i}\frac{\partial A^h_i}{\partial\mu_h}\bigg|_{z=0}^{z=\infty} + \int d^4x\int_0^\infty dz\,\partial_2\frac{\partial\mathcal{L}_h}{\partial\,\partial_2 A^h_i}\frac{\partial A^h_i}{\partial\mu_h}\right],
\end{aligned} \tag{5.47}$$

where we have used partial integration and added and subtracted the derivative term in x_2 in order to make use of the equations of motion. Now we use

$$\frac{\partial A^h_0}{\partial\mu_h}\bigg|_{z=\infty} = 1\,, \qquad \frac{\partial A^h_0}{\partial\mu_h}\bigg|_{z=0} = \frac{\partial A^h_3}{\partial\mu_h}\bigg|_{z=\infty} = \frac{\partial\mathcal{L}_h}{\partial\,\partial_z A^h_3}\bigg|_{z=0} = 0\,, \tag{5.48}$$

which follows from the explicit solutions (5.37), whose behavior at $z = 0$, $z = \infty$ is obtained with the help of eqs. (C.68), (C.69), and (C.70). With these relations and the definition of the

current from eq. (5.44) we obtain

$$-\frac{\partial\Omega}{\partial\mu} = \mathcal{J}^0 - \frac{T}{V}\sum_{h=L,R}\sum_{i=0,3}\int d^4x\int_0^\infty dz\,\partial_2\frac{\partial\mathcal{L}_h}{\partial\,\partial_2 A_i^h}\frac{\partial A_i^h}{\partial\mu_h}\,. \tag{5.49}$$

This is the general form of the difference between the density defined as the 0-component of the current defined via eq. (5.44) and the density defined via the thermodynamic relation (5.46). For an explicit check of this relation one inserts the expressions

$$\partial_2\frac{\partial\mathcal{L}_{L/R}}{\partial\,\partial_2 A_0^{L/R}} = \pm\frac{4\kappa M_{\rm KK}^2}{3}\beta\partial_z A_3^{L/R}\,, \tag{5.50a}$$

$$\partial_2\frac{\partial\mathcal{L}_{L/R}}{\partial\,\partial_2 A_3^{L/R}} = \mp\frac{4\kappa M_{\rm KK}^2}{3}\beta\partial_z A_0^{L/R}\,, \tag{5.50b}$$

and

$$\frac{\partial A_0^{L/R}}{\partial\mu_{L/R}} = p(z) - \frac{p_0}{q_0}q(z)\,, \tag{5.51a}$$

$$\frac{\partial A_3^{L/R}}{\partial\mu_{L/R}} = \pm\frac{\theta^3}{2\beta}\left[k_0\partial_z p - \frac{p_0}{q_0}\left(1+k_0\partial_z q\right)\right]\,, \tag{5.51b}$$

into eq. (5.49). This yields

$$-\frac{\partial\Omega}{\partial\mu} = \mathcal{J}^0 + \frac{4\kappa M_{\rm KK}^2\theta^3}{3}\mu\left[I_0 - \left(\frac{2\beta}{\theta^3}\right)^2 I_3 - \frac{p_0}{q_0}\right]\,. \tag{5.52}$$

With the definition (5.42) this confirms the difference between n and $\mathcal{J}^0$ obtained from eqs. (5.45) and (5.46).

From the general form (5.49) we see that the additional term is a boundary term at the spatial boundary of the system. This suggests that the ambiguity in the currents is related to the terms we have dropped in Section 5.1.1, see eqs. (5.4). These terms correspond to currents at the spatial boundary and disappear in the presence of a homogeneous magnetic field only if the variation $\delta A_\mu(x, z=\pm\infty)$ can be chosen to vanish at this boundary. So this problem might be resolved by considering more complicated, spatially inhomogeneous gauge fields. In our homogeneous ansatz, it is however a priori not clear which definition of the currents corresponds to the correct physics.

A possible solution to this ambiguity was suggested and applied in Refs. [91, 108, 127]. In these references, the CS action has been modified according to

$$\begin{aligned} S'^h_{\rm CS} = \frac{N_c}{12\pi^2}\int d^4x\int_0^\infty dz\,\Big\{&\frac{3}{2}(\partial_2 A_1^h)\left[A_0^h(\partial_z A_3^h) - A_3^h(\partial_z A_0^h)\right] \\ &- \frac{1}{2}(\partial_z A_1^h)\left[A_0^h(\partial_2 A_3^h) - A_3^h(\partial_2 A_0^h)\right]\Big\}\,. \end{aligned} \tag{5.53}$$

This modified action (marked by a prime) is obtained from the original CS action (5.33b) by adding a boundary term at the holographic and the spatial boundary,

$$S'^h_{\rm CS} = S^h_{\rm CS} + S^h_{\rm boundary}\,, \tag{5.54}$$

with

$$\begin{aligned} S^h_{\rm boundary} = \frac{N_c}{24\pi^2}\Big\{&\int d^3x\int_0^\infty dz\,A_1^h\Big[A_0^h(\partial_z A_3^h) - A_3^h(\partial_z A_0^h)\Big]_{x_2} \\ &- \int d^4x\,A_1^h\Big[A_0^h(\partial_2 A_3^h) - A_3^h(\partial_2 A_0^h)\Big]_{z=0}^{z=\infty}\Big\}\,. \end{aligned} \tag{5.55}$$

Note that this boundary term cannot be considered as a holographic counterterm since it involves an integration over z. From eq. (5.53) we see that the addition of S^h_{boundary} effectively amounts to a multiplication of the on-shell action by 3/2 because the second line in eq. (5.53) vanishes on-shell. The benefit of the modified action is that the integrand on the right-hand side of eq. (5.49) vanishes now, *i.e.*, there is no ambiguity in the currents anymore.

Modifications of a CS action by boundary terms are in fact sometimes necessary in order to ensure validity of the variational principle in the presence of nontrivial boundary values [128]. However, this is not what the above modification is achieving. Instead, it leads to gauge invariance under the residual gauge transformations $A_1 \to A_1 + \partial_1\Lambda(x_1)$ which are compatible with the boundary conditions of our ansatz and which do not vanish at spatial infinity $x_2 = \pm\infty$ [91]. In fact, by this modification one loses all anomalies for the (now uniquely defined) currents, as we show now. To this end, we switch on the electric fields again. Then, the currents of the original action in the symmetric phase are

$$T > T_c: \quad \mathcal{J}^0_{L/R} = 2\kappa M^2_{\text{KK}} \frac{p_0}{q_0} \left[\theta^3(\mu_t \mp \mu_{5,t}) \pm \frac{2}{3}\frac{q_0}{p_0}\beta(E \mp \epsilon)t\right], \tag{5.56a}$$

$$\mathcal{J}^1_{L/R} = 0\,, \tag{5.56b}$$

$$\mathcal{J}^2_{L/R} = \pm\frac{4\kappa M^2_{\text{KK}}}{3}\beta\, x_2(E \mp \epsilon)\,, \tag{5.56c}$$

$$\mathcal{J}^3_{L/R} = \mp 4\kappa M^2_{\text{KK}}\beta\,(\mu_t \mp \mu_{5,t})\left(1 - \frac{1}{3}\right), \tag{5.56d}$$

where we have used the definition (5.43) and the gauge fields (5.37) and field strengths (5.38). All terms containing a 1/3 originate from the CS contribution of the current, *i.e.*, from the second term in eq. (5.43). All other terms are YM contributions. In particular, the 2-component of the current is a pure CS term. This component is unphysical because it depends on our choice to introduce the magnetic field via the gauge field A_1. We could have introduced the same magnetic field via A_2 or a combination of A_1 and A_2, in which case the 1- and 2-components of the currents would have been different. We shall see below that Bardeen's counterterm solves this problem by canceling the 2-component. Here, however, it gives a nonzero contribution to the anomaly. Namely, the divergence of the (unmodified) currents becomes

$$\partial_\mu \mathcal{J}^\mu_{L/R} = \partial_t \mathcal{J}^0_{L/R} + \partial_2 \mathcal{J}^2_{L/R} = \mp\frac{N_c}{12\pi^2} B(E \mp \epsilon)\,, \tag{5.57}$$

where we have used the definition of $\mu_{5,t}$ (5.40) and $\kappa M^2_{\text{KK}}\beta \equiv N_c B/16\pi^2$. This is exactly the consistent anomaly (5.8), because

$$\mp\frac{N_c}{48\pi^2} F^{L/R}_{\mu\nu}\widetilde{F}^{\mu\nu}_{L/R}\bigg|_{z=\infty} = \mp\frac{N_c}{12\pi^2} B(E \mp \epsilon)\,. \tag{5.58}$$

The new currents $\mathcal{J}'^\mu_{L/R}$ from the modified action are simply obtained by multiplying the CS contribution of the currents (5.56) by 3/2. Doing so in the explicit results (5.56), this yields

$$\partial_\mu \mathcal{J}'^\mu_{L/R} = \partial_t \mathcal{J}'^0_{L/R} + \partial_2 \mathcal{J}'^2_{L/R} = 0\,, \tag{5.59}$$

which can also be inferred in generality from (5.8). Consequently, the anomaly has disappeared. In other words, the new vector and the axial currents are both conserved. Nevertheless, one finds nonzero currents in the direction of the magnetic field. Multiplying the CS contribution in eq. (5.56d) by 3/2 one obtains $\mathcal{J}'^3_R + \mathcal{J}'^3_L = N_c/(4\pi^2)\, B\mu_5$ and $\mathcal{J}'^3_R - \mathcal{J}'^3_L = N_c/(4\pi^2)\, B\mu$ [91], both of which are 1/2 times the results of refs. [96] and [103, 129], respectively (cf. sec. 5.3.1 below).

In the remainder of this chapter we shall again consider the full, unmodified chiral currents (5.5) which contain the complete covariant anomaly upon inclusion of the counterterm (5.11).

5.3 Axial and vector currents

In this section we shall use the results from the previous Sections to compute the vector and axial currents in the presence of a magnetic field and a quark chemical potential μ as well as an axial chemical potential μ_5. We have seen that a consistent definition of the currents is not obvious in the given setup. We shall focus on the definition of the currents presented in Section 5.1.1 since they reproduce, together with Bardeen's counterterm, the correct anomaly. Before going into the details, let us explain the expected physics behind the vector current, in other words the chiral magnetic effect.

5.3.1 The chiral magnetic effect

A (noncentral) heavy-ion collision, where the chiral magnetic effect is expected to occur, is more complicated than we can capture with our thermodynamic description. The physical situation and its simplified description within a thermodynamic approach is as follows [96]. In the high-temperature phase gluonic sphaleron configurations with nonzero winding number should be produced with relatively high probability, inducing an imbalance in left- and right-handed quarks due to the QCD anomaly and thus a nonzero axial number density n_5. In the simple picture applied in Ref. [96], such chirality changing transitions are assumed to have taken place in a nonequilibrium situation, after which in equilibrium a finite n_5 is no longer changed by the QCD anomaly. The QED anomaly on the other hand does not change n_5 as long as only a magnetic field is present, so n_5 can be considered a conserved quantity for which we may introduce μ_5 as the corresponding chemical potential. (We have introduced also electric fields above for the sake of checking the axial anomaly, but shall set them to zero in the final results.) Nonzero quark masses and/or nonzero chiral condensates can be expected to lead to a decay of n_5. In the given context, it is thus questionable to apply the equilibrium description also to the chirally broken phase, and strictly speaking our approach should be extended to a nonequilibrium calculation.

Let us now briefly recapitulate the physics behind the occurrence of the vector current which constitutes the chiral magnetic effect in terms of a (quasi)particle picture [95, 96]. Suppose the magnetic field leads to a spin polarization of all fermions, *i.e.*, the spins of all quarks are aligned parallel or antiparallel to the magnetic field depending on their charge being positive or negative. Massless right-handed fermions, which have positive helicity, have momenta parallel to their spin, so they move parallel to the magnetic field if they have positive charge, and antiparallel otherwise. For left-handed fermions with negative helicity, the situation is exactly reversed. If there are more right-handed than left-handed fermions, $n_5 > 0$, there is a resulting net electromagnetic current parallel to the magnetic field. (Antifermions have helicity opposite to chirality but also opposite charge, so they give a current in the same direction.) For weakly-coupled fermions this picture applies since in the lowest Landau level indeed all fermions have their spins aligned in the direction of the magnetic field according to their charge. The chiral magnetic effect then results solely from the lowest Landau level. The contribution of fermions in higher Landau levels, where both parallel and antiparallel spin projections are populated, cancels out. This can be seen explicitly upon using the thermodynamic potential of free fermions in a magnetic field, and the resulting current is [96]

$$J = \frac{N_c}{2\pi^2}\mu_5 B\,. \tag{5.60}$$

In our model we cannot see any Landau levels directly. Therefore, let us also repeat another, apparently more general, derivation of the chiral magnetic effect. It is based on an energy conservation argument originally pointed out by Nielsen and Ninomiya [130] and applied in Ref. [96]. It states that an energy $2\mu_5$ is needed to replace a fermion at the left-handed Fermi

surface μ_L with a fermion at the right-handed Fermi surface μ_R. This conversion changes the axial number density by $dN_5 = 2$, *i.e.*, the energy actually is $\mu_5 dN_5$. Such a change in N_5 is possible through the QED anomaly in the presence of an electric and a (non-orthogonal) magnetic field. The energy can thus be provided by an electric current. Hence, the change in N_5 per unit volume and time is given by the electric power per unit volume $\mathbf{J}\cdot\mathbf{E}$,

$$\mathbf{J}\cdot\mathbf{E} = \mu_5 \frac{dn_5}{dt}\,. \tag{5.61}$$

Now we know from the (covariant) axial anomaly (5.17b) that, with $\nabla\cdot\mathbf{J}_5 = 0$ and $n_5 = \mathcal{J}_5^0$,

$$\frac{dn_5}{dt} = \frac{N_c}{2\pi^2}\mathbf{B}\cdot\mathbf{E}\,. \tag{5.62}$$

Inserting this into eq. (5.61) and taking $\mathbf{B}$ and $\mathbf{E}$ parallel yields a current $\mathbf{J}$ in the direction of $\mathbf{B}$, given by eq. (5.60). Note that this argument only works for a nonzero, although arbitrarily small, electric field.

Besides the vector current we shall also compute the axial current for which the analogous topological result is [103, 129]

$$J_5 = \frac{N_c}{2\pi^2}\mu B\,, \tag{5.63}$$

which is proportional to the ordinary quark chemical potential and thus of potential interest in neutron and quark star physics.

5.3.2 Currents with consistent anomaly

We have already computed the currents in the symmetric phase, see eqs. (5.56). The analogue for the broken phase, obtained from the definition (5.5) and the gauge fields and field strengths (6.27) and (5.27) is

$$\begin{aligned}
T<T_c: \quad \mathcal{J}^0_{L/R} &= \pm 4\kappa M_{\rm KK}^2\beta\left[-\mu_{5,t}\coth\beta\pi \mp (\jmath_t-\epsilon t) + \frac{Et\pm(\jmath_t-\epsilon t)}{3}\right], && \text{(5.64a)}\\
\mathcal{J}^1_{L/R} &= 0\,, && \text{(5.64b)}\\
\mathcal{J}^2_{L/R} &= \pm\frac{4\kappa M_{\rm KK}^2}{3}\beta\, x_2\left[E\mp\epsilon\frac{\beta\coth\beta\pi}{2\rho(\beta)}\right], && \text{(5.64c)}\\
\mathcal{J}^3_{L/R} &= \mp 4\kappa M_{\rm KK}^2\beta\left[\mp\mu_{5,t} - (\jmath_t-\epsilon t)\coth\beta\pi - \frac{\mu_t\mp\mu_{5,t}}{3}\right]. && \text{(5.64d)}
\end{aligned}$$

Again, to make the origin of the various terms transparent we have written the CS contributions separately. All terms containing a $1/3$ come from the CS action. As for the symmetric phase, we can easily check the consistent anomaly (5.8). Using the expression for the supercurrent (6.31) and $\kappa M_{\rm KK}^2\beta \equiv N_c B/16\pi^2$ we find

$$\partial_t\mathcal{J}^0_{L/R} + \partial_2\mathcal{J}^2_{L/R} = \mp\frac{N_c}{12\pi^2}B\left(E\mp\epsilon\frac{\beta\coth\beta\pi}{2\rho(\beta)}\right) \tag{5.65}$$

and

$$\mp\frac{N_c}{48\pi^2}F^{L/R}_{\mu\nu}\widetilde{F}^{\mu\nu}_{L/R} = \mp\frac{N_c}{12\pi^2}B\left(E\mp\epsilon\frac{\beta\coth\beta\pi}{2\rho(\beta)}\right), \tag{5.66}$$

which confirms eq. (5.8). The axial electric field seems to be modified by a complicated function of the dimensionless magnetic field. This originates from the mixing of the electric field with the supercurrent, which both enter the boundary value of A_3. We shall see that this somewhat strange structure disappears after adding Bardeen's counterterm. From the results (5.56) and

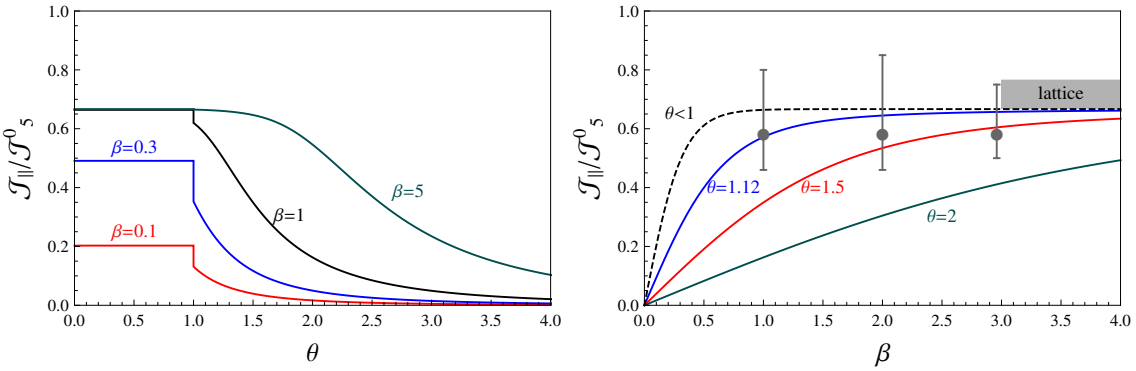

Figure 5.3: Vector current $\mathcal{J}_\parallel = \mathcal{J}_3$ per imbalance of right- and left-handed fermions $n_5 = \mathcal{J}^0_5$ as a function of the dimensionless temperature $\theta = 2\pi T/M_{\rm KK}$ for different values of the dimensionless magnetic field $\beta = \alpha B/M^2_{\rm KK} \simeq B/(0.35\,{\rm GeV}^2) \simeq B/(2\cdot 10^{19}\,{\rm G})$ (left panel) and as a function of β for different values of θ (right panel). The critical temperature for the chiral phase transition is $T_c = M_{\rm KK}/(2\pi)$, *i.e.*, $\theta_c = 1$. The currents in this plot are obtained using the consistent anomaly, *i.e.*, *before* adding Bardeen's counterterm to fulfill the covariant anomaly. After this term is added, the vector current vanishes exactly. The left plot shows the discontinuity at the first order chiral phase transition. This discontinuity vanishes for asymptotically large magnetic fields. The right panel shows that the current saturates at a value of $\mathcal{J}_\parallel = \frac{2}{3}\mathcal{J}^0_5$, in very good agreement with the lattice data for the root mean square value of fluctuations of vector currents and axial densities [109]. The three lattice data points are taken from from figs. 4 and 8 of ref. [109] and correspond to a temperature $T = 1.12\,T_c$. The shaded area indicates the results read off from Figure 11 of ref. [109] for the cleaner case of a ($T = 0$) instanton-like configuration, where the corresponding points lie between $\mathcal{J}_\parallel/\mathcal{J}^0_5 \simeq 0.66 - 0.77$ for magnetic fields of $\beta \simeq 3.0$ and higher.

(5.64) we may compute the vector currents in the chirally symmetric and broken phases. For the following results we set $E = \epsilon = 0$. We find the same result for both phases which is

$$\mathcal{J}_3 = (\mathcal{J}_{\rm YM} + \mathcal{J}_{\rm CS})_3 = \left(1 - \frac{1}{3}\right)\frac{N_c}{2\pi^2} B\mu_5\,. \tag{5.67}$$

This differs by a factor 2/3 from the topological result (5.60). This difference is not surprising since we have not implemented the covariant anomaly yet. To this end we must add Bardeen's counterterm. Before doing so we point out an interesting result which we obtain by considering the ratio of the vector current over the axial density. From eqs. (5.56) and (5.64) we obtain

$$\frac{\mathcal{J}_3}{\mathcal{J}^0_5} = \frac{2}{3}\begin{cases} \dfrac{2\beta}{\theta^3}\dfrac{q_0}{p_0} & \text{for } T > T_c \\ \tanh\beta\pi & \text{for } T < T_c \end{cases}, \tag{5.68}$$

which is displayed in Figure 5.3. In the left panel we see that the first order chiral phase transition manifests itself in the discontinuity of the ratio $\mathcal{J}_3/\mathcal{J}^0_5$. Interestingly, the jump vanishes for asymptotically large magnetic fields. The curves for the symmetric phase are in qualitative agreement with the weak-coupling results in Figure 2 of Ref. [96]. The right panel shows an intriguing agreement of our result for the ratio $\mathcal{J}_3/\mathcal{J}^0_5$ with recent lattice results [109] for the root mean square values of electric currents and chiral densities at large magnetic fields. While the very good numerical agreement might be a coincidence, the lattice results as well as our result clearly show an asymptotic value significantly smaller than 1. If it were 1, the entire imbalance $\mathcal{J}^0_5$ in right-and left-handed fermions, *i.e.*, all excess right-handed fermions, would

contribute to the current for asymptotically large magnetic fields. This is expected at least at weak coupling. In this case, for sufficiently large magnetic fields, all fermions populate the lowest Landau level. Consequently, since the current originates solely from the lowest Landau level, as explained above, one expects $\mathcal{J}_3/\mathcal{J}_5^0 \to 1$. This is confirmed in the weak-coupling calculation of ref. [96], see Figure 6 in this Reference. The lattice result suggests that at strong coupling there may be important modifications to the Landau level picture. We emphasize, however, that Figure 5.3 is not yet our final physical prediction. The model has not yet been appropriately renormalized in order to exhibit the covariant anomaly.

We also remark that the scale of our magnetic fields is very large such that for all physical applications, be it in heavy-ion collisions or in magnetars, the limit of weak magnetic fields is sufficient. In fact, a dimensionless magnetic field $\beta = 1$ corresponds roughly to a magnetic field $B \simeq 2 \cdot 10^{19}\,\mathrm{G}$ if one follows Refs. [29, 131] and sets $N_c = 3$, $M_{\mathrm{KK}} \simeq 949\,\mathrm{MeV}$, $\kappa \simeq 0.00745$, which fits the experimental values for the pion decay constant and the rho meson mass. Therefore, for all applications we have in mind, $\beta \ll 1$. Moreover, one should recall that we have used the YM approximation for the DBI action. This is of course a good approximation for small magnetic fields, but our extrapolation to larger magnetic fields may be subject to modification when the full DBI action is employed. On the other hand, in the limit $\beta \gg 1$, the results for the on-shell action, eqs. (C.60) and (C.80) exhibit a strong suppression of the YM action compared to the CS action. This suggests that our approximation is reliable also for asymptotically large magnetic fields.

5.3.3 Currents with covariant anomaly and absence of the chiral magnetic effect

The next step is to include Bardeen's counterterm (5.11) in order to implement the covariant anomaly. In the broken phase there is a slight complication because the counterterm should only involve genuine background gauge fields, and not those boundary values of the bulk gauge fields that due to the gauge choice $A_z = 0$ represent gradients of the pion field. This means that we have to subtract the time-independent part of the supercurrent $\jmath = -\beta\mu/2\rho$ from the boundary values of the $A_3^{L/R}$. Then, with eq. (5.13) and the value of c from eq. (5.16), the contributions of the counterterm to the currents are

$$
\begin{aligned}
T < T_c: \quad \Delta\mathcal{J}^0_{L/R} &= \pm\frac{2\kappa M_{\mathrm{KK}}^2}{3}\beta[3(A_3^{R/L} \mp \jmath) - (A_3^{L/R} \pm \jmath)] \\
&= \mp\frac{4\kappa M_{\mathrm{KK}}^2}{3}\beta t\left[E \pm 2\epsilon\frac{\beta\coth\beta\pi}{2\rho(\beta)}\right], && \text{(5.69a)} \\
\Delta\mathcal{J}^1_{L/R} &= 0\,, && \text{(5.69b)} \\
\Delta\mathcal{J}^2_{L/R} &= \mp\frac{4\kappa M_{\mathrm{KK}}^2}{3}\beta\, x_2\left[E \mp \frac{\beta\coth\beta\pi}{2\rho(\beta)}\right], && \text{(5.69c)} \\
\Delta\mathcal{J}^3_{L/R} &= \mp\frac{2\kappa M_{\mathrm{KK}}^2}{3}\beta(3A_0^{R/L} - A_0^{L/R}) = \mp\frac{4\kappa M_{\mathrm{KK}}^2}{3}\beta(\mu_t \pm 2\mu_{5,t})\,. && \text{(5.69d)}
\end{aligned}
$$

The first observation is that the 2-component of the current vanishes after adding the counterterm. As mentioned above, this 2-component was unphysical anyway. The cancellation of this component is therefore, besides the covariant anomaly, another sign for the necessity of the counterterm. The covariant anomaly is now correctly contained in the renormalized currents $\bar{\mathcal{J}}^\mu_{L/R} = \mathcal{J}^\mu_{L/R} + \Delta\mathcal{J}^\mu_{L/R}$. This is clear by construction, and can also be verified explicitly: adding eqs. (5.69) to eqs. (5.64), yields

$$
\partial_\mu\bar{\mathcal{J}}^\mu = 0\,, \qquad \partial_\mu\bar{\mathcal{J}}^\mu_5 = \partial_t\bar{\mathcal{J}}^0_5 = \frac{N_c}{2\pi^2}BE\,, \tag{5.70}
$$

	$\bar{\mathcal{J}}^0$	$\bar{\mathcal{J}}^0_5$	$\bar{\mathcal{J}}_\parallel$	$\bar{\mathcal{J}}^5_\parallel$
$T > T_c$	$\frac{N_c}{4\pi^2}\mu B\,\frac{\theta^3}{\beta}\frac{p_0}{q_0}$	$\frac{N_c}{4\pi^2}\mu_5 B\,\frac{\theta^3}{\beta}\frac{p_0}{q_0}$	0	$\frac{N_c}{2\pi^2}\mu B$
$T < T_c$	$\frac{N_c}{6\pi^2}\mu B\,\frac{\beta}{\rho}$	$\frac{N_c}{2\pi^2}\mu_5 B\,\coth\beta\pi$	0	$\frac{N_c}{4\pi^2}\mu B\,\frac{\beta\coth\beta\pi}{\rho}$

Table 5.1: Vector and axial densities $\bar{\mathcal{J}}^0$, $\bar{\mathcal{J}}^0_5$, and vector and axial currents $\bar{\mathcal{J}}_\parallel$, $\bar{\mathcal{J}}^5_\parallel$ in the direction of the magnetic field B after adding Bardeen's counterterm. All results are given as functions of the dimensionless temperature $\theta = 2\pi T/M_{\rm KK}$ and the dimensionless magnetic field $\beta = \alpha B/M^2_{\rm KK}$. The densities in the chirally symmetric phase ($T > T_c$) depend on temperature; the ratio p_0/q_0 behaves as $p_0/q_0 \to 1$ for $\beta/\theta^3 \to 0$ and $p_0/q_0 \to 2\beta/\theta^3$ for $\beta/\theta^3 \to \infty$. In the chirally broken phase ($T < T_c$), all quantities are independent of temperature; the function ρ behaves as $\rho \to 3/(2\pi)$ for $\beta \to 0$ and $\rho \to \beta$ for $\beta \to \infty$. The vector current vanishes exactly in both symmetric and broken phases; this indicates the absence of a chiral magnetic effect in the Sakai-Sugimoto model, see discussion in the text. For the axial current, the temperature-independent topological result is reproduced in the symmetric phase. See Figure 5.4 for the comparison of the axial currents in the symmetric and broken phases.

with the vector and axial currents $\bar{\mathcal{J}}^\mu$, $\bar{\mathcal{J}}^\mu_5$.

The contributions of the counterterm to the currents in the symmetric phase are

$$T > T_c: \quad \Delta\mathcal{J}^0_{L/R} = \pm\frac{2\kappa M^2_{\rm KK}}{3}\beta(3A_3^{R/L} - A_3^{L/R}) = \mp\frac{4\kappa M^2_{\rm KK}}{3}\beta t(E \pm 2\epsilon)\,, \tag{5.71a}$$

$$\Delta\mathcal{J}^1_{L/R} = 0\,, \tag{5.71b}$$

$$\Delta\mathcal{J}^2_{L/R} = \mp\frac{4\kappa M^2_{\rm KK}}{3}\beta\, x_2(E \mp \epsilon)\,, \tag{5.71c}$$

$$\Delta\mathcal{J}^3_{L/R} = \mp\frac{2\kappa M^2_{\rm KK}}{3}\beta(3A_0^{R/L} - A_0^{L/R}) = \mp\frac{4\kappa M^2_{\rm KK}}{3}\beta(\mu_t \pm 2\mu_{5,t})\,. \tag{5.71d}$$

These counterterms have to be added to the currents (5.56). Again, the 2-component of the currents is canceled, and the covariant anomaly can again be verified explicitly. The results for the currents after setting $E = \epsilon = 0$ are given in Table 5.1 for both the symmetric and the chirally broken phase. For the axial current we find that the counterterm exactly cancels the CS part of the current,

$$\bar{\mathcal{J}}^3_5 = \mathcal{J}^3_5 + \Delta\mathcal{J}^3_5 = (\mathcal{J}_{\rm YM})^3_5\,. \tag{5.72}$$

In the chirally symmetric phase, this yields exactly the expected topological result (5.63). In the broken phase, the current is suppressed (but nonvanishing, in contrast to the results obtained with a modified CS action [91]). To lowest order in the magnetic fields as well as for asymptotically large magnetic fields this suppression is simply given by a numerical factor. For intermediate magnetic fields the difference to the symmetric phase is given by a complicated function of B. We plot this result in Figure 5.4.

The most striking of our results shown in Table 5.1 is that for both phases the renormalized vector current is zero for all magnetic fields,

$$\bar{\mathcal{J}}_3 = (\mathcal{J}_{\rm YM} + \mathcal{J}_{\rm CS} + \Delta\mathcal{J})_3 = \left(1 - \frac{1}{3} - \frac{2}{3}\right)\frac{N_c}{2\pi^2}B\mu_5 = 0, \tag{5.73}$$

i.e., the chiral magnetic effect has completely disappeared after adding Bardeen's counterterm. The vector current has been computed in the Sakai-Sugimoto model before, and both existing

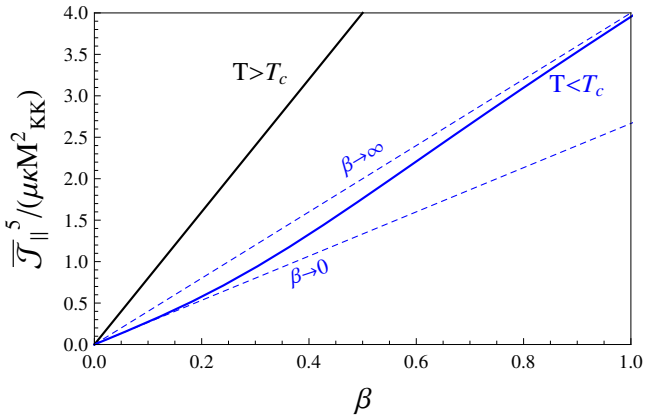

Figure 5.4: Axial current $\bar{\mathcal{J}}^5_{\parallel}$ in chirally symmetric ($T > T_c$) and chirally broken ($T < T_c$) phases in the presence of chemical potential μ as functions of the dimensionless magnetic field $\beta = \alpha B/M^2_{\rm KK}$, *i.e.*, the magnetic field in units of $M^2_{\rm KK}/\alpha \simeq 2\cdot 10^{19}\,$G. In the symmetric phase the current is linear in B, while the current in the broken phase is linear only for small B and asymptotically large B as indicated by the dashed lines. Due to the huge scale for the magnetic field, the small-B approximation for the axial current is sufficient for astrophysical applications. In this case the current in the broken phase is simply 1/3 of the current in the symmetric phase. The analytical results are given in Table 5.1 where it is also shown that the vector current vanishes.

(but differing) results are nonvanishing. One of the results [91] is 1/2 of the topological result (5.60). This result, however, has been obtained with the modified action discussed in Section 5.2.3 which amounts to multiplying the CS contribution by 3/2 (and leaving out the counterterm). As we have seen, this modified action leads to a vanishing anomaly. Another result has recently been presented in Ref. [101] as a limit case of a more general frequency-dependent calculation, but using only the YM part of the current. This gives the topological result (5.60), as can also be seen from eq. (5.73). However, as we have shown, this does not produce the complete covariant anomaly, see eqs. (5.19).

One of the purposes of our work is to point out the differences of these results and the problems of the various approaches regarding the correct anomaly. A summary of our findings is given in table 5.2. Although in our approach the correct anomaly is ensured, we do not claim to have the final answer since the problem of the ambiguity of the currents, see Section 5.2.3, remains. Our approach shows that the CS part of the currents is important for two reasons. First, as realized already in earlier works [34, 110, 111], it naturally gives a nonzero contribution when the currents are defined by varying the full action. Second, and maybe more importantly, only by including the CS contribution does one reproduce the standard result for the consistent anomaly. And only then one can completely implement the covariant anomaly (*i.e.*, a conserved vector current even in the presence of axial gauge fields) by adding an appropriate counterterm as a holographic renormalization. We have explained why this counterterm, even in the absence of axial field strengths, but in the presence of an axial chemical potential, changes the result for the vector current. We do not, however, see a general reason why the counterterm must render the vector current zero, *i.e.*, why by requiring the current to be conserved the current itself should disappear as it turned out to be the case in our explicit calculation.

After having understood the difference of our result to previous results in the same model, let us discuss its significance in view of the apparent contradiction to the result (5.60). As explained above, this result can be derived by using the Landau-level structure of fermions in a magnetic field. One might thus view our result as an indication that there are no fermionic

	$\mathcal{J}_{\rm YM}$	$\mathcal{J}_{\rm YM+CS}$	$\mathcal{J}_{\rm YM+CS}+\Delta\mathcal{J}$	$\mathcal{J}'_{\rm YM+CS}$
anomaly	"semi-covariant":	consistent:	<u>covariant:</u>	absent:
$\partial_\mu \mathcal{J}_5^\mu / \frac{N_c}{24\pi^2}$	$\underline{3F_V\widetilde{F}_V + 3F_A\widetilde{F}_A}$	$F_V\widetilde{F}_V + F_A\widetilde{F}_A$	$\underline{3F_V\widetilde{F}_V + F_A\widetilde{F}_A}$	0
$\partial_\mu \mathcal{J}^\mu / \frac{N_c}{24\pi^2}$	$6F_V\widetilde{F}_A$	$2F_V\widetilde{F}_A$	$\underline{0}$	0
$(\mathcal{J}_\parallel^5 / \frac{\mu B N_c}{2\pi^2})\big\vert_{T>T_c}$	1	$\frac{2}{3}$	1	$\frac{1}{2}$
$\mathcal{J}_\parallel / \frac{\mu_5 B N_c}{2\pi^2}$	1	$\frac{2}{3}$	0	$\frac{1}{2}$
$(\mathcal{J}_\parallel / \mathcal{J}_5^0)\big\vert_{B\to\infty}$	1	$\frac{2}{3}$	0	$\frac{1}{2}$

Table 5.2: Summary of results for the different (parts of the) chiral currents: the Yang-Mills part $\mathcal{J}_{\rm YM}$ (exclusively considered in Ref. [101]), the complete current prior to renormalization $\mathcal{J}_{\rm YM+CS}$ ($\equiv \mathcal{J}$ in the text), the complete current plus Bardeen's counterterm $\mathcal{J}_{\rm YM+CS} + \Delta\mathcal{J} \equiv \bar{\mathcal{J}}$, and the chiral current obtained by modifying the Chern-Simons action according to Ref. [91, 108], $\mathcal{J}'_{\rm YM+CS}$. The correct result for the covariant anomaly is underlined. A "1" in the results for the axial current $\mathcal{J}_\parallel^5$ means agreement with the exact QCD result of ref. [103, 129]; a "1" in the results for the electromagnetic current $\mathcal{J}_\parallel$ means agreement with the weak-coupling approach of ref. [96].

quasiparticles filling Landau levels in the Sakai-Sugimoto model. This may be particularly interesting in view of the recent attempts to see Landau-level-like structures in holographic models [132, 133]. However, as we have pointed out, the derivation of the chiral magnetic effect via the energy conservation argument by Nielsen and Ninomiya appears to be more general. Obviously, the energy conservation (5.61) does not hold with our results because the left-hand side is zero while the right-hand side yields the expected nonzero result from the anomaly, see eq. (5.70). More precisely, one can check that eq. (5.61) holds before adding Bardeen's counterterm while the counterterm itself violates eq. (5.61). However, the form of the counterterm seems to be uniquely determined by the requirements of parity and the possibility of accommodating it in holographic renormalization. This raises the question whether the apparently general energy argument actually uses properties of the system which are different in our strong-coupling approach. Clearly, also in our system, chirality is converted by a rate simply given by the anomaly. Possibly the energy needed for this conversion cannot be written as in eq. (5.61). A reason might be that this energy makes use of the existence of Fermi surfaces for the right- and left-handed particles which are absent in our model. It is tempting to speculate that the chiral magnetic effect indeed vanishes in the strong-coupling limit and that the weak-coupling results together with the recent observations of charge separation in heavy-ion collisions suggest that the quark-gluon plasma generated in such a collision is sufficiently weakly coupled to exhibit the chiral magnetic effect. A deeper understanding of our result, however, seems required before drawing this conclusion.

We recall that in the context of heavy-ion collisions the magnetic field clearly is time-dependent, in contrast to our assumption of a constant magnetic field. Therefore, in order to compute the induced current, one has to consider the frequency-dependent chiral conductivity [97, 101], whereas our result only corresponds to the zero-frequency limit[2]. In other words, even if the conductivity at zero frequency vanishes, a nonzero (time-dependent) current can be

[2] Judging from the calculation of the chiral magnetic conductivity in Ref. [101] (where only the YM part was taken into account), one might expect that the full result, taking into account also the (frequency-independent) CS part and Bardeen's counterterm, leads to a nonzero conductivity for asymptotically large frequency [134]. This seems curious, although we do not see a fundamental reason for this to be unphysical.

expected if there is a nonvanishing conductivity at nonzero frequencies. However, this does not imply electric charge separation because the separation of charges is proportional to the zero-frequency limit of the conductivity [97]. This is easy to understand in analogy to a capacitor which cannot be charged with an alternating current, *i.e.*, integrating the induced current over time will lead to a vanishing charge separation as long as there is no direct current.

Chapter 6

Meson supercurrents and the Meissner effect in the Sakai-Sugimoto model

This chapter is based on [34]. In dense quark matter, chiral symmetry can be broken by the usual chiral condensates $\langle\bar{\psi}\psi\rangle$ or, in a three-flavor system at sufficiently large densities, by diquark condensates $\langle\psi\psi\rangle$ in the color-flavor locked state [8]. In this chapter we shall consider a two-flavor system at finite baryon and isospin chemical potential in the strong-coupling regime at large N_c, which may form different kinds of chiral condensates $\langle\bar{\psi}\psi\rangle$ depending on the values of temperature, the chemical potentials, and the external magnetic field.

It has been shown using a Nambu-Jona-Lasinio (NJL) model that a magnetic field can act as a catalyst for chiral symmetry breaking [135, 136], see also [137, 138]. Also chiral perturbation theory has been used to study the effect of magnetic fields [139, 140], recently for instance in the context of the deconfinement and chiral phase transitions in Refs. [141] and [142, 143], respectively. All these studies are restricted to the vacuum, *i.e.*, they are done for the case of vanishing chemical potentials. Dense matter with nonvanishing chemical potentials in a magnetic field has been studied in the context of color superconductivity [144, 145, 146], which, due to Goldstone boson currents and the axial anomaly, can be ferromagnetic [147]. We use the holographic model by Sakai and Sugimoto, see Chapter 4, at nonzero isospin and baryon chemical potentials to study the effect of a magnetic field on chirally broken phases.[1]

We shall find meson supercurrents and the Meissner effect in the chirally broken phases. Both phenomena are best understood as an analogy to (weak-coupling) superfluidity or superconductivity. For instance, a charged pion condensate of the form $\langle\bar{d}\gamma_5 u\rangle$ can be viewed as Cooper pairing of two different fermion species, here an anti-down-quark and an up-quark. In general, Cooper pairing of two fermion species with chemical potentials μ_1 and μ_2 takes place at a common Fermi surface given by $\bar{\mu} = (\mu_1 + \mu_2)/2$. A mismatch in chemical potentials $\delta\mu = (\mu_1 - \mu_2)/2$ induces a "stress" on the pairing in trying to move the two Fermi surfaces apart. For not too large values of $\delta\mu$, the system can sustain the stress and the densities of the two fermion species are (at zero temperature) "locked" together, *i.e.*, the difference in densities $\delta n = n_1 - n_2$ vanishes. For larger values of $\delta\mu$, and before completely breaking the condensate, the system may respond to the stress by leaving some, but not all, fermions around the Fermi surfaces unpaired, allowing for a nonzero δn. The resulting state breaks rotational invariance, and it may even break translational invariance by giving rise to a crystalline structure. Anisotropic pion condensates in nuclear matter have been discussed a long time ago [150, 151, 152, 153]; crystalline structures of the superfluid order parameter are well-known in

[1] For effects of magnetic fields in other holographic models of strongly coupled gauge theories with flavor degrees of freedom see e.g. Refs. [57, 148, 149].

condensed matter physics [154, 155] as well as in dense quark matter [156], and also have been discussed in the context of chiral condensates [157]. In either case, be it in a homogeneous manner or in a complicated crystalline structure, this unconventional pairing induces nonzero "supercurrents" in the system, see for instance Refs. [158, 159, 160]. These supercurrents are cancelled by counter-propagating currents, typically coming from unpaired fermions, such that the net current in the system vanishes.

In the case of a pion condensate of the form $\langle \bar{d}\gamma_5 u\rangle$, $\bar{\mu}$ and $\delta\mu$ correspond to the isospin, μ_I, and baryon, μ_B, chemical potential, respectively. Consequently, one might expect anisotropic pairing upon increasing the "mismatch" μ_B. And, corresponding to the above δn, a nonzero baryon number n_B is expected. In the Sakai-Sugimoto model, a finite baryon number is taken into account via the Chern-Simons term. Localized baryons can be described by instantons of the effective gauge theory of the flavor branes [93, 111, 161] corresponding to chiral skyrmions, which in the ground state form crystals rather than a liquid [162, 163, 125]. However, we are interested in a homogeneous distribution of baryon (and isospin) density. It turns out that this can be achieved by a nonzero magnetic field in the model [91, 90], which is anyway of interest in the context of neutron star physics.

A magnetic field, however, is expelled from the charged pion condensate because a condensate of charged bosons (be it Cooper pairs or, in our case, Goldstone bosons) acts as a superconductor and thus exhibits a Meissner effect.[2] Accordingly, we shall find the above expectations of a supercurrent and nonzero baryon number not realized in the charged pion condensate which remains unmodified for (not too large) magnetic fields. A meson supercurrent as well as nonzero baryon (and isospin) numbers occur, for nonzero magnetic field, instead in the phase with a neutral pion condensate.

This chapter is organized as follows. In Section 6.1 we discuss our ansatz for solutions in the presence of baryon and isospin chemical potentials and a magnetic field and derive the equations of motion and the free energy for the chirally broken phases. The main part of this chapter is Section 6.2. In this part we first discuss how to incorporate different chiral condensates into the model, see Section 6.2.1. In Section 6.2.2 we solve the equations of motion for the sigma and the charged pion phase and compute their free energies. In particular, we discuss the Meissner effect in Section 6.2.4. The results are used to discuss the currents and number densities in these phases in Section 6.2.5. Finally, we compare their free energies and discuss the resulting phase diagram in Section 6.2.6.

6.1 Equation of motion and free energy in the chirally broken phase

In this Section we specify our ansatz according to the physical situation we are interested in and write down the corresponding equations of motion and we explain how to renormalize the free energy. In this chapter we shall be concerned with the confined, *i.e.*, chirally broken, phase whose metric g is given in Eq. (4.11a). For completeness we present the equations of motion and the free energy of the deconfined, *i.e.*, chirally restored, phase in Appendix C.4.

6.1.1 Equations of motion and ansatz including magnetic field, chemical potentials, and supercurrents

Now we specify our ansatz for the gauge fields. As already mentioned in Section 4.2, we set all components of the gauge field proportional to to τ_1 and τ_2 in flavor space to zero and write the gauge fields and field strengths proportional to $\mathbf{1}$ as $(\hat{A}, \hat{F})$ and the ones proportional to

[2] Holographic models of superconductors and superfluids have recently been investigated in Refs. [164, 165, 166, 167], see Ref. [168] for a discussion of the Meissner effect.

τ_3 as (A, F). First, we set all components proportional to τ_1 and τ_2 in flavor space to zero and may then, for notational convenience drop the superscript 3 from the gauge fields and field strengths. Consequently, in the following we are only left with gauge field and field strength components with a hat $(\hat{A}, \hat{F})$, corresponding to the $\mathbf{1}$-components, and without any flavor index (A, F), corresponding to the τ_3-components. This choice simplifies the calculations significantly but is a restriction for the possible chiral condensates we can capture, as we shall explain in Section 6.2.1.

The magnetic field is introduced as follows. The electromagnetic gauge group with generator $Q = \mathrm{diag}(q_1, q_2)$, where q_1 and q_2 are the electric charges of the quark flavors, is a subgroup of $U(2)_L \times U(2)_R$. The magnetic field $\mathcal{B}_{\mathrm{em}}$ thus has baryon and isospin components, $Q\mathcal{B}_{\mathrm{em}} = \hat{\mathcal{B}}\mathbf{1} + \mathcal{B}\tau_3$, or

$$\hat{\mathcal{B}} = \frac{q_1 + q_2}{2}\mathcal{B}_{\mathrm{em}}\,, \qquad \mathcal{B} = \frac{q_1 - q_2}{2}\mathcal{B}_{\mathrm{em}}\,. \tag{6.1}$$

We are interested in a system of up and down flavors, *i.e.*, $q_1 = 2/3\,e$, $q_2 = -1/3\,e$ with $e^2 = 4\pi/137$ and $\hat{\mathcal{B}} = e\mathcal{B}_{\mathrm{em}}/6$, $\mathcal{B} = e\mathcal{B}_{\mathrm{em}}/2$, but mostly we shall derive general results, keeping $\hat{\mathcal{B}}$ and $\mathcal{B}$ independent of each other. We should recall that the gauge symmetry in the bulk corresponds to a global symmetry at the boundary. Therefore, there is no electromagnetic gauge symmetry at the boundary, and in this sense $\mathcal{B}_{\mathrm{em}}$ is not a dynamical magnetic field.

We consider a spatially homogeneous magnetic field and, without loss of generality, let it point into the 3-direction. This requires nonzero field strengths $\hat{F}_{12}$ and F_{12}. We can therefore choose the ansatz

$$\hat{A}_1(\mathbf{x}, z) = -x_2\frac{\hat{b}(z)}{2}\,, \qquad \hat{A}_2(\mathbf{x}, z) = x_1\frac{\hat{b}(z)}{2}\,, \tag{6.2a}$$

$$A_1(\mathbf{x}, z) = -x_2\frac{b(z)}{2}\,, \qquad A_2(\mathbf{x}, z) = x_1\frac{b(z)}{2}\,, \tag{6.2b}$$

such that $\hat{F}_{12}(z) = \hat{b}(z)$, $F_{12}(z) = b(z)$, and the boundary values at $z = \pm\infty$ of $\hat{b}(z)$, $b(z)$ given by $\hat{\mathcal{B}}$, $\mathcal{B}$. (Note that for non-constant $\hat{b}(z)$, $b(z)$, we also have nonzero field strengths $\hat{F}_{iz}$, F_{iz}.)

Next we account for the chemical potentials. This is done by identifying the boundary values at $z = \pm\infty$ for the gauge fields $\hat{A}_0(z)$ and $A_0(z)$ with the baryon and isospin chemical potentials μ_B and μ_I [162, 88, 92]. Consequently, we may have nonzero field strengths $\hat{F}_{0z}$, F_{0z}. It turns out that within this ansatz nonzero values of the spatial gauge fields may be induced, *i.e.*, we have to take into account $\hat{A}_3(z)$, $A_3(z)$ and thus the field strengths $\hat{F}_{3z}$, F_{3z}. The boundary values at $z = \pm\infty$ of the spatial gauge fields are identified with the gradients of the meson fields [29, 91]. These gradients correspond, according to the usual hydrodynamic theory of a superfluid [169, 170], to "supercurrents", *i.e.*, currents of the condensate, in our context for instance the current of a pion condensate; see also Refs. [158, 159]. Consequently, we shall identify $\hat{A}_3(\pm\infty)$, $A_3(\pm\infty)$ with meson supercurrents $\hat{\jmath}$, $\jmath$. The supercurrents are not external parameters, hence we shall minimize the free energy with respect to them [91, 90]. They should not be confused with the "normal" currents $\mathcal{J}_i = \delta S_{\mathrm{eff}}/\delta A^i$, discussed in the Sakai-Sugimoto model in detail in Refs. [110, 111] and Chapter 5, and computed below in Section 6.2.3. The supercurrents rather act as a source for the normal currents.

Now we can insert the ansatz into the general equations of motion (4.23). We then need to replace $\mathcal{A}_0 \to i\mathcal{A}_0$, since we are working in euclidean space. We find the following equations for the magnetic field

$$\partial_z[k(z)\partial_z\hat{b}] = \partial_z[k(z)\partial_z b] = 0\,, \tag{6.3}$$

where

$$k(z) \equiv u_{\mathrm{KK}}^3 + u_{\mathrm{KK}}z^2\,. \tag{6.4}$$

They arise from the Yang-Mills variation with respect to the spatial gauge field, Eqs. (C.2b) and (C.3b) and contain no contribution from the Chern-Simons term. Moreover, they decouple

from the equations for the other fields, which are

$$\partial_z[k(z)\hat{F}_{z0}] = \frac{\alpha u_{\rm KK}^2}{M_{\rm KK}^2}\left[b(z)F_{z3}+\hat{b}(z)\hat{F}_{z3}\right], \tag{6.5a}$$

$$\partial_z[k(z)F_{z0}] = \frac{\alpha u_{\rm KK}^2}{M_{\rm KK}^2}\left[b(z)\hat{F}_{z3}+\hat{b}(z)F_{z3}\right], \tag{6.5b}$$

$$\partial_z[k(z)\hat{F}_{z3}] = \frac{\alpha u_{\rm KK}^2}{M_{\rm KK}^2}\left[b(z)F_{z0}+\hat{b}(z)\hat{F}_{z0}\right], \tag{6.5c}$$

$$\partial_z[k(z)F_{z3}] = \frac{\alpha u_{\rm KK}^2}{M_{\rm KK}^2}\left[b(z)\hat{F}_{z0}+\hat{b}(z)F_{z0}\right], \tag{6.5d}$$

where

$$\alpha \equiv \frac{27\pi}{2\lambda}\,. \tag{6.6}$$

In all four equations in (6.5) the left-hand side comes from the variation of the Yang-Mills contribution, while the right-hand side originates from the Chern-Simons contribution. We see that the latter is proportional to the magnetic field. The equations (6.3) and (6.5) shall be solved analytically in Section 6.2. Before doing so we use these equations to derive a simple expression for the free energy.

6.1.2 Free energy and holographic renormalization

In order to compute the free energy we have to evaluate the action for our specific ansatz. Recall that the Yang-Mills part of the action can be written as

$$S_{\rm YM} = \kappa\int d^4x\int_{-\infty}^{\infty}dz\left\{\frac{16M_{\rm KK}^2k^{2/3}(z)}{9(2\pi\alpha')^2u_{\rm KK}}+\frac{M_{\rm KK}^2}{u_{\rm KK}^2}k(z){\rm Tr}[\mathcal{F}_{z\mu}^2]+\frac{1}{2}h(z){\rm Tr}[\mathcal{F}_{\mu\nu}^2]\right\}, \tag{6.7}$$

where $\mu,\nu=0,1,2,3$ and the functions $k(z)$ and $h(z)$ are given in (4.21). To compute the Chern-Simons contribution to the free energy we first note that the surface term (last term on the right-hand side of Eq. (4.18)) gives a nonzero contribution. Within our ansatz the term $\propto d(\hat{A}{\rm Tr}[A^3])$ vanishes since our only nonzero flavor components of the gauge fields are proportional to $\mathbf{1}$ and τ_3; however, the term $\propto d(\hat{A}{\rm Tr}[FA])$ does not vanish. We find

$$\hat{A}_\mu F_{\nu\rho}F_{\sigma\lambda}\epsilon^{\mu\nu\rho\sigma\lambda} = 8b(\hat{A}_3F_{z0}-\hat{A}_0F_{z3})\,, \tag{6.8a}$$

$$\hat{A}_\mu \hat{F}_{\nu\rho}\hat{F}_{\sigma\lambda}\epsilon^{\mu\nu\rho\sigma\lambda} = 8\hat{b}(\hat{A}_3\hat{F}_{z0}-\hat{A}_0\hat{F}_{z3})\,, \tag{6.8b}$$

$$\begin{aligned}\partial_\mu(\hat{A}_\nu F_{\rho\sigma}A_\lambda)\epsilon^{\mu\nu\rho\sigma\lambda} &= 2b(A_3\hat{F}_{z0}-A_0\hat{F}_{z3}+2\hat{A}_0F_{z3}-2\hat{A}_3F_{z0})\\ &\quad+2\hat{b}(A_3F_{z0}-A_0F_{z3})\,.\end{aligned} \tag{6.8c}$$

Inserting these expressions into the Chern-Simons action (4.18) yields, with $\mathcal{A}_0\to i\mathcal{A}_0$ and $N_c/(16\pi^2)=\alpha\kappa$,

$$\begin{aligned}S_{\rm CS} &= \frac{\alpha\kappa}{3}\int dx^4\int_{-\infty}^{\infty}dz\,\Big[\hat{b}\left(\hat{A}_3\hat{F}_{z0}+A_3F_{z0}-\hat{A}_0\hat{F}_{z3}-A_0F_{z3}\right)\\ &\qquad+b\left(\hat{A}_3F_{z0}+A_3\hat{F}_{z0}-\hat{A}_0F_{z3}-A_0\hat{F}_{z3}\right)\Big]\\ &= \frac{\kappa M_{\rm KK}^2}{3u_{\rm KK}^2}\frac{V}{T}\left\{\int_{-\infty}^{\infty}dz\,k(z)(\hat{F}_{z0}^2+F_{z0}^2-\hat{F}_{z3}^2-F_{z3}^2)\right.\\ &\qquad\left.-\Big[k(z)(\hat{A}_0\hat{F}_{z0}+A_0F_{z0}-\hat{A}_3\hat{F}_{z3}-A_3F_{z3})\Big]_{z=-\infty}^{z=+\infty}\right\},\end{aligned} \tag{6.9}$$

where, in the second step, we have used the equations of motion (6.5), and where V is the three-dimensional volume of space and T the temperature. In changing the integration over the holographic coordinate from $u \in [u_{\rm KK}, \infty]$ to $z \in [-\infty, \infty]$ we have assumed that the integrand is symmetric in z. In all phases we consider this turns out to be the case. Putting the Yang-Mills and Chern-Simons contribution together, we obtain the free energy density $\Omega \equiv T(S_{\rm YM} + S_{\rm CS})/V$

$$\begin{aligned}\Omega &= \Omega_g + \Omega_b + \frac{\kappa M_{\rm KK}^2}{6u_{\rm KK}^2}\int_{-\infty}^{\infty} dz\, k(z)(-\hat{F}_{z0}^2 - F_{z0}^2 + \hat{F}_{z3}^2 + F_{z3}^2) \\ &\quad - \frac{\kappa M_{\rm KK}^2}{3u_{\rm KK}^2}\left[k(z)(\hat{A}_0\hat{F}_{z0} + A_0F_{z0} - \hat{A}_3\hat{F}_{z3} - A_3F_{z3})\right]_{z=-\infty}^{z=+\infty}, \end{aligned} \tag{6.10}$$

where the geometric contribution Ω_g is given by the field-independent first term on the right-hand side of Eq. (4.20). This term is independent of all gauge fields and field strengths and thus plays no role in discussing the physical properties of a given phase. For free energy comparisons of phases with different geometries one can handle this term with the proper renormalization explained in Ref. [21]. We shall only compare free energies of phases with identical embedding of the flavor branes. Hence, for our purpose, this term can simply be dropped from now on. The term Ω_b in Eq. (6.10) is given by

$$\begin{aligned}\Omega_b &\equiv \frac{\kappa}{4}\int_{-\infty}^{\infty} dz\, h(z)[\hat{b}^2(z) + b^2(z)] \\ &\quad + \frac{\kappa M_{\rm KK}^2}{4u_{\rm KK}^2}\frac{\int dx_1 dx_2 (x_1^2 + x_2^2)}{\int dx_1 dx_2}\int_{-\infty}^{\infty} dz\, k(z)[(\partial_z\hat{b})^2 + (\partial_z b)^2]\,. \end{aligned} \tag{6.11}$$

Both contributions of Ω_b solely depend on the magnetic field (remember that the equations of motion for $\hat{b}$ and b (6.3) decouple from the other field equations). Therefore, Ω_b is irrelevant for minimizing the free energy with respect to the supercurrents $\hat{\jmath}$ and $\jmath$. However, both terms of Ω_b are divergent.

Let us first consider only constant functions $b(z) = \mathcal{B}$ and $\hat{b}(z) = \hat{\mathcal{B}}$, for which only the first term in Ω_b is present. Since we have already divided by the volume V of 3-space, we would expect a finite energy density from a homogeneous magnetic field, but because of the extra holographic dimension, this is not the case. In fact, since $h(z) \sim z^{-2/3}$, the divergence of Ω_b comes from the $|z| \to \infty$ limits of integration and is thus a typical holographic divergence which can be treated by holographic renormalization [171]. Here we do not attempt to provide a complete discussion of this procedure, which for the (nonconformal) Sakai-Sugimoto model has been introduced only recently [172, 173]. We rather follow the method outlined in these papers and subtract a counterterm, fixed by a physical renormalization condition, as follows. After restricting the holographic integration in Ω_b to a finite interval $-\Lambda < z < \Lambda$, we subtract a counterterm $\delta\Omega_b(\Lambda)$ which cancels the divergence and obtain a renormalized contribution $\Omega_b^{\rm ren}$. We also include a finite counterterm which is fixed by requiring the free energy in the absence of any chemical potential to vanish,

$$\Omega(\mu_{B,I} = 0) = 0\,. \tag{6.12}$$

This condition is motivated by the observation that Ω should be the matter part of the free energy, *i.e.*, it should describe the fermions and their interaction with the magnetic field. In particular, we thus require that the energy density of the (nondynamical) magnetic field in the absence of any matter be left out. This we shall later treat separately when we consider the Gibbs free energy (the Legendre transform from fixed internal magnetic field to fixed external magnetic field) in Section 6.2.6. The condition (6.12) implies that we have to require

$$0 = \Omega_b^{\rm ren} \equiv \lim_{\Lambda\to\infty}[\Omega_b(\Lambda) - \delta\Omega_b(\Lambda)]\,. \tag{6.13}$$

To find the exact form of the counterterms we first note that, for constant $\hat{b}(z) = \hat{\mathcal{B}}$ and $b(z) = \mathcal{B}$,

$$\Omega_b(\Lambda) = \frac{3\kappa}{2}(\hat{\mathcal{B}}^2 + \mathcal{B}^2)\left[\frac{\Lambda^{1/3}}{u_{\rm KK}^{1/3}} - \sqrt{\pi}\,\frac{\Gamma(5/6)}{\Gamma(1/3)} + \mathcal{O}\left(\frac{u_{\rm KK}^{5/3}}{\Lambda^{5/3}}\right)\right] . \tag{6.14}$$

The counterterm $\delta\Omega_b(\Lambda)$ should depend only on fields and geometric data on the slice $z = \Lambda$, in particular it should only involve the induced metric $\gamma_{\mu\nu}$ on the slice and not the complete metric g. By including appropriate factors of the dilaton [172, 173] and an appropriate numerical factor to fulfill the condition (6.13) we find

$$\delta\Omega_b(\Lambda) = R\left[\left(\frac{e^{\Phi}}{g_s}\right)^{1/3} - \frac{\sqrt{\pi}\,\Gamma(5/6)}{\Gamma(1/3)}\left(\frac{u_{\rm KK}}{R}\right)^{1/2}\left(\frac{e^{\Phi}}{g_s}\right)^{-1/3}\right]\mathcal{C}(\Lambda)\,, \tag{6.15}$$

with

$$\begin{aligned}\mathcal{C}(\Lambda) &\equiv -T_8 V_4 (2\pi\alpha')^2 e^{-\Phi}\sqrt{\gamma}\,\gamma^{\mu\nu}\gamma^{\rho\sigma}{\rm Tr}[\mathcal{F}_{\nu\rho}\mathcal{F}_{\sigma\mu}] \\ &= \frac{3\kappa}{2u_{\rm KK}^{1/4}R^{3/4}}(\hat{\mathcal{B}}^2 + \mathcal{B}^2)\left[\frac{\Lambda^{1/6}}{u_{\rm KK}^{1/6}} + \mathcal{O}\left(\frac{1}{\Lambda^{11/6}}\right)\right] ,\end{aligned} \tag{6.16}$$

where we have used Eq. (C.4) and where the indices μ, ν, ρ, σ run over $0, 1, 2, 3$. With this counterterm, the term proportional to $\Lambda^{1/3}$ (Λ^0) in Eq. (6.14) are cancelled by the first (second) term in Eq. (6.15)[3] .

In the case of a magnetic field which is not constant in the bulk, the second term in Ω_b as given by Eq. (6.11) is also divergent, but its divergence comes from the integration over the spatial directions perpendicular to the magnetic field, regardless of whether the holographic z-integration is finite or not. Therefore, we cannot treat this term by the usual holographic renormalization and we interpret this divergence, when present, as a Meissner effect: a phase where a homogeneous magnetic field $\mathcal{B}_{\rm em}$, which fixes the boundary values of $\hat{b}(z)$ and $b(z)$, is only possible for non-constant functions in z, is infinitely penalized such that only $\mathcal{B}_{\rm em} = 0$ is allowed. As we shall see, this will be the case for the charged pion condensate, to be discussed further in Section 6.2.4. At this point we already observe that the role of the spatial directions transverse to the magnetic field is no coincidence. It points to the necessity of currents in these directions which produce a magnetic field equal in magnitude but with opposite direction compared to the external magnetic field. This leads to a vanishing total magnetic field in the system, which is nothing but the Meissner effect for superconductors.

6.2 Chirally broken phases in a magnetic field

In this section we solve the equations of motion for the chirally broken phase. We shall distinguish between two different chirally broken phases, the σ and the π phase. This is the main part of this chapter, and the main physical results can be found in Sections. 6.2.5 and 6.2.6.

6.2.1 Chiral rotations and resulting boundary conditions

In $N_f = 2$ chiral perturbation theory the chiral field $U \in U(2)$ describing the Goldstone bosons is given by

$$U = e^{i(\eta + \varphi_a\tau_a)/f_\pi} , \tag{6.17}$$

[3]Note that equations (6.11)-(6.16) have different prefactors than equations (3.14)-(3.19) in Ref. [34] where we used a wrong prefactor in (3.19) and missed a factor of 1/2 in the first term in (3.14).

where f_π is the pion decay constant (in the Sakai-Sugimoto model, $f_\pi = 2M_{\rm KK}\sqrt{\kappa/\pi}$ [29, 111]). The η meson becomes massive in QCD due to the explicit breaking of the $U(1)_A$. This is realized in the Sakai-Sugimoto model through the Chern-Simons term, and the mass of the η can be computed within the model, $m_\eta = \lambda M_{\rm KK}\sqrt{N_f/N_c}/(3\sqrt{3}\pi)$ [29], see also Refs. [174, 175, 176]. For the purpose of the following arguments we assume the full $U(2)_L \times U(2)_R$ symmetry to be intact, *i.e.*, the η meson appears massless. We comment on this assumption below Eq. (6.22). In the Sakai-Sugimoto model the chiral field is given by the holonomy [29]

$$U = P\exp\left(i\int_{-\infty}^{\infty} dz\, \mathcal{A}_z\right) . \tag{6.18}$$

As mentioned above, we work in a gauge where $\mathcal{A}_z = 0$. It seems we can then only consider the vacuum $U = \mathbf{1}$. However, we can keep the $\mathcal{A}_z = 0$ gauge and recover other vacua encoded in the boundary values of the gauge fields. This is explained in detail for instance in Ref. [94]. We shall now recapitulate this explanation and apply it to our case.

Consider a potential $V[\mu_L, \mu_R, U(\phi)]$ which is invariant under $U(N_f)_L \times U(N_f)_R$. Here, $\mu_L, \mu_R \in U(N_f)$ are fixed external parameters. For the following argument we denote these parameters simply by μ_L, μ_R, reminiscent of the chemical potentials, but one should keep in mind that this notation also includes the external magnetic field. The chiral field U is written as a function of a parameter ϕ with respect to which we have to minimize the potential to find the vacuum. This parameter is a symbol for the fields φ_a given in Eq. (6.17). The external parameters transform under the global symmetry as $\mu_L \to g_L^{-1}\mu_L g_L$, $\mu_R \to g_R^{-1}\mu_R g_R$, while the chiral field transforms as $U \to g_L^{-1} U g_R$, where $g_L \in U(N_f)_L$, $g_R \in U(N_f)_R$. Via a global symmetry transformation we have $V[\mu_L, \mu_R, U(\phi)] = V[g_L^{-1}(\phi)\mu_L g_L(\phi), g_R^{-1}(\phi)\mu_R g_R(\phi), \mathbf{1}]$ with ϕ-dependent transformations $g_L(\phi)$, $g_R(\phi)$ such that $g_L^{-1}(\phi)U(\phi)g_R(\phi) = \mathbf{1}$. To find the vacuum of the theory it obviously does not matter whether we use the original potential or the potential with the transformed quantities because both expressions are simply identical. Consequently, instead of keeping the external parameters fixed and varying the chiral field we can fix the chiral field to be the unit matrix and vary the external parameters. Of course we cannot simply treat the external parameters as arbitrary continuous quantities with respect to which we minimize the potential. We need to ensure that they are connected by a transformation to their physical values. We shall see below that within our ansatz the allowed rotated parameters only assume two discrete values, such that we simply have to compare two separate phases with each other. After minimization of the potential, the physical vacuum is given by applying the rotation found from minimization "backwards" onto the unit matrix, *i.e.*,

$$U = g_L g_R^{-1} . \tag{6.19}$$

Without loss of generality we can set $g_R = \mathbf{1}$ and thus $U = g_L$. We can write

$$g_L = e^{i(\eta + \varphi_a\tau_a)/f_\pi} = e^{i\eta/f_\pi}\frac{\sigma + i\pi_a\tau_a}{f_\pi} , \tag{6.20}$$

where $\sigma/f_\pi \equiv \cos(\varphi/f_\pi)$, $\pi_a/f_\pi = \varphi_a/\varphi\,\sin(\varphi/f_\pi)$ with $\varphi \equiv (\varphi_1^2+\varphi_2^2+\varphi_3^2)^{1/2}$. This is the usual form of the chiral field in chiral perturbation theory, where the massive mode, the "sigma", is frozen and the effective theory describes the remaining light Goldstone modes, the pions. Therefore, both sides of Eq. (6.20) contain four degrees of freedom; for the right-hand side we have the condition $\sigma^2 + \pi^2 = f_\pi^2$ which is obvious from the definitions of σ and π_a.

To apply a rotation given by g_L on the (left-handed) external parameter μ_L note that our physical chemical potentials and the magnetic field are diagonal in flavor space and identical for L and R, $\mu_L = \mu_R = \mu_B\mathbf{1} + \mu_I\tau_3$, $\mathcal{B}_{{\rm em},L} = \mathcal{B}_{{\rm em},R} = \hat{\mathcal{B}}\mathbf{1} + \mathcal{B}\tau_3$. The baryon part $\propto \mathbf{1}$ does obviously not change under an $SU(2)$ transformation. We thus only have to consider how the

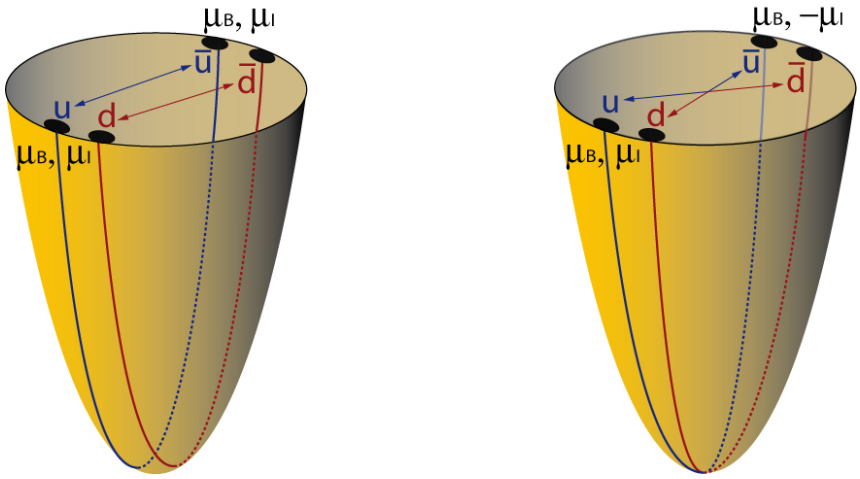

Figure 6.1: A cartoon of our condensates. Left: σ condensate: $\langle\bar{u}\gamma_5 u\rangle - \langle\bar{d}\gamma_5 d\rangle$. The left handed up brane is connected with the right handed up brane. Right: $\pi^{\pm}$ condensate with nonzero $\langle\bar{d}\gamma_5 u\rangle$ and $\langle\bar{u}\gamma_5 d\rangle$. The left handed up brane is connected with the left handed down brane and vice versa. The u and d branes are separated ony for illustrative purpose.

isospin part $\propto \tau_3$ transforms. We find

$$g_L^{-1}\tau_3 g_L = \frac{1}{f_\pi}\left[\pi^+(\pi^0 + i\sigma)\tau_+ + \pi^-(\pi^0 - i\sigma)\tau_- + (1 - 2\pi^+\pi^-)\tau_3\right] , \tag{6.21}$$

where $\tau_\pm \equiv \tau_1 \pm i\tau_2$, and where we have introduced the neutral pion $\pi^0 = \pi_3$ and the charged pions $\pi^\pm \equiv \pi_1 \mp i\pi_2$. In our ansatz described in Section 6.1.1 we have restricted ourselves to diagonal gauge fields. Since the chemical potentials and the magnetic field are the boundary values for the gauge fields, they have to be diagonal too. Consequently, we can only allow for transformations (6.21) that transform τ_3 into a matrix $\propto \tau_3$. There are two (nontrivial) possibilities to make the coefficients in front of τ_+, τ_- vanish: (i) $\pi^+ = \pi^- = 0$ which leads to $g_L^{-1}\tau_3 g_L = \tau_3$ and (ii) $\pi^0 = \sigma = 0$ which leads to $g_L^{-1}\tau_3 g_L = -\tau_3$. Hence we can either leave the isospin components of the chemical potentials and the magnetic field invariant or flip their sign. This means that the parameter ϕ in $U(\phi)$ above is in fact discrete, not continuous. Had we allowed for off-diagonal components in the gauge fields, we could have described arbitrary linear combinations of the pion fields.

These somewhat formal arguments have a very intuitive geometric interpretation [92]: another (simpler, but less precise) way of saying what we have just explained is the following. Think of the D8-branes as a left-handed up-brane and a left-handed down-brane and of the $\overline{\text{D8}}$-branes as a right-handed up-brane and a right-handed down-brane. Then, a chirally broken phase can be constructed by connecting (i) the left-handed up-brane with the right-handed up-brane and likewise for the down-branes or (ii) the left-handed up-brane with the right-handed down-brane and vice versa. These two possibilities correspond exactly to the two cases from the above formal argument: case (i) corresponds to a condensate where equal quark flavors participate, *i.e.*, a combination of σ and π^0 with $\bar{u} - u$ and $\bar{d} - d$ pairing. In the remainder of this chapter we shall refer to this case as the σ phase. Case (ii) corresponds to a charged pion condensate with nonzero $\langle\bar{d}\gamma_5 u\rangle$, $\langle\bar{u}\gamma_5 d\rangle$, to which we shall refer as the π phase (this phase is sometimes called "ρ" [92, 177]). As a summary of this section and a reminder for the subsequent sections, we present the resulting boundary conditions for the σ and the π phases in Table 6.1 [4].

[4] In [34] we used twice the boundary conditions for the chemical potentials and supercurrents as we do here

	$\hat{A}_0(\pm\infty)$	$A_0(\pm\infty)$	$\hat{b}(\pm\infty)$	$b(\pm\infty)$	$\hat{A}_3(\pm\infty)$	$A_3(\pm\infty)$
σ	μ_B	μ_I	$\hat{\mathcal{B}}$	$\mathcal{B}$	$\mp\hat{\jmath}$	$\mp\jmath$
π	μ_B	$\pm\mu_I$	$\hat{\mathcal{B}}\,(0)$	$\pm\mathcal{B}\,(0)$	$\mp\hat{\jmath}$	0

Table 6.1: Boundary conditions in the sigma and pion phases. The boundary conditions for the temporal components of the gauge fields correspond to the baryon and isospin chemical potentials, while the boundary conditions for the field strengths $\hat{F}_{12} \equiv \hat{b}$, $F_{12} \equiv b$ correspond to the baryon and isospin components of the magnetic field. The boundary conditions for the spatial components $\hat{A}_3$, A_3 are given by the meson supercurrents $\hat{\jmath}$, $\jmath$. These currents are not external parameters but have to be determined by minimizing the free energy. In the π phase $A_3(\pm\infty)$ has to vanish to ensure a well-defined behavior of the gauge fields under parity transformations, see Eq. (C.29) and discussion above this equation. The zeros in parantheses for the magnetic fields in the charged pion condensed phase indicate that eventually we shall set $\hat{\mathcal{B}} = \mathcal{B} = 0$ because of the Meissner effect in this phase, see Section 6.2.4.

In this Table we also have included the supercurrents which, in our gauge $g_L = U$, have the form $g_L^{-1}\nabla g_L$ [29]. With Eq. (6.20) this becomes for the two phases

$$(i)\ \ \sigma \text{ phase}: \qquad ig_L^{-1}\nabla g_L = -\frac{\nabla\eta}{f_\pi} + \frac{\tau_3}{f_\pi^2}\left(\pi^0\nabla\sigma - \sigma\nabla\pi^0\right)\,, \tag{6.22a}$$

$$(ii)\ \ \pi \text{ phase}: \qquad ig_L^{-1}\nabla g_L = -\frac{\nabla\eta}{f_\pi} + \frac{i\tau_3}{2f_\pi^2}\left(\pi^+\nabla\pi^- - \pi^-\nabla\pi^+\right)\,. \tag{6.22b}$$

Note that the right-hand sides of both equations are real. We see that the supercurrents are diagonal, *i.e.*, our ansatz with nonvanishing $\mathbf{1}$-component $\hat{\jmath}$ and τ_3-component $\jmath$ is consistent. Interestingly, an anisotropic η condensate appears in the $\mathbf{1}$-components $\hat{\jmath}$. The η condensate has dropped out in Eq. (6.21), and thus our boundary conditions, given by the chemical potentials and the magnetic field modified by the rotation (6.21), do not seem to reveal whether there is an admixture of an η condensate in the σ phase. On the other hand, a nonzero supercurrent $\hat{\jmath}$ seems to indicate the presence of an η supercurrent. Indeed, we shall see later that in the σ phase a nonzero $\hat{\jmath}$ is induced. The term $\nabla\eta$ in Eqs. (6.22) appears due to our use of the full $U(2)_L \times U(2)_R$ symmetry. Strictly speaking, our Lagrangian breaks the axial $U(1)_A$ because of the presence of the Chern-Simons term. However, this symmetry is preserved if one compensates a $U(1)_A$ rotation by a shift of the θ parameter, whose realization in the Sakai-Sugimoto model is discussed in Ref. [29], see also Ref. [178]. We thus implicitly adjust the θ parameter to apply the full gauge symmetry. We shall proceed within this simplification, but have to keep in mind that in a more complete approach one would have to consider a fixed θ. Such an approach would be of interest especially in view of recent studies of possible (CP-violating) η condensates in an NJL model calculation [179], or, including a magnetic field, in the linear sigma model [143].

We finally remark that our setup does not include the possibility of diquark condensation of the form $\langle ud\rangle$, which is expected to lead to color superconductivity of quark matter at sufficiently large baryon chemical potential [9]. However, color superconductivity does not necessarily occur in the large N_c limit where a "chiral density wave" is a strong candidate for the ground state [180, 181], or, as suggested recently, quark matter may be confined even for large chemical potentials [86, 182].

to ensure thermodynamic consistency (see discussion below (6.50)). Also note that we exchanged $R \leftrightarrow L$ in (C.8) compared to [34] to be consistent with Chapter 5.

6.2.2 Solutions of the equations of motion and free energies

We can now solve the equations of motion (6.3) and (6.5) for the two sets of boundary conditions given in Table 6.1. For notational convenience we set $u_{\rm KK} = 1$ (the final results in Secs. 6.2.5 and 6.2.6 do not depend on $u_{\rm KK}$ and thus all physical quantities will have the correct dimensions). For both sets of boundary conditions we first note that the differential equations (6.5) can be solved by defining the new functions

$$F_0^\pm(z) \equiv k(z)\frac{\hat{F}_{z0} \pm F_{z0}}{2}\,, \qquad F_3^\pm(z) \equiv k(z)\frac{\hat{F}_{z3} \pm F_{z3}}{2}\,. \tag{6.23}$$

Then, the four equations (6.5) are equivalent to

$$\partial_z F_0^\pm = \frac{\alpha[\hat{b}(z) \pm b(z)]}{k(z) M_{\rm KK}^2}\, F_3^\pm(z)\,, \qquad \partial_z F_3^\pm = \frac{\alpha[\hat{b}(z) \pm b(z)]}{k(z) M_{\rm KK}^2}\, F_0^\pm(z)\,. \tag{6.24}$$

Now the two equations with the upper sign are decoupled from the two equations with the lower sign. To proceed, we have to distinguish between the two chirally broken phases.

6.2.3 Sigma phase

With the boundary conditions of the σ phase from Table 6.1 and with Eqs. (6.3) we conclude that the magnetic fields are constant in the bulk

$$\hat{b}(z) = \hat{\mathcal{B}}\,, \qquad b(z) = \mathcal{B}\,. \tag{6.25}$$

In the following, we shall denote the dimensionless magnetic fields by

$$\hat{B} \equiv \frac{\alpha\hat{\mathcal{B}}}{M_{\rm KK}^2}\,, \qquad B \equiv \frac{\alpha\mathcal{B}}{M_{\rm KK}^2}\,, \qquad B_{\rm em} \equiv \frac{\alpha\mathcal{B}_{\rm em}}{M_{\rm KK}^2}\,. \tag{6.26}$$

We can now solve Eqs. (6.24) for completely general boundary conditions for the gauge fields. This is done in Appendix C.2, where we also present some technical details. Here we proceed with the specific solution obtained from the boundary conditions given in the first row of Table 6.1. This solution yields the gauge fields

$$\hat{A}_0(z) = \mu_B - \frac{\hat{\jmath}}{2}[C_+(z) + C_-(z) - T_+] - \frac{\jmath}{2}[C_+(z) - C_-(z) - T_-]\,, \tag{6.27a}$$

$$A_0(z) = \mu_I - \frac{\jmath}{2}[C_+(z) + C_-(z) - T_+] - \frac{\hat{\jmath}}{2}[C_+(z) - C_-(z) - T_-]\,, \tag{6.27b}$$

$$\hat{A}_3(z) = -\frac{\hat{\jmath}}{2}[S_+(z) + S_-(z)] - \frac{\jmath}{2}[S_+(z) - S_-(z)]\,, \tag{6.27c}$$

$$A_3(z) = -\frac{\jmath}{2}[S_+(z) + S_-(z)] - \frac{\hat{\jmath}}{2}[S_+(z) - S_-(z)]\,, \tag{6.27d}$$

where we have abbreviated

$$C_\pm(z) \equiv \frac{\cosh[(\hat{B} \pm B)\arctan z]}{\sinh[\pi(\hat{B} \pm B)/2]}\,, \qquad S_\pm(z) \equiv \frac{\sinh[(\hat{B} \pm B)\arctan z]}{\sinh[\pi(\hat{B} \pm B)/2]}\,, \tag{6.28a}$$

$$T_\pm \equiv \coth\frac{\pi(\hat{B} + B)}{2} \pm \coth\frac{\pi(\hat{B} - B)}{2}\,. \tag{6.28b}$$

Note that $T_\pm = C_+(\infty) \pm C_-(\infty) = C_+(-\infty) \pm C_-(-\infty)$. Since the functions $C_\pm(z)$ and $S_\pm(z)$ are symmetric and antisymmetric in z, respectively, both temporal components of the gauge fields are symmetric while both spatial components are antisymmetric. Together with

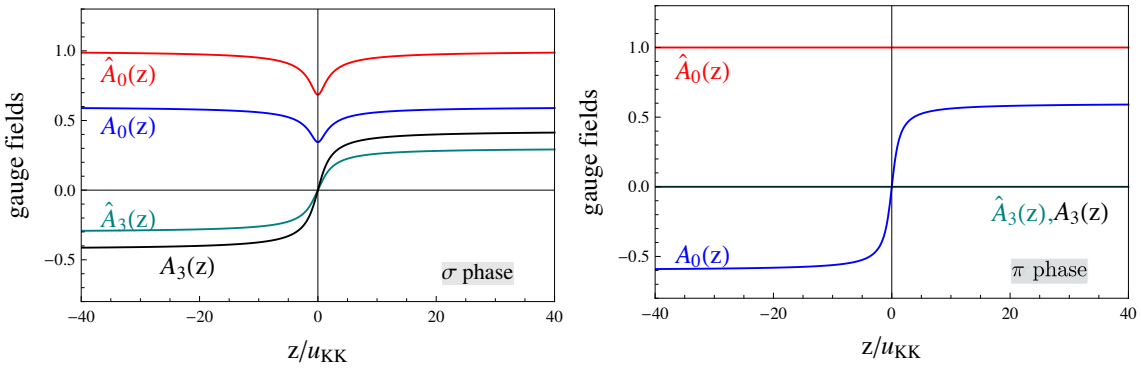

Figure 6.2: Energetically preferred configuration of the gauge fields as a function of the holographic coordinate z for sigma phase (left panel) and the charged pion phase (right panel). For the sigma phase we have chosen a dimensionless magnetic field $eB_{\rm em} = 2$. In the pion phase, $B_{\rm em} = 0$ due to the Meissner effect. The boundary values for $\hat{A}_0(z)$ and $A_0(z)$ are given by the baryon and isospin chemical potentials, respectively. The boundary values of $\hat{A}_3(z)$ and $A_3(z)$ yield the meson supercurrents and are determined dynamically from minimization of the free energy.

the behavior of the supercurrents under a parity transformation this ensures that the gauge fields transform as a vector under parity, see discussion below Eq. (C.16). We plot the gauge fields with the supercurrents determined from minimization of the free energy, see Eqs. (6.31), in the left panel of Figure 6.2. Next, we insert the gauge fields and the resulting field strengths into the free energy (6.10) and obtain (for details see Appendix C.2)

$$\begin{aligned}\Omega &= \frac{\kappa M_{\rm KK}^2}{6}\Big[(\hat{\jmath}+\jmath)^2\rho_+(\hat{B},B)+(\hat{\jmath}-\jmath)^2\rho_-(\hat{B},B)\\ &\qquad +4\mu_B(\hat{\jmath}\hat{B}+\jmath B)+4\mu_I(\hat{\jmath}B+\jmath\hat{B})\Big]\,,\end{aligned} \tag{6.29}$$

with

$$\rho_\pm(\hat{B},B)\equiv 2(\hat{B}\pm B)\coth\frac{\pi(\hat{B}\pm B)}{2}+\frac{\pi(\hat{B}\pm B)^2}{2\sinh^2[\pi(\hat{B}\pm B)/2]}\,. \tag{6.30}$$

The asymptotic values of the functions $\rho_\pm(\hat{B},B)$ at small and large magnetic fields are shown in Table C.1 in Appendix C.2.

Minimizing Ω with respect to $\hat{\jmath}$, $\jmath$ yields

$$\hat{\jmath} = -\frac{\mu_B+\mu_I}{2}\frac{\hat{B}+B}{\rho_+(\hat{B},B)}-\frac{\mu_B-\mu_I}{2}\frac{\hat{B}-B}{\rho_-(\hat{B},B)}\,, \tag{6.31a}$$

$$\jmath = -\frac{\mu_B+\mu_I}{2}\frac{\hat{B}+B}{\rho_+(\hat{B},B)}+\frac{\mu_B-\mu_I}{2}\frac{\hat{B}-B}{\rho_-(\hat{B},B)}\,. \tag{6.31b}$$

One can check that this is indeed a minimum of Ω: the matrix of second derivatives of Ω with respect to the supercurrents has eigenvalues $8\kappa M_{\rm KK}^2\rho_+/3$, $8\kappa M_{\rm KK}^2\rho_-/3$, which are independent of $\hat{\jmath}$ and $\jmath$ and positive for all $\hat{B}$, B.

As already mentioned below Eq. (6.2) we recall that the supercurrents $\hat{\jmath}$, $\jmath$ act as a source for the currents $\hat{\mathcal{J}}$, $\mathcal{J}$ which we compute now. The currents $\hat{\mathcal{J}}$, $\mathcal{J}$ are the spatial 3-components of the currents

$$\bar{\mathcal{J}}^\mu_{L/R}=\mathcal{J}^\mu_{{\rm YM},L/R}+\mathcal{J}^\mu_{{\rm CS},L/R}+\Delta\mathcal{J}^\mu_{L/R}, \tag{6.32}$$

we derived in (5.1). The Yang-Mills, Chern-Simons and Bardeen contributions are given by (5.5) and (5.11)

$$\mathcal{J}^{\mu}_{\mathrm{YM},L/R} = \mp 2\kappa M_{\mathrm{KK}}^2 k(z)\mathcal{F}^{z\mu}\Big|_{z=\pm\infty}, \tag{6.33a}$$

$$\mathcal{J}^{\mu}_{\mathrm{CS},L/R} = \pm\frac{N_c}{24\pi^2}\epsilon^{\mu\nu\rho\sigma}\mathcal{A}_\nu\mathcal{F}_{\rho\sigma}\Big|_{z=\pm\infty}, \tag{6.33b}$$

$$\Delta\mathcal{J}^{\mu}_{L/R} = \mp\frac{N_c}{48\pi^2}\left(\mathcal{A}_\nu^{R/L}\mathcal{F}_{\rho\sigma}^{R/L} - \mathcal{A}_\nu^{L/R}\mathcal{F}_{\rho\sigma}^{R/L} + 2\mathcal{A}_\nu^{R/L}\mathcal{F}_{\rho\sigma}^{L/R}\right)\epsilon^{\mu\nu\rho\sigma}\Big|_{z=\pm\infty}. \tag{6.33c}$$

Here, the indices μ,ν,ρ,σ run over 0,1,2,3, the upper (lower) signs correspond to L (R), and we have, in the CS contribution, already used that in our ansatz the off-diagonal components of the gauge fields in flavor space vanish. With the gauge field (6.27) and the field strengths (C.16) we obtain the baryon and isospin components of the spatial currents,

$$\begin{aligned}\hat{\mathcal{J}} = \hat{\mathcal{J}}_{\mathrm{YM}} + \hat{\mathcal{J}}_{\mathrm{CS}} \equiv \hat{\mathcal{J}}_L = -\hat{\mathcal{J}}_R = -\frac{\kappa M_{\mathrm{KK}}^2}{2}\Bigg[&(\mu_B+\mu_I)\frac{(\hat{B}+B)^2}{\rho_+(\hat{B},B)}\coth\frac{\pi(\hat{B}+B)}{2}\\ &+(\mu_B-\mu_I)\frac{(\hat{B}-B)^2}{\rho_-(\hat{B},B)}\coth\frac{\pi(\hat{B}-B)}{2} - \frac{2}{3}(\mu_B\hat{B}+\mu_I B)\Bigg],\end{aligned} \tag{6.34a}$$

$$\begin{aligned}\mathcal{J} = \mathcal{J}_{\mathrm{YM}} + \mathcal{J}_{\mathrm{CS}} \equiv \mathcal{J}_L = -\mathcal{J}_R = \frac{\kappa M_{\mathrm{KK}}^2}{2}\Bigg[&(\mu_B+\mu_I)\frac{(\hat{B}+B)^2}{\rho_+(\hat{B},B)}\coth\frac{\pi(\hat{B}+B)}{2}\\ &-(\mu_B-\mu_I)\frac{(\hat{B}-B)^2}{\rho_-(\hat{B},B)}\coth\frac{\pi(\hat{B}-B)}{2} - \frac{2}{3}(\mu_B B+\mu_I\hat{B})\Bigg],\end{aligned} \tag{6.34b}$$

where the terms with prefactor 2/3 are the Chern-Simons contributions and we used $N_c\mathcal{B} = 16\pi^2 M_{KK}^2\kappa$. These currents are already evaluated at the minimum of the free energy, *i.e.*, we have inserted the supercurrents (6.31). After adding Barddeen's counterterm (6.33c) only the YM parts of the currents (6.34) survive

$$\bar{\hat{\mathcal{J}}}_{L/R} = \hat{\mathcal{J}}_{\mathrm{YM}}, \qquad \bar{\mathcal{J}}_{L/R} = \mathcal{J}_{\mathrm{YM},L/R}. \tag{6.35}$$

Note that Bardeen's counterterm only cancels the (CS) contribution in the case of vanishing axial chemical potential. They add up to zero in the sums $\mathcal{J}_L+\mathcal{J}_R$ and $\hat{\mathcal{J}}_L+\hat{\mathcal{J}}_R$, corresponding to vanishing baryon and isospin currents, however they yield nonzero axial currents (see Section 5.3. We remark that the subleading term in the expansion of the 3-component of the gauge fields only agrees with the current (6.33) after adding Bardeen's counterterm.

$$\hat{A}_3(z) = \mp\hat{\jmath} \pm \frac{\hat{\mathcal{J}}_{\mathrm{YM},L/R}}{\kappa M_{\mathrm{KK}}^2}\frac{1}{z} + \mathcal{O}\left(\frac{1}{z^2}\right), \quad A_3(z) = \mp\jmath \pm \frac{\mathcal{J}_{\mathrm{YM},L/R}}{\kappa M_{\mathrm{KK}}^2}\frac{1}{z} + \mathcal{O}\left(\frac{1}{z^2}\right). \tag{6.36}$$

Finally, we insert the values (6.31) back into Ω yields the value of the free energy at the minimum,

$$\Omega_\sigma = -\frac{\kappa M_{\mathrm{KK}}^2}{6}\left[(\mu_B+\mu_I)^2\frac{(\hat{B}+B)^2}{\rho_+(\hat{B},B)} + (\mu_B-\mu_I)^2\frac{(\hat{B}-B)^2}{\rho_-(\hat{B},B)}\right]. \tag{6.37}$$

We see that for vanishing magnetic fields $\Omega_\sigma = 0$, *i.e.*, the free energy does not depend on any of the chemical potentials. This is the expected result for the sigma phase and has also been observed in Ref. [92].

6.2.4 Pion phase and Meissner effect

In this case the boundary conditions are given in the second row of Table 6.1, and the differential equations (6.3) for the magnetic fields have the solution

$$\hat{b}(z) = \hat{\mathcal{B}}\,, \qquad b(z) = \frac{2\mathcal{B}}{\pi} \arctan z\,. \tag{6.38}$$

As we have discussed at the end of Section 6.1.2, nonconstant functions $\hat{b}$ or b lead to an infinite contribution to the free energy which cannot be removed by holographic renormalization, but which enforces a vanishing magnetic field, indicating a Meissner effect. In the π phase, it is the nonconstant isospin component $b(z)$ which leads to this conclusion. This is only to be expected since the condensate of pions carries an electric charge, and thus the system is an electromagnetic superconductor. By the Meissner effect, a magnetic field is induced which is opposite, but equal in magnitude, to the applied magnetic field, such that $\mathcal{B}_{\text{em}} = 0$ and thus $\hat{B} = B = 0$. Of course our electromagnetic group is only global and thus the microscopic description of the Meissner effect, for instance in terms of a Meissner mass for the photon, is not straightforward. However, in terms of supercurrents, the effect can be described quite naturally: in fact we have to allow for a supercurrent in the directions transverse to the magnetic field, *i.e.*, $\boldsymbol{\jmath}_s(\mathbf{x}, z) = \frac{1}{2} b(z)\,(x_2, -x_1, 0)$, such that $\operatorname{curl} \boldsymbol{\jmath}_s = -b$ (and the same for the components $\hat{\boldsymbol{\jmath}}_s$, $\hat{b}$). This is the usual London equation for a superconductor, see for instance Ref. [183]. Consequently, we need to add the supercurrents $\hat{\boldsymbol{\jmath}}_s$, $\boldsymbol{\jmath}_s$ to the boundary conditions of the gauge fields $\hat{A}_1(\mathbf{x}, z)$, $\hat{A}_2(\mathbf{x}, z)$, $A_1(\mathbf{x}, z)$, $A_2(\mathbf{x}, z)$ from Eqs. (6.2) such that the total boundary conditions (and thereby the total magnetic field in the superconductor) vanish, $\hat{B} = B = 0$. This condition renders the equations of motion for the pion phase very simple. We shall, however, solve these equations for arbitrary magnetic fields and only at the end set $\hat{B} = B = 0$. This provides us with a better understanding of the structure of the solution, for instance its behavior under parity transformations.

We defer all technical details and the solution for general boundary conditions with the magnetic fields (6.38) to Appendix C.3. For the specific boundary conditions characterizing the charged pion condensate we find the solutions

$$\hat{A}_0(z) = \mu_B + \frac{\mu_I}{2}\left[\tilde{C}_+(z) + \tilde{C}_-(z) - \tilde{T}_+\right] - \frac{\hat{\jmath}}{2}\left[[\tilde{C}_+(z) - \tilde{C}_-(z) - \tilde{T}_-\right], \tag{6.39a}$$

$$A_0(z) = \frac{\mu_I}{2}\left[\tilde{S}_+(z) + \tilde{S}_-(z)\right] - \frac{\hat{\jmath}}{2}\left[\tilde{S}_+(z) - \tilde{S}_-(z)\right], \tag{6.39b}$$

$$\hat{A}_3(z) = -\frac{\hat{\jmath}}{2}\left[\tilde{S}_+(z) + \tilde{S}_-(z)\right] + \frac{\mu_I}{2}\left[\tilde{S}_+(z) - \tilde{S}_-(z)\right], \tag{6.39c}$$

$$A_3(z) = -\frac{\hat{\jmath}}{2}\left[\tilde{C}_+(z) + \tilde{C}_-(z) - \tilde{T}_-\right] + \frac{\mu_I}{2}\left[\tilde{C}_+(z) - \tilde{C}_-(z) - \tilde{T}_+\right], \tag{6.39d}$$

where we abbreviated

$$\tilde{C}_+(z) \equiv \frac{P_+(z) + P_-(z)}{P_+^+ - P_+^-}\,, \qquad \tilde{C}_-(z) \equiv \frac{Q_+(z) + Q_-(z)}{Q_+^+ - Q_+^-}\,, \tag{6.40a}$$

$$\tilde{S}_+(z) \equiv \frac{P_+(z) - P_-(z)}{P_+^+ - P_+^-}\,, \qquad \tilde{S}_-(z) \equiv \frac{Q_+(z) - Q_-(z)}{Q_+^+ - Q_+^-}\,, \tag{6.40b}$$

$$\tilde{T}_\pm \equiv \frac{P_+^+ + P_+^-}{P_+^+ - P_+^-} \pm \frac{Q_+^+ + Q_+^-}{Q_+^+ - Q_+^-}\,, \tag{6.40c}$$

with

$$Q_\pm(z) \equiv \frac{\pi}{2\sqrt{B}} e^{\frac{\pi\hat{B}^2}{4B}} \operatorname{erf}\left(\frac{\pi\hat{B} \pm 2B \arctan z}{2\sqrt{\pi B}}\right), \tag{6.41a}$$

$$P_\pm(z) \equiv \frac{\pi}{2\sqrt{B}} e^{-\frac{\pi\hat{B}^2}{4B}} \operatorname{erfi}\left(\frac{\pi\hat{B} \pm 2B \arctan z}{2\sqrt{\pi B}}\right), \tag{6.41b}$$

and $Q_+^\pm \equiv Q_+(\pm\infty)$, $P_+^\pm \equiv P_+(\pm\infty)$. Here, erf is the error function and $\operatorname{erfi}(z) \equiv \operatorname{erf}(iz)/i$. The functions $\tilde{C}_\pm$, $\tilde{S}_\pm$, $\tilde{T}_\pm$ are the more complicated counterparts of the functions $C_\pm$, $S_\pm$, $T_\pm$ from Eqs. (6.28). They share the same property $\tilde{T}_\pm = \tilde{C}_+(\infty) \pm \tilde{C}_-(\infty) = \tilde{C}_+(-\infty) \pm \tilde{C}_-(-\infty)$, and, as their counterparts, $\tilde{C}_\pm(z)$ and $\tilde{S}_\pm(z)$ are symmetric and antisymmetric in z, respectively. This means that the temporal $\mathbf{1}$ component and the spatial τ_3 component are symmetric in z while the temporal τ_3 component and the spatial $\mathbf{1}$ component are antisymmetric. Again, together with the parity transformations of the current, this gives the correct parity behavior of the gauge fields, see discussion in Appendix C.3. In particular, the requirement of a well-defined parity leads to the condition $\jmath = 0$.

Inserting Eqs. (6.39) and the corresponding field strengths into the free energy (6.10) yields

$$\Omega = \frac{\kappa M_{\mathrm{KK}}^2}{6} \left\{ \hat{\jmath}^2 - \mu_I^2 \, \rho(\hat{B}, B) - 2\mu_B \left[\mu_I \, \eta_+(\hat{B}, B) - \hat{\jmath} \, \eta_-(\hat{B}, B) \right] \right\} + \Omega_b \,, \tag{6.42}$$

with Ω_b given in Eq. (6.11) and

$$\rho(\hat{B}, B) \equiv \frac{4\pi}{(P_+^+ - P_+^-)(Q_+^+ - Q_+^-)} + 4 \cosh \frac{\pi\hat{B}}{2} \left(\frac{e^{\frac{\pi B}{4}}}{P_+^+ - P_+^-} + \frac{e^{-\frac{\pi B}{4}}}{Q_+^+ - Q_+^-} \right), \tag{6.43a}$$

$$\eta_\pm(\hat{B}, B) \equiv 2 \sinh \frac{\pi\hat{B}}{2} \left(\frac{e^{\frac{\pi B}{4}}}{P_+^+ - P_+^-} \mp \frac{e^{-\frac{\pi B}{4}}}{Q_+^+ - Q_+^-} \right). \tag{6.43b}$$

Again, the asymptotic values of these functions are given in Table C.1 in Appendix C.2.

Minimization of Ω with respect to $\hat{\jmath}$ yields

$$\hat{\jmath} = -\mu_B \frac{\eta_-(\hat{B}, B)}{\rho(\hat{B}, B)} \,, \tag{6.44}$$

and the minimum of the free energy becomes

$$\Omega_\pi = -\frac{\kappa M_{\mathrm{KK}}^2}{6} \left[\mu_B^2 \frac{\eta_-^2(\hat{B}, B)}{\rho(\hat{B}, B)} + \mu_I^2 \, \rho(\hat{B}, B) + 2\mu_B \mu_I \, \eta_+(\hat{B}, B) \right] + \Omega_b \,. \tag{6.45}$$

We see that for vanishing magnetic fields the free energy depends on the isospin chemical potential, giving rise to a nonzero isospin density. This is expected from the quark content of the charged pion condensate and was also observed within the Sakai-Sugimoto model in Ref. [92].

Taking into account the Meissner effect, which is enforced by the infrared divergence in Ω_b as discussed at the beginning of this subsection, we have to set $\hat{B} = B = 0$, leading to the simple result for the free energy

$$\Omega_\pi = -\frac{2\kappa M_{\mathrm{KK}}^2}{\pi} \, \mu_I^2 \,. \tag{6.46}$$

From Eq. (6.44) we conclude that for $\hat{B} = B = 0$ we have $\hat{\jmath} = 0$. And, from the definitions (6.33), we see that in the absence of a magnetic field also the normal currents vanish, $\hat{\mathcal{J}} = \mathcal{J} = 0$. In the following we shall discuss the results of the pion phase only in the presence of the Meissner effect.

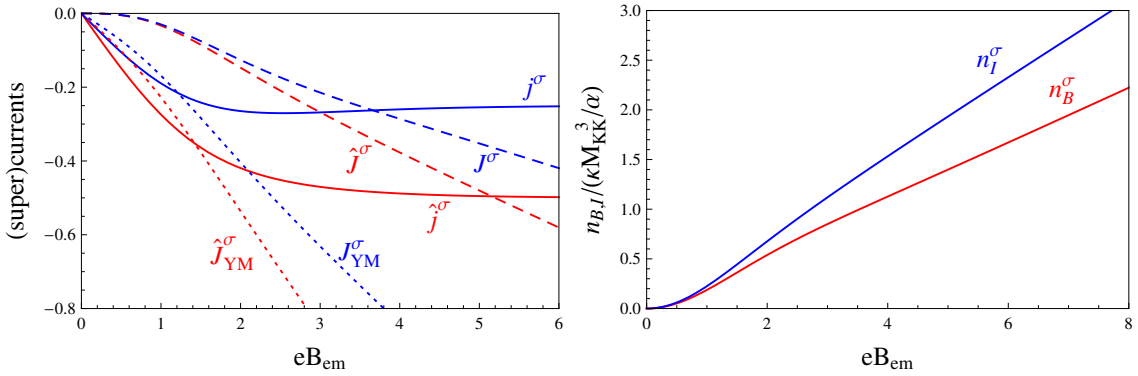

Figure 6.3: Left panel: Meson supercurrents $\hat{\jmath}^\sigma$ (red solid) and $\jmath^\sigma$ (blue solid), normal currents $\hat{\mathcal{J}}^\sigma$ (red dashed) and $\mathcal{J}^\sigma$ (blue dashed) and the Yang-Mills currents $\hat{\mathcal{J}}^\sigma_{YM}$ (red dotted) and $\mathcal{J}^\sigma_{YM}$ (blue dotted) as a function of the dimensionless magnetic field $eB_{\rm em}$ in the sigma phase. The units are $M_{\rm KK}/\alpha$ for $\hat{\jmath}^\sigma$, $\jmath^\sigma$ and $\kappa M_{\rm KK}^3/\alpha$ for $\hat{\mathcal{J}}^\sigma$, $\mathcal{J}^\sigma$,$\hat{\mathcal{J}}^\sigma_{YM}$, $\mathcal{J}^\sigma_{YM}$. Right panel: baryon and isospin number densities as a function of the dimensionless magnetic field in the sigma phase. The analytical expressions for the functions are given in Eqs. (6.31), (6.34), and (6.48). We have fixed $\mu_B = 2\mu_I = M_{\rm KK}\alpha$. In the (charged) pion phase, all currents as well as the baryon density vanish due to the Meissner effect; the isospin density is given by the simple expression (6.52b).

6.2.5 Meson supercurrents and number densities

We have seen that all currents in the charged pion phase vanish (except for the supercurrents in the transverse 1- and 2-directions which cancel the applied magnetic field). The supercurrents and normal currents in the sigma phase, given in Eqs. (6.31) and (6.34), respectively, are shown in the left panel of Figure 6.3 as a function of the magnetic field. We have used the electromagnetic field $B_{\rm em}$, defined in Eq. (6.1), with the electric charges of up and down quarks. We see that the supercurrents behave linear in $B_{\rm em}$ for small $B_{\rm em}$ and approach an asymptotic value for a large magnetic field. These limit cases assume very simple forms in terms of the electric quark charges q_i and the quark chemical potentials $\mu_{1,2} \equiv \mu_B \pm \mu_I$. The quark supercurrents $\jmath_{1,2} \equiv \hat{\jmath} \pm \jmath$ then are

$$\jmath_i^\sigma \simeq -\frac{1}{2}\begin{cases} \dfrac{\pi q_i \mu_i B_{\rm em}}{3} & \text{for small } B_{\rm em} \\ \mu_i \,\mathrm{sgn}\, q_i & \text{for large } B_{\rm em} \end{cases} . \tag{6.47}$$

The limit of a large magnetic field is strictly speaking not consistent with our approximations. Firstly, we have expanded the DBI action for small gauge fields. Secondly, we have treated the flavor branes as probe branes which becomes questionable for large magnetic fields since one would have to consider the backreaction on the background geometry. As mentioned in Ref. [90] in the same context, the case of a large magnetic field within the present approach can only be meaningful if one thinks of the action (4.13) as a "bottom-up" model for QCD, which is not derived from an AdS/CFT correspondence. Indeed, with appropriate functions $k(z)$, $h(z)$, the bottom-up model from Ref. [184] can be recovered from Eq. (4.20). Thus, in the following we shall use our analytical functions to discuss the whole range of magnetic fields with this qualification in mind.

We can compute the baryon and isospin densities from the 0-component of the current defined in Eq. (6.32). For a vanishing electric field Bardeen's counterterm does not contribute

to the densities as can be seen from (5.69a). We obtain for the sigma phase

$$n_B^\sigma = \frac{\kappa M_{\rm KK}^2}{3}\left[(\mu_B+\mu_I)\frac{(\hat{B}+B)^2}{\rho_+}+(\mu_B-\mu_I)\frac{(\hat{B}-B)^2}{\rho_-}\right], \tag{6.48a}$$

$$n_I^\sigma = \frac{\kappa M_{\rm KK}^2}{3}\left[(\mu_B+\mu_I)\frac{(\hat{B}+B)^2}{\rho_+}-(\mu_B-\mu_I)\frac{(\hat{B}-B)^2}{\rho_-}\right]. \tag{6.48b}$$

In principle one could also compute the densities from the free energies computed in the previous section via

$$n_{B,I} = -\frac{\partial\Omega}{\partial\mu_{B,I}}\,. \tag{6.49}$$

It turns out that

$$\frac{1}{2}(\mathcal{J}_R^0+\mathcal{J}_L^0) = -\frac{\partial\Omega}{\partial\mu_B}-\frac{\partial\Omega}{\partial\mu_I}\,\tau_3\,. \tag{6.50}$$

As we explained in (5.2.3) this thermodynamic inconsistency can be traced back to spatial boundary terms of the system. In [34] we used different boundary conditions to ensure thermodynamic consistency, namely twice the values for the chemical potentials and supercurrents we use here. By comparing the results of this chapter with [34] one can check that the different boundary conditions only lead to quantitative changes due to the rescaling of the chemical potentials and supercurrents by a factor 1/2. Using a modified action as in Ref.[91] cures this problem but one looses all anomalies. See Section (5.5) for a detailed discussion of this problem. In Appendix C.5 we give the results obtained with the modified action for comparison. It is still not clear to us how to ensure thermodynamic consistency and keep the anomaly at the same time. In what follows we use the densities obtained via Eq. (6.32) with the result given in (6.48).

The densities are plotted in the right panel of Figure 6.3. As expected, both densities vanish in the case of a vanishing magnetic field. Switching on a magnetic field induces currents as well as nonzero densities. Again, it is convenient to express the number densities in terms of the quark flavor components, $n_{1,2} \equiv n_B \pm n_I$, rather than in baryon and isospin components. We obtain for small and large magnetic fields

$$n_i^\sigma \simeq \frac{\kappa M_{\rm KK}^2}{3}\begin{cases}\dfrac{\pi q_i^2\mu_i B_{\rm em}^2}{3} & \text{for small } B_{\rm em}\\[2ex] \mu_i|q_i|B_{\rm em} & \text{for large } B_{\rm em}\end{cases}. \tag{6.51}$$

For the pion phase we find from the free energy (6.46)

$$n_B^\pi = 0\,, \tag{6.52a}$$

$$n_I^\pi = \frac{2\kappa M_{\rm KK}^2}{\pi}\mu_I\,. \tag{6.52b}$$

From the baryon and isospin densities we can immediately deduce the electric charge density $n_Q = q_1 n_1 + q_2 n_2$. The electric charge of the system is relevant for example in the astrophysical context because in a neutron star the overall electric charge has to vanish. Here we simply observe which electric charge is carried by our system for given chemical potentials. For more realistic applications one would have to require charge neutrality and possibly counterbalance the charge of the chiral condensate for instance by the presence of electrons or protons. For the σ condensate we find $n_Q^\sigma = 0$ for vanishing magnetic fields, as expected. Switching on a magnetic field induces electric charges in the system. For infinitesimally small $B_{\rm em}$ a straight

line $\mu_B = -9\mu_I/7$ appears in the μ_B-μ_I plane dividing the plane into a region with infinitesimally positive (above/right of the line) and negative (below/left of the line) charge. With increasing magnetic field, giving rise to larger charges, the slope of the line slightly decreases and approaches the value $\mu_B = -5\mu_I/3$ asymptotically for large $B_{\rm em}$. For the pion phase we have $n_Q^\pi = n_I^\pi$, which is positive (negative) for positive (negative) isospin chemical potentials and independent of the baryon chemical potential.

We may finally recover the scenario considered in Ref. [90] as a limit of our more general results. In that paper, a vanishing isospin chemical potential, a vanishing baryon component of the magnetic field, and an isospin magnetic field constant in the holographic coordinate z (as in Eq. (6.38)) was considered. For a comparison it is thus instructive to compute the energy density ϵ of the sigma phase. We write the free energy (6.29) as $\Omega = \epsilon - \mu_B n_B - \mu_I n_I$ with n_B, n_I given in Eqs. (6.48). Then we can express the energy density in terms of the number densities,

$$\epsilon_\sigma = \frac{3}{8\kappa M_{\rm KK}^2}\left[(n_B^\sigma + n_I^\sigma)^2\frac{\rho_+}{(\hat{B}+B)^2} + (n_B^\sigma - n_I^\sigma)^2\frac{\rho_-}{(\hat{B}-B)^2}\right]. \tag{6.53}$$

For small and large magnetic fields we obtain

$$\epsilon_\sigma \simeq \begin{cases} \dfrac{8\lambda M_{\rm KK}^2}{3N_c}\left[\dfrac{(n_B^\sigma + n_I^\sigma)^2}{(\hat{\mathcal{B}}+\mathcal{B})^2} + \dfrac{(n_B^\sigma - n_I^\sigma)^2}{(\hat{\mathcal{B}}-\mathcal{B})^2}\right] & \text{for small } \hat{\mathcal{B}}, \mathcal{B} \\ \dfrac{12\pi^2}{N_c}\left[\dfrac{(n_B^\sigma + n_I^\sigma)^2}{|\hat{\mathcal{B}}+\mathcal{B}|} + \dfrac{(n_B^\sigma - n_I^\sigma)^2}{|\hat{\mathcal{B}}-\mathcal{B}|}\right] & \text{for large } \hat{\mathcal{B}}, \mathcal{B} \end{cases}, \tag{6.54}$$

where we have reinstated the dimensionful magnetic fields according to Eq. (6.26). For large magnetic fields we thus obtain, up to a numerical prefactor, an equation of state as for a free fermion gas in a magnetic field: setting $n_I^\sigma = \hat{\mathcal{B}} = 0$ we have $\epsilon_\sigma = 24\pi^2(n_B^\sigma)^2/(\mathcal{B}N_c)$ while for a free gas $\epsilon_0 = \pi^2 n_B^2/(\mathcal{B}N_c)$ [90]. In Ref. [90] even the prefactor is exactly that of the free gas. We have checked that this discrepancy comes from the surface term in the Chern-Simons action.

6.2.6 Phase diagram and critical magnetic field

In this section we determine which of the two phases is favored for given values of the chemical potentials and the magnetic field. Since we want to compare the phases at a fixed external magnetic field $\mathcal{H}_{\rm em}$ (and not at fixed $\mathcal{B}_{\rm em}$), we need the Gibbs free energy G. In the case of the charged pion condensate, where $\mathcal{B}_{\rm em} = 0$, the Gibbs free energy is identical to the above computed free energy,

$$G_\pi = \Omega_\pi = -\frac{2\kappa M_{\rm KK}^2}{\pi}\,\mu_I^2\,. \tag{6.55}$$

It is convenient to introduce dimensionless free energies $\omega_{\sigma,\pi}$ via

$$\Omega_{\sigma,\pi} = \frac{M_{\rm KK}^4}{\alpha^2}\,\kappa\,\omega_{\sigma,\pi}\,. \tag{6.56}$$

As we shall see below, κ is the only parameter of the model on which the structure of the phase diagram depends, see Eq. (6.67). The other constants $M_{\rm KK}$ and α only set the energy scale. To make this κ dependence explicit, we have pulled the dimensionless constant κ out of

$\omega_{\sigma,\pi}$. The dimensionless free energies are (using Eqs. (6.37) and (6.46))

$$\omega_\pi = -\frac{2\tilde{\mu}_I^2}{\pi}\,, \tag{6.57a}$$

$$\omega_\sigma = -\frac{1}{6}\left[(\tilde{\mu}_B+\tilde{\mu}_I)^2\frac{(\hat{B}+B)^2}{\rho_+(\hat{B},B)}+(\tilde{\mu}_B-\tilde{\mu}_I)^2\frac{(\hat{B}-B)^2}{\rho_-(\hat{B},B)}\right]\,, \tag{6.57b}$$

where we have introduced the dimensionless chemical potentials

$$\tilde{\mu}_B \equiv \frac{\alpha\mu_B}{M_{\rm KK}}\,, \qquad \tilde{\mu}_I \equiv \frac{\alpha\mu_I}{M_{\rm KK}}\,. \tag{6.58}$$

To obtain the Gibbs free energy in the sigma phase we add the contribution $\mathcal{B}_{\rm em}^2/2$ and Legendre transform the free energy with respect to the change of variable $\mathcal{B}_{\rm em} \to \mathcal{H}_{\rm em}$. Consequently,

$$G_\sigma = \frac{1}{2}\mathcal{B}_{\rm em}^2 + \Omega_\sigma - \mathcal{B}_{\rm em}\mathcal{H}_{\rm em}\,. \tag{6.59}$$

For a given external field $\mathcal{H}_{\rm em}$ one determines $\mathcal{B}_{\rm em}$ from the stationarity condition

$$0 = \frac{\partial G_\sigma}{\partial \mathcal{B}_{\rm em}} = \mathcal{B}_{\rm em} - \mathcal{M}_\sigma - \mathcal{H}_{\rm em}\,, \tag{6.60}$$

where we defined the magnetization in the sigma phase

$$\mathcal{M}_\sigma = -\frac{\partial\Omega_\sigma}{\partial\mathcal{B}_{\rm em}} = \frac{M_{\rm KK}^2}{\alpha}\,\kappa\,M_\sigma\,. \tag{6.61}$$

Here, the dimensionless magnetization is given by

$$M_\sigma = \frac{1}{3}\left[q_1\tilde{\mu}_1^2\frac{\hat{B}+B}{\rho_+}\left(1-\frac{\hat{B}+B}{2\rho_+}\frac{\partial\rho_+}{\partial\hat{B}}\right)+q_2\tilde{\mu}_2^2\frac{\hat{B}-B}{\rho_-}\left(1-\frac{\hat{B}-B}{2\rho_-}\frac{\partial\rho_-}{\partial\hat{B}}\right)\right]\,. \tag{6.62}$$

We have used Eq. (6.1) for the electromagnetic field, and expressed the derivatives with respect to B through derivatives with respect to $\hat{B}$. Before coming back to the Gibbs free energy let us discuss the magnetization and the resulting magnetic susceptibility χ_σ. To obtain M_σ as a function of the external magnetic field we first solve Eq. (6.60), which, in dimensionless quantities reads

$$H_{\rm em} = B_{\rm em} - \kappa\,M_\sigma\,, \tag{6.63}$$

numerically for $B_{\rm em}$. (Here, the dimensionless field $H_{\rm em}$ is defined analogously to the field $B_{\rm em}$, see Eq. (6.26).) Then, we insert the solution back into Eq. (6.62). The result depends on κ, for which we have to choose a numerical value. In order to get some numerical estimates from our following results we also need to assign values to the other parameters of the model. Following [29, 131, 111] we shall use

$$\kappa = 0.00745, \qquad M_{\rm KK} = 949\,{\rm MeV}\,, \tag{6.64}$$

which has been obtained from fits to the rho meson mass and the pion decay constant. From this value for κ we obtain, with $N_c = 3$ and Eq. (4.22), $\lambda \approx 16.6$, and then, with Eq. (6.6), $\alpha \approx 2.55$.

The full numerical result for the magnetization is shown in Figure 6.4. Our result is in qualitative agreement with Ref. [91], where the magnetization was computed for a one-flavor system. (Note, however, that in this reference the boundary value of the field strength was interpreted as H, not B.) We see that the magnetization behaves linearly for small magnetic

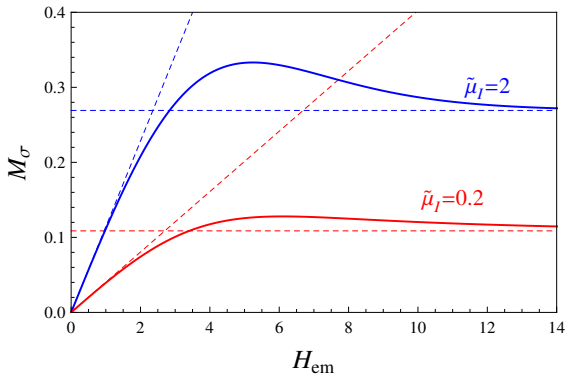

Figure 6.4: Dimensionless magnetization M_σ for the sigma phase as a function of the dimensionless magnetic field $H_{\rm em}$ for two different values of the isospin chemical potential and a baryon chemical potential $\tilde\mu_B = 2$. The dashed lines are the susceptibilities χ_σ from Eq. (6.65), which approximate the magnetization for small magnetic fields, $M_\sigma = \chi_\sigma H_{\rm em}$, and the asymptotic values from Eq. (6.66).

fields. The slope is the magnetic susceptibility, *i.e.*, $M_\sigma \simeq \chi_\sigma H_{\rm em}$. Upon expanding Eq. (6.62) for small magnetic fields we find

$$\chi_\sigma = \frac{\pi}{18}\frac{q_1^2\tilde\mu_1^2 + q_2^2\tilde\mu_2^2}{1 - \frac{2\kappa\pi}{9}(q_1^2\tilde\mu_1^2 + q_2^2\tilde\mu_2^2)}\,. \tag{6.65}$$

Since we neither expect the susceptibility to diverge nor to change sign, this result can only be trusted for sufficiently small chemical potentials, roughly speaking $\tilde\mu_i^2 \ll 1/(\kappa e^2)$. Given the numerical value $(\kappa e^2)^{-1/2} \simeq 38$ and given that one unit of the quark chemical potential $\tilde\mu_i = 1$ corresponds to $\mu_i \simeq 400\,\text{MeV}$, this is not a severe restriction for realistic values of μ_i. However, this result shows that in principle one has to be careful with large chemical potentials in the present approximation where we not only have expanded the DBI action for small gauge fields but also neglected the backreaction of the branes to the background geometry.

For large magnetic fields the magnetization saturates. From Eq. (6.62) we find the constant value

$$\lim_{H_{\rm em}\to\infty} M_\sigma = \frac{q_1\tilde\mu_1^2 - q_2\tilde\mu_2^2}{12}\,, \tag{6.66}$$

where we have used that $B > \hat B$ for a two-flavor system with up and down quarks. We now return to the free energy comparison. For the sigma phase we insert Eq. (6.60) into the Gibbs free energy (6.59). Then we obtain the following difference in Gibbs free energies

$$\frac{\Delta G}{M_{\rm KK}^4/\alpha^2} \equiv \frac{G_\sigma - G_\pi}{M_{\rm KK}^4/\alpha^2} = -\frac{1}{2}H_{\rm em}^2 + \frac{1}{2}\kappa^2 M_\sigma^2 + \kappa(\omega_\sigma - \omega_\pi)\,. \tag{6.67}$$

If $\Delta G > 0$ ($\Delta G < 0$) the π (σ) phase is preferred. It is instructive to relate the comparison between the sigma and pion phases to a usual superconducting material, say a metal, where we compare the superconducting phase (corresponding to the pion phase) and the normal-conducting phase (corresponding to the sigma phase). With the help of this analogy we can understand the various terms in ΔG. The term quadratic in $H_{\rm em}$ is negative, *i.e.*, it works in favor of the normal-conducting phase. This term is the free energy cost which the superconducting phase has to pay for creating a counter magnetic field in order to expel the external magnetic field. In a usual superconductor, this term is thus responsible for a critical magnetic field beyond which the Cooper pair condensate breaks down. There is an additional term, working against the normal-conducting phase, proportional to M_σ^2. This term is absent

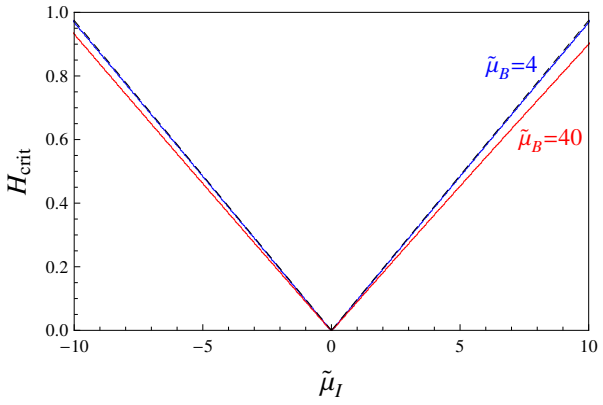

Figure 6.5: Critical magnetic field for the phase transition from the pion to the sigma phase as a function of the isospin chemical potential for baryon chemical potentials $\tilde{\mu}_B = 4$ (red curve) and $\tilde{\mu}_B = 40$ (blue curve). The dashed line is the approximation from Eq. (6.69) and almost coincides with the curve for $\tilde{\mu}_B = 4$. Our model does not include a finite pion mass. It can be expected that the effect of the pion mass shifts the curves such that they start at $\mu_I = \pm m_\pi$ (corresponding to $\tilde{\mu}_I \simeq \pm 0.375$) instead of $\mu_I = 0$.

in most usual superconductors which, to a good approximation, have no magnetic properties in their normal-conducting phase. We thus expect a competition between the two terms, *i.e.*, between the costs that the sigma and charged pion phase have to pay for the magnetization and the Meissner effect, respectively. This competition, together with the difference $\omega_\sigma - \omega_\pi$, will determine the resulting phase diagram.

For small magnetic fields, $H_{\rm em} \ll 1$, and dimensionless chemical potentials of order one, $\tilde{\mu}_{B,I} \lesssim 1$, we can discuss the phase transition between the sigma and the charged pion phase analytically. In this case, the term $\kappa^2 M_\sigma^2$ is of the order of $\kappa^2 e^4$ and thus negligible. The free energy of the sigma phase $\kappa\omega_\sigma$ is proportional to κe^2 and thus also small compared to the remaining terms. We are left with the simple result

$$\frac{\Delta G}{M_{\rm KK}^4/\alpha^2} \simeq -\frac{1}{2}H_{\rm em}^2 + \frac{8\kappa}{\pi}\tilde{\mu}_I^2 \,. \tag{6.68}$$

At the phase transition $\Delta G = 0$ we thus have

$$\tilde{\mu}_I = \pm\sqrt{\frac{\pi}{\kappa}}\frac{H_{\rm em}}{4} \approx \pm 5.13 H_{\rm em} \,. \tag{6.69}$$

This relation can be read as an equation for the critical magnetic field for a given chemical potential, or as an equation for the critical chemical potential for a given magnetic field. We see that, in this approximation, the phase transition is independent of the baryon chemical potential. In Figure 6.5 we plot the critical magnetic field as a function of the isospin chemical potential for two different values of the baryon chemical potential.

Let us now discuss the resulting phase diagram in the μ_B-μ_I plane. Firstly, we consider the case of vanishing magnetic field, $H_{\rm em} = 0$. From Eq. (6.68) we see that, in this case, the pion phase is favored in the entire μ_B-μ_I plane except for the μ_B axis. To understand this result we recall several features of our model. We treat the fermions as massless (in most applications of the Sakai-Sugimoto model, this approximation is used; for a discussion about how to incorporate finite mass effects into the model see the recent Ref. [185]). Therefore, a charged pion condensate appears for arbitrarily small isospin chemical potentials, and not only beyond a finite threshold given by the pion mass. Moreover, since we consider the confined phase, we cannot account for phases where there is a vanishing $\langle\bar{u}u\rangle$ and a nonvanishing $\langle\bar{d}d\rangle$

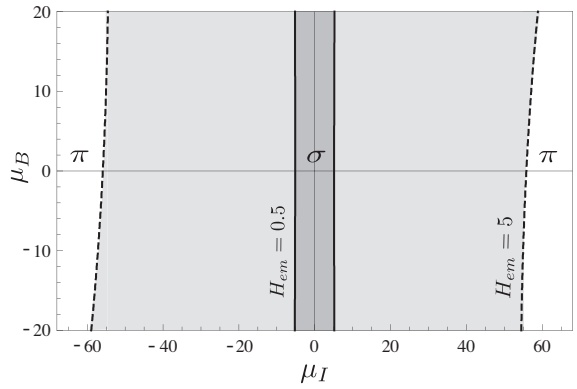

Figure 6.6: Phase diagram for the σ and π phases in the plane of baryon and isospin chemical potentials. We have chosen two different values of the dimensionless magnetic field, $H_{\rm em} = 0.5$ (solid lines, dark shaded sigma phase) and $H_{\rm em} = 5$ (dashed lines, light shaded sigma phase). The sigma phase contains meson supercurrents while the pion phase contains an isotropic $\pi^{\pm}$ condensate and exhibits the Meissner effect. All lines indicate first order phase transitions. The units of this plot, upon fitting the parameters of the model according to (6.64), are $\tilde{\mu}_{B,I} \approx \mu_{B,I}/(370\,\mathrm{MeV})$ and $H_{\rm em} \approx \mathcal{H}_{\rm em}/(1.8 \cdot 10^{19}\,\mathrm{G})$. Hence, due to the huge scales even compared to magnetar scales, this phase diagram is rather of academic interest; for more realistic chemical potentials and magnetic fields, the simple approximation (6.69) is sufficient.

condensate or vice versa. In other words, we cannot connect the up-flavor branes and leave the down-flavor branes disconnected, as done in Ref. [92], where the deconfined (but chirally broken) phase was considered. And finally, in our approach we do not see a phase transition to the chirally restored phase. Since we are in the confined phase, where the subspace of the compactified extra dimension x_4 and the holographic coordinate z is cigar-shaped, the D8 and $\overline{\rm D8}$-branes *must* connect, *i.e.*, chiral symmetry must be broken for all values of the chemical potentials. The chiral symmetry can only be restored above the deconfinement phase transition. Taking into account these restrictions, our phase diagram at vanishing magnetic field is in accordance for instance with Refs. [92, 179].

Next, we discuss the case of a nonzero magnetic field. The phase diagram for two different magnetic fields is shown in Figure 6.6. From Eq. (6.69) we see that a region for the sigma phase opens up, with straight phase transition lines independent of μ_B. These lines start to bend for larger magnetic fields. We may use the numerical values of the parameters of the model given below Eq. (6.63) for some (very) rough quantitative predictions from this phase diagram. First we notice that a dimensionless field $H_{\rm em} = 1$ corresponds to[5] $\mathcal{H}_{\rm em} \simeq 2 \cdot 10^{19}\,\mathrm{G}$, about $4-5$ orders of magnitude larger than the surface field of magnetars, and most likely even larger than the magnetic field in the interior of the star. For the chemical potentials we find that $\tilde{\mu}_{B,I} = 1$ corresponds to $\mu_{B,I} \simeq 400\,\mathrm{MeV}$. As a comparison, a typical baryon chemical potential for neutron stars is at most $\mu_B \lesssim 1500\,\mathrm{MeV}$, corresponding to $\tilde{\mu}_B \simeq 4$. Now, as a rough estimate, let us assume an isospin chemical potential of $1/10$ times the baryon chemical potential in a neutron star, *i.e.*, $\tilde{\mu}_I \simeq 0.4$. Then, the phase transition from the charged pion condensed phase to the sigma phase occurs at a very large magnetic field of approximately $\mathcal{H}_{\rm em} \simeq 1.6 \cdot 10^{18}\,\mathrm{G}$. In other words, the charged pion condensate at finite isospin chemical potentials appears to be, in terms of realistic values for the magnetic field, very robust.

The superconducting properties of a charged pion condensate have been studied in conventional chiral models [186, 187, 188, 189]. There, for an isotropic charged pion condensate,

[5] In the natural Heavyside-Lorentz system of units of particle physics, a magnetic field strength of 1 eV^2 corresponds to $51.189\ldots\,\mathrm{G}$ in the Gaussian system.

the scale of the critical magnetic field is set by m_π^2, which is of the order of $10^{18}\,\mathrm{G}$, whereas an anisotropic charged pion condensate has been argued to give a critical magnetic field of the order of $10^{19}\,\mathrm{G}$. In our model, in the π phase we have an isotropic π condensate and a vanishing m_π, but nevertheless we have obtained a critical field of comparable magnitude. It should be noted that in conventional chiral models the charged pion condensate has been found to behave as a type-II superconductor [186, 187, 188], which means that there is another, smaller critical field strength, above which the magnetic field can penetrate in the form of magnetic vortices. By considering only homogeneous fields, we have of course not taken this possibility into account. Our result for the critical magnetic field corresponds to the larger value where the charged pion condensate is destroyed completely.

Chapter 7

Conclusions and Outlook

In this thesis we have used the gauge/gravity duality to investigate properties of strongly coupled matter. The gauge/gravity duality relates string theory living on asymptotically anti de Sitter space with a gauge theory living on the boundary of this space. When one side is weakly coupled the other side is strongly coupled and vice versa. This duality gives us a new tool to study strongly coupled gauge theories from the low energy limit of string theory, which is supergravity. Since the original statement of the correspondence, great effort has been put into the construction of new dual theories to come closer to QCD. Unfortunately so far no perfect dual string theory to QCD has been found. In this chapter we summarize our findings from the Sakai-Sugimoto model and the D3-D7 brane setup.

7.1 D3-D7 setup

In Chapter 3 we have used the D3-D7 brane setup to calculate the energy spectrum of heavy-light mesons. Our heavy light mesons are described by a string stretching between two D7 branes separated by a finite distance proportional to the mass difference between the hypermultiplets. In the heavy quark limit the meson spectrum is not well approximated by the D7 brane fluctuations but by the fluctuations of the string itself which can be treated semi-classically. In Section 3.5 we calculated a portion of the energy spectrum of heavy-light mesons in $\mathcal{N}=2$ SYM with two massive hypermultiplets. One generic feature of the energy spectrum of the heavy-light meson spectrum is the m_h independence of the excitation energies in the infinite heavy quark mass limit. For example, for low lying fluctuations in the x and y_6 directions we found the energy spectrum

$$E_n = m_h - m_l + m_l \frac{2\pi^2 n}{\sqrt{\lambda}} + \mathcal{O}\left(\frac{m_l^2}{m_h}\right) \ . \tag{7.1}$$

For the ρ fluctuations, we were not able to determine a spectrum analytically, but were nevertheless able to determine this m_h independence numerically. The x fluctuations should correspond to vector-like mesons, while the y_6 and ρ fluctuations should correspond to scalar-like mesons.

We have also studied spinning strings in Section 3.6. For the strings spinning in real space, we have found several branches, characterized by a radial excitation number n. For small angular momentum J, we were able to determine the analytic formula

$$E_n^J = m_h - m_l + m_l \frac{2\pi^2 n J}{\sqrt{\lambda}} + \mathcal{O}\left(\frac{m_l^2}{m_h}\right) \ , \tag{7.2}$$

which displays this m_h independence. Finally we have studied strings spinning in the internal space, which correspond to mesons with R-charge Q from the field theory perspective. For

small Q, we have found the analytic formulae of Eqs. (3.75) and (3.88) which again displays m_h independence. The m_h independence at leading order is in agreement with heavy quark effective theory.

We have also found a degeneracy in the spectrum. For example, the lowest lying mode in the x direction had the same energy as the lowest lying excitation in the y_6 direction.

In Section 3.7.1 we have shown that this degeneracy is a consequence of supersymmetry and that it can be removed upon breaking supersymmetry. By tilting the heavy brane in the internal $\mathbb{R}^6$ space by an angle θ we have broken supersymmetry completely. The analysis of the energy spectrum has revealed the emergence of hyperfine splitting, *e.g.* the energy spectrum for the y_6 fluctuations was

$$E_{y_6} = m_h - m_l + m_l \frac{2\pi^2 n}{\sqrt{\lambda}} - \frac{m_l^2}{m_h} \frac{2n\pi^2 \sin^2\theta}{\sqrt{\lambda}}, \tag{7.3}$$

giving splitting terms proportional to $\sin^2(\theta)/m_h$.

In Section 3.7.2 we have broken supersymmetry by applying an external magnetic field and found Zeeman splitting effects proportional to b/m_h^2 for weak magnetic fields b. Increasing the value of b we found an interesting effect, where the Zeeman split frequencies rejoined in the limit $b \to \infty$.

While we have chosen to approach the question of hadron spectra in QCD-like theories by considering field theories with well-known gravity duals rather than trying to build phenomenological models for QCD itself, it is interesting to note how some effects characterizing the QCD meson spectrum can be realized in relatively simple settings. Our holographic heavy-light mesons certainly deserve further investigation. We have commented in Section 3.8 that it is possible to tune the mass of the ground state to be anything between $m_h - m_l$ and $m_h + m_l$. It would be an interesting project for the future to study this more general heavy-light mesons. The setup involving a tilted heavy D7 brane certainly warrants further work. In particular, one should try to find a way to stabilize the positions of the two D7-branes. We are also interested in performing a detailed analysis of the bound states of the theory at weak coupling, building on the results of Refs. [79, 190, 77].

7.2 Sakai-Sugimoto model

In the rest of this work we have used the Sakai-Sugimoto model, which is the model that at present comes closest to providing a gravity dual to (large-N_c) QCD. The model consists of an D4/D8-$\overline{\text{D8}}$ system in which a bulk gauge symmetry on the D8 and $\overline{\text{D8}}$ branes corresponds to a global (flavor) symmetry at the boundary which is interpreted as chiral symmetry. Here, left- and right-handed fermions are separated by a fifth extra dimension. The electromagnetic subgroup of this flavor symmetry group has been used to incorporate an external magnetic and electric field.

In Chapter 5 we have studied the strong-coupling behavior of chiral fermions in the presence of a chemical potential and a background magnetic field in the chirally broken and the chirally symmetric phases. In particular, we have investigated the chiral magnetic effect, which has been studied previously in a weak-coupling approach [96] and on the lattice [109]. We have pointed out that a reliable calculation within the Sakai-Sugimoto model requires a careful discussion of the QED anomaly in the model. The standard value of the *consistent* anomaly arises naturally in the model for the most straightforward definition of the current. For this

result it is crucial to include the contributions from the CS term which are sometimes ignored in the literature. The *covariant* anomaly can then be implemented by adding Bardeen's counterterm [114], which is also known to be required in chiral models with a Wess-Zumino-Witten term [118], and we have pointed out that this (finite) counterterm has a form that appears consistent with the procedure of holographic renormalization.

After these general discussions we have solved the equations of motion for the chirally broken and the chirally symmetric phases explicitly. In our approximation of the DBI action to lowest order in the gauge fields, the solutions are completely analytical. Electric (vector and axial) fields parallel to the magnetic field have been considered in order to check the anomaly explicitly, but they are not needed and set to zero for our physical (equilibrium) results, which only require magnetic fields in the presence of chemical potentials.

In the presence of a quark chemical potential and a large magnetic field, we have calculated the axial current, which may be of interest for astrophysical phenomena such as pulsar kicks [104]. In the chirally symmetric phase we have reproduced the known topological result [103, 129], while in the chirally broken phase, the current has turned out to be smaller but nonvanishing. These results can also be obtained by using only the YM part of the current, *i.e.*, in the case of the axial current the CS contribution and the contribution of Bardeen's counterterm cancel each other.

This is different for the vector current. In this case, only the YM contribution yields the expected topological result for both phases in in agreement with ref. [96]. With the full current, and after adding Bardeen's counterterm, the vector current becomes zero for both phases. The absence of the chiral magnetic effect in the deconfined phase comes as surprise. One might have expected the known topological result because it can be derived from the anomaly only [130] and we have made sure to incorporate the correct covariant anomaly. Our result of a vanishing vector current in the confined phase seems less puzzling. The usual explanation of the chiral magnetic effect, using a quasiparticle picture (which is not guaranteed to hold in our strong-coupling approach), relies on individual, electrically charged, massless quarks which move in different directions according to their chirality. A suppression of the effect may thus indeed be expected in the confined, chirally broken phase [96, 191].

In comparison to the result from recent lattice calculations [109] we have pointed out an intriguing agreement *before* adding Bardeen's counterterm, *i.e.*, within the consistent anomaly. There the vector current per chirality approaches approximately the value 2/3 for asymptotically large magnetic field. This is clearly different from the weak-coupling approach where this ratio approaches 1. This raises the question whether this asymptotic value can distinguish between strong and weak coupling. It also raises the question whether the lattice result relates to the consistent, as opposed to the covariant, anomaly.

There are several problems in our current approach that certainly need further studies. First, although we have implemented the correct covariant anomaly, a problem remains. Namely, upon computing the free energy explicitly and then taking the derivative with respect to the appropriate source, the currents turn out to be different from the straightforward definition via the gauge/gravity correspondence. This somewhat disturbing discrepancy can be attributed to boundary terms at spatial infinity. We have discussed that a previously suggested fix of this problem by modifying the action [91] seems to be not acceptable because it entirely eliminates the axial anomaly from the correspondingly modified currents. Only the YM part of these currents are anomalous, but those suffer from the same thermodynamic inconsistency that this modification was meant to fix (see also ref. [110] for other issues concerning the definition of chiral currents in the Sakai-Sugimoto model). Second, the introduction of an axial chemical potential might be problematic. It has been argued that a chemical potential can only be introduced if it is associated to a conserved charge N. Only then it is possible to obtain

a physically meaningful vector current. This conserved charge is only gauge invariant when integrated over all of space in spatially homogeneous situations [192, 193]. But for charge separation in heavy-ion collisions one needs inhomogeneous situations, because with $\nabla \mathbf{B} \equiv 0$ we have [194]

$$\frac{\partial \rho}{\partial t} = -\nabla \mathbf{J} = -\frac{e^2 N_c}{2\pi} \mathbf{B} \nabla \mu_5. \tag{7.4}$$

In [194] a toy model similar to the Sakai-Sugimoto model has been considered. There it has been pointed out that it is important to carefully distinguish between the boundary values of the gauge field and the definition of the chemical potential. According to the dictionary the boundary value of the gauge field is the source for an operator and the chemical potential is the difference between the value of the gauge field at the horizon and the boundary. Using linear response theory and the distinction between sources and chemical potentials the topological result has been obtained. The reason is that one can set the sources to zero in the end which leads to vanishing Chern-Simons contribution to the currents.

It has also been suggested that the canonical ensemble is more appropriate for describing the chiral magnetic effect in heavy-ion collisions. We have tried to combine the different approaches, namely using the modified action, going to the canonical ensemble and distinguishing between the sources and chemical potentials. With this combination we were able to satisfy thermodynamic consistency, and obtain the topological result for the axial and vector current. However, by setting the sources to zero we also lost the axial anomaly. It is still not clear to us how to satisfy thermodynamic consistency and keep the anomaly at the same time.

Quantitative improvements could be achieved by extending our calculation to the full DBI action, though they should be minor for magnetic field strengths of practical interest. More critical, but also considerably more difficult, would be the generalization of our ansatz to allow for inhomogeneous field configurations and/or inhomogeneous solutions. This might be required to resolve the ambiguities in the definition of the chiral currents that we have discussed, since those are related to spatial surface contributions in the CS action. With our present definition of the chiral currents we have been led to question the very existence of the chiral magnetic effect in the strong-coupling regime of the Sakai-Sugimoto model (which is gravity dual to large-N_c QCD only in its inaccessible weak coupling limit). In this context it would be important to understand whether in the strong-coupling regime one has Landau-level-like structures, as conjectured in ref. [90]. This is interesting also in view of recent studies in different gauge/gravity models [132, 133].

In Chapter 6 we studied chiral symmetry breaking in a two-flavor system with a magnetic field and baryon and isospin chemical potentials. Our results are independent of temperature, valid for temperatures below the critical temperature for chiral symmetry breaking. We have discussed how the model can account for different Goldstone boson condensates, two of which we have described within our ansatz of abelian gauge field components. Starting from the D-brane action, consisting of Yang-Mills plus Chern-Simons contributions, we have analytically solved the equations of motion and computed the Gibbs free energies of these two phases.

The first phase, briefly termed sigma phase, is a linear combination of the usual chiral sigma condensate and a neutral pion condensate. We have found that for nonzero magnetic fields this phase exhibits a nonzero meson supercurrent. In addition, a normal current is generated which carries baryon and isospin charge. For both currents, there exist counter-propagating currents such that the net current of the system is zero. This is reminiscent of unconventional (anisotropic) superfluids and superconductors in condensed matter systems or deconfined dense quark matter. In accordance with our results for the normal currents, we have found that the baryon and isospin densities in the system, which obviously vanish without a magnetic field, become nonzero once a magnetic field is switched on. As a consequence, also

an electric charge appears in the sigma phase.

In the second phase, briefly termed pion phase, charged pions form a condensate. This phase reacts very differently to a magnetic field. It acts as an electromagnetic superconductor, and thus expels the magnetic field due to the Meissner effect. We have seen that the assumption of a nonzero magnetic field would lead to infrared divergencies in the energy density which cannot be removed by holographic renormalization. Therefore, we have introduced supercurrents which induce a magnetic field opposite, but equal in magnitude, to the externally applied field. Then the total magnetic field in the π phase vanishes, and a consistent treatment without divergencies is possible. In contrast to the σ phase, the π phase, due to the Meissner effect, appears unaltered under the influence of a magnetic field. In particular, the baryon number and all currents (except for the supercurrents cancelling the external magnetic field) vanish.

Besides the calculation of the supercurrent and the observation of the Meissner effect in the charged π condensate, the main result of Chapter 6 is the free energy comparison between the two phases and the resulting phase diagram in the μ_B-μ_I plane. For a vanishing magnetic field, a nonzero isospin chemical potential leads to the rotation of the sigma condensate into a charged pion condensate. This is expected from studies using the same and other models [92, 177, 179, 195]. In the present study, which does not include quark masses, this means that in the absence of a magnetic field the pion condensate is favored over the sigma condensate in the entire μ_B-μ_I plane. For a nonzero magnetic field the rotation is partially undone, *i.e.*, for a given external magnetic field, there is a region for sufficiently small μ_I where the σ phase is favored over the π phase. This is not unlike the transition in a metal from its superconducting to its normal conducting state. We have found that for small magnetic fields, the critical magnetic field for this phase transition is linear in μ_I and independent of μ_B, $H_c \propto |\mu_I|$. As a quantitative estimate from our result we have discussed that for magnetic fields on compact star scales, the charged pion phase at nonzero μ_I is very robust. We have estimated that magnetic fields of the order of 10^{18} G (well beyond surface magnetic fields of magnetars) are needed to induce a phase transition from the π to the σ phase for isospin chemical potentials of the order of 150 MeV.

There are several interesting extensions to our work. One may study the question whether the solutions found here (anisotropic but homogeneous) are stable against formation of crystalline structures. Moreover, since charged pion condensates have been found to behave as type-II superconductors in conventional chiral models [186, 187, 188], it would be interesting to consider inhomogeneous vortex-like configurations of magnetic fields. It is also important to check whether the states we have described are stable with respect to other meson condensates. We already know that without magnetic field a rho meson condensate is expected to form for sufficiently large isospin chemical potentials [94].

One question posed in [34], how the magnetic field affects chiral symmetry restoration in the Sakai-Sugimoto model, was answered in [196] where it was found that the addition of a magnetic field decreases the critical chemical potential for chiral symmetry restoration. This effect is called "inverse magnetic catalysis", in contrast to the usual "magnetic catalysis", where a magnetic field favors the chirally broken phase for vanishing chemical potential.

7.3 Final remarks

To conclude let us make some final remarks. As we have pointed out several times, the AdS/CFT correspondence is a duality between strongly coupled gauge theory and weakly coupled string theory and vice versa. We have used the duality to gain insights into strongly coupled matter by using supergravity and then translating it into the field theory quantities.

There is huge progress in this field and recently it has also been applied to condensed matter systems, such as high temperature superconductors and superfluids [164, 165]. One obstacle that makes it difficult to come closer to the real world is the large N limit which is taken in all the applications of the correspondence. Resolving this problem would be huge step towards a gravity dual of QCD.

There is also the other side of the duality where one can use the field theory to learn something about quantum gravity because all physical degrees of freedom from quantum gravity are encoded in the boundary theory [197]. This approach turns out to be rather difficult because it is not clear how local operators living on the boundary can be matched to local observables living deep inside the bulk but it seems to be a promising way to learn something about quantum gravity.

Despite these difficulties the AdS/CFT correspondence is one of the most ground breaking discoveries in theoretical physics and will certainly surprise us many times on our way to understand the laws of nature.

Acknowledgements

First of all I would like to thank my adviser Anton Rebhan for giving me the opportunity to stay in physics, for his patience with my never ending questions and for motivating me when I needed it most.

I would like to thank Gabor Kunstatter who supervised me in the first months of my studies in Winnipeg and also introduced me into the topic of general relativity, which was essential for my further studies.

I am especially grateful to Aleksi Vuorinen. When he was a postdoc in Vienna we became close friends. We often talked about life and physics and he always encouraged me when I was struggling with problems regarding my work and i profited tremendously from his knowledge. When my first project turned out to be a dead end he included me in a project with Christopher Herzog. Working together with Aleksi on a project was an unforgettable experience and I hope there are many more to come.

I would also like to thank Christopher Herzog for giving me something to work on and sharing his insights in physics with me. It was amazing to see his ability to reduce at the first sight difficult problems to ones I could understand.

I am also very thankfull to Andreas Schmitt. He spent hours after hours sharing all his experience with me. I learned a lot from him and he always took his time answering my questions. Without him, working on my thesis would not have been that much fun and I hope we will also work together in the future.

I would also like to mention Radoslav Rashkov who always had an open ear for my questions.

Many thanks to Ivan Iliev and Matthias Grieder who helped me out with the illustrations for my thesis.

I loved going to work because it was such a nice atmosphere. It was always nice to see my colleagues and many of them are good friends and I would like to thank them for making this period of my life unforgettable. Like Maximilian Attems, with whom I had some of my best climbing experiences. Or David Burke who often joined me for pint or two after work. Others I would like to mention are Florian Preis, Dominik Steineder, Christoph Mayerhofer, Andreas Braun, Andreas Ipp and Niklas Johanson.

Last but not least, I would like to thank all my close friends who always took it with a smile when I could not stop talking about physics.

This thesis has been supported by FWF project no. P19958.

Appendix A

Fields in AdS

In this appendix we want to illustrate how correlation functions are computed via the correspondence (2.51).

A.1 Massless scalar field in AdS

We calculate the correlation function of a massless field in d+1 dimensional AdS space. Note that in this appendix we will use the following notation

$$x_\mu = \{z, \vec{x}\}, \qquad \vec{x} = t, x_1 \ldots x_{d-1}, \tag{A.1}$$

and we will work in Euclidean space $\mathbb{R}^n$. We start with the action

$$S = \int d^{d+1}x\sqrt{g}\left(\frac{1}{2}\left(\partial\phi\right)^2\right), \tag{A.2}$$

with the equation of motion

$$\frac{1}{\sqrt{g}}\partial_\mu\left(\sqrt{g}\partial^\mu\phi(x)\right) = 0 \tag{A.3}$$

We want to solve for $\phi(x)$ in terms of the boundary field $\phi_0(x')$, where $x \in AdS_{d+1}$ and $x' \in \mathbb{R}$, in order to compute the two point correlation function of the operator $\mathcal{O}$ in (2.51). To do so we first look for a Green's function $K(z, \vec{x}; \vec{x}')$ of the Laplace equation whose boundary value is a delta function at the boundary:

$$\Box K(z, \vec{x}; \vec{x}') = \delta^d(\vec{x} - \vec{x}'). \tag{A.4}$$

Then we can construct the classical solution as

$$\phi(z, \vec{x}) = \int d^d x' K(z, \vec{x}; \vec{x}')\phi_0(\vec{x}'). \tag{A.5}$$

To find this function it is convenient to use the metric (2.19). In this representation the boundary consists of a copy of $\mathbb{R}^d$, at $z = 0$, together with a single point P at $z = \infty$. Note that the propagator is invariant under the isometry group of AdS space. We let the boundary point $\vec{x}'$ represent the point P at $z = \infty$: $K(z, \vec{x}; \vec{x}') = K(z, \vec{x}; P)$. Since the boundary condition and the metric are invariant under translations of the $\vec{x}$ the propagator will also have this symmetry and will be only a function of z.

Thus we seek a solution to the problem

$$\frac{d}{dz}z^{-d+1}\frac{d}{dz}K(z) = 0. \tag{A.6}$$

We keep the solution that vanishes at the boundary $z = 0$, which is

$$K(z, \vec{x}; P) = cz^d, \tag{A.7}$$

with c a constant. There is some sort of singularity at the boundary point P, since this solution diverges at infinity. To show that this singularity is a delta function at the boundary we make an $SO(1, d+1)$ transformation (which is an isometry of AdS space and preserves the parametrization space)

$$x_\mu \to \frac{x_\mu}{z^2 + \vec{x}^2} \tag{A.8}$$

that maps P to the origin, $P \to \vec{x}' = 0$, and transforms $K(z, \vec{x}; P)$ to

$$K(z, \vec{x}; 0) = c\frac{z^d}{(z^2 + \vec{x}^2)^d}. \tag{A.9}$$

From translational invariance on the boundary we find

$$K(z, \vec{x}; 0) = c\frac{z^d}{(z^2 + |\vec{x} - \vec{x}'|^2)^d}.$$

Now lets check if this is indeed proportional to a delta function at the boundary. Firstly, by scaling, $\vec{x} \to \vec{x}/z$, we see that

$$c\int d^d x \frac{z^d}{(z^2 + \vec{x}^2)^d} \to c\int d^d x \frac{1}{(1 + \vec{x}^2)^n} = c\sqrt{\pi}\frac{\Gamma\left(n - \frac{1}{2}\right)}{\Gamma(n)}$$

is independent of z and convergent. By requiring that above integral is equal to one the integration constant can be fixed. Secondly, as $z \to 0$, K vanishes except at $\vec{x} = 0$. We conclude that K becomes a delta function at the boundary supported at $\vec{x} = 0$ with unit coefficient if c is chosen properly.

Using this Greens function, the solution to the Laplace equation is

$$\phi(z, \vec{x}) = \frac{\Gamma(d)}{\pi^{\frac{d}{2}}\Gamma\left(d - \frac{1}{2}\right)} \int d^d \vec{x}' \frac{z^d}{(z^2 + |\vec{x} - \vec{x}'|^2)^d} \phi_0(\vec{x}'). \tag{A.10}$$

In order to compute the two point function we need to evaluate the on shell action

$$\begin{aligned} S(\phi) &= \int d^{d+1}x_\mu \sqrt{g}\left(\frac{1}{2}(\partial\phi)^2\right) = \frac{1}{2}\int d^{d+1}x_\mu \, z^{1-d}\partial_\mu\phi\partial_\mu\phi & \text{(A.11)} \\ &= \frac{1}{2}\int d^{d+1}x_\mu \, \partial_\mu\left(z^{1-d}\phi\partial_\mu\phi\right) - \frac{1}{2}\int d^{d+1}x_\mu \, \phi\partial_\mu\left(z^{-d+1}\partial_\mu\phi\right). & \text{(A.12)} \end{aligned}$$

The last term vanishes due to the equation of motions and the total derivative term vanishes in all directions except in the z direction where we have the boundary. We are left with

$$S(\phi) = \frac{1}{2}\int d^d\vec{x} \, z^{1-d}\phi(z, \vec{x})\partial_\mu\phi(z, \vec{x})|_{z=\epsilon}, \tag{A.13}$$

where we have introduced a cutoff to avoid divergencies. In the limit $z \to 0$ we use $\phi_0(z, \vec{x}) = \phi_0(\vec{x})$ and evaluate

$$\begin{aligned} \partial_\mu\phi(z, \vec{x}) &= c\int d^d\vec{x}' \frac{z^n}{(z^2 + |\vec{x} - \vec{x}'|^2)^d}\phi_0(\vec{x}') & \text{(A.14)} \\ &= \frac{\Gamma(d)}{\pi^{\frac{d}{2}}\Gamma\left(d - \frac{1}{2}\right)} dz^{d-1}\int d^d\vec{x}' \frac{\phi_0(\vec{x}')}{(|\vec{x} - \vec{x}'|^2)^d} + O\left(z^{d+1}\right). & \text{(A.15)} \end{aligned}$$

Inserting this into (A.13) we get for the on-shell action

$$S(\phi) = \frac{d}{2} \frac{\Gamma(d)}{\pi^{\frac{d}{2}} \Gamma\left(d - \frac{1}{2}\right)} \int d^d\vec{x} d^d\vec{x}' \frac{\phi_0(\vec{x})\phi_0(\vec{x}')}{(z^2 + |\vec{x} - \vec{x}'|^2)^d}, \tag{A.16}$$

where the singular behavior for $z \to 0$ dropped out. Plugging this action into (2.51) and taking two derivatives w.r.t. the boundary fields we obtain the two point correlation function of the operator $\mathcal{O}$

$$\left\langle \mathcal{O}(\vec{x})\mathcal{O}(\vec{x}') \right\rangle = \frac{\Gamma(d)}{\pi^{\frac{d}{2}} \Gamma\left(d - \frac{1}{2}\right)} \frac{d}{(|\vec{x} - \vec{x}'|^2)^d}, \tag{A.17}$$

as expected for a field of conformal dimension d.

A.2 Massive scalar field in AdS

Now we are ready to repeat the computation from the previous section for massive scalars but now we are looking for a function that obeys the massive wave equation and behaves as $f^{-\Delta_+}\phi_0$ at the boundary. Again the first step is to find a Green's function only depending on z that vanishes at the boundary except for one point P at $z = \infty$ where it becomes a delta function. The action of a massive scalar in AdS_{d+1} is

$$S = \int d^{d+1}x_\mu \sqrt{g} \left(\frac{1}{2} (\partial\phi)^2 + \frac{1}{2} m^2 \phi^2 \right), \tag{A.18}$$

leading to the equation of motion

$$\left(z^{d+1} \frac{d}{dz} z^{-d+1} \frac{d}{dz} - m^2 \right) K(z) = 0. \tag{A.19}$$

There are two linearly independent solutions of the form

$$K(z) \sim z^{\lambda_\pm}, \qquad \Delta_\pm = \frac{1}{2} \left(d \pm \sqrt{d^2 + 4m^2} \right) \tag{A.20}$$

The solution that vanishes at $z = 0$ is $K(z) = z^{\Delta_+}$ but there is again some sort of singularity at $z = \infty$. To show that this becomes a delta function we use the inversion transformation (A.8)

$$K(z, \vec{x}) = C \frac{z^{\Delta_+}}{(z^2 + |\vec{x} - \vec{x}'|)^{\Delta_+}}. \tag{A.21}$$

Note that K does not tend to a delta function at $z = 0$ but

$$\lim_{z \to 0} \frac{z^{\Delta_+ - \Delta_-}}{(z^2 + \vec{x}^2)^{\Delta_+}} = C\delta^d(\vec{x} - \vec{x}') \tag{A.22}$$

does, where we have used $\Delta_+ = d - \Delta_-$. To see this one uses the same arguments as in the previous section. C is a normalization constant given by

$$C = \pi^{\frac{d}{2}} \frac{\Gamma\left(\Delta - \frac{1}{2}\right)}{\Gamma(\Delta)}. \tag{A.23}$$

Now we can build the classical solution

$$\phi(z, \vec{x}) = C^{-1} z^{\Delta_-} \int d^n\vec{x}' \frac{z^{\Delta_+ - \Delta_-}}{(z^2 + |\vec{x} - \vec{x}'|^2)^{\Delta_+}} \phi_0(\vec{x}'). \tag{A.24}$$

The asymptotic solution near the boundary is given by

$$\phi(z,\vec{x})|_{z\to 0} = C^{-1} z^{\Delta_-}\phi_0(\vec{x}) + C^{-1} z^{\Delta_+}\int d^d\vec{x}'\frac{\phi_0(\vec{x}')}{|\vec{x}-\vec{x}'|^{2\Delta}}. \tag{A.25}$$

The boundary condition $\lim_{z\to 0}\Phi(z,\vec{x}) = C^{-1}z^{\Delta_-}\phi_0(\vec{x})$ reflects the important point that the theory on the boundary is only defined up to conformal transformations.

The dimension of the operator $\mathcal{O}$ can be obtained in the following way. We know from the action (A.18) that the five dimensional scalar field is dimensionless and therefore we conclude from (A.25) that the boundary field has dimension $[\text{length}]^{-\Delta_-}$. This implies, through the right hand side of (2.51), that the associated operator $\mathcal{O}$ has mass dimension

$$\Delta = d - \Delta_- = \frac{d}{2} + \frac{1}{2}\sqrt{4+4m^2} = \Delta_+. \tag{A.26}$$

With the solution (A.24) we can evaluate the on shell action as in the massless case and find

$$S(\phi_0) = -\left(\Delta - \frac{d}{2}\right)\frac{\pi^{-\frac{d}{2}}\Gamma(\Delta)}{\Gamma\left(\Delta-\frac{1}{2}\right)}\int d^d\vec{x}d^d\vec{x}'\frac{\phi_0(\vec{x})\phi_0(\vec{x}')}{|\vec{x}-\vec{x}'|^{2\Delta}}. \tag{A.27}$$

Taking one derivative with respect to the source function ϕ_0 gives the expectation value of the operator of conformal dimension Δ and taking two derivatives gives the two point function

$$\left\langle\mathcal{O}(\vec{x})\right\rangle = \frac{2\Delta-d}{C}\int d^d\vec{x'}\frac{\phi_0(\vec{x}')}{(|\vec{x}-\vec{x}'|^2)^{\Delta}}, \qquad \left\langle\mathcal{O}(\vec{x})\mathcal{O}(\vec{x}')\right\rangle = \frac{2\Delta-d}{C}\frac{1}{(|\vec{x}-\vec{x}'|^2)^{\Delta}}, \tag{A.28}$$

where we reinstalled the constant C.

Appendix B

Supergravity solution

The supergravity action is given by

$$S_p = \frac{1}{2\kappa_{10}} \int d^{10}x\sqrt{-g}\left[e^{-2\Phi}\left(R + 4(\nabla\Phi)^2\right) - \frac{2}{2(p+2)!}F_{p+2}^2\right], \tag{B.1}$$

where R is the Ricci scalar, Φ is the dilaton and $F_{p+2} = dC_{p+1}$ is the field strength of the (p+1)-form potential. The equations of motion stemming from varying the action (B.1) are

$$R_{\mu\nu} + 2\nabla_\mu\nabla_\nu\Phi = \frac{e^{2\Phi}}{2(p+1)!}\left[F_{\mu\nu}^2 - \frac{g_{\mu\nu}}{2(p+2)}F^2\right] \tag{B.2}$$

$$d^\star F_{p+2} = 0, \qquad R = 4(\nabla\Phi)^2 - 4\Box\Phi\,. \tag{B.3}$$

The solutions to these equations are given by

$$ds^2 = \frac{\left(-f(u)dt^2 + d\vec{x}_p^2\right)}{\sqrt{H_p(u)}} + \sqrt{H_p(u)}\left(\frac{du^2}{f(u)} + u^2 d\Omega_{8-p}^2\right) \tag{B.4}$$

$$e^{-2\phi} = H_p(u)^{\frac{p-3}{2}}, \qquad H_p(u) = 1 + \frac{L^{7-p}}{u^{7-p}}, \qquad f(u) = 1 - \frac{u_0^{7-p}}{u^{7-p}}\,, \tag{B.5}$$

$$F_{01\ldots pu} = -\sqrt{1 + \frac{u_0^{7-p}}{L^{7-p}}}\frac{H_p'(u)}{H_p^2(u)}. \tag{B.6}$$

In order to calculate the RR-charge we need to impose Dirac's quantization condition: We integrate $\frac{1}{\kappa_{10}}{}^\star F_{p+2}$ over S^{8-p} and set it equal to an integer times the tension. We obtain

$$N = \frac{(7-p)\Omega_{8-p}^2}{2\kappa_{10}^2 T_p} L^{(7-p)/2}\sqrt{u_0^{7-p} + L^{7-p}}. \tag{B.7}$$

The ADM mass of the solution is

$$M = \frac{\Omega_{8-p}V_p}{2\kappa_{10}^2}\left[(8-p)u_0^{7-p} + (7-p)L^{7-p}\right]. \tag{B.8}$$

In order to understand the geometry better its useful to change coordinates to extend the metric past $u = 0$.

$$\rho^{7-p} = L^{7-p} + u^{7-p}, \qquad r_- = L, \qquad r_+^{7-p} = u_0^{7-p} + L^{7-p} \tag{B.9}$$

The metric now becomes

$$ds^2 = -\frac{f_+(\rho)}{\sqrt{f_-(\rho)}}dt^2 + \sqrt{f_-(\rho)}d\vec{x}_p^2 + \frac{f_-(\rho)^{-\frac{1}{2}-\frac{5-p}{7-p}}}{f_+(\rho)} + r^2 f_-(\rho)^{\frac{1}{2}-\frac{5-p}{7-p}}d\Omega_{8-p}^2, \tag{B.10}$$

where the dilaton and harmonic functions are given by

$$e^{-\Phi} = g_s^{-2} f_-(\rho)^{-\frac{p-3}{2}}, \qquad f_\pm(\rho) = 1 - \left(\frac{r_\pm}{\rho}\right)^{7-p}. \tag{B.11}$$

The parameters r_+ and r_- are related to the ADM mass and the RR-charge N of the solution by

$$M = \frac{\Omega_{8-p} V_p}{2\kappa_{10}^2}\left[(8-p) r_+^{7-p} - r_-^{7-p}\right], \qquad N = \frac{(7-p)\Omega_{8-p}^2}{2\kappa_{10}^2 T_p}(r_+ r_-)^{(7-p)/2}. \tag{B.12}$$

The metric (B.10) has a horizon at $\rho = r_+$ and a curvature singularity at $\rho = r_-$ for $p \leq 6$. For an acceptable brane solution we must have $r_+ \geq r_-$, otherwise we will have a naked singularity. The condition $r_+ \geq r_-$ translates into an inequality between the mass M and the R-R charge N. For a fixed value of N, according to (B.12), the mass is an increasing function of r_+ and takes the form

$$M \geq T_p V_p N. \tag{B.13}$$

Solutions whose mass is at the lower bound, $r_+ = r_-$ (or equivalently $u_0 = 0$), are called extremal p-branes. Equation (B.13) is also the BPS bound with respect to the 10-dimensional supersymmetry. In supersymmetry a BPS state is a state that carries conserved charges and the supersymmetry algebra determines the mass of the state in terms of its charges. In what follows we will always consider extremal or near-extremal p-branes. For extremal p-branes the metric (B.4) takes the form

$$ds^2 = H(u)^{-\frac{1}{2}}\left(-dt^2 + d\vec{x}_p^2\right) + H_p(u)^{\frac{1}{2}}\left(du^2 + u^2 d\Omega_{8-p}^2\right). \tag{B.14}$$

The region around $u = 0$ is known as the "throat" of the solution or its near horizon region. From (B.7) we see that the throat size L is proportional to the charge

$$\left(\frac{L}{2\pi l_s}\right)^{7-p} = \frac{g_s N}{7-p}\frac{\Gamma\left[\frac{9-p}{2}\right]}{2\pi^{(9-p)/2}}. \tag{B.15}$$

This relation is very important for the AdS/CFT correspondence because it gives a relation between supergravity and field theory quantities. For near extremal p-branes the horizon is located far down its throat. This means that we can use the throat approximation $u \ll L$ and the metric becomes

$$ds^2 = \left(\frac{u}{L}\right)^{\frac{7-p}{2}}\left(-f(u)dt^2 + d\vec{x}_p^2\right) + \left(\frac{L}{u}\right)^{\frac{7-p}{2}}\left(\frac{du^2}{f(u)} + u^2 d\Omega_{8-p}^2\right) \tag{B.16}$$

B.1 Important Relations

$$2\kappa_{10} = 2\kappa_0^2 g_s^2 = 16\pi G_N = (2\pi)^7 \alpha'^4 g_s^2 \tag{B.17}$$

$$\Omega_n = \frac{2\pi^{(n+1)/2}}{\Gamma[(n+1)/2]} \tag{B.18}$$

$$G_d = \frac{G_{10}}{(2\pi)^{10-d} V_{10-d}} \tag{B.19}$$

$$T_{D_p} = \frac{\sqrt{\pi}}{\kappa_{10}(2\pi l_s)^{p-3}} = \frac{1}{(2\pi)^p g_s l_s^{p+1}} \tag{B.20}$$

Appendix C

Equation of motions and solutions for the Sakai-Sugimoto model

C.1 General form of equations of motion

Here we present the general form of the variations of the Yang-Mills Lagrangian $\mathcal{L}_{\rm YM}$ and the Chern-Simons Lagrangian $\mathcal{L}_{\rm CS}$ (which can be read off from Eqs. (5.2a) and (5.2b)) for the chirally broken phase. The variation of the Yang-Mills Lagrangian is

$$\frac{\delta\mathcal{L}_{\rm YM}}{\delta\mathcal{A}^a_\lambda} = -2T_8V_4(2\pi\alpha')^2{\rm Tr}\left[(t_a\partial_\rho - i[t_a,\mathcal{A}_\rho])e^{-\Phi}\sqrt{g}\,g^{\mu\lambda}g^{\rho\sigma}\mathcal{F}_{\sigma\mu}\right], \tag{C.1}$$

where the greek indices run over $0,1,2,3,u$, and where $t_0 \equiv \mathbf{1}/2$, $t_a \equiv \tau_a/2$, according to the convention (4.16). Consequently,

$$-\frac{3u_{\rm KK}^{3/2}}{4\kappa M_{\rm KK}^2}\frac{\delta\mathcal{L}_{\rm YM}}{\delta\hat{A}_0} = \partial_u\left(\frac{u^{5/2}f^{1/2}}{v}\hat{F}_{u0}\right) + \partial_i\left(\frac{R^3v}{u^{1/2}f^{1/2}}\hat{F}_{i0}\right), \tag{C.2a}$$

$$-\frac{3u_{\rm KK}^{3/2}}{4\kappa M_{\rm KK}^2}\frac{\delta\mathcal{L}_{\rm YM}}{\delta\hat{A}_i} = \partial_u\left(\frac{u^{5/2}f^{1/2}}{v}\hat{F}_{ui}\right) + \partial_0\left(\frac{R^3v}{u^{1/2}f^{1/2}}\hat{F}_{0i}\right) + \partial_j\left(\frac{R^3v}{u^{1/2}f^{1/2}}\hat{F}_{ji}\right), \tag{C.2b}$$

$$-\frac{3u_{\rm KK}^{3/2}}{4\kappa M_{\rm KK}^2}\frac{\delta\mathcal{L}_{\rm YM}}{\delta\hat{A}_u} = \partial_0\left(\frac{u^{5/2}f^{1/2}}{v}\hat{F}_{0u}\right) + \partial_i\left(\frac{u^{5/2}f^{1/2}}{v}\hat{F}_{iu}\right), \tag{C.2c}$$

and

$$-\frac{3u_{\rm KK}^{3/2}}{4\kappa M_{\rm KK}^2}\frac{\delta\mathcal{L}_{\rm YM}}{\delta A^a_0} = (\delta_{ac}\partial_u + A^b_u\epsilon_{abc})\frac{u^{5/2}f^{1/2}}{v}F^c_{u0} + (\delta_{ac}\partial_i + A^b_i\epsilon_{abc})\frac{R^3v}{u^{1/2}f^{1/2}}F^c_{i0}, \tag{C.3a}$$

$$-\frac{3u_{\rm KK}^{3/2}}{4\kappa M_{\rm KK}^2}\frac{\delta\mathcal{L}_{\rm YM}}{\delta A^a_i} = (\delta_{ac}\partial_u + A^b_u\epsilon_{abc})\frac{u^{5/2}f^{1/2}}{v}F^c_{ui} + (\delta_{ac}\partial_0 + A^b_0\epsilon_{abc})\frac{R^3v}{u^{1/2}f^{1/2}}F^c_{0i} + (\delta_{ac}\partial_j + A^b_j\epsilon_{abc})\frac{R^3v}{u^{1/2}f^{1/2}}F^c_{ji}, \tag{C.3b}$$

$$-\frac{3u_{\rm KK}^{3/2}}{4\kappa M_{\rm KK}^2}\frac{\delta\mathcal{L}_{\rm YM}}{\delta A^a_u} = (\delta_{ac}\partial_0 + A^b_0\epsilon_{abc})\frac{u^{5/2}f^{1/2}}{v}F^c_{0u} + (\delta_{ac}\partial_i + A^b_i\epsilon_{abc})\frac{u^{5/2}f^{1/2}}{v}F^c_{iu}, \tag{C.3c}$$

where the indices i,j,k run over 1,2,3, and where we used

$$\frac{T_8V_4(2\pi\alpha')^2R^{3/2}}{g_s} = \frac{4\kappa M_{\rm KK}^2}{3u_{\rm KK}^{3/2}}, \tag{C.4}$$

with κ defined in Eq. (4.22).

The variations of the Chern-Simons Lagrangian with respect to the $\mathbf{1}$ and τ_3 components are

$$\frac{\delta\mathcal{L}_{\rm CS}}{\delta\hat{A}_\mu} = -i\frac{\kappa\alpha}{4}(F^a_{\nu\rho}F^a_{\sigma\lambda}+\hat{F}_{\nu\rho}\hat{F}_{\sigma\lambda})\epsilon^{\mu\nu\rho\sigma\lambda}\,, \tag{C.5a}$$

$$\frac{\delta\mathcal{L}_{\rm CS}}{\delta A^a_\mu} = -i\frac{\kappa\alpha}{2}\hat{F}_{\nu\rho}F^a_{\sigma\lambda}\epsilon^{\mu\nu\rho\sigma\lambda}\,, \tag{C.5b}$$

with α defined in Eq. (6.6). Consequently,

$$\frac{\delta\mathcal{L}_{\rm CS}}{\delta\hat{A}_0} = i\kappa\alpha(F^a_{ui}F^a_{jk}+\hat{F}_{ui}\hat{F}_{jk})\epsilon^{ijk}\,, \tag{C.6a}$$

$$\frac{\delta\mathcal{L}_{\rm CS}}{\delta\hat{A}_i} = i\kappa\alpha\left(2F^a_{j0}F^a_{uk}-F^a_{u0}F^a_{jk}+2\hat{F}_{j0}\hat{F}_{uk}-\hat{F}_{u0}\hat{F}_{jk}\right)\epsilon^{ijk}\,, \tag{C.6b}$$

$$\frac{\delta\mathcal{L}_{\rm CS}}{\delta\hat{A}_u} = i\kappa\alpha(F^a_{i0}F^a_{jk}+\hat{F}_{i0}\hat{F}_{jk})\epsilon^{ijk}\,, \tag{C.6c}$$

and

$$\frac{\delta\mathcal{L}_{\rm CS}}{\delta A^a_0} = i\kappa\alpha(F^a_{ui}\hat{F}_{jk}+F^a_{jk}\hat{F}_{ui})\epsilon^{ijk}\,, \tag{C.7a}$$

$$\frac{\delta\mathcal{L}_{\rm CS}}{\delta A^a_i} = i\kappa\alpha\left(2F^a_{uk}\hat{F}_{j0}-F^a_{jk}\hat{F}_{u0}+2F^a_{j0}\hat{F}_{uk}-F^a_{u0}\hat{F}_{jk}\right)\epsilon^{ijk}\,, \tag{C.7b}$$

$$\frac{\delta\mathcal{L}_{\rm CS}}{\delta A^a_u} = i\kappa\alpha(F^a_{i0}\hat{F}_{jk}+F^a_{jk}\hat{F}_{i0})\epsilon^{ijk}\,. \tag{C.7c}$$

As mentioned in the Chapter 4, we consider maximally separated branes $L=\pi/M_{\rm KK}$, for which the embedding of the D8-branes is trivial, $\partial_u x_4=0$, and thus $v=1$ (see Eq. (4.12)). This simplifies the above expressions and also ensures that there is no equation of motion for $x_4(u)$. The expressions (C.2), (C.3), (C.6), (C.7) are used in Sec. 6.1.1 to derive the field equations for our specific ansatz.

C.2 Solving the equations of motion for constant magnetic fields

In this appendix we solve the equations of motion for a constant magnetic field for general boundary conditions. The resulting general expressions are instructive to see the structure and symmetries of the solution. By inserting the boundary conditions from Table 6.1 into the general expressions we obtain the solution for the sigma phase, see Eqs. (6.27) (the charged pion condensate requires a nonconstant magnetic field and is discussed in Appendix C.3). The general boundary conditions used here are denoted by

$$\hat{A}_0(\pm\infty) = \mu_B^{L,R}\,, \qquad A_0(\pm\infty)=\mu_I^{L,R}\,, \tag{C.8a}$$

$$\hat{A}_3(\pm\infty) = \hat{\jmath}^{L,R}\,, \qquad A_3(\pm\infty)=\jmath^{L,R}\,, \tag{C.8b}$$

where the upper (lower) sign corresponds to R (L). It is convenient to express the boundary values in terms of their sums and differences,

$$\mu^V_{B,I} \equiv \frac{\mu^R_{B,I}+\mu^L_{B,I}}{2}\,, \qquad \mu^A_{B,I}\equiv\frac{\mu^R_{B,I}-\mu^L_{B,I}}{2}\,, \tag{C.9a}$$

$$\hat{J} \equiv \frac{\hat{\jmath}^R+\hat{\jmath}^L}{2}\,, \qquad \hat{\jmath}\equiv\frac{\hat{\jmath}^R-\hat{\jmath}^L}{2}\,, \qquad J\equiv\frac{\jmath^R+\jmath^L}{2}\,, \qquad \jmath\equiv\frac{\jmath^R-\jmath^L}{2}\,. \tag{C.9b}$$

Here, V and A stand for the vector and axial parts of the chemical potentials.

The general solution for (6.24) with the magnetic field (6.25) is

$$F_0^+ = c_1\zeta_+^{-1} + c_2\zeta_+\,, \qquad F_0^- = d_1\zeta_-^{-1} + d_2\zeta_-\,, \tag{C.10a}$$
$$F_3^+ = -c_1\zeta_+^{-1} + c_2\zeta_+\,, \qquad F_3^- = -d_1\zeta_-^{-1} + d_2\zeta_-\,, \tag{C.10b}$$

with constants c_1, c_2, d_1, d_2 and with

$$\zeta_\pm(z) \equiv e^{(\hat{B}\pm B)\arctan z}\,. \tag{C.11}$$

Consequently, from Eqs. (6.23) we obtain

$$k\hat{F}_{z0} = c_1\zeta_+^{-1} + c_2\zeta_+ + d_1\zeta_-^{-1} + d_2\zeta_-\,, \tag{C.12a}$$
$$kF_{z0} = c_1\zeta_+^{-1} + c_2\zeta_+ - d_1\zeta_-^{-1} - d_2\zeta_-\,, \tag{C.12b}$$
$$k\hat{F}_{z3} = -c_1\zeta_+^{-1} + c_2\zeta_+ - d_1\zeta_-^{-1} + d_2\zeta_-\,, \tag{C.12c}$$
$$kF_{z3} = -c_1\zeta_+^{-1} + c_2\zeta_+ + d_1\zeta_-^{-1} - d_2\zeta_-\,. \tag{C.12d}$$

Here and in the remainder of this and the following appendices we often omit the argument z in the various functions for the sake of brevity. For the integration of the field strengths we use

$$\int dz\frac{\zeta_\pm(z)}{k(z)} = \frac{\zeta_\pm(z)}{\hat{B}\pm B}\,, \qquad \int dz\frac{\zeta_\pm^{-1}(z)}{k(z)} = -\frac{\zeta_\pm^{-1}(z)}{\hat{B}\pm B}\,. \tag{C.13}$$

This yields the gauge fields

$$\hat{A}_0 = -\frac{c_1\zeta_+^{-1}}{\hat{B}+B} + \frac{c_2\zeta_+}{\hat{B}+B} - \frac{d_1\zeta_-^{-1}}{\hat{B}-B} + \frac{d_2\zeta_-}{\hat{B}-B} + \hat{a}_0\,, \tag{C.14a}$$
$$A_0 = -\frac{c_1\zeta_+^{-1}}{\hat{B}+B} + \frac{c_2\zeta_+}{\hat{B}+B} + \frac{d_1\zeta_-^{-1}}{\hat{B}-B} - \frac{d_2\zeta_-}{\hat{B}-B} + a_0\,, \tag{C.14b}$$
$$\hat{A}_3 = \frac{c_1\zeta_+^{-1}}{\hat{B}+B} + \frac{c_2\zeta_+}{\hat{B}+B} + \frac{d_1\zeta_-^{-1}}{\hat{B}-B} + \frac{d_2\zeta_-}{\hat{B}-B} + \hat{a}_3\,, \tag{C.14c}$$
$$A_3 = \frac{c_1\zeta_+^{-1}}{\hat{B}+B} + \frac{c_2\zeta_+}{\hat{B}+B} - \frac{d_1\zeta_-^{-1}}{\hat{B}-B} - \frac{d_2\zeta_-}{\hat{B}-B} + a_3\,, \tag{C.14d}$$

with integration constants $\hat{a}_0$, a_0, $\hat{a}_3$, a_3. We determine the eight constants from the eight boundary conditions (C.8). This yields the gauge fields

$$\begin{aligned}\hat{A}_0 = {} & \mu_B^V - \frac{\mu_B^A}{2}(S_+ + S_-) - \frac{\mu_I^A}{2}(S_+ - S_-) \\ & - \frac{\hat{\jmath}}{2}(C_+ + C_- - T_+) - \frac{\jmath}{2}(C_+ - C_- - T_-)\,,\end{aligned} \tag{C.15a}$$
$$\begin{aligned}A_0 = {} & \mu_I^V - \frac{\mu_I^A}{2}(S_+ + S_-) - \frac{\mu_B^A}{2}(S_+ - S_-) \\ & - \frac{\jmath}{2}(C_+ + C_- - T_+) - \frac{\hat{\jmath}}{2}(C_+ - C_- - T_-)\,,\end{aligned} \tag{C.15b}$$
$$\begin{aligned}\hat{A}_3 = {} & \hat{J} - \frac{\hat{\jmath}}{2}(S_+ + S_-) - \frac{\jmath}{2}(S_+ - S_-) \\ & - \frac{\mu_B^A}{2}(C_+ + C_- - T_+) - \frac{\mu_I^A}{2}(C_+ - C_- - T_-)\,,\end{aligned} \tag{C.15c}$$
$$\begin{aligned}A_3 = {} & J - \frac{\jmath}{2}(S_+ + S_-) - \frac{\hat{\jmath}}{2}(S_+ - S_-) \\ & - \frac{\mu_I^A}{2}(C_+ + C_- - T_+) - \frac{\mu_B^A}{2}(C_+ - C_- - T_-)\,,\end{aligned} \tag{C.15d}$$

and ($k(z)$ times) the field strengths

$$
\begin{aligned}
k\hat{F}_{z0} &= -\frac{\mu_B^A}{2}\left[\hat{B}(C_+ + C_-) + B(C_+ - C_-)\right] - \frac{\mu_I^A}{2}\left[\hat{B}(C_+ - C_-) + B(C_+ + C_-)\right] \\
&\quad -\frac{\hat{\jmath}}{2}\left[\hat{B}(S_+ + S_-) + B(S_+ - S_-)\right] - \frac{\jmath}{2}\left[\hat{B}(S_+ - S_-) + B(S_+ + S_-)\right], \quad \text{(C.16a)} \\
kF_{z0} &= -\frac{\mu_B^A}{2}\left[\hat{B}(C_+ - C_-) + B(C_+ + C_-)\right] - \frac{\mu_I^A}{2}\left[\hat{B}(C_+ + C_-) + B(C_+ - C_-)\right] \\
&\quad -\frac{\hat{\jmath}}{2}\left[\hat{B}(S_+ - S_-) + B(S_+ + S_-)\right] - \frac{\jmath}{2}\left[\hat{B}(S_+ + S_-) + B(S_+ - S_-)\right], \quad \text{(C.16b)} \\
k\hat{F}_{z3} &= -\frac{\mu_B^A}{2}\left[\hat{B}(S_+ + S_-) + B(S_+ - S_-)\right] - \frac{\mu_I^A}{2}\left[\hat{B}(S_+ - S_-) + B(S_+ + S_-)\right] \\
&\quad -\frac{\hat{\jmath}}{2}\left[\hat{B}(C_+ + C_-) + B(C_+ - C_-)\right] - \frac{\jmath}{2}\left[\hat{B}(C_+ - C_-) + B(C_+ + C_-)\right], \quad \text{(C.16c)} \\
kF_{z3} &= -\frac{\mu_B^A}{2}\left[\hat{B}(S_+ - S_-) + B(S_+ + S_-)\right] - \frac{\mu_I^A}{2}\left[\hat{B}(S_+ + S_-) + B(S_+ - S_-)\right] \\
&\quad -\frac{\hat{\jmath}}{2}\left[\hat{B}(C_+ - C_-) + B(C_+ + C_-)\right] - \frac{\jmath}{2}\left[\hat{B}(C_+ + C_-) + B(C_+ - C_-)\right], \quad \text{(C.16d)}
\end{aligned}
$$

where the functions $C_\pm(z)$, $S_\pm(z)$, and $T_\pm$ are defined in Eqs. (6.28). As it should be, the gauge fields (C.15) transform as a vector under a parity transformation once we impose the physical boundary conditions of the σ condensate which imply $\mu_B^A = \mu_I^A = 0$. This can be seen as follows. A parity transformation is given by $(x_1, x_2, x_3, z) \to (-x_1, -x_2, -x_3, -z)$. In particular, the transformation $z \to -z$ implies a chirality transformation $L \to R$ since the two halves of the D8/$\overline{\text{D8}}$-branes, namely $z > 0$ and $z < 0$, correspond to right- and left-handed fermions. Consequently, a parity transformation acts as $C_\pm(z) \to +C_\pm(z)$, $S_\pm(z) \to -S_\pm(z)$ (since the magnetic fields $\hat{B}$, B are even under parity). For the supercurrents we have $\hat{\jmath}, \jmath \to +\hat{\jmath}, +\jmath$ and $\hat{J}, J \to -\hat{J}, -J$. Here we have used that the Goldstone boson is a pseudoscalar (for a detailed discussion of the parity of the mesons in the Sakai-Sugimoto model see Ref. [29]). As a result we see that the temporal components (C.15a), (C.15b) have even parity, while the spatial components (C.15c), (C.15d) have odd parity. This statement is true for arbitrary values of the currents $\hat{\jmath}, \jmath, \hat{J}, J$. We shall see below that in the case of a charged pion condensate the requirement of a well-defined parity results in conditions for the supercurrents, see discussion below Eq. (C.33).

In order to compute the free energy we note that

$$
C_\pm^2 - S_\pm^2 = \frac{1}{\sinh^2[\pi(\hat{B} \pm B)/2]}\,. \tag{C.17}
$$

Therefore, the following combination of field strengths, needed for the free energy, becomes independent of z,

$$
\begin{aligned}
k^2\left(-\hat{F}_{z0}^2 - F_{z0}^2 + \hat{F}_{z3}^2 + F_{z3}^2\right) &= [(\hat{\jmath} + \jmath)^2 - (\mu_B^A + \mu_I^A)^2]\,\frac{(\hat{B} + B)^2}{2\sinh^2[\pi(\hat{B} + B)/2]} \\
&\quad + [(\hat{\jmath} - \jmath)^2 - (\mu_B^A - \mu_I^A)^2]\,\frac{(\hat{B} - B)^2}{2\sinh^2[\pi(\hat{B} - B)/2]}\,. \qquad \text{(C.18)}
\end{aligned}
$$

Next we use the fact that $S_\pm$ and $C_\pm$ are antisymmetric and symmetric in z, respectively, as well as

$$
C_\pm(\infty) = \coth\frac{\pi(\hat{B} \pm B)}{2}\,, \qquad S_\pm(\infty) = 1\,, \tag{C.19}
$$

	small $\hat{B}, B$	large $\lvert\hat{B}\rvert, \lvert B\rvert$	
		$\lvert\hat{B}\rvert > \lvert B\rvert$	$\lvert\hat{B}\rvert < \lvert B\rvert$
$\rho_\pm$	$\frac{6}{\pi} + \frac{\pi(\hat{B} \pm B)^2}{6}$	$2\lvert\hat{B} \pm B\rvert$	
ρ	$\frac{12}{\pi} + \frac{5\hat{B}^2 + B^2}{15}\pi$	$4\lvert\hat{B}\rvert$	$2(\lvert\hat{B}\rvert + \lvert B\rvert)$
η_+	$\frac{\pi\hat{B}B}{3}$	$2B \operatorname{sgn}\hat{B}$	$B \operatorname{sgn}\hat{B} + \hat{B} \operatorname{sgn} B$
η_-	$2\hat{B}$	$2\hat{B}$	$(\lvert\hat{B}\rvert + \lvert B\rvert) \operatorname{sgn}\hat{B}$

Table C.1: Behavior of the functions ρ, $\rho_\pm$, $\eta_\pm$, defined in Eqs. (6.30), (6.43) for small and large magnetic fields $\hat{B}$, B. We have kept relative magnitude and sign of baryon and isospion components arbitrary. They can then later be inserted according to the electric charges of the quarks. We show the behavior for small magnetic fields up to second order and the behavior for large magnetic fields in leading linear order.

to obtain

$$\begin{aligned}
&\Big(\hat{A}_0 k\hat{F}_{z0} + A_0 kF_{z0} - \hat{A}_3 k\hat{F}_{z3} - A_3 kF_{z3}\Big)_{z=-\infty}^{z=\infty} \\
&= -2\mu_B^V(\hat{\jmath}\hat{B} + \jmath B) - 2\mu_I^V(\hat{\jmath}B + \jmath\hat{B}) + 2\hat{J}(\mu_B^A\hat{B} + \mu_I^A B) + 2J(\mu_B^A B + \mu_I^A\hat{B}) \\
&+ [(\mu_B^A + \mu_I^A)^2 - (\hat{\jmath} + \jmath)^2](\hat{B} + B)\coth\frac{\pi(\hat{B} + B)}{2} \\
&+ [(\mu_B^A - \mu_I^A)^2 - (\hat{\jmath} - \jmath)^2](\hat{B} - B)\coth\frac{\pi(\hat{B} - B)}{2}\,.
\end{aligned} \tag{C.20}$$

Inserting Eqs. (C.18) and (C.20) into Eq. (6.10) yields the free energy

$$\begin{aligned}
\Omega \;=\; & \frac{\kappa M_{\mathrm{KK}}^2}{6}\Big\{\left[(\jmath + \hat{\jmath})^2 - (\mu_B^A + \mu_I^A)^2\right]\rho_+ + \left[(\jmath - \hat{\jmath})^2 - (\mu_B^A - \mu_I^A)^2\right]\rho_- \\
& + \mu_B^V(\hat{\jmath}\hat{B} + \jmath B) + \mu_I^V(\hat{\jmath}B + \jmath\hat{B}) \\
& - \hat{J}(\mu_B^A\hat{B} + \mu_I^A B) - J(\mu_B^A B + \mu_I^A\hat{B})\Big\}\,,
\end{aligned} \tag{C.21}$$

with $\rho_\pm$ defined in Eq. (6.30). For the behavior of $\rho_\pm$ for small and large magnetic fields see Table C.1. We see that if we allowed for nonzero axial chemical potentials μ_B^A, μ_I^A, the free energy would be unbounded from below in the directions of the sum of left- and right-handed supercurrents $\hat{J}$ and J. However, in the physical case of the σ condensate where $\mu_B^A = \mu_I^A = 0$ the free energy remains bounded and independent of $\hat{J}$ and J. The latter is a manifestation of a residual gauge symmetry ("residual" since we have already employed the gauge $\mathcal{A}_z = 0$), i.e., we can choose a gauge where $\hat{J} = J = 0$. This is in accordance with the discussion in Ref. [29], see in particular Eq. (5.23) in this reference.

Minimization of Ω with respect to the currents $\hat{\jmath}$, $\jmath$ yields

$$\hat{\jmath} \;=\; -\frac{\mu_B^V + \mu_I^V}{2}\frac{\hat{B} + B}{\rho_+} - \frac{\mu_B^V - \mu_I^V}{2}\frac{\hat{B} - B}{\rho_-}\,, \tag{C.22a}$$

$$\jmath \;=\; -\frac{\mu_B^V + \mu_I^V}{2}\frac{\hat{B} + B}{\rho_+} + \frac{\mu_B^V - \mu_I^V}{2}\frac{\hat{B} - B}{\rho_-}\,, \tag{C.22b}$$

and the minimum of the free energy becomes (with $\mu_B^A = \mu_I^A = 0$)

$$\Omega_0 = -\frac{\kappa M_{\rm KK}^2}{6}\left[(\mu_B^V+\mu_I^V)^2\frac{(\hat{B}+B)^2}{\rho_+}+(\mu_B^V-\mu_I^V)^2\frac{(\hat{B}-B)^2}{\rho_-}\right]. \tag{C.23}$$

C.3 Solving the equations of motion for nonconstant magnetic fields

In this appendix we present the general solution to the differential equations (6.24) for the case of a nonconstant isospin magnetic field given in Eq. (6.38). The general expressions given below reduce to the results for the charged pion phase upon inserting the specific boundary conditions from the second row of Table 6.1. The general boundary conditions considered here are the same as the ones given in Eqs. (C.8).

Then, the solution of (6.24) has the same form as given in Eqs. (C.10) and (C.12), with $\zeta_\pm(z)$ replaced by

$$\tilde{\zeta}_\pm(z) \equiv e^{(\hat{B}\pm\frac{B}{\pi}\arctan z)\arctan z}. \tag{C.24}$$

To obtain the gauge fields we need

$$\int dz\frac{\tilde{\zeta}_+(z)}{k(z)} = P_+(z), \qquad \int dz\frac{\tilde{\zeta}_-^{-1}(z)}{k(z)} = -P_-(z), \tag{C.25a}$$

$$\int dz\frac{\tilde{\zeta}_+^{-1}(z)}{k(z)} = Q_+(z), \qquad \int dz\frac{\tilde{\zeta}_-(z)}{k(z)} = -Q_-(z), \tag{C.25b}$$

with $P_\pm$, $Q_\pm$ given in Eqs. (6.41). We shall denote $Q_\pm^+ \equiv Q_\pm(+\infty)$, $Q_\pm^- \equiv Q_\pm(-\infty)$, $P_\pm^+ \equiv P_\pm(+\infty)$, $P_\pm^- \equiv P_\pm(-\infty)$, and use $P_-^\pm = P_+^\mp$, $Q_-^\pm = Q_+^\mp$. Hence we can express the values of P_-, Q_- at $z = \pm\infty$ through the values of P_+, Q_+ at $z = \mp\infty$. Then, after determining the integration constants from the boundary conditions we can write the gauge fields as

$$\begin{aligned}\hat{A}_0 &= \mu_B^V - \frac{\mu_B^A}{2}(\tilde{S}_+ + \tilde{S}_-) - \frac{\jmath}{2}(\tilde{S}_+ - \tilde{S}_-)\\ &\quad - \frac{\mu_I^A}{2}(\tilde{C}_+ + \tilde{C}_- - \tilde{T}_+) - \frac{\hat{\jmath}}{2}(\tilde{C}_+ - \tilde{C}_- - \tilde{T}_-),\end{aligned} \tag{C.26a}$$

$$\begin{aligned}A_0 &= \mu_I^V - \frac{\mu_I^A}{2}(\tilde{S}_+ + \tilde{S}_-) - \frac{\hat{\jmath}}{2}(\tilde{S}_+ - \tilde{S}_-)\\ &\quad - \frac{\mu_B^A}{2}(\tilde{C}_+ + \tilde{C}_- - \tilde{T}_+) - \frac{\jmath}{2}(\tilde{C}_+ - \tilde{C}_- - \tilde{T}_-),\end{aligned} \tag{C.26b}$$

$$\begin{aligned}\hat{A}_3 &= \hat{J} - \frac{\hat{\jmath}}{2}(\tilde{S}_+ + \tilde{S}_-) - \frac{\mu_I^A}{2}(\tilde{S}_+ - \tilde{S}_-)\\ &\quad - \frac{\jmath}{2}(\tilde{C}_+ + \tilde{C}_- - \tilde{T}_+) - \frac{\mu_B^A}{2}(\tilde{C}_+ - \tilde{C}_- - \tilde{T}_-),\end{aligned} \tag{C.26c}$$

$$\begin{aligned}A_3 &= J - \frac{\jmath}{2}(\tilde{S}_+ + \tilde{S}_-) - \frac{\mu_B^A}{2}(\tilde{S}_+ - \tilde{S}_-)\\ &\quad - \frac{\hat{\jmath}}{2}(\tilde{C}_+ + \tilde{C}_- - \tilde{T}_+) - \frac{\mu_I^A}{2}(\tilde{C}_+ - \tilde{C}_- - \tilde{T}_-),\end{aligned} \tag{C.26d}$$

and the field strengths as

$$
\begin{aligned}
k\hat{F}_{z0} &= -\frac{\mu_B^A}{2}(c_+ + c_-) - \frac{\jmath}{2}(c_+ - c_-) - \frac{\mu_I^A}{2}(s_+ + s_-) - \frac{\hat{\jmath}}{2}(s_+ - s_-)\,, && \text{(C.27a)}\\
kF_{z0} &= -\frac{\mu_I^A}{2}(c_+ + c_-) - \frac{\hat{\jmath}}{2}(c_+ - c_-) - \frac{\mu_B^A}{2}(s_+ + s_-) - \jmath(s_+ - s_-)\,, && \text{(C.27b)}\\
k\hat{F}_{z3} &= -\frac{\hat{\jmath}}{2}(c_+ + c_-) - frac\mu_I^A 2(c_+ - c_-) - \frac{\jmath}{2}(s_+ + s_-) - \frac{\mu_B^A}{2}(s_+ - s_-)\,, && \text{(C.27c)}\\
kF_{z3} &= -\frac{\jmath}{2}(c_+ + c_-) - \frac{\mu_B^A}{2}(c_+ - c_-) - \frac{\hat{\jmath}}{2}(s_+ + s_-) - \frac{\mu_I^A}{2}(s_+ - s_-)\,, && \text{(C.27d)}
\end{aligned}
$$

where $\tilde{C}_\pm$, $\tilde{S}_\pm$, and $\tilde{T}_\pm$ are defined in Eqs. (6.40), and where

$$
\begin{aligned}
c_+(z) &\equiv \frac{\tilde{\zeta}_+(z) + \tilde{\zeta}_-^{-1}(z)}{P_+^+ - P_+^-}\,, \qquad c_-(z) \equiv \frac{\tilde{\zeta}_+^{-1}(z) + \tilde{\zeta}_-(z)}{Q_+^+ - Q_+^-}\,, && \text{(C.28a)}\\
s_+(z) &\equiv \frac{\tilde{\zeta}_+(z) - \tilde{\zeta}_-^{-1}(z)}{P_+^+ - P_+^-}\,, \qquad s_-(z) \equiv \frac{\tilde{\zeta}_+^{-1}(z) - \tilde{\zeta}_-(z)}{Q_+^+ - Q_+^-}\,. && \text{(C.28b)}
\end{aligned}
$$

(These additional definitions were not necessary in the case of constant magnetic fields, since there the integration of the solution could be expressed in terms of the same functions as the solution itself.)

We now have to check the behavior of the gauge fields (C.26) under a parity transformation. For the pion phase we have $\mu_B^A = \mu_I^V = 0$. We have to require $\hat{A}_0 \to +\hat{A}_0$, $A_0 \to -A_0$, $\hat{A}_3 \to -\hat{A}_3$, $A_3 \to +A_3$ (note the additional "twist" for the isospin components originating from the isospin rotation explained in Sec. 6.2.1). Since $\tilde{C}_\pm(z) \to +\tilde{C}_\pm(z)$, $\tilde{S}_\pm(z) \to -\tilde{S}_\pm(z)$, and $\hat{\jmath}, \jmath \to +\hat{\jmath}, +\jmath$ and $\hat{J}, J \to -\hat{J}, -J$ under a parity transformation, we have to require

$$
J = \jmath = 0\,. \tag{C.29}
$$

We shall continue with the general solution but have to keep this condition in mind for the final result.

For the free energy we first note that the following combinations are independent of z,

$$
c_+c_- + s_+s_- = \frac{4}{(P_+^+ - P_+^-)(Q_+^+ - Q_+^-)}\,, \qquad s_+c_- + s_-c_+ = 0\,. \tag{C.30}
$$

Then, we find

$$
k^2\left(-\hat{F}_{z0}^2 - F_{z0}^2 + \hat{F}_{z3}^2 + F_{z3}^2\right) = 16\frac{(\hat{\jmath}^2 + \jmath^2) - [(\mu_B^A)^2 + (\mu_I^A)^2]}{(P_+^+ - P_+^-)(Q_+^+ - Q_+^-)}\,. \tag{C.31}
$$

Next we use that $c_\pm$ and $s_\pm$ are symmetric and antisymmetric in z, respectively, and denote $c_\pm^+ \equiv c_\pm(\infty) = c_\pm(-\infty)$, $s_\pm^+ \equiv s_\pm(\infty) = -s_\pm(-\infty)$. Then,

$$
\begin{aligned}
&\left(\hat{A}_0 k\hat{F}_{z0} + A_0 kF_{z0} - \hat{A}_3 k\hat{F}_{z3} - A_3 kF_{z3}\right)_{z=-\infty}^{z=\infty}\\
&= (s_+^+ + s_-^+)(\jmath\hat{J} + \hat{\jmath}J - \mu_B^V\mu_I^A - \mu_I^V\mu_B^A) + (s_+^+ - s_-^+)(\hat{J}\mu_B^A + J\mu_I^A - \hat{\jmath}\mu_B^V - \jmath\mu_I^V)\\
&+(c_+^+ + c_-^+)[(\mu_B^A)^2 + (\mu_I^A)^2 - (\hat{\jmath}^2 + \jmath^2)]\,. \qquad \text{(C.32)}
\end{aligned}
$$

Inserting this into the free energy (6.10) yields

$$
\begin{aligned}
\Omega &= \frac{\kappa M_{\rm KK}^2}{6}\Big\{\left[\hat{\jmath}^2 + \jmath^2 - (\mu_B^A)^2 - (\mu_I^A)^2\right]\rho + 2(\mu_B^V\mu_I^A + \mu_I^V\mu_B^A)\,\eta_+ + 2(\mu_B^V\hat{\jmath} + \mu_I^V\jmath)\,\eta_-\\
&\quad - 2\hat{J}(\mu_B^A\eta_- + \jmath\eta_+) - 2J(\mu_I^A\eta_- + \hat{\jmath}\eta_+)\Big\}\,, \qquad \text{(C.33)}
\end{aligned}
$$

with ρ and $\eta_\pm \equiv s_+^+ \pm s_-^+$ given in Eqs. (6.43); their behavior for small and large magnetic fields can be found in Table C.1. As in the case of constant magnetic fields discussed in the previous appendix, see Eq. (C.21), the free energy is unbounded from below without further constraints. This can be seen by computing the matrix of second derivatives $\partial^2\Omega/(\partial x_m \partial x_n)$ with $x_m, x_n = \hat{\jmath}, \jmath, \hat{J}, J$. This matrix has eigenvalues $2\kappa M_{\rm KK}^2/3\,[\rho \pm (\rho^2 + 4\eta_+^2)^{1/2}]$, two of which are negative for all magnetic fields. However, we already know from the requirement of a well-defined parity of the gauge fields that $J = \jmath = 0$. Then, with $\mu_B^A = \mu_I^V = 0$, as required for the charged pion condensate, we see that the free energy becomes bounded from below. The only remaining current with respect to which we need to minimize the free energy is then $\hat{\jmath}$. The sum of left- and right-handed currents, $\hat{J}$, remains undetermined, which is, as mentioned for the case of the sigma phase below Eq. (C.21), a consequence of the residual gauge freedom. We may thus set $\hat{J} = 0$.

We can now minimize with respect to $\hat{\jmath}$,

$$\hat{\jmath} = -\mu_B^V \frac{\eta_-}{\rho}\,, \tag{C.34}$$

and insert this back into the free energy,

$$\Omega_0 = -\frac{\kappa M_{\rm KK}^2}{6}\left\{(\mu_B^V)^2\frac{\eta_-^2}{\rho} + (\mu_I^A)^2\rho + 2\eta_+\mu_B^V\mu_I^A\right\}. \tag{C.35}$$

C.4 Equations of motion and free energy in the chirally restored phase

Within our approximation of treating the flavor branes as probe branes, the free energies discussed in the main part of the paper are negligible for the finite-temperature phase transition to the chirally restored phase. It is rather the background geometry which is responsible for this phase transition [21, 88]. Therefore, our approach cannot show magnetic-field induced corrections beyond the order of N_f/N_c to the critical temperature T_c for chiral symmetry breaking. This is different when the D8 and $\overline{\rm D8}$-branes are not maximally separated in the extra dimension [123, 198].

Therefore, in this appendix we simply give the equations of motion and the free energy for the chirally restored phase without discussing the solutions. We do so for the sake of completeness but also because these expressions may be useful to compute possible small corrections to T_c of the order of N_f/N_c. One might then speculate whether these corrections persist for smaller and thus more realistic values of N_c. We leave such a study for the future.

The derivation of the equations of motion and the free energy of the chirally restored phase is analogous to the one for the confined phase given in Section 6.1.2 and Appendix C.1. The only difference is the use of the metric (4.11b) instead of (4.11a) and Eq. (4.8) instead of (4.5). We use the same coordinate transformation as in the chirally broken phase, i.e., Eq. (4.19) with $u_{\rm KK}$ replaced by u_T and with $z \in [0, \infty]$. This is not really a simplifiaction in this case but it helps to compare the result to the one for the chirally broken phase. We find for the equations of motion

$$\partial_z[k_3(z)\partial_z\hat{b}] = \partial_z[k_3(z)\partial_z b] = 0\,, \tag{C.36}$$

and

$$\partial_z[k_0(z)\hat{F}_{z0}] = \frac{\alpha M_{\rm KK} u_T^2}{(2\pi T)^3}\left[b(z)F_{z3}+\hat{b}(z)\hat{F}_{z3}\right], \tag{C.37a}$$

$$\partial_z[k_0(z)F_{z0}] = \frac{\alpha M_{\rm KK} u_T^2}{(2\pi T)^3}\left[b(z)\hat{F}_{z3}+\hat{b}(z)F_{z3}\right], \tag{C.37b}$$

$$\partial_z[k_3(z)\hat{F}_{z3}] = \frac{\alpha M_{\rm KK} u_T^2}{(2\pi T)^3}\left[b(z)F_{z0}+\hat{b}(z)\hat{F}_{z0}\right], \tag{C.37c}$$

$$\partial_z[k_3(z)F_{z3}] = \frac{\alpha M_{\rm KK} u_T^2}{(2\pi T)^3}\left[b(z)\hat{F}_{z0}+\hat{b}(z)F_{z0}\right]. \tag{C.37d}$$

In contrast to the confined phase, there are now two different functions appearing for the temporal and spatial components,

$$k_0(z) \equiv \frac{(u_T^3+u_T z^2)^{3/2}}{z\,u_T^{1/2}}, \qquad k_3(z) \equiv z\,u_T^{1/2}(u_T^3+u_T z^2)^{1/2}. \tag{C.38}$$

The free energy becomes

$$\begin{aligned}\Omega^{\rm deconf} &= \Omega_g^{\rm deconf}+\Omega_b^{\rm deconf}+\frac{\kappa(2\pi T)^3}{3M_{\rm KK}u_T^2}\int_0^\infty dz\,\left[-k_0(z)(\hat{F}_{z0}^2+F_{z0}^2)+k_3(z)(\hat{F}_{z3}^2+F_{z3}^2)\right]\\ &\quad-\frac{2\kappa(2\pi T)^3}{3M_{\rm KK}u_T^2}\left[k_0(z)(\hat{A}_0\hat{F}_{z0}+A_0F_{z0})-k_3(z)(\hat{A}_3\hat{F}_{z3}-A_3F_{z3})\right]_{z=0}^{z=+\infty},\end{aligned} \tag{C.39}$$

where

$$\Omega_g^{\rm deconf} \equiv \frac{32\kappa(2\pi T)^3}{9(2\pi\alpha')^2u_T^2M_{\rm KK}}\int_0^\infty dz\,z\,u_T^{3/2}(u_T^3+u_Tz^2)^{1/6}, \tag{C.40a}$$

$$\Omega_b^{\rm deconf} \equiv \frac{\kappa(2\pi T)}{M_{\rm KK}}(\hat{\mathcal{B}}^2+\mathcal{B}^2)\int_0^\infty dz\,z\,u_T^{1/2}(u_T^3+u_Tz^2)^{-5/6}. \tag{C.40b}$$

Here we have assumed the magnetic field to be constant in z, $\hat{b}(z)=\hat{\mathcal{B}}$, $b(z)=\mathcal{B}$, which solves Eq. (C.36). We see that at the critical temperature where $2\pi T = M_{\rm KK}$ and thus $u_T = u_{\rm KK}$ the free energy assumes a form very similar to the one in the confined phase. The only differences are then the functions $k_0(z)$ and $k_3(z)$ (vs. the single function $k(z)$ in the confined phase) and the different integrands in Ω_g and Ω_b.

C.5 Phase diagram with modified action

The modified action (5.53) suggested in [91] restores thermodynamic consistency in the sense that the number densities defined via the thermodynamic potential agree with the holographic definition (5.6). However, one looses the axial anomaly, see Section 5.2.3. Since there has not been a resolution to this problem, we present here the main results of (6) with the modified action for comparison.

The modified action is given by

$$\tilde{S} = S_{YM}+\frac{3}{2}S_{CS}, \tag{C.41}$$

where S_{YM} and S_{CS} are given by (5.2a) and (5.2b) respectively. By using the equation of motion the YM part of the action drops out and only boundary terms survive. The action is given by

$$\tilde{\Omega} = \frac{\kappa M_{\rm KK}^2}{u_{\rm KK}^2}\left[k(z)(\hat{A}_0\hat{F}_{z0}+A_0F_{z0}-\hat{A}_3\hat{F}_{z3}-A_3F_{z3})\right]_{z=-\infty}^{z=+\infty}. \tag{C.42}$$

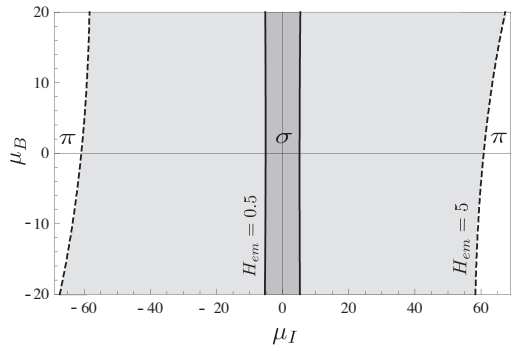

Figure C.1: Phase diagram for the σ and π phases in the plane of baryon and isospin chemical potentials with the modified action with the same values for the magnetic field and units as in Figure 6.6. This diagram almost coincides with Figure 6.6, with the only difference that the bending of the first order phase transition line sets in earlier but is still only visible for magnetic fields several times larger than those expected in compact stars. For $H_{em} = 5$ the interval for μ_I where the phase transition lies is twice as the interval in Figure 6.6.

With the solutions for the gauge fields (6.27) and fieldstrengths (C.16) we obtain

$$\tilde{\Omega} = \frac{\kappa}{2}\Big\{2\tilde{\tilde{j}}(\mu_B\tilde{B}+\mu_I B)+2\tilde{j}(\mu_I\hat{B}+\mu_B B)+(\tilde{\tilde{j}}+\tilde{j})^2(\hat{B}+B)\coth\Big[\frac{\pi}{2}(\hat{B}+B)\Big] \tag{C.43}$$

$$+ \ (\tilde{\tilde{j}}-\tilde{j})^2(\hat{B}-B)\coth\Big[\frac{\pi}{2}(\hat{B}-B)\Big]\Big\}. \tag{C.44}$$

Minimizing with respect to the supercurrents yields

$$\tilde{\tilde{j}} = -\frac{\mu_B+\mu_I}{4}\tanh\Big[\frac{\pi}{2}(\hat{B}+B)\Big]-\frac{\mu_B-\mu_I}{4}\tanh\Big[\frac{\pi}{2}(\hat{B}-B)\Big], \tag{C.45a}$$

$$\jmath = -\frac{\mu_B+\mu_I}{4}\tanh\Big[\frac{\pi}{2}(\hat{B}+B)\Big]+\frac{\mu_B-\mu_I}{4}\tanh\Big[\frac{\pi}{2}(\hat{B}-B)\Big]. \tag{C.45b}$$

Inserting this back into $\tilde{\Omega}$ yields the free energy at the minimum

$$\tilde{\Omega}_\sigma = \frac{\kappa M_{\rm KK}}{2}\Big[(\hat{B}+B)(\mu_B+\mu_I)^2\tanh\Big[\frac{\pi}{2}(\hat{B}+B)\Big]+(\hat{B}-B)(\mu_B-\mu_I)^2\tanh\Big[\frac{\pi}{2}(\hat{B}-B)\Big]\Big]. \tag{C.46}$$

Now one can check that the 0-component of the four current (6.33) agrees with the definition via the free energy

$$\tilde{\mathcal{J}}_L^0+\tilde{\mathcal{J}}_R^0 = -\frac{\partial\tilde{\Omega}}{\partial\mu_B}-\frac{\partial\tilde{\Omega}}{\partial\mu_I}\tau_3, \tag{C.47}$$

and therefore thermodynamic consistency is ensured.

C.6 Solving the equations of motion with electric field

C.6.1 Chirally broken phase

In this appendix we solve the equations of motion in the broken phase, eqs. (5.24). The equation of motion for A_z (5.24c) is trivially integrated with respect to time t to yield

$$k\partial_z A_0 = -2\beta t e(z) + k\partial_z \widetilde{A}_0 \,, \tag{C.48}$$

where we have denoted $e(z) \equiv -\partial_t A_3$ and where we have written the t-independent integration constant as $k\partial_z \widetilde{A}_0$, to be determined below. Inserting this into eqs. (5.24a) and (5.24b) yields

$$\begin{aligned} \partial_z(k\partial_z \widetilde{A}_0) &= 2\beta\partial_z A_3 + 2\beta t\partial_z e \,, & \text{(C.49a)} \\ \partial_z(k\partial_z A_3) &= 2\beta\partial_z \widetilde{A}_0 - (2\beta)^2 t\frac{e(z)}{k(z)} \,. & \text{(C.49b)} \end{aligned}$$

Since the left-hand side of eq. (C.49a) does not depend on t, the right-hand side must be independent of t too which implies

$$\partial_z A_3 = -t\partial_z e + \partial_z \widetilde{A}_3 \,, \tag{C.50}$$

where we have written the t-independent part as $\partial_z \widetilde{A}_3$. Consequently, eqs. (C.49a) and (C.49b) become

$$\begin{aligned} \partial_z(k\partial_z \widetilde{A}_0) &= 2\beta\partial_z \widetilde{A}_3 \,, & \text{(C.51a)} \\ \partial_z(k\partial_z \widetilde{A}_3) &= 2\beta\partial_z \widetilde{A}_0 - t\left[(2\beta)^2\frac{e(z)}{k(z)} - \partial_z(k\partial_z e)\right] \,. & \text{(C.51b)} \end{aligned}$$

Now the square bracket on the right-hand side of eq. (C.51b) must vanish because all other terms in the equation do not depend on t. This yields a differential equation for $e(z)$. Since $e(z) = -\partial_t A_3$, the boundary conditions for A_3 (5.22) imply $e(\pm\infty) = E \mp (\epsilon - \jmath_1)$, where we have decomposed the supercurrent as

$$\jmath_t = \jmath + \jmath_1 t \,, \tag{C.52}$$

with $\jmath$, $\jmath_1$ being t-independent. With these boundary conditions the equation for $e(z)$ is solved by

$$e(z) = E\frac{\cosh(2\beta\arctan z)}{\cosh\beta\pi} - (\epsilon - \jmath_1)\frac{\sinh(2\beta\arctan z)}{\sinh\beta\pi} \,. \tag{C.53}$$

To find the solution for A_0 and A_3 we first conclude from eqs. (C.48) and (C.50),

$$\begin{aligned} A_0(t,z) &= \widetilde{A}_0(z) + g_0(t) \\ &\quad -t\left[E\frac{\sinh(2\beta\arctan z)}{\cosh\beta\pi} - (\epsilon - \jmath_1)\frac{\cosh(2\beta\arctan z)}{\sinh\beta\pi}\right] \,, & \text{(C.54a)} \\ A_3(t,z) &= \widetilde{A}_3(z) - t\left[E\frac{\cosh(2\beta\arctan z)}{\cosh\beta\pi} - (\epsilon - \jmath_1)\frac{\sinh(2\beta\arctan z)}{\sinh\beta\pi}\right] \,. & \text{(C.54b)} \end{aligned}$$

From the z-integration in eq. (C.48) we have obtained a t-dependent integration constant $g_0(t)$. Such a constant is not permissible in A_3 because of the constraint $e(z) = -\partial_t A_3$. Integration constants independent of z *and* t are included in $\widetilde{A}_0(z)$, $\widetilde{A}_3(z)$. We shall fix $g_0(t) = \jmath_1 t\coth\beta\pi$. This removes the supercurrent from the vector boundary value of $A_0(t,z)$. We cannot at the same time remove the axial field ϵ from this boundary value. This becomes clear in hindsight after determining $\jmath_t$ from minimization of the free energy. Only with the given choice of $g_0(t)$

this minimization leads to a consistent, *i.e.*, time-independent, result for $\jmath$, $\jmath_1$. It is thus unavoidable for the boundary values of $A_0(t,z)$ to become time-dependent,

$$A_0(t, z = \pm\infty) = \mu_t \mp \mu_{5,t}\,, \tag{C.55}$$

where we defined

$$\mu_t \equiv \mu + t\epsilon \coth \beta\pi\,, \qquad \mu_{5,t} \equiv \mu_5 + tE \tanh \beta\pi\,. \tag{C.56}$$

We have now reduced the equations of motion (C.51) to equations for $\widetilde{A}_0(z)$, $\widetilde{A}_3(z)$ which are simply the gauge fields in the absence of an electric field. These equations can be solved in general,

$$\widetilde{A}_0(z) = a_0 - \frac{c}{2\beta} e^{-2\beta \arctan z} + \frac{d}{2\beta} e^{2\beta \arctan z}\,, \tag{C.57a}$$

$$\widetilde{A}_3(z) = a_3 + \frac{c}{2\beta} e^{-2\beta \arctan z} + \frac{d}{2\beta} e^{2\beta \arctan z}\,, \tag{C.57b}$$

with integration constants a_0, a_3, c, and d which are fixed by the boundary conditions $\widetilde{A}_0(\pm\infty) = \mu \mp \mu_5$, $\widetilde{A}_3(\pm\infty) = \mp\jmath$. The resulting gauge fields $\widetilde{A}_0(z)$, $\widetilde{A}_3(z)$ are then inserted into the gauge fields $A_0(t,z)$ $A_3(t,z)$ from eqs. (C.54) to obtain the final solution

$$\begin{aligned} A_0(t,z) &= \mu_t - \mu_{5,t} \frac{\sinh(2\beta \arctan z)}{\sinh \beta\pi} \\ &\quad -(\jmath_t - \epsilon t)\left[\frac{\cosh(2\beta \arctan z)}{\sinh \beta\pi} - \coth \beta\pi\right], \end{aligned} \tag{C.58a}$$

$$\begin{aligned} A_3(t,z) &= -tE - \mu_{5,t}\left[\frac{\cosh(2\beta \arctan z)}{\sinh \beta\pi} - \coth \beta\pi\right] \\ &\quad -(\jmath_t - \epsilon t)\frac{\sinh(2\beta \arctan z)}{\sinh \beta\pi}\,. \end{aligned} \tag{C.58b}$$

For the free energy we also need the field strengths (times $k(z)$),

$$k\partial_z A_0 = -2\beta\left[\mu_{5,t}\frac{\cosh(2\beta \arctan z)}{\sinh \beta\pi} + (\jmath_t - \epsilon t)\frac{\sinh(2\beta \arctan z)}{\sinh \beta\pi}\right], \tag{C.59a}$$

$$k\partial_z A_3 = -2\beta\left[\mu_{5,t}\frac{\sinh(2\beta \arctan z)}{\sinh \beta\pi} + (\jmath_t - \epsilon t)\frac{\cosh(2\beta \arctan z)}{\sinh \beta\pi}\right]. \tag{C.59b}$$

As a check, we can perform a parity transformation on the gauge fields. With $\mu \to +\mu$, $\mu_5 \to -\mu_5$, $\jmath_t \to +\jmath_t$, $B \to +B$, $E \to -E$, $\epsilon \to +\epsilon$ and $z \to -z$ we find $A_0(t,z) \to A_0(t,z)$ and $A_3(t,z) \to -A_3(t,z)$, *i.e.*, the fields have the correct behavior under parity transformations for each t and z.

We can now insert the gauge fields and field strengths into the action (5.23) to obtain the thermodynamic potential $\Omega = \frac{T}{V} S_{\text{on-shell}}$. The YM and CS contributions are

$$\Omega_{\text{YM}} = \kappa M_{\text{KK}}^2 \frac{4\pi\beta^2}{\sinh^2 \beta\pi}\left[(\jmath_t - \epsilon t)^2 - \mu_{5,t}^2\right], \tag{C.60a}$$

$$\begin{aligned} \Omega_{\text{CS}} &= \frac{8\kappa M_{\text{KK}}^2}{3}\left(\beta \coth \beta\pi - \frac{\pi\beta^2}{\sinh^2 \beta\pi}\right)\left[(\jmath_t - \epsilon t)^2 - \mu_{5,t}^2\right] \\ &\quad + \frac{8\kappa M_{\text{KK}}^2}{3}\beta\left[\mu_t(\jmath_t - \epsilon t) + tE\mu_{5,t}\right], \end{aligned} \tag{C.60b}$$

where the real time parameter t is treated as an external parameter, unrelated to the imaginary time τ, whose integration is assumed to just give a factor $1/T$. In the YM part we have dropped the terms $\propto B^2, E^2$. This vacuum subtraction can be understood in terms of holographic renormalization and follows from the renormalization condition that the thermodynamic potential be zero for vanishing chemical potentials; for the explicit procedure see ref. [34].

C.6.2 Chirally symmetric phase

Here we solve the equations of motion for the chirally symmetric phase, eqs. (5.36). For notational convenience, let us, in this subsection, denote

$$\beta' \equiv \frac{\beta}{\theta^3}\,. \tag{C.61}$$

The time-dependence of the gauge fields is treated analogously to the broken phase. Thus, eqs. (5.36c) and (5.36b) imply

$$k_0\partial_z A_0^{L/R} = \mp 2\beta' t e_{L/R}(z) + k_0\partial_z \widetilde{A}_0^{L/R}\,, \tag{C.62}$$

and

$$\partial_z A_3^{L/R} = -t\partial_z e_{L/R}(z) + \partial_z \widetilde{A}_3^{L/R}\,, \tag{C.63}$$

where $\widetilde{A}_0^{L/R}$, $\widetilde{A}_3^{L/R}$ are constant in t, and where $e_{L/R} \equiv -\partial_t A_3^{L/R}$. Then, eqs. (5.36a) and (5.36b) read

$$\begin{aligned}
\partial_z(k_0\partial_z \widetilde{A}_0^{L/R}) &= \pm 2\beta'\partial_z \widetilde{A}_3^{L/R}\,, &\text{(C.64a)}\\
\partial_z(k_3\partial_z \widetilde{A}_3^{L/R}) &= \pm 2\beta'\partial_z \widetilde{A}_0^{L/R} - t\left[(2\beta')^2\frac{e_{L/R}(z)}{k_0(z)} - \partial_z(k_3\partial_z e_{L/R})\right]\,. &\text{(C.64b)}
\end{aligned}$$

This is analogous to eq. (C.51), the only difference being the two functions $k_0(z)$ and $k_3(z)$ instead of the single function $k(z)$. Again the square bracket in eq. (C.64b) has to vanish. This yields a differential equation for $e_{L/R}(z)$ which is solved as follows. With $\widetilde{e}_{L/R} = k_3\partial_z e_{L/R}$ one can rewrite this differential equation as

$$\partial_z(k_0\partial_z \widetilde{e}_{L/R}) = (2\beta')^2\frac{\widetilde{e}_{L/R}}{k_3}\,. \tag{C.65}$$

This equation has the two independent solutions

$$\begin{aligned}
p(z) &= {}_2F_1\left[-\frac{\sqrt{1-16\beta'^2}+1}{4}, \frac{\sqrt{1-16\beta'^2}-1}{4}, \frac{1}{2}, \frac{1}{1+z^2}\right]\,, &\text{(C.66a)}\\
q(z) &= \frac{1}{\sqrt{1+z^2}}\,{}_2F_1\left[-\frac{\sqrt{1-16\beta'^2}-1}{4}, \frac{\sqrt{1-16\beta'^2}+1}{4}, \frac{3}{2}, \frac{1}{1+z^2}\right]\,. &\text{(C.66b)}
\end{aligned}$$

Consequently, $\widetilde{e}_{L/R}(z) = P_{L/R}\,p(z) + Q_{L/R}\,q(z)$, with constants $P_{L/R}$, $Q_{L/R}$, and thus

$$e_{L/R}(z) = \frac{1}{(2\beta')^2}\left(P_{L/R}\,k_0\partial_z p + Q_{L/R}\,k_0\partial_z q\right)\,. \tag{C.67}$$

In the following we need the behavior of the functions $p(z)$, $q(z)$, $k_0\partial_z p$, $k_0\partial_z q$ at $z=\infty$ and $z=0$. At $z=\infty$ we have

$$p(\infty) = -k_0\partial_z q(\infty) = 1\,, \qquad q(\infty) = k_0\partial_z p(\infty) = 0\,. \tag{C.68}$$

At $z=0$ one finds

$$\begin{aligned}
p_0 &\equiv p(0) = \frac{\sqrt{\pi}}{\Gamma\left[\left(3-\sqrt{1-16\beta'^2}\right)/4\right]\Gamma\left[\left(3+\sqrt{1-16\beta'^2}\right)/4\right]}\,, &\text{(C.69a)}\\
q_0 &\equiv q(0) = \frac{\sqrt{\pi}}{2\Gamma\left[\left(5-\sqrt{1-16\beta'^2}\right)/4\right]\Gamma\left[\left(5+\sqrt{1-16\beta'^2}\right)/4\right]}\,, &\text{(C.69b)}
\end{aligned}$$

and

$$k_0\partial_z p(z\to 0) = (2\beta')^2 p_0 \ln z\,, \qquad k_0\partial_z q(z\to 0) = (2\beta')^2 q_0 \ln z\,. \tag{C.70}$$

The boundary conditions $e_{L/R}(z=\infty) = E \mp \epsilon$ yield $Q_{L/R} = -(2\beta')^2(E\mp\epsilon)$. Inserting this constant into eq. (C.67), the result into eqs. (C.62), (C.63), and integrating the resulting equations over z yields the gauge fields

$$A_0^{L/R}(t,z) = \mp 2\beta' t\left[\frac{P_{L/R}}{(2\beta')^2}\,p(z) - (E\mp\epsilon)\,q(z)\right] + g_0^{L/R}(t) + \widetilde{A}_0^{L/R}(z)\,, \tag{C.71a}$$

$$A_3^{L/R}(t,z) = -t\left[\frac{P_{L/R}}{(2\beta')^2}\,k_0\partial_z p(z) - (E\mp\epsilon)\,k_0\partial_z q\right] + \widetilde{A}_3^{L/R}(z)\,. \tag{C.71b}$$

Here, $g_0^{L/R}(t)$ are time-dependent integration constants from the z integration. We proceed by solving eqs. (C.64) for $\widetilde{A}_0^{L/R}$, $\widetilde{A}_3^{L/R}$. Recalling that $p(z)$, $q(z)$ fulfill the differential equation (C.65) one easily checks that the functions

$$\widetilde{A}_0^{L/R}(z) = a_0^{L/R} \pm 2\beta'\left[C_{L/R}\,p(z) + D_{L/R}\,q(z)\right]\,, \tag{C.72a}$$

$$\widetilde{A}_3^{L/R}(z) = a_3^{L/R} + C_{L/R}\,k_0\partial_z p + D_{L/R}\,k_0\partial_z q\,, \tag{C.72b}$$

with integration constants $a_0^{L/R}$, $a_3^{L/R}$, $C_{L/R}$ and $D_{L/R}$, are solutions of eqs. (C.64). One now inserts these functions into eqs. (C.71) and determines the integration constants as follows. First we recall that all constants except for $g_0^{L/R}(t)$ must not depend on t. This will be used repeatedly in the following. Then we require the boundary condition $A_3^{L/R}(t,z=\infty) = -t(E\mp\epsilon)$ which implies $D_{L/R} = a_3^{L/R}$. Next, we require regularity of $A_3^{L/R}(t,z)$ at $z=0$. With eq. (C.70) we find that $A_3^{L/R}(t,z\to 0)$ diverges logarithmically. Requiring the factor in front of the $\ln z$ term to vanish yields the conditions

$$C_{L/R} = -\frac{q_0}{p_0}D_{L/R}\,, \qquad P_{L/R} = (2\beta')^2\frac{q_0}{p_0}(E\mp\epsilon)\,. \tag{C.73}$$

For the temporal component we need to require $A_0^{L/R}(t,z=0) = 0$ [88] which yields $a_0^{L/R} = g_0^{L/R}(t) = 0$. With these results the boundary value of $A_0^{L/R}(t,z)$ becomes

$$A_0^{L/R}(t,z=\infty) = \mp 2\beta'\frac{q_0}{p_0}[D_{L/R} + t(E\mp\epsilon)]\,. \tag{C.74}$$

This result shows that, as in the broken phase, the boundary values of axial and vector parts of A_0 necessarily become time-dependent. In other words, in the presence of an electric field one cannot fix these boundary values to be time-independent chemical potentials. At $t=0$ we require $A_0^{L/R}(t=0,z=\infty) = \mu \mp \mu_5$. With these initial values we find

$$D_{L/R} = \mp\frac{p_0}{q_0}\frac{\mu\mp\mu_5}{2\beta'}\,, \tag{C.75}$$

and the time-dependent chemical potentials become

$$A_0^{L/R}(t,z=\infty) = \mu_t \mp \mu_{5,t}\,, \tag{C.76}$$

with

$$\mu_t \equiv \mu + 2\beta' t\epsilon\frac{q_0}{p_0}\,, \qquad \mu_{5,t} \equiv \mu_5 + 2\beta' tE\frac{q_0}{p_0}\,. \tag{C.77}$$

Collecting all the integration constants, we obtain from eqs. (C.71) and (C.72) the final solution for the gauge fields,

$$A_0^{L/R}(t,z) = (\mu_t \mp \mu_{5,t})\left[p(z) - \frac{p_0}{q_0}\,q(z)\right], \tag{C.78a}$$

$$A_3^{L/R}(t,z) = -t(E \mp \epsilon) \pm \frac{\mu_t \mp \mu_{5,t}}{2\beta'}\left[k_0\partial_z p - \frac{p_0}{q_0}(1 + k_0\partial_z q)\right]. \tag{C.78b}$$

Again we can check the behavior of the gauge fields under parity transformations. In contrast to the broken phase, we have separate right- and left-handed fields which transform as $A_0^{L/R}(t,z) \to A_0^{R/L}(t,z)$, and $A_3^{L/R}(t,z) \to -A_3^{R/L}(t,z)$, as it should be. The field strengths become

$$k_0\partial_z A_0^{L/R} = (\mu_t \mp \mu_{5,t})\left(k_0\partial_z p - \frac{p_0}{q_0}k_0\partial_z q\right), \tag{C.79a}$$

$$k_3\partial_z A_3^{L/R} = \pm 2\beta'(\mu_t \mp \mu_{5,t})\left[p(z) - \frac{p_0}{q_0}q(z)\right]. \tag{C.79b}$$

Inserting these results into the action, given by eqs. (5.32) and (5.33), yields the YM and CS contributions to the free energy,

$$\Omega_{\rm YM} = -2\kappa\theta^3 M_{\rm KK}^2(\mu_t^2 + \mu_{5,t}^2)[I_0 - (2\beta')^2 I_3], \tag{C.80a}$$

$$\Omega_{\rm CS} = \frac{4\kappa M_{\rm KK}^2\theta^3}{3}\Big\{(\mu_t^2 + \mu_{5,t}^2)\Big[I_0 - (2\beta')^2 I_3 - \frac{p_0}{q_0}\Big] + 2\beta'\,t\,(\mu_t\epsilon + \mu_{5,t}E)\Big\}, \tag{C.80b}$$

where we abbreviated the integrals

$$I_0 \equiv \int_0^\infty \frac{dz}{k_0}\left(k_0\partial_z p - \frac{p_0}{q_0}k_0\partial_z q\right)^2, \tag{C.81}$$

$$I_3 \equiv \int_0^\infty \frac{dz}{k_3}\left[p(z) - \frac{p_0}{q_0}q(z)\right]^2. \tag{C.82}$$

In the limit $\beta \gg 1$, the combination $I_0 - (2\beta')^2 I_3 \to 0$, so that for very strong magnetic fields $\Omega_{\rm CS} \gg \Omega_{\rm YM}$, as is also the case in the chirally broken phase, see eqs. (C.60).

Bibliography

[1] S. L. Glashow, *Partial-symmetries of weak interactions*, *Nuclear Physics* **22** (1961), no. 4 579 – 588.

[2] S. Weinberg, *A model of leptons*, *Phys. Rev. Lett.* **19** (Nov, 1967) 1264–1266.

[3] A. Salam, *Relativistic groups and analyticity*, *N. Svartholm. ed. Elementary Particle Physics:* (1968).

[4] D. J. Gross and F. Wilczek, *ULTRAVIOLET BEHAVIOR OF NON-ABELIAN GAUGE THEORIES*, *Phys. Rev. Lett.* **30** (1973) 1343–1346.

[5] H. D. Politzer, *RELIABLE PERTURBATIVE RESULTS FOR STRONG INTERACTIONS?*, *Phys. Rev. Lett.* **30** (1973) 1346–1349.

[6] K. Kajantie, M. Laine, K. Rummukainen and Y. Schroder, *The Pressure of hot QCD up to g6 ln(1/g)*, *Phys.Rev.* **D67** (2003) 105008 [hep-ph/0211321].

[7] A. Vuorinen, *The Pressure of QCD at finite temperatures and chemical potentials*, *Phys.Rev.* **D68** (2003) 054017 [hep-ph/0305183].

[8] M. G. Alford, K. Rajagopal and F. Wilczek, *Color-flavor locking and chiral symmetry breaking in high density QCD*, *Nucl. Phys.* **B537** (1999) 443–458 [hep-ph/9804403].

[9] M. G. Alford, A. Schmitt, K. Rajagopal and T. Schäfer, *Color superconductivity in dense quark matter*, *Rev. Mod. Phys.* **80** (2008) 1455–1515 [0709.4635].

[10] H. Georgi, *Effective Field Theory*, *Annual Review of Nuclear and Particle Science* **43** (1993), no. 1 209–252.

[11] A. Pich, *Effective field theory*, hep-ph/9806303.

[12] J. Smit, *Introduction to quantum fields on the lattice*, *Cambrifge Lecture Notes in Physics* (2002).

[13] J. Rothe, Heinz, *Lattice gauge theories: An introduction*, *Bookmark and Share World Scientific Lecture Notes in Physics* **74**.

[14] J. M. Maldacena, *The large N limit of superconformal field theories and supergravity*, *Adv. Theor. Math. Phys.* **2** (1998) 231–252 [hep-th/9711200].

[15] A. Buchel and J. T. Liu, *Universality of the shear viscosity in supergravity*, *Phys.Rev.Lett.* **93** (2004) 090602 [hep-th/0311175].

[16] S. Borsanyi, G. Endrodi, Z. Fodor, A. Jakovac, S. D. Katz *et. al.*, *The QCD equation of state with dynamical quarks*, *JHEP* **1011** (2010) 077 [1007.2580].

[17] P. Kovtun, D. Son and A. Starinets, *Viscosity in strongly interacting quantum field theories from black hole physics*, *Phys.Rev.Lett.* **94** (2005) 111601 [hep-th/0405231]. An Essay submitted to 2004 Gravity Research Foundation competition.

[18] J. Casalderrey-Solana, H. Liu, D. Mateos, K. Rajagopal and U. A. Wiedemann, *Gauge/String Duality, Hot QCD and Heavy Ion Collisions*, 1101.0618.

[19] S. Sachdev, *Condensed matter and AdS/CFT*, 1002.2947.

[20] G. T. Horowitz and J. Polchinski, *Gauge / gravity duality*, gr-qc/0602037.

[21] E. Witten, *Anti-de Sitter space, thermal phase transition, and confinement in gauge theories*, *Adv. Theor. Math. Phys.* **2** (1998) 505–532 [hep-th/9803131].

[22] O. Aharony, O. Bergman, D. L. Jafferis and J. Maldacena, *N=6 superconformal Chern-Simons-matter theories, M2-branes and their gravity duals*, *JHEP* **0810** (2008) 091 [0806.1218].

[23] G. 't Hooft, *Dimensional reduction in quantum gravity*, *Published in Salamfest :0284-296* (1993) [gr-qc/9310026].

[24] L. Susskind, *The World as a hologram*, *J. Math. Phys.* **36** (1995) 6377–6396 [hep-th/9409089].

[25] R. Bousso, *The Holographic principle*, *Rev.Mod.Phys.* **74** (2002) 825–874 [hep-th/0203101].

[26] J. Erlich, E. Katz, D. T. Son and M. A. Stephanov, *QCD and a holographic model of hadrons*, *Phys. Rev. Lett.* **95** (2005) 261602 [hep-ph/0501128].

[27] A. Karch, E. Katz, D. T. Son and M. A. Stephanov, *Linear confinement and AdS/QCD*, *Phys.Rev.* **D74** (2006) 015005 [hep-ph/0602229].

[28] U. Gursoy and E. Kiritsis, *Exploring improved holographic theories for QCD: Part I*, *JHEP* **02** (2008) 032 [0707.1324].

[29] T. Sakai and S. Sugimoto, *Low energy hadron physics in holographic QCD*, *Prog. Theor. Phys.* **113** (2005) 843–882 [hep-th/0412141].

[30] A. Karch and E. Katz, *Adding flavor to AdS/CFT*, *JHEP* **06** (2002) 043 [hep-th/0205236].

[31] C. P. Herzog, S. A. Stricker and A. Vuorinen, *Remarks on Heavy-Light Mesons from AdS/CFT*, *JHEP* **05** (2008) 070 [0802.2956].

[32] C. P. Herzog, S. A. Stricker and A. Vuorinen, *Hyperfine Splitting and the Zeeman Effect in Holographic Heavy-Light Mesons*, *Phys. Rev.* **D82** (2010) 041701 [1005.3285].

[33] A. Rebhan, A. Schmitt and S. A. Stricker, *Anomalies and the chiral magnetic effect in the Sakai- Sugimoto model*, *JHEP* **01** (2010) 026 [0909.4782].

[34] A. Rebhan, A. Schmitt and S. A. Stricker, *Meson supercurrents and the Meissner effect in the Sakai- Sugimoto model*, *JHEP* **05** (2009) 084 [0811.3533].

[35] O. Aharony, S. S. Gubser, J. M. Maldacena, H. Ooguri and Y. Oz, *Large N field theories, string theory and gravity*, *Phys. Rept.* **323** (2000) 183–386 [hep-th/9905111].

[36] E. D'Hoker and Freedman, *Supersymmetric gauge theories and the AdS / CFT correspondence*, hep-th/0201253.

[37] H. Nastase, *Introduction to AdS-CFT*, 0712.0689.

[38] M. B. Green, J. H. Schwarz and E. Witten, *Superstring Theory: Volume 1, Introduction. Volume II: Loop Amplitudes, Anomalies and Phenomenology.* Cambridge University Press, July, 1988.

[39] J. Polchinski, *String Theory, Vol. 1 An introduction to the bosonic string, String theory. Vol. 2: Superstring theory and beyond.* Cambridge University Press, June, 2005.

[40] E. Kiritsis, *String Theory in a Nutshell.* Princeton University Press, March, 2007.

[41] S. W. Hawking and G. F. R. Ellis, *The Large Scale Structure of Space-Time.* Cambridge University Press, Feb., 1975.

[42] C. R. Graham and E. Witten, *Conformal anomaly of submanifold observables in AdS/CFT correspondence*, *Nucl. Phys.* **B546** (1999) 52–64 [hep-th/9901021].

[43] C. A. Bayona and N. R. Braga, *Anti-de Sitter boundary in Poincare coordinates*, *Gen.Rel.Grav.* **39** (2007) 1367–1379 [hep-th/0512182].

[44] S. Coleman and J. Mandula, *All possible symmetries of the s matrix*, *Phys. Rev.* **159** (Jul, 1967) 1251–1256.

[45] J. Wess and J. Bagger, *Supersymmetry and Supergravity.* Princeton University Press, 2 revised ed., Mar., 1992.

[46] R. Grimm, M. Sohnius and J. Wess, *Extended Supersymmetry and Gauge Theories*, *Nucl. Phys.* **B133** (1978) 275.

[47] G. 't Hooft, *A planar diagram theory for strong interactions*, *Nucl. Phys.* **B72** (1974) 461.

[48] D. J. Gross and A. Neveu, *Dynamical symmetry breaking in asymptotically free field theories*, *Phys. Rev. D* **10** (Nov, 1974) 3235–3253.

[49] J. Polchinski, *Dirichlet-Branes and Ramond-Ramond Charges*, *Phys. Rev. Lett.* **75** (1995) 4724–4727 [hep-th/9510017].

[50] D. Z. Freedman, S. D. Mathur, A. Matusis and L. Rastelli, *Correlation functions in the CFT(d)/AdS(d + 1) correspondence*, *Nucl. Phys.* **B546** (1999) 96–118 [hep-th/9804058].

[51] S. Lee, S. Minwalla, M. Rangamani and N. Seiberg, *Three-point functions of chiral operators in D = 4, N = 4 SYM at large N*, *Adv. Theor. Math. Phys.* **2** (1998) 697–718 [hep-th/9806074].

[52] E. Witten, *Anti-de Sitter space and holography*, *Adv. Theor. Math. Phys.* **2** (1998) 253–291 [hep-th/9802150].

[53] S. S. Gubser, I. R. Klebanov and A. M. Polyakov, *Gauge theory correlators from non-critical string theory*, *Phys. Lett.* **B428** (1998) 105–114 [hep-th/9802109].

[54] I. R. Klebanov and E. Witten, *AdS/CFT correspondence and symmetry breaking*, *Nucl. Phys.* **B556** (1999) 89–114 [hep-th/9905104].

[55] P. Breitenlohner and D. Z. Freedman, *Stability in Gauged Extended Supergravity*, *Ann. Phys.* **144** (1982) 249.

[56] E. Bergshoeff, R. Kallosh, T. Ortin and G. Papadopoulos, *Kappa symmetry, supersymmetry and intersecting branes*, *Nucl.Phys.* **B502** (1997) 149–169 [hep-th/9705040].

[57] V. G. Filev, C. V. Johnson, R. C. Rashkov and K. S. Viswanathan, *Flavoured large N gauge theory in an external magnetic field*, *JHEP* **10** (2007) 019 [hep-th/0701001].

[58] M. Neubert, *Heavy quark symmetry*, *Phys. Rept.* **245** (1994) 259–396 [hep-ph/9306320].

[59] J. M. Maldacena, *The large N limit of superconformal field theories and supergravity*, *Adv. Theor. Math. Phys.* **2** (1998) 231–252 [hep-th/9711200].

[60] I. R. Klebanov and M. J. Strassler, *Supergravity and a confining gauge theory: Duality cascades and chiSB-resolution of naked singularities*, *JHEP* **08** (2000) 052 [hep-th/0007191].

[61] E. Shuryak, *Why does the quark gluon plasma at RHIC behave as a nearly ideal fluid?*, *Prog. Part. Nucl. Phys.* **53** (2004) 273–303 [hep-ph/0312227].

[62] E. V. Shuryak, *What RHIC experiments and theory tell us about properties of quark-gluon plasma?*, *Nucl. Phys.* **A750** (2005) 64–83 [hep-ph/0405066].

[63] S. S. Gubser, I. R. Klebanov and A. W. Peet, *Entropy and Temperature of Black 3-Branes*, *Phys. Rev.* **D54** (1996) 3915–3919 [hep-th/9602135].

[64] P. Romatschke and U. Romatschke, *Viscosity Information from Relativistic Nuclear Collisions: How Perfect is the Fluid Observed at RHIC?*, *Phys. Rev. Lett.* **99** (2007) 172301 [0706.1522].

[65] G. Policastro, D. T. Son and A. O. Starinets, *The shear viscosity of strongly coupled N = 4 supersymmetric Yang-Mills plasma*, *Phys. Rev. Lett.* **87** (2001) 081601 [hep-th/0104066].

[66] A. Karch, E. Katz and N. Weiner, *Hadron masses and screening from AdS Wilson loops*, *Phys.Rev.Lett.* **90** (2003) 091601 [hep-th/0211107].

[67] M. Kruczenski, D. Mateos, R. C. Myers and D. J. Winters, *Meson spectroscopy in AdS/CFT with flavour*, *JHEP* **07** (2003) 049 [hep-th/0304032].

[68] J. Erdmenger, N. Evans, I. Kirsch and E. Threlfall, *Mesons in Gauge/Gravity Duals - A Review*, *Eur.Phys.J.* **A35** (2008) 81–133 [0711.4467].

[69] A. Paredes and P. Talavera, *Multiflavor excited mesons from the fifth dimension*, *Nucl.Phys.* **B713** (2005) 438–464 [hep-th/0412260].

[70] J. Erdmenger, N. Evans and J. Grosse, *Heavy-light mesons from the AdS/CFT correspondence*, *JHEP* **0701** (2007) 098 [hep-th/0605241].

[71] J. Erdmenger, K. Ghoroku and I. Kirsch, *Holographic heavy-light mesons from non-Abelian DBI*, *JHEP* **0709** (2007) 111 [0706.3978].

[72] J. Gomis, F. Marchesano and D. Mateos, *An Open string landscape*, *JHEP* **0511** (2005) 021 [hep-th/0506179].

[73] C. Herzog, A. Karch, P. Kovtun, C. Kozcaz and L. Yaffe, *Energy loss of a heavy quark moving through N=4 supersymmetric Yang-Mills plasma*, *JHEP* **0607** (2006) 013 [hep-th/0605158].

[74] A. Cotrone, L. Martucci and W. Troost, *String splitting and strong coupling meson decay*, *Phys.Rev.Lett.* **96** (2006) 141601 [hep-th/0511045].

[75] K. Peeters, J. Sonnenschein and M. Zamaklar, *Holographic decays of large-spin mesons*, *JHEP* **0602** (2006) 009 [hep-th/0511044].

[76] P. Chesler and A. Vuorinen, *Heavy flavor diffusion in weakly coupled N=4 super Yang-Mills theory*, *JHEP* **0611** (2006) 037 [hep-ph/0607148].

[77] E. Pomoni and L. Rastelli, *Intersecting Flavor Branes*, 1002.0006.

[78] H. Arfaei and M. Sheikh Jabbari, *Different d-brane interactions*, *Phys.Lett.* **B394** (1997) 288–296 [hep-th/9608167].

[79] C. P. Herzog and T. Klose, *The Perfect Atom: Bound States of Supersymmetric Quantum Electrodynamics*, *Nucl.Phys.* **B839** (2010) 129–156 [0912.0733].

[80] J.-H. Cho, P. Oh, C. Park and J. Shin, *String pair creations in D-brane systems*, *JHEP* **0505** (2005) 004 [hep-th/0501190].

[81] K. Nakamura and P. D. Group, *Review of particle physics*, *Journal of Physics G: Nuclear and Particle Physics* **37** (2010), no. 7A 075021.

[82] R. L. Jaffe and K. Johnson, *Unconventional States of Confined Quarks and Gluons*, *Phys. Lett.* **B60** (1976) 201.

[83] N. Isgur and J. E. Paton, *A Flux Tube Model for Hadrons*, *Phys. Lett.* **B124** (1983) 247.

[84] N. R. Constable and R. C. Myers, *Exotic scalar states in the AdS / CFT correspondence*, *JHEP* **9911** (1999) 020 [hep-th/9905081].

[85] M. Kruczenski, D. Mateos, R. C. Myers and D. J. Winters, *Towards a holographic dual of large-N(c) QCD*, *JHEP* **05** (2004) 041 [hep-th/0311270].

[86] L. McLerran and R. D. Pisarski, *Phases of Cold, Dense Quarks at Large N_c*, *Nucl. Phys.* **A796** (2007) 83–100 [0706.2191].

[87] O. Aharony, J. Sonnenschein and S. Yankielowicz, *A holographic model of deconfinement and chiral symmetry restoration*, *Annals Phys.* **322** (2007) 1420–1443 [hep-th/0604161].

[88] N. Horigome and Y. Tanii, *Holographic chiral phase transition with chemical potential*, *JHEP* **01** (2007) 072 [hep-th/0608198].

[89] E. Antonyan, J. A. Harvey, S. Jensen and D. Kutasov, *NJL and QCD from string theory*, hep-th/0604017.

[90] E. G. Thompson and D. T. Son, *Magnetized baryonic matter in holographic QCD*, *Phys. Rev.* **D78** (2008) 066007 [0806.0367].

[91] O. Bergman, G. Lifschytz and M. Lippert, *Magnetic properties of dense holographic QCD*, 0806.0366.

[92] A. Parnachev, *Holographic QCD with Isospin Chemical Potential*, *JHEP* **02** (2008) 062 [0708.3170].

[93] H. Hata, T. Sakai, S. Sugimoto and S. Yamato, *Baryons from instantons in holographic QCD*, hep-th/0701280.

[94] O. Aharony, K. Peeters, J. Sonnenschein and M. Zamaklar, *Rho meson condensation at finite isospin chemical potential in a holographic model for QCD*, *JHEP* **02** (2008) 071 [0709.3948].

[95] D. E. Kharzeev, L. D. McLerran and H. J. Warringa, *The effects of topological charge change in heavy ion collisions: 'Event by event P and CP violation'*, *Nucl. Phys.* **A803** (2008) 227–253 [0711.0950].

[96] K. Fukushima, D. E. Kharzeev and H. J. Warringa, *The Chiral Magnetic Effect*, *Phys. Rev.* **D78** (2008) 074033 [0808.3382].

[97] D. E. Kharzeev and H. J. Warringa, *Chiral Magnetic conductivity*, *Phys.Rev.* **D80** (2009) 034028 [0907.5007].

[98] **STAR** Collaboration, S. A. Voloshin, *Probe for the strong parity violation effects at RHIC with three particle correlations*, 0806.0029.

[99] **STAR Collaboration** Collaboration, B. Abelev *et. al.*, *Azimuthal Charged-Particle Correlations and Possible Local Strong Parity Violation*, *Phys.Rev.Lett.* **103** (2009) 251601 [0909.1739].

[100] F. Wang, *Effects of Cluster Particle Correlations on Local Parity Violation Observables*, *Phys.Rev.* **C81** (2010) 064902 [0911.1482].

[101] H.-U. Yee, *Holographic Chiral Magnetic Conductivity*, *JHEP* **0911** (2009) 085 [0908.4189].

[102] D. T. Son and A. R. Zhitnitsky, *Quantum anomalies in dense matter*, *Phys. Rev.* **D70** (2004) 074018 [hep-ph/0405216].

[103] M. A. Metlitski and A. R. Zhitnitsky, *Anomalous axion interactions and topological currents in dense matter*, *Phys. Rev.* **D72** (2005) 045011 [hep-ph/0505072].

[104] E. V. Gorbar, V. A. Miransky and I. A. Shovkovy, *Chiral asymmetry of the Fermi surface in dense relativistic matter in a magnetic field*, 0904.2164.

[105] J. Charbonneau and A. Zhitnitsky, *Topological Currents in Neutron Stars: Kicks, Precession, Toroidal Fields, and Magnetic Helicity*, 0903.4450.

[106] S. S. Gubser, I. R. Klebanov and A. M. Polyakov, *Gauge theory correlators from non-critical string theory*, *Phys. Lett.* **B428** (1998) 105–114 [hep-th/9802109].

[107] E. Witten, *Anti-de Sitter space and holography*, *Adv. Theor. Math. Phys.* **2** (1998) 253–291 [hep-th/9802150].

[108] G. Lifschytz and M. Lippert, *Anomalous conductivity in holographic QCD*, 0904.4772.

[109] P. V. Buividovich, M. N. Chernodub, E. V. Luschevskaya and M. I. Polikarpov, *Numerical evidence of chiral magnetic effect in lattice gauge theory*, 0907.0494.

[110] H. Hata, M. Murata and S. Yamato, *Chiral currents and static properties of nucleons in holographic QCD*, *Phys. Rev.* **D78** (2008) 086006 [0803.0180].

[111] K. Hashimoto, T. Sakai and S. Sugimoto, *Holographic Baryons : Static Properties and Form Factors from Gauge/String Duality*, 0806.3122.

[112] K.-Y. Kim and I. Zahed, *Electromagnetic Baryon Form Factors from Holographic QCD*, *JHEP* **0809** (2008) 007 [0807.0033].

[113] K.-Y. Kim and I. Zahed, *Nucleon-Nucleon Potential from Holography*, *JHEP* **0903** (2009) 131 [0901.0012].

[114] W. A. Bardeen, *Anomalous Ward identities in spinor field theories*, *Phys. Rev.* **184** (1969) 1848–1857.

[115] C. T. Hill, *Anomalies, Chern-Simons terms and chiral delocalization in extra dimensions*, *Phys.Rev.* **D73** (2006) 085001 [hep-th/0601154].

[116] J. S. Bell and R. Jackiw, *A PCAC puzzle: pi0 → gamma gamma in the sigma model*, *Nuovo Cim.* **A60** (1969) 47–61.

[117] S. L. Adler, *Axial vector vertex in spinor electrodynamics*, *Phys. Rev.* **177** (1969) 2426–2438.

[118] O. Kaymakcalan, S. Rajeev and J. Schechter, *Nonabelian Anomaly and Vector Meson Decays*, *Phys. Rev.* **D30** (1984) 594.

[119] J. Erdmenger, M. Haack, M. Kaminski and A. Yarom, *Fluid dynamics of R-charged black holes*, *JHEP* **0901** (2009) 055 [0809.2488].

[120] N. Banerjee, J. Bhattacharya, S. Bhattacharyya, S. Dutta, R. Loganayagam *et. al.*, *Hydrodynamics from charged black branes*, 0809.2596.

[121] M. Torabian and H.-U. Yee, *Holographic nonlinear hydrodynamics from AdS/CFT with multiple/non-Abelian symmetries*, *JHEP* **0908** (2009) 020 [0903.4894].

[122] D. T. Son and P. Surowka, *Hydrodynamics with Triangle Anomalies*, *Phys.Rev.Lett.* **103** (2009) 191601 [0906.5044].

[123] O. Bergman, G. Lifschytz and M. Lippert, *Response of Holographic QCD to Electric and Magnetic Fields*, *JHEP* **05** (2008) 007 [0802.3720].

[124] C. V. Johnson and A. Kundu, *External Fields and Chiral Symmetry Breaking in the Sakai- Sugimoto Model*, *JHEP* **12** (2008) 053 [0803.0038].

[125] K.-Y. Kim, S.-J. Sin and I. Zahed, *Dense Holographic QCD in the Wigner-Seitz Approximation*, *JHEP* **09** (2008) 001 [0712.1582].

[126] J. Ambjorn, J. Greensite and C. Peterson, *THE AXIAL ANOMALY AND THE LATTICE DIRAC SEA*, *Nucl. Phys.* **B221** (1983) 381.

[127] G. Lifschytz and M. Lippert, *Holographic Magnetic Phase Transition*, *Phys.Rev.* **D80** (2009) 066007 [0906.3892].

[128] S. Elitzur, G. W. Moore, A. Schwimmer and N. Seiberg, *Remarks on the Canonical Quantization of the Chern-Simons- Witten Theory*, *Nucl. Phys.* **B326** (1989) 108.

[129] G. M. Newman and D. T. Son, *Response of strongly-interacting matter to magnetic field: Some exact results*, *Phys. Rev.* **D73** (2006) 045006 [hep-ph/0510049].

[130] H. B. Nielsen and M. Ninomiya, *ADLER-BELL-JACKIW ANOMALY AND WEYL FERMIONS IN CRYSTAL*, *Phys. Lett.* **B130** (1983) 389.

[131] T. Sakai and S. Sugimoto, *More on a holographic dual of QCD*, *Prog. Theor. Phys.* **114** (2005) 1083–1118 [hep-th/0507073].

[132] P. Basu, J. He, A. Mukherjee and H.-H. Shieh, *Holographic Non-Fermi Liquid in a Background Magnetic Field*, *Phys. Rev.* **D82** (2010) 044036 [0908.1436].

[133] F. Denef, S. A. Hartnoll and S. Sachdev, *Quantum oscillations and black hole ringing*, *Phys. Rev.* **D80** (2009) 126016 [0908.1788].

[134] H.-U. Yee, *private communication*, .

[135] V. P. Gusynin, V. A. Miransky and I. A. Shovkovy, *Catalysis of dynamical flavor symmetry breaking by a magnetic field in (2+1)-dimensions*, *Phys. Rev. Lett.* **73** (1994) 3499–3502 [hep-ph/9405262].

[136] V. P. Gusynin, V. A. Miransky and I. A. Shovkovy, *Dimensional reduction and catalysis of dynamical symmetry breaking by a magnetic field*, *Nucl. Phys.* **B462** (1996) 249–290 [hep-ph/9509320].

[137] S. P. Klevansky and R. H. Lemmer, *Chiral symmetry restoration in the Nambu-Jona-Lasinio model with a constant electromagnetic field*, *Phys. Rev.* **D39** (1989) 3478–3489.

[138] S. P. Klevansky, *The Nambu-Jona-Lasinio model of quantum chromodynamics*, *Rev. Mod. Phys.* **64** (1992) 649–708.

[139] N. O. Agasian and I. A. Shushpanov, *Gell-Mann-Oakes-Renner relation in a magnetic field at finite temperature*, *JHEP* **10** (2001) 006 [hep-ph/0107128].

[140] T. D. Cohen, D. A. McGady and E. S. Werbos, *The chiral condensate in a constant electromagnetic field*, *Phys. Rev.* **C76** (2007) 055201 [0706.3208].

[141] N. O. Agasian and S. M. Fedorov, *Quark-hadron phase transition in a magnetic field*, *Phys. Lett.* **B663** (2008) 445–449 [0803.3156].

[142] E. S. Fraga and A. J. Mizher, *Chiral transition in a strong magnetic background*, *Phys. Rev.* **D78** (2008) 025016 [0804.1452].

[143] A. J. Mizher and E. S. Fraga, *CP violation and chiral symmetry restoration in the hot linear sigma model in a strong magnetic background*, 0810.5162.

[144] E. J. Ferrer, V. de la Incera and C. Manuel, *Magnetic color flavor locking phase in high density QCD*, *Phys. Rev. Lett.* **95** (2005) 152002 [hep-ph/0503162].

[145] K. Fukushima and H. J. Warringa, *Color superconducting matter in a magnetic field*, *Phys. Rev. Lett.* **100** (2008) 032007 [0707.3785].

[146] J. L. Noronha and I. A. Shovkovy, *Color-flavor locked superconductor in a magnetic field*, *Phys. Rev.* **D76** (2007) 105030 [0708.0307].

[147] D. T. Son and M. A. Stephanov, *Axial anomaly and magnetism of nuclear and quark matter*, *Phys. Rev.* **D77** (2008) 014021 [0710.1084].

[148] T. Albash, V. G. Filev, C. V. Johnson and A. Kundu, *Finite Temperature Large N Gauge Theory with Quarks in an External Magnetic Field*, *JHEP* **07** (2008) 080 [0709.1547].

[149] J. Erdmenger, R. Meyer and J. P. Shock, *AdS/CFT with Flavour in Electric and Magnetic Kalb-Ramond Fields*, *JHEP* **12** (2007) 091 [0709.1551].

[150] A. B. Migdal, *Phase Transition in Nuclear Matter and Non-pair Nuclear Forces*, *Sov. Phys. JETP* **36** (1973) 1052.

[151] R. F. Sawyer, *Condensed π^- phase in neutron star matter*, *Phys. Rev. Lett.* **29** (1972) 382–385.

[152] D. J. Scalapino, *π^- condensate in dense nuclear matter*, *Phys. Rev. Lett.* **29** (1972) 386–388.

[153] G. Baym, *Pion condensation in nuclear and neutron star matter*, *Phys. Rev. Lett.* **30** (1973) 1340–1342.

[154] A. I. Larkin and Y. N. Ovchinnikov, *Inhomogeneous state of superconductors*, *Sov. Phys. JETP* **20** (1965) 762.

[155] P. Fulde and R. A. Ferrell, *Superconductivity in a strong spin-exchange field*, *Phys. Rev.* **135** (1964) A550.

[156] M. G. Alford, J. A. Bowers and K. Rajagopal, *Crystalline color superconductivity*, *Phys. Rev.* **D63** (2001) 074016 [hep-ph/0008208].

[157] O. Schnetz, M. Thies and K. Urlichs, *Phase diagram of the Gross-Neveu model: Exact results and condensed matter precursors*, *Ann. Phys.* **314** (2004) 425–447 [hep-th/0402014].

[158] A. Kryjevski, *Spontaneous superfluid current generation in the kaon condensed color flavor locked phase at nonzero strange quark mass*, *Phys. Rev.* **D77** (2008) 014018 [hep-ph/0508180].

[159] T. Schäfer, *Meson supercurrent state in high density QCD*, *Phys. Rev. Lett.* **96** (2006) 012305 [hep-ph/0508190].

[160] A. Schmitt, *Supercurrents in color-superconducting quark matter*, *Nucl. Phys.* **A820** (2009) 49c–56c [0810.4243].

[161] S. Seki and J. Sonnenschein, *Comments on Baryons in Holographic QCD*, *JHEP* **01** (2009) 053 [0810.1633].

[162] M. Rozali, H.-H. Shieh, M. Van Raamsdonk and J. Wu, *Cold Nuclear Matter In Holographic QCD*, *JHEP* **01** (2008) 053 [0708.1322].

[163] K.-Y. Kim, S.-J. Sin and I. Zahed, *The Chiral Model of Sakai-Sugimoto at Finite Baryon Density*, *JHEP* **01** (2008) 002 [0708.1469].

[164] S. A. Hartnoll, C. P. Herzog and G. T. Horowitz, *Building a Holographic Superconductor*, *Phys. Rev. Lett.* **101** (2008) 031601 [0803.3295].

[165] S. S. Gubser and S. S. Pufu, *The gravity dual of a p-wave superconductor*, *JHEP* **11** (2008) 033 [0805.2960].

[166] C. P. Herzog, P. K. Kovtun and D. T. Son, *Holographic model of superfluidity*, 0809.4870.

[167] M. Ammon, J. Erdmenger, M. Kaminski and P. Kerner, *Superconductivity from gauge/gravity duality with flavor*, 0810.2316.

[168] S. A. Hartnoll, C. P. Herzog and G. T. Horowitz, *Holographic Superconductors*, *JHEP* **12** (2008) 015 [0810.1563].

[169] D. Vollhardt and P. Wölfle, *The Superfluid Phases of Helium 3*. Taylor & Francis, London, 1990.

[170] D. T. Son, *Low-energy quantum effective action for relativistic superfluids*, hep-ph/0204199.

[171] A. Karch, A. O'Bannon and K. Skenderis, *Holographic renormalization of probe D-branes in AdS/CFT*, *JHEP* **04** (2006) 015 [hep-th/0512125].

[172] T. Wiseman and B. Withers, *Holographic renormalization for coincident Dp-branes*, *JHEP* **10** (2008) 037 [0807.0755].

[173] I. Kanitscheider, K. Skenderis and M. Taylor, *Precision holography for non-conformal branes*, *JHEP* **09** (2008) 094 [0807.3324].

[174] A. Armoni, *Witten-Veneziano from Green-Schwarz*, *JHEP* **06** (2004) 019 [hep-th/0404248].

[175] J. L. F. Barbon, C. Hoyos-Badajoz, D. Mateos and R. C. Myers, *The holographic life of the η'*, *JHEP* **10** (2004) 029 [hep-th/0404260].

[176] A. Parnachev and A. R. Zhitnitsky, *Phase Transitions, θ Behavior and Instantons in QCD and its Holographic Model*, 0806.1736.

[177] B. Klein, D. Toublan and J. J. M. Verbaarschot, *The QCD phase diagram at nonzero temperature, baryon and isospin chemical potentials in random matrix theory*, *Phys. Rev.* **D68** (2003) 014009 [hep-ph/0301143].

[178] E. Witten, *Theta dependence in the large N limit of four-dimensional gauge theories*, *Phys. Rev. Lett.* **81** (1998) 2862–2865 [hep-th/9807109].

[179] D. Boer and J. K. Boomsma, *Spontaneous CP-violation in the strong interaction at $\theta = \pi$*, *Phys. Rev.* **D78** (2008) 054027 [0806.1669].

[180] D. V. Deryagin, D. Y. Grigoriev and V. A. Rubakov, *Standing wave ground state in high density, zero temperature QCD at large N_c*, *Int. J. Mod. Phys.* **A7** (1992) 659–681.

[181] E. Shuster and D. T. Son, *On finite-density QCD at large N_c*, *Nucl. Phys.* **B573** (2000) 434–446 [hep-ph/9905448].

[182] L. Y. Glozman and R. F. Wagenbrunn, *Chirally symmetric but confining dense and cold matter*, *Phys. Rev.* **D77** (2008) 054027 [0709.3080].

[183] A. Fetter and J. Walecka, *Quantum theory of many-particle systems*. McGraw-Hill, New York, 1971.

[184] D. T. Son and M. A. Stephanov, *QCD and dimensional deconstruction*, *Phys. Rev.* **D69** (2004) 065020 [hep-ph/0304182].

[185] R. McNees, R. C. Myers and A. Sinha, *On quark masses in holographic QCD*, 0807.5127.

[186] B. J. Harrington and H. K. Shepard, *Superconducting properties of pion condensates*, *Phys. Rev.* **D16** (1977) 3437.

[187] B. J. Harrington and H. K. Shepard, *Superconducting properties of pion condensates. II*, *Phys. Rev.* **D19** (1979) 1713.

[188] N. Y. Anisimov and D. N. Voskresensky, *Superconductivity of pion condensate*, *Sov. J. Nucl. Phys.* **30** (1979) 612–615.

[189] A. B. Migdal, E. E. Saperstein, M. A. Troitsky and D. N. Voskresensky, *Pion degrees of freedom in nuclear matter*, *Phys. Rept.* **192** (1990) 179–437.

[190] T. Rube and J. G. Wacker, *The Simplicity of Perfect Atoms: Degeneracies in Supersymmetric Hydrogen*, 0912.2543.

[191] W.-j. Fu, Y.-x. Liu and Y.-l. Wu, *Chiral Magnetic Effect and QCD Phase Transitions with Effective Models*, 1003.4169.

[192] V. Rubakov, *On chiral magnetic effect and holography*, 1005.1888.

[193] A. Y. Alekseev, V. V. Cheianov and J. Frohlich, *Universality of transport properties in equilibrium, Goldstone theorem and chiral anomaly*, cond-mat/9803346.

[194] A. Gynther, K. Landsteiner, F. Pena-Benitez and A. Rebhan, *Holographic Anomalous Conductivities and the Chiral Magnetic Effect*, 1005.2587.

[195] J. O. Andersen and L. Kyllingstad, *Pion condensation at finite temperature and density: The role of charge neutrality*, hep-ph/0701033.

[196] F. Preis, A. Rebhan and A. Schmitt, *Inverse magnetic catalysis in dense holographic matter*, 1012.4785.

[197] A. Hamilton, D. N. Kabat, G. Lifschytz and D. A. Lowe, *Local bulk operators in AdS/CFT: A boundary view of horizons and locality*, *Phys. Rev.* **D73** (2006) 086003 [hep-th/0506118].

[198] C. V. Johnson and A. Kundu, *External Fields and Chiral Symmetry Breaking in the Sakai- Sugimoto Model*, 0803.0038.